STUDIES OF PROTEIN COMPLEXES INVOLVED IN THE ADENYLYLATION CASCADE OF THE NITROGEN SIGNALLING PATHWAY IN *Escherichia coli.*

Thesis submitted by
Paula Clancy BSc (JCU), MSc (JCU)
in March 2004.

For the degree of Doctor of Philosophy
in the Department of Biochemistry and Molecular Biology
James Cook University of North Queensland.

I dedicate this work to my father who was always very proud of his girls, and won't be here to see its completion.

DECLARATION

I declare that this thesis is my own work and has not been submitted in any form for another degree or diploma at any university or other institute of tertiary education. Information derived from the published or unpublished work of others has been acknowledged in the text and a list of references is given.

……. **……**

Paula Clancy **Mar 2004**

STATEMENT OF ACCESS

I, the undersigned, the author of this thesis, understand that James Cook University of North Queensland will make it available for use within the University Library and, by microfilm or other means, allow access to users in other approved libraries. All users consulting this thesis will have to sign the following statement:

> In consulting with this thesis I agree not to copy or closely paraphrase it in whole or part without written consent of the author and to make proper written acknowledgement for any assistance, which I have obtained from it.

Beyond this, I do not wish to pace any restriction on access of this thesis.

…… **……...**

Paula Clancy **Mar 2004**

ABSTRACT

Adenylyl transferase (ATase), the *glnE* gene product from *Escherichia coli*, is a bifunctional enzyme that catalyses the opposing adenylylation and deadenylylation of glutamine synthetase (GS). The overall aim of this thesis was elucidation of the molecular mechanisms of the adenylylation cascade.

A new central domain has been identified using ATase truncation constructs in activity assays and solubility trials. This new regulatory domain is flanked by two flexible Q-linkers, Q1 and Q2. Thus the topology of ATase can be represented as N-Q1-R-Q2-C. The N domain was PII-UMP independent in *in vitro* deadenylylation assays, and had 1000 fold less activity then entire ATase, suggesting PII-UMP binding impacts on the conformation of the deadenylylation active site.

Monoclonal antibodies (mAbs) generated in this work against ATase were characterised using ATase mutants and the truncated proteins. Two mAbs, 5A7 (binds residues 502-548) and 39G11 (binds residues 466-501) both binding in the R domain, blocked the binding of PII, GlnK, PII-UMP and GlnK-UMP to ATase. This is the first report that pinpoints the effector-protein binding sites to within the R domain of ATase.

Both PII and ATase bound α-ketoglutarate (α-kg) in direct binding assays. Several lines of evidence suggested that PII contains the high affinity α-kg binding site and ATase the low affinity site. This study demonstrates for the first time that the two small effector-molecules α-kg and glutamine (gln) probably bind in the last 340 residues of ATase (Q2-C domain), possibly near the adenylylation active site.

The demonstration that the ATase mutant W694G presented a gln independent phenotype suggests that the bulky side chain of Trp 694 must move out of the adenylylation active site, so that GS can dock and be modified. Surface plasmon resonance (SPR) data suggested the binding of gln within Q2-C is transmitted to the R domain as an allosteric inhibitor of PII-UMP binding, and consequently deadenylylation.

A panel of mAbs was also produced against PII and characterised using a series of PII mutants. Two of the PII mAbs 19G4 (binds PII/GlnK) and 24H2 (binds PII) were used further to demonstrate that heterotrimers are formed between PII and GlnK *in vivo* in nitrogen starved cells.

It is well documented that the T-loops of PII and GlnK are probably the principal regions used by these signalling proteins to bind to the various receptor-proteins such as ATase, UTase and NRII. This study suggests PII and GlnK also interact with GS. Using PII mutants carrying specific GlnK residues at positions 43, 52 and 54 in the T-loop this study demonstrated the Asp at position 54 was the critical determinant of PII T-loop binding to GS, whereas the interaction with UTase involved both Asp54 and Thr43.

PUBLISHED PAPERS

Hall, R. A., Kay, B. H., Burgess, G. W., **Clancy, P.,** and Fanning, I. D. (1990). Epitope analysis of the envelope and non-structural glycoproteins of Murray Valley encephalitis. *J. Gen. Virol.* **71**: 2923-2930.

Hall, R. A., Burgess, G. W., Kay, B. H., and **Clancy, P.** (1991). Monoclonal antibodies to Kunjin and Kokobera viruses. *Immunol. Cell. Biol.* **69**: 47-49.

Breinl, R. A. **Clancy, P.**, McBride, W. J. H., and Vasudevan, S. G. (1997). Cloning and expression of the exposed portion of the four dengue virus serotypes. *Arbovir. Res. In Aust.* **7**: 21-24.

van Heeswijk, W. C., Wen, D., **Clancy, P.**, Jaggi, R., Ollis, D. L., Westerhoff, H., V., and Vasudevan, S. G. (2000). The *Escherichia coli* signal transducers PII (GlnB) and GlnK form heterotrimers *in vivo*: Fine tuning the nitrogen signal cascade. *Proc. Nat. Acad. Sci. USA* **97**: 3942-3947.

Xu, Y., Carr, P. D., **Clancy, P.,** Garcia-Dominguez, M., Forchhammer, K., Florencio, F., Tandeau de Marsac, N., Vasudevan, S., and Ollis, D. (2003). The structures of the PII proteins from the cyanobacteria *Synechococcus* sp. PCC 7942 and *Synechocystis* sp. PCC 6803. *Acta Cryst D.* **59**: 2183-2190.

Xu, Y., Wen, D., **Clancy, P.,** Carr, P. D., Ollis, D. L., and Vasudevan, S. G. (2004). Expression, purification, crystallization and preliminary X-ray analysis of the N-terminal domain of *Escherichia coli* adenylyltransferase. *Protein Expr. Purif.* **34**:142-6.

MANUSCRIPTS IN PREPARATION

Clancy, P., Teakle, L and Vasudevan, S. G. Production and characterization of monoclonal antibodies to proteins in the nitrogen assimilation cascade in *Escherichia coli*.

Clancy, P., Xu, Y, Carr, P. D., Vasudevan, S. G. and Ollis, D. L. Structure and function of PII: mapping small molecule binding using mutants

Clancy, P., and Vasudevan, S. G. Adenylyl transferase is a mutidomain protein containing a central regulatory domain that controls the two opposing activity domains

CONFERENCE PRESENTATIONS

Hall, R. A., Burgess, G. W., Kay, B. H., and **Clancy, P.** (1988). Application of monoclonal antibodies to the study of Australian flaviviruses. Presented to the Australian Society for Immunology annual Conference, Canberra.

Hall, R. A., Kay, B. H., Burgess, G. W., **Clancy, P.**, and Fanning, I. D. (1989). Examination of Flavivirus epitopes using monoclonal antibodies to Murray Valley encephalitis, Kunjin and Kokobera viruses. Presented as a poster at the 5th Australian Arbovirus Symposium, Brisbane.

Hall, R. A., Burgess, G. W., **Clancy, P.**, and Kay, B. H. (1989). Detection of serum antibodies to specific flavivirus epitopes using monoclonal antibodies. Presented to the 5th Australian Arbovirus Symposium, Brisbane.

Burgess, G. W., **Clancy, P.**, and Yan, M. (1992). Development of monoclonal antibody based ELISA diagnostic for alphaviruses. Presented to the Arbovirus Research in Australia Symposium, Brisbane.

Clancy, P., and Vasudevan, S. G. (1999). The Role of Small Effector Molecules in Nitrogen Signal Transduction Studied Using Surface Plasmon Resonance. Presented as a poster at COMBIO conference for Australian Society for Biochemistry and Molecular Biology, Gold Coast.

Clancy, P., Xu, Y., Carr, P. D., Ollis, D. L., and Vasudevan, S. G. (2001). Mutational analysis of PII. Presented as a poster at COMBIO conference for Australian Society for Biochemistry and Molecular Biology, Canberra.

Clancy, P.*, McLoughlin, S.*, Xu, Y., Ollis, D. L., and Vasudevan, S. G. (2002). Site-Directed Mutagenesis Analysis Indicates That The Two Opposing Activities Of Adenylyl Transferase Are Carried Out Within Active Sites That Are Very Similar To Human DNA Polymerase β. Presented as a poster at COMBIO conference for Australian Society for Biochemistry and Molecular Biology, Sydney.

CONTENTS

LIST OF FIGURES

LIST OF TABLES

ABBREVIATIONS

Ab	Antibody
ABTS	2,2'-azino-bis 3-ethylbenzthiazoline 6-sulphonic acid
ADP	Adenosine diphosphate
Ag	Antigen
Ala	Alanine residue
AMP	Adenosine monophosphate
Arg	Arginine residue
Asn	Asparagine
Asp	Aspartate residue
ATase	Adenylyltransferase
ATP	Adenosine triphosphate
BCIP	15-bromo-4-chloro-3-indolyl phosphate p-toluidine salt
bp	Base pair
C	Carbon
^{o}C	Degrees Celsius
cm^2	Centimetres squared
CPU	Central processing unit
CTAB	Cetyltrimethyl ammonium bromide
CTP	Cytidine triphosphate
d	Day
DEAE	Diethylaminoethyl
DMEM	Dulbeccos minimal essential media
DMF	Dimethylformamide
DMSO	Dimethylsuphoxide
DNA	Deoxyribonucleic acid
DPM	Disintegrations per minute
EDTA	Ethylenediaminetetraacetic acid
ELISA	Enzyme linked immunoassay
Ep	Epitope
g	Gram
GDH	Glutamate dehydrogenase
gln	Glutamine
Gln	Glutamine residue
glu	Glutamate
Glu	Glutamate residue
Gly	Glycine residue
GOGAT	Gltuamine amide-2-oxoglutarate amino transferase
GS	Glutamine synthetase
GS_{MT}	Glutamine synthetase from *Mycobacterium tuberculosis*
GS_{ST}	Glutamine synthetase from *Salmonella typhimurium*
HEPES	4-(2-hydroxyethyl)-1-piperazineethanesulfonic acid
His	Histidine residue
HRPO	Horseraddish peroxidase
IgG	Immunoglobulin G

IgM	Immunoglobulin M
Ile	Isoleucine residue
IP	Intraperitoneally
IPTG	Isopropyl-beta-D-thiogalactopyranoside
IV	Intravenously
K_d	Disassociation constant
K_m	Michaelis constant
kD	Kilodalton
α-kg	α-Ketoglutarate
L	Litre
λ	Wavelength
LB	Luria Bertani broth
Leu	Leucine residue
Lys	Lysine residue
M	Molar
mAb	Monoclonal antibody
Met	Methionine residue
Mg^{2+}	Magnesium ion
min	Minute
mg	Miligram
mL	Mililitre
mL^{-1}	Per mililitre
mM	Milimolar
Mn^{2+}	Manganese ion
N	Nitrogen
$NADP^+$	Nicotinamide adenine dinucleotide phosphate, oxidised form
NADPH	Nicotinamide adenine dinucleotide phosphate, reduced form
NBT	Nitrobluetetrazolium
NH_3	Ammonia
nm	Nanometre
NMR	Nuclear magnetic resonance
NP40	Nonidet P40
OD_{405}	Optical density measured at wavelength 405 nanometres
OD_{492}	Optical density measured at wavelength 492 nanometres
OD_{595}	Optical density measured at wavelength 595 nanometres
PAGE	Polyacrylamide gel electrophoresis
PEG	Polyethyleneglycol
Phe	Phenylalanine residue
PMSF	Phenylmethylsulphonyl fluoride
Pro	Proline residue
RNA	Ribonucleic acid
rpm	Revolutions per minute
SDS	Sodiumdodecylsulphate
Ser	Serine residue
SPR	Surface plasmon resonance
TCA	Trichloracetic acid
TEMED	N,N,N,N-tetramethylethylenediamine
Thr	Threonine residue

Tyr	Tyrosine residue
μCi	Microcuries
μg	Microgram
μL	Microlitre
μm	Micrometre
μM	Micromolar
UMP	Uridine monosphate
UTase	Uridylyltransferase-uridylyl removing enzyme
UTP	Uridine triphosphate
UV	Ultraviolet
V	Volts
Val	Valine residue
v/v	Volume per volume
well^{-1}	Per well
w/v	Weight per volume
3D	Three dimensional

AKNOWLEDGEMENTS

First and foremost I thank my daughter, Erin for her patience in this long, drawn out endeavour, which has covered most of her lifetime.

I would also like to thank my supervisor Dr Vasudevan for his guidance and support.

Many of the truncation constructs and mutants used in this work were produced by other workers from Dr Vasudevans laboratory. To them I offer my thanks. A special thanks also to Dr Arcondeguy for her generous gift of the swapped T-loop PII mutant plasmids.

The last person I wish to thank is Dr Yibin Xu who produced all the 3D protein diagrams presented in this thesis. Unfailingly altering diagrams for me until they were just right. Never once complaining.

CHAPTER 1 Introduction

1.1 The nitrogen signalling pathway in *Escherichia coli*

Nitrogen assimilation is one of the cornerstones of macromolecular biosynthesis in the microbial world. The level of intracellular nitrogen (N) appears to be the important factor in determining the expression of several of the enzymes of N metabolism (Merrick and Edwards, 1995). Ammonia, which is the preferred source of N, but not the only source is assimilated within the bacterial cell into glutamine (gln) or glutamate (glu). These two amino acids then serve as N donors for biosynthetic reactions and the formation of many organic molecules, such as proteins, RNA and DNA (Merrick and Edwards, 1995).

Enteric bacteria possess two pathways for incorporating ammonia (NH_3) into biological compounds: the glutamate dehydrogenase (GDH) pathway (Pathway 1) and the glutamine synthetase/glutamine amide-2-oxoglutarate amino transferase (GS/GOGAT) pathway (Pathway 2).

$$\textbf{Pathway 1:} \quad \alpha\text{-kg} + NH_3 + NADPH \xrightarrow{\text{GDH}} glu + NADP^+ \qquad (1)$$

$$\textbf{Pathway 2:} \quad gln + \alpha\text{-kg} + NADPH \xrightarrow{\text{GOGAT}} 2\ glu + NADP^+ \qquad (2)$$

$$glu + NH_3 + ATP \xrightarrow{\text{GS}} gln + ADP + P_i \qquad (3)$$

Both these pathways result in the incorporation of NH_3 into glu. Glutamate dehydrogenase has a K_m for NH_3 of 1.1-3mM and GS has a K_m for NH_3 of 0.2mM (Miller and Stadtman, 1972). Therefore, GS is the predominant controller of N assimilation during limiting N conditions. The GS pathway predominates when environmental N conditions are poor but is more expensive in terms of energy (utilising an ATP molecule during gln synthesis); consequently the transcription and enzymatic activity of GS are tightly regulated.

The GS enzyme is regulated at several levels. Firstly, there is direct feedback inhibition from various components of the biosynthetic processes e.g. CTP, AMP, histidine, alanine and glycine, where the N donated from gln is critical. For more sophisticated control, there are also proteins in the bacterial cell for sensing the level of N (uridylyltransferase-uridylyl removing enzyme; UTase) and regulating the transcription (NRI and NRII) and enzymatic activity (adenylyltransferase; ATase) of GS.

The PII protein acts as the signalling molecule in response to intracellular N levels, linking all these enzymes and their respective activities into a concerted controlling force on the activities of GS (Magasanik, 1993). PII is capable of binding to at least three different bifunctional receptor-proteins (ATase, UTase and NRII) and consequently influencing their activities. If PII is in its uridylylated form it can further influence the actions of two of these receptor-proteins (ATase and UTase). The GlnK protein is also capable of most of these interactions (Jaggi, 1998) (see scheme in Figure 1.1). How GlnK fits into the pathway is not yet fully understood, particularly when it was demonstrated that these two signalling proteins could form heterotrimers *in vivo* in *E. coli* in conditions of N limitation (Forchhammer *et al.*, 1999; van Heeswijk *et al.*, 2000). However, a clear association with the AmtB protein has been demonstrated in *E. coli* (Coutts *et al.*, 2002; Blauwkamp and Ninfa, 2003) (see later).

It has been suggested that PII may act as a carbon (C) sensor, due to the binding of α-ketoglutarate (α-kg) (Ninfa *et al.*, 1995). PII has a vastly diminished capacity to bind ADP (Kamberov *et al.*, 1995b), at the highly conserved ATP-binding cleft formed in all PII-like molecules (Xu *et al.*, 1998). The poorer binding capacity of ADP suggests PII may also act as a free energy sensor. Ninfa and Atkinson (2000) likened the PII molecule to the central processing unit of a computer suggesting it was the N signal transduction CPU controlling N assimilation by integrating the antagonistic signals of N and C status within the bacterial cell.

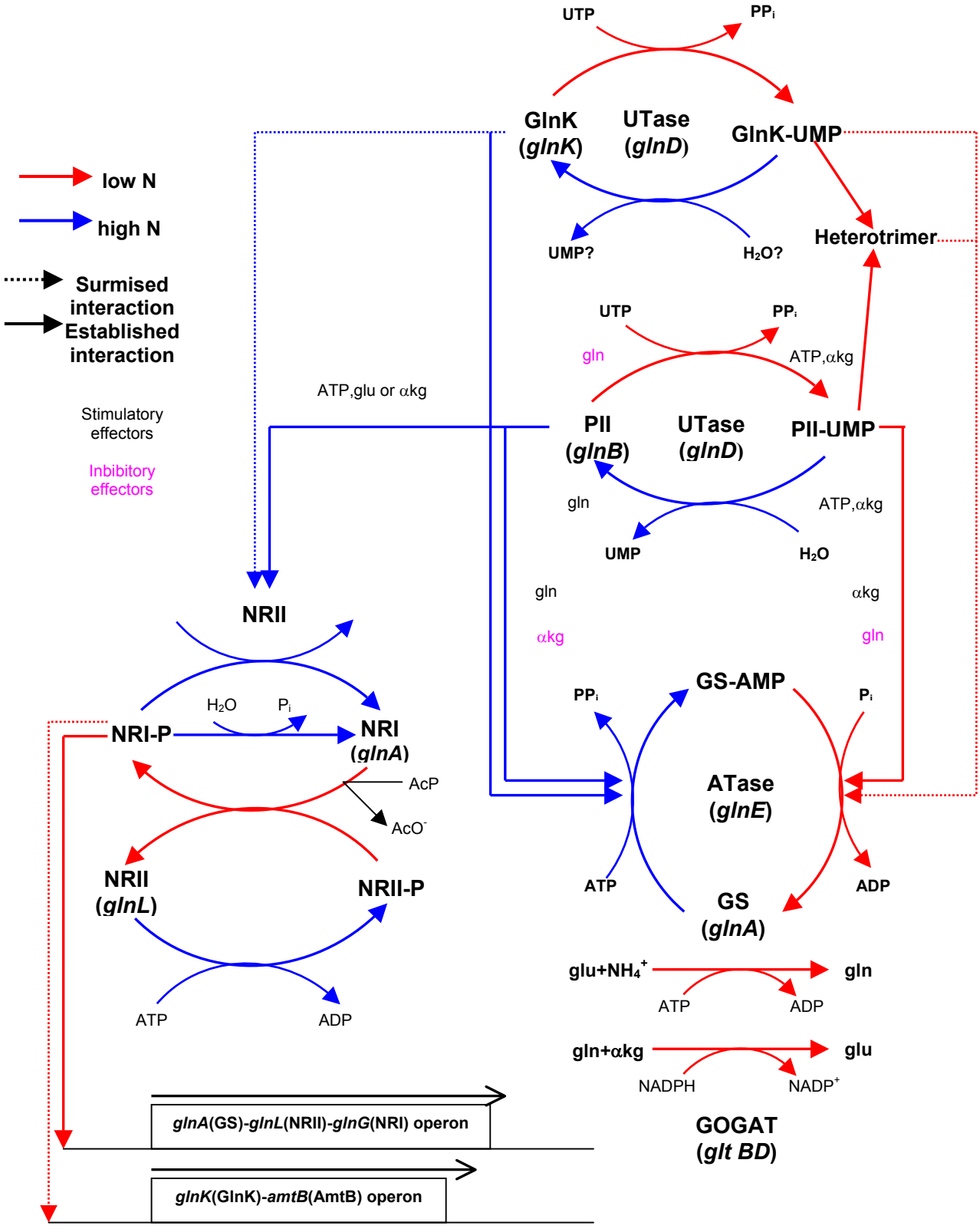

Figure 1.1 ***Diagrammatic presentation of the nitrogen-signalling pathway in E. coli.*** Derived from van Heeswijk (1998). Cellular N level sensed by UTase. In high N conditions UTase deuridylylates the signalling molecules PII-UMP/GlnK-UMP. PII then stimulates ATase to adenylylate GS (inactivation). PII also interacts with NRII stimulating it to phosphorylate NRI. NRI-P activates expression of *glnA* (GS). In low N conditions PII is uridylylated by UTase. PII-UMP then stimulates ATase to deadenylylate GS-AMP (activation)

1.1.1 The nitrogen signalling pathway's response to high levels of nitrogen

When the level of intracellular N increases, the uridylyl removing activity of the sensor molecule UTase predominates, causing it to deuridylylate covalently modified PII-UMP. PII then promotes the inactivation of GS by interacting with ATase stimulating its adenylylation activity. ATase progressively adenylylates each of the twelve subunits of GS by covalent addition of an AMP group to Tyr397 in each monomer, gradually rendering GS inactive (Adler *et al.*, 1975).

UTase and PII also regulate transcription of the *glnA* gene, which encodes for the production of GS, consequently affecting GS expression levels. Transcription of the *glnA* gene is modulated through the interaction of PII with the two component regulation system of the histidine protein kinase NRII and the response regulator NRI (Merrick and Edwards, 1995).

The activities of NRII are affected by the binding of PII. If N levels are high then unmodified PII is the predominant form of the signalling protein. PII binds to NRII causing it to dephosphorylate NRI-P rendering it incapable of activating transcription of the *glnA* gene (Merrick and Edwards, 1995).

1.1.2 The nitrogen signalling pathway's response to low levels of nitrogen

In N limiting conditions PII is progressively uridylylated by the sensor protein UTase at residue Tyr51 of each monomer (Son and Rhee, 1987, Jaggi *et al.*, 1996). The resulting PII-UMP interacts with ATase promoting this enzyme's ability to reactivate adenylylated GS by progressively deadenylylating each of its adenylylated monomers (Adler *et al.*, 1975).

When N levels are low the predominant form of PII is PII-UMP, and NRII is free to catalyse the phosphorylation of NRI. NRI in its phosphorylated form, NRI-P activates transcription of the *glnA* gene (and other genes), thereby raising the amount of GS produced in the cell.

NRI can also be phosphorylated by acetyl phosphate, which in turn is regulated by the activities of NRII and GS (Feng *et al.*, 1992). This reaction may facilitate the shift down from N rich to N poor, priming the system in N limiting conditions when the intracellular concentrations of both NRI and NRII would be low. Either route is capable of producing the phosphorylated form of the NRI protein, NRI-P, which enhances the transcription of the *glnA* gene using the σ^{54} factor bound RNA polymerase, however under certain N starvation conditions both routes are needed (Feng *et al.*, 1992).

1.1.3 The role of small effector-molecules in the nitrogen signalling pathway

Early experiments by Senior (1975) demonstrated a correlation between the regulation of the GS adenylylation state and the concentrations of the key stimuli gln and α-kg. The intracellular gln concentration signals N status, and the intracellular α-kg concentration signals C status.

The particular activity of UTase that is stimulated at any given time in the cell is dependent on the ratio of the intracellular concentrations of α-kg and gln (Merrick and Edwards, 1995). The uridylylating activity of the enzyme is stimulated by presentation of PII bound to α-kg and ATP. Both these small effector-molecules bind to PII in a co-operative manner, i.e for either small effector-molecule to bind to PII the other must be present (Kamberov *et al.*, 1995b). Measurements for the *in vivo* concentration range for α-kg (*E. coli*) have been determined as 0.1-0.9mM (Senior, 1975).

The deuridylylating function of UTase is stimulated when there is an excess of N, which is signalled by an increase in the intracellular gln concentration. The *in vivo* concentration range of gln in *Salmonella typhimurium* was determined as ~0.3 to ~2-3mM by Ikeda *et al.* (1996). A high intracellular concentration of gln causes UTase to preferentially deuridylylate PII-UMP (Kamberov *et al.*, 1995a). In a similar manner the capacity of α-kg to inhibit the adenylylation of GS by ATase is dependent on the intracellular concentration of gln, which is necessary for the adenylylation activity of ATase (van Heeswijk, 1998). This ratio can reflect the uridylylation state of PII (the

lower the value for the ratio the more PII-UMP present) and the adenylylation state of GS (Engelman and Francis, 1978; van Heeswijk, 1998).

1.1.4 The role of the PII paralogue GlnK in the nitrogen signalling pathway

In terms of the cascade depicted in Figure 1.1 GlnK is interchangeable with PII, however the two proteins appear to have different functions. Within the cell PII is constituitively expressed, merely alternating its uridylylation state. Whereas the expression of GlnK is N regulated. Under conditions of low N, GlnK is expressed at high levels. Therefore GlnK may be the major contributor (rather than PII) to the deadenylylation activity of ATase in *E. coli* (van Heeswijk *et al.*, 1996). However, their relative *in vitro* activities suggest that PII is the major deadenylylation driving force rather than GlnK (van Heeswijk *et al.*, 1996; Atkinson and Ninfa, 1999).

1.1.4.1 Proposed roles for GlnK

Some of the proposed roles for GlnK in *E. coli* are as follows:

1. Slow down the transcriptional response when N starved cells encounter NH_3 in order to help buffer the signal transduction system against transitory changes in N levels. Thus, the concentrations of the "memory proteins" NRI, NRII and GlnK only drop after prolonged exposure to NH_3 (van Heeswijk *et al.*, 1996; van Heeswijk *et al*., 2000).
2. To uncouple the regulation of NRII and ATase under N limiting conditions (Atkinson and Ninfa, 1998).
3. Act as a governor preventing sustained full expression of certain N regulating genes under all conditions (Atkinson and Ninfa, 1998).
4. Allow fine control of intracellular concentrations of NRI-P at levels in the upper end of the physiological range (Atkinson and Ninfa, 1998).

1.1.4.2 Demonstrated functions of GlnK

Each N-regulating promoter is activated at a different intracellular concentration of NRI-P. Transcription of the *glnA* gene is activated by a very low intracellular NRI-P

concentration, whereas those that give rise to the use of arginine or histidine require a higher intracellular concentration of NRI-P. GlnK appears to regulate certain N regulating promoters (including its own) through *glnL*, but doesn't appear to regulate the *glnA* promoter (Atkinson and Ninfa, 1998). GlnK does not appear to be as effective as PII at reducing the level of the phosphorylated form of the NRI protein NRI-P through NRII. This means GlnK has little effect on the *glnA* promoter, but plays a major role in regulating the other N regulating promoters that require a higher intracellular concentration of NRI-P (Atkinson and Ninfa, 1998).

Until the full complement of target proteins have been identified for PII and GlnK it is difficult to determine the exact physiological role of the GlnK form of the N signalling proteins in the *E. coli* bacterium (Arcondeguy *et al.*, 2001). Coutts *et al.*, (2002) confirmed the long surmised existence of an interaction between GlnK and the AmtB protein. They demonstrated that the sequestration of GlnK (and to a lesser extent PII) to the membrane was due to the AmtB protein and that binding to the membrane is influenced by the signalling proteins uridylylation state.

Blauwkamp and Ninfa (2003) also recently demonstrated a connection between the AmtB protein and the two signalling proteins in *E. coli*. The AmtB protein antagonises signalling by PII through NRII, such that the PII mediated response in the shift from N starvation to N becoming available is diminished. When GlnK is present it prevents the AmtB mediated antagonism of PII signalling after N starvation. The AmtB protein also slowed the deuridylylation of PII-UMP upon addition of NH_3.

He *et al.*, (1998) have demonstrated a specific physiological role for GlnK in the free-living diazotroph *Klebsiella pneumoniae* that the *glnB* derived PII cannot fulfill. *K. pneumoniae* has both a *glnB* and *glnK* form of the N signalling protein like the enteric *E. coli*. The NifA protein activates transcription of various N fixation gene products in the proteobacteria, and is regulated in response to cellular oxygen and/or N status. In this bacterium the NifL protein represses the transcriptional activity of the NifA protein. Initially He *et al.*, (1997) demonstrated that NRI was necessary for relief of NifL transcriptional inhibition. NRI is necessary for the transcription of GlnK, which in turn

inhibits the repressive actions of the NifL protein. Surprisingly uridylylation of GlnK does not affect the inhibitory action of GlnK on the NifL protein (He ***et*** *al.*, 1998). Two residues in the T-loop of GlnK, Asp54 and to a lesser extent Thr43, distinguished it from PII with regards to the interaction with the NifL protein (Arcondeguy ***et*** *al.*, 2000).

1.2 Structure and function of proteins in the nitrogen signalling pathway

The functions of the various proteins involved in regulating GS in E. *coli* are summarised in Table 1.1.

THIS TABLE HAS BEEN REMOVED DUE TO COPYRIGHT RESTRICTIONS

Table 1.1 ***Functions of the GS regulatory proteins.*** Summary of the various functions of the known GS regulatory proteins in E. ***coli.*** (adapted from van Heeswijk (1998)).

Three dimensional structures are now known for several of the GS regulatory proteins. Nuclear magnetic resonance (NMR) spectroscopy was used to determine the 3D structure of the N-terminal domain of NRI (Volkman ***et*** *al.*, 1995). A more recently determined structure for this domain using NMR observed the conformational changes

that occur within the domain upon formation of a complex with a central domain peptide (residues 139-160) (Hastings *et al.*, 2003). Multidimensional heteronuclear NMR was used to determine the 3D solution structure for the C-terminal domain of NRI (DNA binding domain with 3 Ala substitutions) (Pelton *et al.*, 1999). The 3D structures of GS from *Salmonella typhimurium* (Yamashita *et al.*, 1989) and *Mycobacterium tuberculosis* (Gill *et al.*, 2002), PII (Carr *et al.*, 1996) and GlnK (Xu *et al.*, 1998) from *E. coli* have all been determined using X-ray crystallography. More recently the 3D structure of the deadenylylation domain for ATase has also been resolved using X-ray crystallography (Xu *et al.*, 2004). The relationships between structure and function for the GS regulatory proteins have been discussed in this section.

1.2.1 Glutamine synthetase (GS)

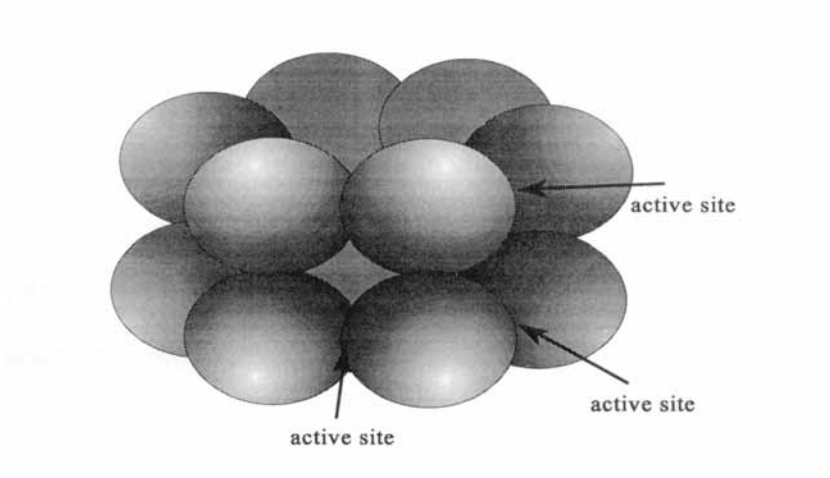

Figure 1.2 ***Structure of Glutamine synthetase.*** Schematic diagram of the GS protein from *Salmonella typhimurium* (GS_{ST}) derived from the 3D X-ray crystal structure (Yamashita *et al*., 1989).

The GS protein has 12 identical monomers of 55 kDa each. The monomers are arranged in 2 hexagonal rings superimposed on each other and held together by hydrophobic interactions and hydrogen bonding (Figure 1.2) (Yamashita *et al.*, 1989).

There is an active site at the interface of pairs of monomers within each ring. The active site is cylindrical formed by six antiparallel β strands from one monomer and two from

the adjacent monomer. Within this active site are the binding sites for gln, ATP (Tyr397 which is located at the outer diameter of the hexagonal ring structure), NH_4^+, and 2 bivalent cations (Liaw *et al.*, 1995).

Recently the 3D structure of the GS I protein from *M. tuberculosis* (GS_{MT}) the infectious agent in the disease tuberculosis has been resolved by X-ray crystallography (Gill *et al.*, 2002). In this organism GS is probably involved in production of a unique constituent (poly L-gln+L-glu chains) in the pathogenic bacterial cell wall (Harth et al., 1994). The two resolved GS proteins have sequences that are 52% identical and all 19 catalytic site residues are conserved as is the lengths of their active site loops (Eisenberg *et al.*, 2000). Their structures, mode of regulation and accompanying regulatory enzymes are also very similar and conserved (Gill *et al.*, 2002). GS from *M. tuberculosis* is also similar enough to GS from *E. coli* to be able to supplement its activity in a GS deficient *E. coli* strain (Gill *et al.*, 2002).

Gill *et al.*, (2002) proposed that several flexibility and conformational differences in protein segments around the active sites were due to the GS_{ST} being in the taut state conformation and GS_{MT} being in the relaxed state conformation as suggested by Hunt and Ginsburg (1972). The major difference between the two models is the position of the residue Glu212, which is in the first metal binding active site of GS_{ST} but it lies outside the GS_{MT} active site. This means that the metal binding pockets in the GS_{MT} "relaxed" molecule, are empty.

1.2.2 Uridylyl transferase/ removing enzyme (UTase)

The UTase protein is a 95 kD protein with 890 amino acid residues (Garcia and Rhee, 1983). UTase is a bifunctional enzyme that uridylylates and deuridylylates PII and GlnK depending on the N level in the bacterial cell. UTase is known to bind gln (probably only at one site), which probably inhibits the transferase activity by binding to the central complex inhibiting the rate of the catalytic step (Kamberov *et al.*, 1995a; Jiang *et al.*, 1998a).

Whether or not both of the enzymes activities reside in separate domains, or are part of the same active site within a single domain is yet to be determined (Jaggi, 1998). Based on detailed sequence comparisons of conserved features of nucleotidyl transferases such as UTase and ATase, Holm and Sander (1995) suggested that there is only one catalytic site in UTase spanning residues 55-116 (Figure 1.3b). Their study was based on a signature sequence determined from rat DNA polymerase β. A more recent analysis of the nucleotidyl transferase superfamily by Aravind and Koonin (1999) concurs with this assessment and predicts that UTase has a single catalytic site and an amino acid binding domain.

The original sequence alignment of Holm and Sander (1995) has been revised by Xu et al., (2004) using an overlay of the 3D structures of several polymerase motifs (Figure 1.3a). This region of the protein contains the two highly conserved Asp residues (Figure 1.3b), which have been shown to be critically important in the catalytic activity of the rat DNA polymerase β protein. These two residues coordinate the correct positioning of the divalent metal ion involved in catalysis (Pelletier *et al.*, 1994; Sawaya *et al.*, 1994). Both of the catalytic activities of UTase are stimulated by the divalent metal ion Mn^{2+} or Mg^{2+}, depending on the other small effector-molecules present. Kinetic data using the two metal ions and activity assays using UTase proteins with point mutations in the β polymerase motif suggest that there is only the one catalytic site in UTase (Jiang *et al.*, 1998a).

1.2.3 Adenylyl transferase (ATase)

ATase is a bifunctional enzyme of 946 amino acid residues responsible for regulating the enzymatic activity of *E. coli* GS, by the reversible adenylylation of each of its twelve monomers. Sequence alignment with rat DNA polymerase β demonstrated the presence of two nucleotidyl transferase signature motifs within ATase: the first site spanning residues 117-184 (deadenylylation) and the second site spanning residues 644-712 (adenylylation) (Holm and Sander, 1995) (Figure 1.3b). The two antagonistic activities of ATase reside in separate terminal domains (AT-N_{423}: residues 1-423 and

AT-C_{521}: residues 425-946) (Figure 1.5) at either end of the protein (Jaggi *et al.*, 1997). Each terminal domain encompasses one of the signature polymerase motifs.

(a)

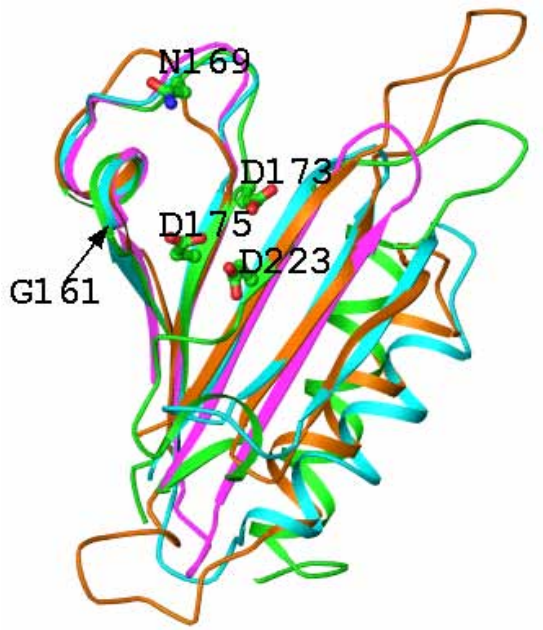

(b)

```
174   IATVCGSFRRGAE-SSGDMDVLLTHPNFT   DNA Polymerase β (human)
33    AIGVYGSLGRQTDGPYSDIEMMCVMSTEE   Kanamycin NT (S. aureus)
83    KIFTYGSYRLGVHGPGSDIDTLVVVPKHV   Poly(A) polymerase (yeast)
156   LILGMGKLGGGELNFSSDIDLIFAWPEHG   ATase (deadenylylation) (E. coli)
684   AVVGYGKLGGWELGYSSDLDLIFLHDCPM   ATase (adenylylation) (E. coli)
88    ALVAVGGYGRGELHPLSDVDLLILSRKKL   UTase (E. coli)
```

Figure 1.3 ***Sequence alignment of various nucleotidyl transferases using polymerase motif.*** (a) Overlay of polymerase motifs from known 3D structures of nucleotidyl transferases (NT). Deadenylylation domain of ATase (AT-N_{440}) (green) (Xu *et al.*, 2004), human polymerase β (orange) (Sawaya *et al.*, 1997), kanamycin NT (magenta) (Pedersen *et al.*, 1995) and yeast poly A polymerase (cyan) (Bard *et al.*, 2000; Martin *et al.*, 2000). (b) Sequence alignment derived from structural overlay (Xu *et al.*, 2004). This sequence alignment differs slightly from the original alignment of Holm and Sander (1995). The UTase protein from *E. coli* has one β polymerase motif and the ATase protein from the same organism has two β polymerase motifs. Highly conserved residues such as the double Asp in the catalytic site of rat DNA polymerase β have been highlighted in red and other residues also mutated in the two ATase active sites are highlighted in black (McLoughlin, 1999).

Further examination of the sequence of ATase by my supervisor, Dr. Vasudevan, demonstrated the presence of two Q-linkers. A Q-linker is described as a region of mainly hydrophilic residues (gln, glu, arg, ser and pro), which acts as a tether between two domains and is commonly found in bacterial transcription factors (Wooton and

Drummond, 1989). The first Q-linker, Q1, spans residues 441-462 and the second Q-linker, Q2, spans residues 606-627. Using a helical wheel projection (Schiffer and Edmundson, 1967) Q1 is predicted to contain an amphipathic α-helix, where one face is predominantly hydrophobic whilst the other is predominantly hydrophilic containing all the charged residues and gln residues (Jaggi, 1998) (Figure 1.4). The discovery of these two Q-linkers within the primary sequence of the protein suggested that there might be three domains within the ATase protein.

(a)

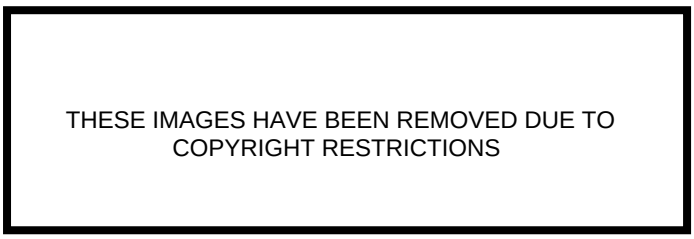

(b)

Figure 1.4 ***Analysis of the α-helix in the ATase Q1 linker.*** (a) Top view representation of the helical region of Q1 from residues 448-461. The respective amino acids and their relative positions in the helix are indicated on the helical wheel. The hydrophobic residues are highlighted in red, whilst the hydrophilic residues are black. The hydrophobicity of the residues was assigned according to Engelman *et al.*, (1986). (b) Schematic representation of AT-C_{521}, which includes the Q1 linker. The hydrophobic side of the α-helix in Q1 is associated with a proposed hydrophobic patch in the N-terminal region of the construct i.e. the putative R domain (diagram courtesy of Jaggi, 1998).

Jaggi (1998), Wen (2000), and O Donnell (2000) produced a panel of N- and C-terminal truncation constructs of ATase based on the domain boundary predictions as well as the location of the two Q-linkers (Figure 1.5) in order to investigate the structure and function of the enzyme. Jaggi (1998) proposed a structural model for ATase (Figure 1.6) based on solubility and activity studies of the ATase truncation constructs (Figure 1.5). The ATase protein probably comprises three domains; the first of which, is the N-terminal domain (residues 1-440) which binds PII and PII-UMP/α-kg and is responsible for the deadenylylation of the inactive GS-AMP protein. The second domain is the central domain (residues 463-604) which probably binds gln, and the third domain is the C-terminal domain (residues 627-946) which is responsible for adenylylation of the active GS protein. There are also two "Q" linker regions: Q1 (residues 441-462) and Q2 (residues 606-627) (Jaggi, 1998).

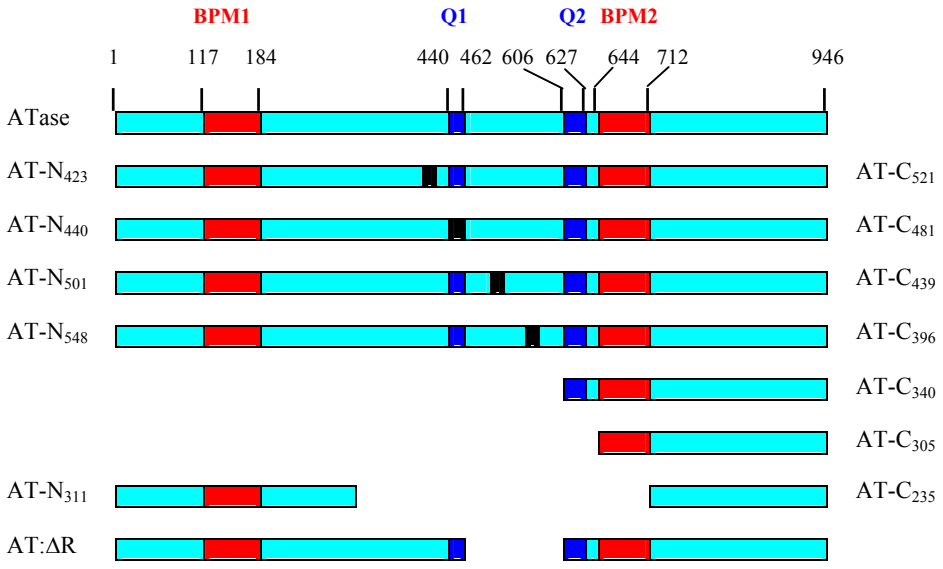

Figure 1.5 ***Schematic representation of the truncation constructs of ATase.*** N- and C-terminal truncation constructs of ATase produced by Jaggi (1998), Wen (2000), and O Donnell (2000). Truncations of the ATase protein (946 residues long) were designated AT-N or AT-C depending on their location in the linear polypeptide chain and the number of amino acid residues contained in each truncation construct is indicated by a subscripted figure (eg. AT-N_{440} refers to the N-terminal 440 residues of ATase). Also indicated on the diagram are the positions of the two predicted β-polymerase motifs (BPM1 & BPM2) (Holm and Sander, 1995) and the two Q-linkers (Q1 & Q2) (Wooton and Drummond, 1989). The black segments represent the boundaries between the adjoining constructs.

McLoughlin (1999) mutated the highly conserved aspartate residues within the two β-polymerase motifs in ATase (Asp173 and Asp175: deadenylylation, Asp700 and Asp702: adenylylation) (Figure 1.3b), to Ala, Glu or Asn individually, or in pairs. These mutations resulted in the complete inactivation of the respective active sites even for such subtle changes as Asp to Glu suggesting that active site conformation is very important for both the activities in ATase (McLoughlin, 1999). Mechanistically the two Asp residues within the polymerase motif are known to be critical for all polymerases and the introduction of mutations to these residues in rat DNA polymerase β also completely inactivated that enzyme (Pelletier *et al.*, 1994). This is the first demonstration that the active site conformation of a prokaryotic nucleotidyl transferase from the nucleotidyl transferase superfamily (determined by sequence similarity) is similar to that of a eukaryotic enzyme in the same superfamily.

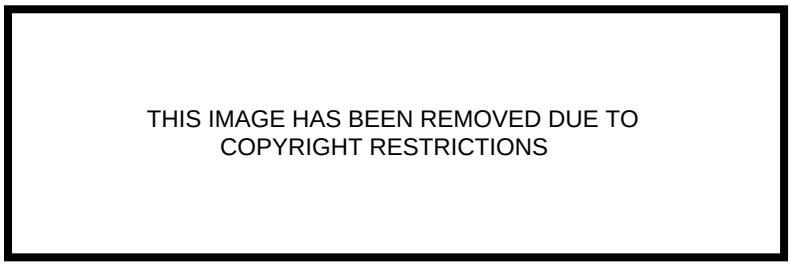

Figure 1.6 ***Structural model proposed for ATase.*** Jaggi (1998) proposed a structural model for ATase based on solubility and activity studies of the ATase truncation constructs (Figure 1.5). The ATase protein probably comprises three domains; the first of which, is the N-terminal domain (residues 1-440) which binds PII and PII-UMP/α-kg and is responsible for the deadenylylation of the inactive GS-AMP protein. The second domain is the central domain (residues 463-604) which probably binds gln, and the third domain is the C-terminal domain (residues 627-946) which is responsible for adenylylation of the active GS protein. There are also two "Q" linker regions: Q1 (residues 441-462) and Q2 (residues 606-627) (Jaggi, 1998).

More recently, the 3D structure of the AT-N_{440} construct (Figure 1.5) has been solved by X-ray crystallography, and the two highly conserved Asp173 and Asp175 residues within the deadenylylation active site are probably very important in positioning the Mg^{2+} ion required for deadenylylation activity (Figure 1.7) (Xu *et al.*, 2004). These two residues are important in positioning the Mg^{2+} ion in rat DNA polymerase-β (Davies *et al.*, 1994; Pelletier *et al.*, 1994) the protein from which the putative active site was determined (Holm and Sander, 1995) (Figure 1.3b).

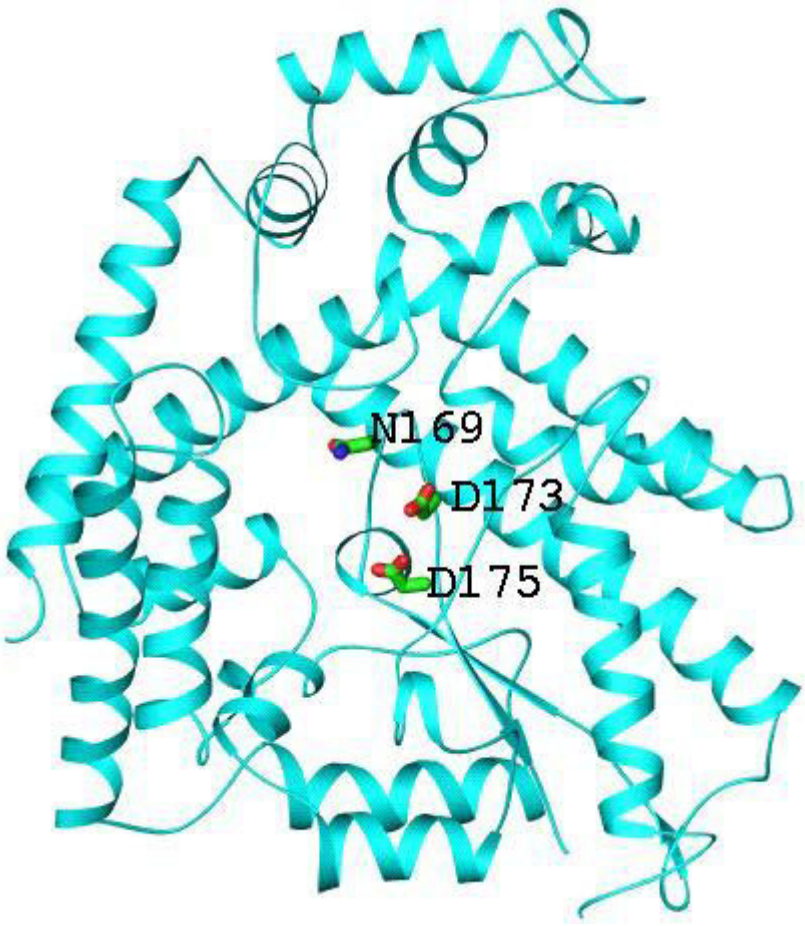

Figure 1.7 ***Structure of N domain of ATase.*** The 3D structure of the AT-N_{440} construct (Figure 1.5) has now been solved with X-ray crystallography (Xu *et al.*, 2004). The two highly conserved Asp173 and Asp175 residues within the deadenylylation active site (Holm and Sander, 1995), which are important for positioning the Mg^{2+} ion required for deadenylylation activity, and the Asn169 residue, which probably helps position the phosphate involved in the deadenylylation reaction correctly have been highlighted.

The other important residue (from the McLoughlin (1999) suite of mutations) highlighted from solving the 3D structure of the AT-N_{440} construct is the Asn169

residue, which probably helps position the phosphate involved in the deadenylylation reaction. The AT:N169G mutant protein also had drastically reduced activity in the deadenylylation assay (McLoughlin, 1999).

Unlike *E. coli* the *glnE* gene product in *M. tuberculosis* was demonstrated to be essential for the latter using gene crossover experiments. In *E. coli* it is the *glnA* gene encoding GS that is essential (Parish and Stoker, 2000). These workers suggested that it was possible that removal of the *glnE* gene in *M. tuberculosis* may lead to the GS I protein being overactive. Since the GS I protein is expressed to a high level in *M. tuberculosis* it is possible that the increase in activity could lead to depletion of the cellular L-glutamate pool, which is very important for cellular metabolism.

1.2.4 Nitrogen regulating protein I (NRI or NtrC)

NRI is a dimeric protein formed from two 55 kD subunits of 486 amino acid residues each. It is divided into three domains (Merrick and Edwards, 1995). The N-terminal domain (~12kD) is characteristic of response regulators and constitutes the receiver domain for the interaction with the sensor domain of NRII (Merrick and Edwards, 1995). Successful interaction with NRII results in the transfer of a phosphate group to the highly conserved Asp54 residue of NRI (Keener and Kustu, 1988). Substitutions at the Asp54 residue significantly impair the response of the bacteria to conditions of N deprivation (Moore *et al.*, 1993). The 3D structure of the N-terminal domain has been described using NMR spectroscopy (Figure 1.8) (Volkman *et al.*, 1995; Hastings *et al.*, 2003). This domain is tethered to the central domain by a Q-linker (Wooton and Drummond, 1989).

The central domain of NRI is 240 amino acids long and characteristic of σ^{54} dependent activator proteins (Kustu *et al.*, 1989). This domain contains a conserved nucleoside-binding site, which interacts with ATP (Wiess *et al.*, 1991). It is also considered to be the domain, which interacts with σ^{N}-containing RNA polymerase ($E\sigma^{N}$) to activate transcription (Merrick and Edwards, 1995). The ATPase activity of NRI is essential for open complex formation with $E\sigma^{N}$ and is stimulated by DNA binding and by phosphorylation at the conserved Asp54 residue (Austin and Dixon, 1992).

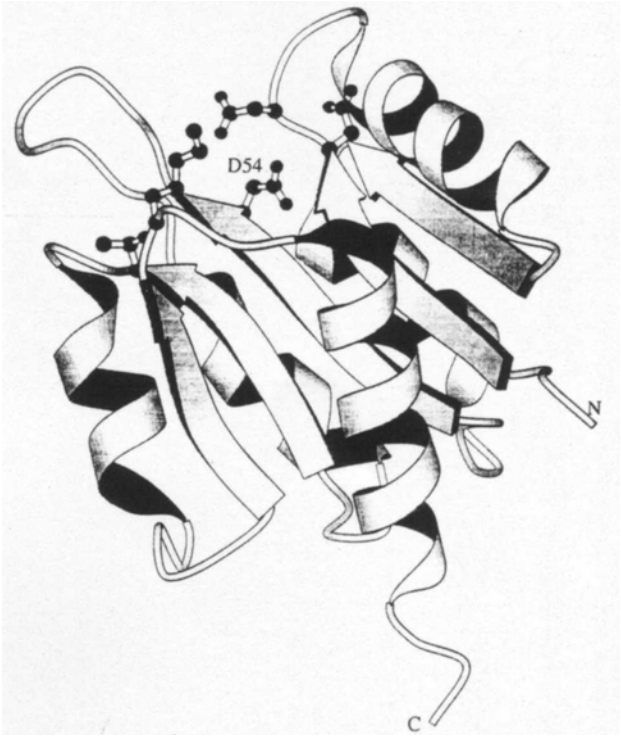

Figure 1.8 ***Structure of N-terminal domain of NRI.*** Structure of the N-terminal domain of the NRI protein, which contains the highly conserved Asp54 residue (site of reversible phosphorylation). This structure was determined using NMR spectroscopy (Volkman *et al.*, 1995).

The C-terminal domain of NRI is comprised of 90 amino acids and mediates DNA binding to the dimer. This domain contains a helix turn helix motif, which allows recognition of upstream enhancer regions (Contreras and Drummond, 1988). These enhancer regions facilitate oligomerisation of NRI to form a complex containing at least two dimers. The complex is required for transcriptional activation and to tether the phosphorylated form of the NRI protein, NRI-P at high local concentrations near the promoter and thereby increase its frequency of contact with $E\sigma^N$ (Su *et al.*, 1990).

Pelton and coworkers (1999) resolved the 3D solution structure for the C-terminal domain of NRI from *Salmonella typhimurium* using a DNA binding mutant with Ala residues replacing Arg456, Asn457 and Arg461. Although this mutation impaired DNA binding in the full length protein other functions of the protein were retained.

In NRI the ability of the N-terminal domain to dimerise is masked by an interaction with the central domain. Phosphorylation at residue Asp54 relieves the inhibition from this interaction allowing dimerisation and hence activating transcription (Fiedler and Wiess, 1995).

1.2.5 Nitrogen regulating protein II (NRII or NtrB)

NRII is a histidine protein kinase comprised of a N-terminal phosphatase sensor domain (110 amino acid residues) and a C-terminal kinase domain. It is ~36 kD and usually forms dimers (Ninfa *et al.*, 1986).

The kinase domain includes three highly conserved motifs, an amino terminal motif including the autophosphorylation site His139, a motif with a conserved Asn residue of unknown function, and a carboxy terminal motif containing a potential nucleoside triphosphate binding site (Stock *et al.*, 1989).

The autophosphorylation of NRII at residue His139 is ATP dependent (Ninfa *et al.*, 1991). The ATP binds in the C-terminal motif (59 amino acid residues) then phosphorylates residue His139 (Ninfa *et al.*, 1995). The phosphate is then transferred to the Asp54 residue of NRI when the kinase activity of NRII is stimulated i.e. when all the PII molecules in the cell are uridylylated.

Initially, indirect evidence suggested PII bound in the N-terminal phosphatase domain regulating the ability of NRII to catalyse the dephosphorylation of the phosphorylated form of the NRI protein, NRI-P (Kamberov *et al.*, 1994). Subsequent studies by Jiang *et al.*, (2000) confirmed NRII comprised three domains: a N-terminal domain (signal transduction), a central domain (phosphotransferase, phosphatase and dimerisation) and a C-terminal domain (kinase). PII was demonstrated to bind to the C-terminal kinase domain resulting in a conformational change, which impacted on the other two domains, causing the central domain to be active in its phosphatase conformation.

1.2.6 The signalling proteins PII and GlnK

Many PII and PII-like proteins have been found across 11 bacterial families, and several lower and higher-plant families. In some instances a single organism can have several PII-like proteins (van Heeswijk *et al.*, 1995) and these PII-like proteins can potentially form heterotrimers (Forchhammer *et al.*, 1999; van Heeswijk *et al.*, 2000). All of the PII-like signalling proteins currently characterised are involved in N signalling. They have been grouped in terms of the 3rd and 5th residue of the monomer into GlnB-like or GlnK-like. The GlnB-like proteins have a Lys at residue 3 and a Glu or Asp at residue 5 (forming a salt bridge), whereas the GlnK-like proteins have a hydrophobic residue, either Leu, Ile, Met or Phe at position 3, and Ile, Thr or Met at position 5. The other feature that classifies the proteins as GlnK-like is the existence of a relationship between the *glnK*-like gene and the *amtB* gene (Arcondeguy *et al.*, 2001).

A sequence alignment of the 50 PII-like and GlnK-like proteins in the Genbank database, demonstrates some highly conserved features of the protein. The functional T-loop from residues 37-55, including the Tyr51 residue is fairly highly conserved in a substantial number of the proteins. The most highly conserved region of the proteins is surprisingly the ATP-binding cleft, rather than residues that maintain structural integrity (Xu *et al.*, 1998).

There are now 5 3D structures for PII and GlnK-like proteins resolved by X-ray crystallography. PII (Carr *et al.*, 1996) and GlnK (Xu *et al.*, 1998) from *E. coli* (Figure 1.9) (Table 1.2), PII from *Herbaspirillum seropedicae* (Benelli *et al.*, 2002), PII from *Synechococcus sp* (Xu *et al.*, 2003), and PII from *Synechocystis sp* (Xu *et al.*, 2003). *E. coli* and *H. seropedicae* are both proteobacteria, *Synechococcus sp* and *Synechocystis sp* are cyanobacteria. All of these proteins are trimeric comprised of three equal ~12 kD monomers. They also have surface exposed T-loops and ATP-binding clefts which, are the primary interaction sites of all PII and GlnK-like proteins.

PII	GlnK
Trimeric protein (Vasudevan *et al.*, 1994).	Trimeric protein (Xu *et al.*, 1998).
Each monomer 112 amino acids and ~12.4kD (Merrick and Edwards, 1995).	Each monomer 112 amino acids and ~12.2kD (van Heeswijk, 1998).
67% homology in primary sequence (van Heeswijk *et al.*, 1995).	
20 residue loop (T-loop) containing the conserved Tyr51 residue the site of uridylylation (Son *et al.*, 1987; Jaggi *et al.*, 1996).	20 residue loop (T-loop) containing the conserved Tyr51 residue the site of uridylylation (van Heeswijk *et al.*, 1995).
The trimer has a compact barrel shape (~5nm in diameter and ~3nm in height), consisting of three tightly interlocking β sheets surrounded by α helices. These two structures contain most of the residues of the protein (Carr *et al.*, 1996).	The trimer has a barrel-like core consisting of a four-stranded β sheet, which packs against two α helices. The core structure is similar to PII, but the monomers differ at the C-terminus and the loops (Xu *et al.*, 1998).
T-loops jut out from the barrel-like core of the protein positioning Tyr51 ~13Á above one of the flat surfaces of the protein (Carr *et al.*, 1996).	The T-loops protrude from the top of the molecule positioning Tyr51 ~8Á above the barrel (Xu *et al.*, 1998).
A cleft is formed on the surface of the protein at the juncture of the β sheets between the B, C and T-loops of neighbouring monomers. One side of the cleft is covered with uncharged residues, while the other side of the cleft is lined with basic residues Arg38, Lys40, Lys85 and Lys90 from one monomer and Arg101 and Arg103 from the adjacent monomer (Carr *et al.*, 1996). This cleft is not as open as that of GlnK (Xu *et al.*, 2001).	A difference can be seen in the cleft of GlnK, which has an anion-binding site within the highly conserved ATP-binding site. There is no anion binding site in PII (Lys85 is in an unfavourable position to bind a sulphate or phosphate ion) further pointing to different functions for the two molecules. Competition between anions and ATP in binding GlnK could be the mechanism for coupling N regulation with the level of sulphate or possibly phosphate (Xu *et al.*, 1998).
The residues Lys3 and Asp5 form a salt bridge (Carr *et al.*, 1996).	There are two neutral residues at the same positions, Leu3 and Val5 (Xu *et al.*, 1998).

Table 1.2 ***Comparison of the structural elements of the signalling proteins PII and GlnK from E. coli.***

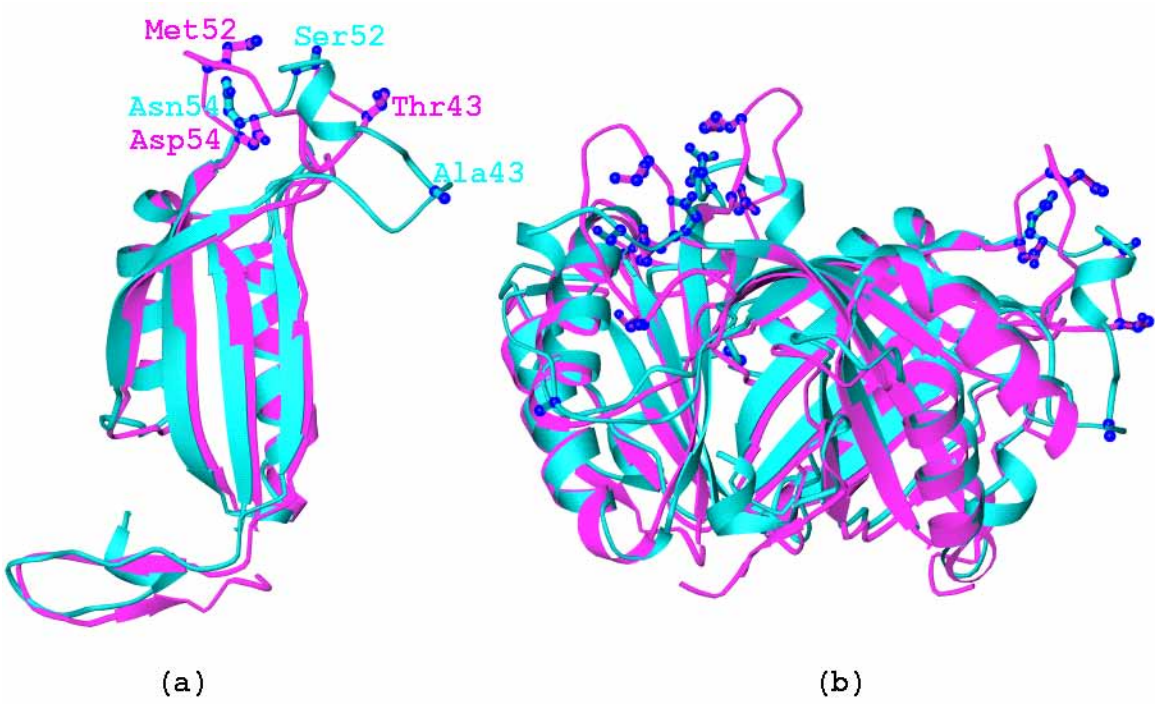

Figure 1.9 ***Structure of the nitrogen signalling proteins PII and GlnK of E. coli.*** X-ray crystal structure of the PII (pink) (Carr *et al.*, 1996) and GlnK (cyan) (Xu *et al.*, 1998) proteins from *E. coli* have been overlaid to demonstrate their structural similarities. In (a) the monomer is depicted and in (b) the trimer is depicted. The three T-loop residues where they differ have also been highlighted. It must be noted that the position of the T-loops in these three dimensional structures is constrained by the crystal lattice of the protein crystal and only indicative of one of the many potential conformations for the T-loop, which is probably mobile in solution.

On the top face of the barrel of PII from *E. coli* there are large charged patches (highly conserved region), which suggests electrostatics may play an important role in guiding target molecules to their correct docking sites (Carr *et al.*, 1996). The central cavity of PII may also contain metals on the threefold axis (Carr *et al.*, 1996). Cobalt has been shown to stimulate the interaction of PII and NRII to dephosphorylate NRI-P (Liu and Magasanik, 1995). Cobalt may bind in the central cavity of PII (Carr *et al.*, 1996).

Small effector-molecules probably bind in the cleft altering the conformation of the apex of the T-loop, activating or inhibiting the interactions with receptors (Jiang *et al.*, 1997a). Only one T-loop is involved in each interaction with the receptor-proteins UTase, ATase and NRII in *E. coli* (Jiang *et al.*, 1997b). In the case of GlnK, ATP binding with Arg residues in the cleft changes the charge distribution of the molecule possibly facilitating its interaction with other proteins. The T-loop is positioned in GlnK

such that ATP binding may affect its mobility and structure; consequently affecting its interactions with receptors (Xu *et al.*, 1998).

Although the binding site for ATP has been determined attempts to isolate the binding site for α-kg have been unsuccessful. Xu *et al.*, (1998) predicted α-kg probably binds to PII at the base of the T-loop, because this was the only region of the protein they could not resolve from PII/α-kg complex crystals, and they did not find α-kg in the resolved regions of the crystal structure. Benelli *et al.*, (2002) aligned several PII structures with two α-keto acid isomerising enzyme/α-kg isomerisation inhibitor complex structures, and suggested there is a binding site for α-kg in the ATP binding-cleft. The binding site is near that of ATP, involving residues Lys90 and Arg 101 from alternate monomers. The PII mutant work by Jiang *et al*., (1997) is consistent with this prediction.

There is a growing body of crystallographic evidence to suggest the T-loop is flexible in solution and that the observed sequence conservation, which doesn't have a matching structural conservation, is actually to confer flexibility to the loop, allowing it to interact with several different receptor-molecules (Xu *et al.*, 1998). Furthermore the T-loop is disordered in ATP complexes of the proteins that have been examined until now, suggesting that this region of the protein adopts different conformations within the crystal.

There are only three residues out of twenty within the T-loop (residues 36-55), where PII and GlnK (*E. coli*) differ (residues 43, 52, and 54) (Figure 1.9). These differences may be sufficient to make the necessary interactions with the different receptor-proteins (Arcondeguy *et al.*, 2000). GlnK has a 3_{10} helix in the middle of its T-loop when stabilised in a crystal lattice (Xu *et al.*, 1998). A similar 3_{10} helix in the interferon γ protein makes intimate contact with its receptor-protein (Walter *et al.*, 1995). It is possible that the T-loop of GlnK and other PII-like proteins may function in a similar way when binding to target receptor-proteins (Xu *et al.*, 1998).

1.3 Aims

The work described in this thesis is a culmination of studies centred around the proteins and small effector-molecules involved in the component of the N assimilation pathway that controls the level of activity of GS, i.e. the adenylylation cascade. The main focus of this study is the elucidation of the underlying molecular mechanisms of this cascade.

1.3.1 Aim 1 Production of monoclonal antibodies to PII and ATase for structure function studies

A panel of monoclonal antibodies (mAbs) was produced against the signalling protein PII and the receptor-protein ATase for use in investigating the interaction between the two proteins. These mAbs were then characterised to determine binding sites on their respective source proteins, and a collection of mutant and truncated proteins. Production and characterisation of these mAbs is covered in Chapter 3. Using a PII specific mAb that did not recognise GlnK and a PII/GlnK specific mAb, created in this work it was demonstrated that these two proteins could form heterotrimers both *in vitro* and *in vivo* (van Heeswijk *et al.*, 2000).

1.3.2 Aim 2 Obtain insight into the structure and function of ATase using a panel of unique PII mutants

It is known that ATP binds in the highly conserved ATP-binding cleft of the PII protein, and it is surmised that α-kg binds somewhere at the base of the T-loop, but how ATP and α-kg binding affect presentation of the T-loop to receptor-proteins is not fully understood. Using a large panel of PII mutants produced in the Vasudevan Laboratory at James Cook University (unpublished) Chapter 4 investigated the role of individual residues within the highly conserved ATP-binding cleft and T-loop of the PII protein, with respect to the binding of several target proteins and small effector-molecules.

1.3.3 Aim 3 Comparison of PII and GlnK function with respect to ATase

In Chapter 5 the differences between the two signalling proteins PII and GlnK are investigated in detail. Participation of several residues within the T-loop is also investigated.

1.3.4 Aim 4 Map the PII binding site in ATase and demonstrate the existence of a central regulatory domain

In Chapter 6 the panel of ATase mAbs generated in this work is used to map the region of the protein where the two forms of the signalling effector-proteins PII and GlnK bind. The prediction that a middle domain separates the two activity domains of ATase is examined by the construction of a central domain polypeptide. The role of the central domain within the multi-domain protein is also investigated.

1.3.5 Aim 5 Investigate intramolecular signal transduction within ATase domains using both truncated proteins and ATase mutants

The final results chapter investigates the role of the small effector-molecules gln and α-kg in regulating the two antagonistic activities of the ATase protein. Several questions involving small effector-molecules are listed below. Where does gln bind and how does it stimulate adenylylation activity and inhibit deadenylylation activity? Where does α-kg bind and how does it stimulate deadenylylation activity? How does α-kg stimulate adenylylation activity at a low concentration and inhibit that same activity at a higher concentration? What is the role of the Q1 linker in small effector-molecule signalling, within the ATase protein? Which residues within the similar catalytic sites give rise to the antagonistic activities? The above questions were addressed in Chapter 7 using all the truncation constructs and mutant proteins at my disposal as well as the ones generated in this study.

This thesis includes a final discussion chapter where all of the results addressing the above specific aims are drawn together for the proposal of a new adenylylation cascade model.

CHAPTER 2 Materials and Methods

2.1 MATERIALS

2.1.1 Chemicals

Manufacturer	Chemical
Ajax chemicals	$CaCl_2$, $MgCl_2$, DMSO, Na_2HPO_4, NaH_2PO_4, $MgSO_4$, KCl, CTAB, CH_2COONa, Na_2CO_3, $NaHCO_3$, $(NH_4)_2SO_4$, $MnCl_2$, K_2HPO_4, KH_2PO_4
BDH chemicals	Acetic acid, ethanol, methanol, NH_4Cl, propan-2-ol, TCA, glycerol, Na arsenate, NH_2OH, α-ketoglutarate
ICN	NaOH, Ecolite scintillation fluid, glycine, SDS, coomassie R-250, bromophenol blue, tris, EDTA, β-mercaptoethanol, BCIP, NBT, triton X-100, tween 20, tween 80, Na azide, EtBr, imidazole, UTP, ATP, ADP, ammonium persulphate
Amyl media	LB broth base
Amersham	UTP-Na salt [^{3}H], ATP-Na salt [^{14}C], α-kg [^{14}C]
Merck	TSK DEAE Fractogel
BioRad	MAPS II protein A agarose kit, Bradford's reagent
Gibco	HEPES, CONCERT miniprep kit, CONCERT midiprep kit, CONCERT gel extraction kit, TEMED, calf serum, foetal bovine serum, gentamicin solution, penicillin/streptomycin solution, glutamine, non-essential amino acids solution, sodium pyruvate solution, complete and incomplete Freund's adjuvant
Astral	Agarose, ampicillin, IPTG, DTT, dNTPs, 40% acrylamide/bis, PMSF, leupeptin, pepstatin
Sigma	Nonidet P40, pristane, dimethyl formamide, ABTS, 30% H_2O_2, mouse mAb isotyping kit, PEG 2000 solution, hypoxanthine, aminopterin, thymidine, OPI solution, citric acid, amphotericin, trypan blue solution

2.1.2 Proteins

2.1.2.1 Restriction enzymes

Manufacturer	Enzyme	Recognition sequence
New England Biolabs	*DpnI*	$\overset{CH_3}{\underset{\vert}{C}}$ 5' GA↓TC 3'
	NdeI	5' CA↓TATG 3'
	SmaI	5' GGTAC↓C 3'

2.1.2.2 Other enzymes

Manufacturer	Enzyme
Gibco	High fidelity supermix PCR enzyme mix
Stratagene	*pfu* turbo DNA polymerase
Sigma	Lysozyme, RNase
Promega	T4 DNA ligase, *Taq* DNA polymerase

2.1.2.3 Antibodies

Manufacturer	Antibody
Sigma	Rabbit-anti-Mouse IgG AP conjugate
	Rabbit-anti-Goat IgG HRPO conjugate
BioRad	Goat-anti-Mouse IgG HRPO conjugate

2.1.2.4 Other proteins

Manufacturer	Protein
Boehringer Mannheim	Bovine serum albumin (BSA)
BioRad	SDS PAGE low molecular weight marker
Sigma	Casein
Nestle	Carnation skim milk powder

2.1.3 Buffers and solutions

2.1.3.1 Antibody production solutions and additives

Phosphate buffered saline (PBS): NaCl (0.8% w/v), KCl (0.2% w/v), Na_2HPO_4 (0.144% w/v), KH_2PO_4 (0.024% w/v). Adjust to pH 7.4, autoclave and store at 4°C.

Hypoxanthine, aminopterin, thymidine (HAT) (100x): hypoxanthine (0.136% w/v), aminopterin (0.018% w/v), thymidine (0.038% w/v). The hypoxanthine was dissolved in a few drops of 1M NaOH, the volume was then made up to 100mL with PBS and the other components added. The solution was filter sterilised through a 0.22μm syringe filter and stored as 5mL aliquots in foil covered bottles at –20°C.

HEPES buffer (100x): HEPES (1M). Adjust pH to 7.5, autoclave and store in 5mL aliquots at –20°C.

HT (100x): As for HAT, without aminopterin added.

Sodium bicarbonate solution (25x): $NaHCO_3$ ($0.06gmL^{-1}$). Autoclave and store in 20mL aliquots at 4°C.

Glutamine solution (50x): glutamine (200mM). The solution was filter sterilised through a 0.22µm syringe filter and stored as 10mL aliquots in foil covered bottles at –20°C.

Double emulsion solution: NaCl (0.85% w/v). Autoclave and store at 4°C, add tween 80 (25% w/v) just prior to use.

Na azide solution (100x): Na azide (10% w/v).

2.1.3.2 DNA manipulations

Restriction enzyme buffer systems: New England Biolabs. **NEB 2**: NaCL (50mM), Tris-HCl (10mM), $MgCl_2$ (10mM), DTT (1mM). **NEB 4**: potassium acetate (50mM), Tris-acetate (20mM), Mg acetate (10mM), DTT (1mM).

Ligation buffer (10x): Promega. Tris-HCl (300mM), $MgCl_2$ (100mM), DTT (100mM), ATP (10mM).

***Taq* DNA polymerase buffer (10x):** Promega. KCl (500mM), Tris-HCl (100mM), Triton X-100 (1% v/v), $MgCl_2$ (15mM).

High fidelity supermix buffer (1.1x): Gibco. Tris-SO_4 (66mM), $(NH_4)_2SO_4$ (19.8µM), $MgSO_4$ (2.2mM), dGTP (220µM), dATP (220µM), dTTP (220µM), dCTP (220µM).

***pfu* turbo DNA polymerase buffer (10x):** Stratagene. Tris-HCl (pH 8.8) (200 mM), MgS04 (20 mM), KCl (100 mM), $(NH_4)_2S0_4$ (100 mM), Triton X-100 (1%v/v), nuclease-free BSA ($1mgmL^{-1}$).

CTAB buffer: CTAB (5% w/v). Autoclave and store at 30°C.

STET buffer: sucrose (8% w/v), Triton X-100 (0.1% w/v), EDTA (50mM), Tris-HCl (50mM, pH 8.0). Autoclave and store at room temperature.

TE buffer: Tris-HCl (10mM), EDTA (1mM, pH 7.6). Autoclave and store at room temperature.

TAE buffer (50x): Tris (2M), glacial acetic acid (5.7% v/v), EDTA (50mM).

Sequencing cleanup mix: Na acetate (112.5mM), ethanol (74.2% v/v). Prepared freshly just prior to use.

2.1.3.3 Protein manipulations

Resuspension buffer: sucrose (25% w/v), Tris (50mM, pH 8.0), EDTA (1mM).

PMSF solution: PMSF (100mM) dissolved in isopropanol and stored in a foil wrapped bottle at –20^{o}C.

Pepstatin solution: pepstatin (2mM). Store in a foil wrapped bottle at 4^{o}C.

Leupeptin solution: leupeptin (10.5mM) dissolved in DMSO and stored in a foil wrapped bottle at –20^{o}C.

ATase DEAE buffer A: sodium phosphate (20mM, pH 7.2), $MgCl_2$ (1mM), β-mercaptoethanol (5mM). Vacuum filter-sterilise and store at 4^{o}C.

ATase DEAE buffer B: buffer A, NaCl (1M). Vacuum filter-sterilise and store at 4^{o}C.

UTase DEAE buffer A: HEPES (20mM, pH 7.4), EDTA (1mM), β-mercaptoethanol (5mM). Vacuum filter-sterilise and store at 4^{o}C.

UTase DEAE buffer B: buffer A, NaCl (1M). Vacuum filter- sterilise and store at 4^{o}C.

PII DEAE buffer A: HEPES (20mM, pH 7.4), EDTA (1mM), β-mercaptoethanol (1mM). Vacuum filter-sterilise and store at 4^{o}C.

PII DEAE buffer B: buffer A, NaCl (1M). Vacuum filter-sterilise and store at 4^{o}C.

GlnK DEAE buffer A: Tris (20mM, pH 8.8), EDTA (1mM), β-mercaptoethanol (1mM).

GlnK DEAE buffer B: buffer A, NaCl (1M). Vacuum filter-sterilise and store at 4^{o}C.

GS buffer: imidazole (10mM, pH 7.0), $MnCl_2$ (10mM), β-mercaptoethanol (2mM). Vacuum filter-sterilise and store at 4^{o}C.

2.1.3.3.1 SDS PAGE

PAGE loading dye (2x): Bromophenol blue (0.2% w/v), glycerol (40% v/v).

PAGE loading dye (4x): Bromophenol blue (0.2% w/v), glycerol (80% v/v).

SDS PAGE sample loading buffer (2x): PAGE loading dye (1.5mL 2x), DTT (0.25mL 1M), SDS (0.25mL 20% w/v), Tris (0.35mL 2M). Prepared fresh every 2wk and stored at –20^{o}C.

SDS PAGE sample loading buffer (4x): PAGE loading dye (1.5mL 4x), DTT (0.25mL 1M), SDS (0.25mL 20% w/v), Tris (0.35mL 2M). Prepared fresh every 2wk and stored at –20^{o}C.

SDS PAGE running buffer (5x): Tris (0.25M), glycine (1.9M), SDS (0.5% w/v).

Ammonium persulphate solution: ammonium persulphate (10% w/v). Store in 1mL aliquots at –20^{o}C.

Coomassie staining solution (R-250): Coomassie blue R-250 (0.1% w/v), methanol (40% v/v), glacial acetic acid (10% v/v). The dye is completely dissolved in the methanol first, then the other components added.

Destaining solution: glacial acetic acid (10% v/v), methanol (10% v/v).

2.1.3.3.2 Native non-denaturing PAGE

Native PAGE sample loading buffer (2x): PAGE loading dye (1.5mL 2x), Tris (0.35mL 2M). Prepared fresh every 2wk and stored at –20^{o}C.

Native PAGE sample loading buffer (4x): PAGE loading dye (1.5mL 4x), Tris (0.35mL 2M). Prepared fresh every 2wk and stored at –20^{o}C.

Native PAGE running buffer (5x): Tris (0.25M), glycine (1.9M).

Nonidet P40 solution: NP 40 (10% v/v).

2.1.3.4 Western blotting

SDS PAGE transfer buffer: SDS PAGE running buffer (20% v/v), methanol (20% v/v).

Native PAGE transfer buffer: native PAGE running buffer (20% v/v), methanol (20% v/v).

TBS: Tris-HCl (20mM, pH 7.6), NaCl (20mM).

TTBS: TBS, tween 20 (0.2% v/v).

MTBS: TBS, Carnation skim milk powder (5% w/v). Stored in 10mL aliquots at –20^{o}C.

MTTBS: TTBS, Carnation skim milk powder (5% w/v). Stored in 10mL aliquots at –20^{o}C.

Alkaline phosphatase buffer: Tris (100mM), NaCl (100mM), $MgCl_2$ (5mM).

BCIP solution: BCIP (1.6% w/v) dissolved in DMF and stored at 4°C in foil wrapped bottle.

NBT solution: NBT (3%w/v) dissolved in DMF (70% v/v). Stored at 4°C in foil wrapped bottle.

2.1.3.5 ELISA

Coating buffer: Na2CO3 (0.13M), NaHCO3 (0.037M). Adjust to pH 9.6 and store at 4°C.

TEN buffer (10x): Tris (0.5M, pH 8.0), EDTA (0.01M), NaCl (1.5M).

TEN-T buffer (10x): TEN, tween 20 (0.5% v/v).

TEN-T-C buffer (10x): TEN-T, casein (2% w/v). Store in 100mL aliquots at –20°C.

Citrate phosphate buffer: A: citric acid (0.1M), B: Na_2HPO_4 (0.2M). Combine A+B to give pH 4.2. Store at 4°C.

ABTS stock: ABTS (2.8% w/v). Store in foil wrapped bottle at room temperature.

H_2O_2 stock: H_2O_2 (0.378% v/v). Prepare just before use.

ELISA buffer: citrate phosphate buffer (10mL), ABTS stock (200µL), H_2O_2 stock (200µL). Prepare just before use.

2.1.3.6 SPR analysis

HBS running buffer: HEPES (10mM, pH 7.4), EDTA (3.4mM), NaCl (300mM), P20 surfactant (0.01% v/v). Vacuum filter-sterilise, degas and store at 4°C in 100mL aliquots.

N-hydroxysuccinimide (NHS) solution: NHS (0.05M). Store in 1mL aliquots at -20°C.

N-ethyl-N'-(3-diethylaminopropyl) carbodimide (EDC) solution: EDC (0.2M). Store in 1mL aliquots at -20°C.

Ethanolamine hydrochloride solution: ethanolamine (1M, pH 8.5). Store in 1mL aliquots at -20°C.

Phosphoric acid: H3PO4 (100mM). Vacuum filter-sterilise and degas solution.

2.1.3.7 GS adenylylation/deadenylylation assay

Adenylylation assay mix (2x): HEPES-HCl (100mM, pH 7.6), BSA (2mgmL^{-1}), K_2PO_4 (50mM), $MgCl_2$ (10mM), ATP (2mM), glutamine (2mM), GS (100nM, n=1) (see section 2.2.7.9), PII (50nM) (see section 2.7.7.7).

Deadenylylation assay mix (2x): HEPES-HCl (100mM, pH 7.6), BSA (2mgmL^{-1}), K_2PO_4 (50mM), $MgCl_2$ (10mM), ATP (2mM), α-ketoglutarate (40mM), GS-AMP (100nM, n=11) (see section 2.2.7.9), PII-UMP (50nM, n=3) (see section 2.2.5.6.1).

GS assay stop mix: $FeCl_2$ (206mM), TCA (123mM), HCl (249mM).

γ-glutamyl transferase assay mix A: imidazole-HCl (0.16M, pH 7.2), glutamine (0.16M), NH_2OH (42mM), $MgCl_2$ (62.5mM), $MnCl_2$ (0.42mM).

γ-glutamyl transferase assay mix B: assay mix A, ADP (0.42mM), Na_2HAsO_4 (21mM).

γ-glutamyl transferase assay mix C: assay mix A without $MgCl_2$.

γ-glutamyl transferase assay mix D: assay mix B without $MgCl_2$.

2.1.3.8 Uridylylation assay

Uridylylation reaction mix: HEPES (20mM, pH 7.5), $MgCl_2$ (20mM), KCl (100mM), DTT (1mM), α-ketoglutarate (2mM), UTP (0.4mM), ATP (4mM).

2.1.3.9 Radio-labelled effector binding assay

Small effector binding assay buffer (pH 7.5): Tris-HCl (50mM, pH 7.5), KCl (100mM), $MgCl_2$ (10mM). Vacuum filter-sterilise and store at 4^{o}C.

Small effector binding assay buffer (pH 6.0): Tris-HCl (50mM, pH 7.5), KCl (100mM), $MgCl_2$ (10mM). Adjust pH to 6.0. Vacuum filter-sterilise and store at 4^{o}C.

2.1.4 Bacterial strains

Strain	Genotype	Source/Reference
AN1459	F$^-$ *ilv leu thr supE recA srlA*:: Tn*10*	Elvin *et al.*, (1986)
BL21 (DE3) RecA	B F$^-$ *dcm ompT hsdS(r_B- m_B-) gal recA srlA*:: Tn*10*	Studier *et al.*, (1990)
DH5α	F$^-$ *supE44 hsdR17 recA1 end A1gyrA96 thi-1 relA1*	Raleigh *et al.*, (1989)
JM109	*recA1 supE44 end A1 hsdR17 gyrA96 relA1 thiΔ(lac-proAB)* F'[*traD36 proAB*$^+$ *lacI*^{q} *lacZ*ΔM15]	Yanisch-Perron *et al.*, (1985)
RB9017	*endA1 thi-1 hsdR17 supE44 ΔlacU169 hutC$_{klebs}$* MU *lysogen glnE*::Tn*5*	Bueno *et al.*, (1985)
RB9040	*endA1 thi-1 hsdR17 supE44 ΔlacU169 hutC$_{klebs}$* MU *lysogen glnD99*::Tn*10*	Bueno *et al.*, (1985)
RB9065	*endA1 thi-1 hsdR17 supE44 ΔlacU169 hutC$_{klebs}$* MU *lysogen glnD99*::Tn*10 ΔglnB2306*	Bueno *et al.*, (1985)
TG1	K12 *Δ(lac-pro) supE thi hsd* D5/F' *tra* D36 *Pro A+B+laclq lacZΔ*M15	Gibson (1984)

2.1.5 Bacterial growth medium and additives

2.1.5.1 Non-selective media

LB medium: tryptone (10g), yeast extract (5g), NaCl (5g), NaOH (2.5mL of 1M), dissolved in 1L ddH_2O and autoclaved.

LB plate medium: LB medium, agar (1.5% w/v), dissolved in 1L ddH_2O and autoclaved. Mix thoroughly, cool to 50^{o}C and pour into plates.

2.1.5.2 Selective media

LBA medium: cold LB medium, 100μgmL^{-1} ampicillin (100mgmL^{-1} stock in ddH_2O)

LBAC medium: LBA medium, 25μgmL^{-1} chloramphenicol (25mgmL^{-1} stock in absolute ethanol).

LBA plate medium: 50^{o}C LB medium, 100μgmL^{-1} ampicillin (100mgmL^{-1} stock in ddH_2O). Mix thoroughly and pour into plates.

LBAC plate medium: 50^{o}C LBA medium, 25μgmL^{-1} chloramphenicol (25mgmL^{-1} stock in absolute ethanol). Mix thoroughly and pour into plates.

2.1.6 Vectors

2.1.6.1 Parent vectors

Vector	Description	Source/Reference
pND707	λ P_R-P_L promoter	Love *et al.*, (1996)
pETMCS I	pET expression vector	Neylon *et al.*, (2000)
pBluescript	lac promoter	Short *et al.*, (1998)

2.1.6.2 Recombinant vectors

Plasmid	Description	Source/Reference
pRJ001	*glnB* (PII) in pND707	Jaggi *et al.*, (1996)
pRJ001:G24A	*glnB* (PII:G24A) in pND707	Vasudevan lab unpublished
pRJ001:G24AT26A	*glnB* (PII:G24AT26A) in pND707	Vasudevan lab unpublished
pRJ001:G24D	*glnB* (PII:G24D) in pND707	Vasudevan lab unpublished
pRJ001:T26A	*glnB* (PII:T26A) in pND707	Vasudevan lab unpublished
pRJ001:H42N	*glnB* (PII:H42N) in pND707	Vasudevan lab unpublished
pRJ001:T43A	*glnB* (PII:T43A) in pND707	Vasudevan lab unpublished
pRJ001:Y46F	*glnB* (PII:Y46F) in pND707	Jaggi (1998)
pRJ001:Y51F	*glnB* (PII:Y51F) in pND707	Jaggi (1998)
pRJ001:Y51S	*glnB* (PII:Y51S) in pND707	Vasudevan lab unpublished
pRJ001:V64AP66S	*glnB* (PII:V64AP66S) in pND707	Vasudevan lab unpublished
pRJ001:V64AP66T	*glnB* (PII:V64AP66T) in pND707	Vasudevan lab unpublished
pRJ001:K90N	*glnB* (PII:K90N) in pND707	Vasudevan lab unpublished
pRJ001:R103D	*glnB* (PII:R103D) in pND707	Vasudevan lab unpublished
pRJ001:R103CT104A	*glnB* (PII:R103CT104A) in pND707	Vasudevan lab unpublished
pRJ001:R103HT104A	*glnB* (PII:R103HT104A) in pND707	Vasudevan lab unpublished
pRJ001:T104A	*glnB* (PII:T104A) in pND707	Vasudevan lab unpublished
pRJ001:E106A	*glnB* (PII:E106A) in pND707	Vasudevan lab unpublished
pSC003	*glnB* (PII:K3LD5T) in pND707	Canyon (1998)
pNV101	*glnD* (UTase) in pND707	Jaggi *et al.*, (1996)
pNV103	*glnK* (GlnK) in pND707	Vasudevan lab unpublished
pWVH57	*glnA* (GS) in pBluescript II KS+	van Heeswijk *et al.*, (1996)
pJRV001	*glnA* (GS) in pND707	Vasudevan lab unpublished
pTA52	*glnB* (PII:T43A) in pBluescript II KS+	Arcondeguy *et al.*, (2000)
pTA53	*glnB* (PII:M52S) in pBluescript II KS+	Arcondeguy *et al.*, (2000)
pTA54	*glnB* (PII:D54N) in pBluescript II KS+	Arcondeguy *et al.*, (2000)
pTA55	*glnB* (PII:D54NM52S) in pBluescript II KS+	Arcondeguy *et al.*, (2000)
pTA56	*glnB* (PII:D54NT43A) in pBluescript II KS+	Arcondeguy *et al.*, (2000)
pTA57	*glnB* (PII:D54NM52ST43A) in pBluescript II KS+	Arcondeguy *et al.*, (2000)
pTA58	*glnB* (PII:M52ST43A) in pBluescript II KS+	Arcondeguy *et al.*, (2000)
PRJ002	*glnE* (AT-C_{522}) in pND707	Jaggi *et al.*, (1997)
pRJ007	*glnE* (AT-N_{423}) in pND707	Jaggi *et al.*, (1997)
pRJ009	*glnE* (ATase) in pND707	Jaggi *et al.*, (1997)
pRJ0012	*glnE* (AT-N_{548}) in pND707	Jaggi (1998)
pRJ0013	*glnE* (AT-N_{501}) in pND707	Jaggi (1998)
pRJ0014	*glnE* (AT-C_{439}) in pND707	Jaggi (1998)
pRJ0015	*glnE* (AT-C_{396}) in pND707	Jaggi (1998)
pDW1	*glnE* (AT-N_{440}) in pND707	Wen (2000)
pDW2	*glnE* (AT-C_{481}) in pND707	Wen (2000)
pDW3	*glnE* (AT-N_{467}) in pND707	Wen (2000)
pDW4	*glnE* (AT-C_{518}) in pND707	Wen (2000)
pDW7	*glnE* (AT-C_{340}) in pETDW2	Wen (2000)

Plasmid	Description	Source/Reference
pDW8+glnB	*glnE* (AT-C_{305})+*glnB* in pETDW2	Wen (2000)
p235+glnB	*glnE* (AT-C_{235})+*glnB* in pETDW2	Vasudevan lab unpublished
pETDW2	pETMCS I ΔSph I ΔSal I upstream of PT7	Wen (2000)
pET AT:ΔR	*glnE* (AT:ΔR) in pETDW2	O'Donnell (2000)
pRJ009:$Q1^2$	*glnE* (AT:$Q1^2$) in pND707	O'Donnell (2000)
pRJ009:W452A	*glnE* (AT:W452A) in pND707	O'Donnell (2000)
pRJ009:E454A	*glnE* (AT:E454A) in pND707	O'Donnell (2000)
pRJ009:N169G	*glnE* (AT:N169G) in pBluescript II	Mc Loughlin (1999)
pRJ009:D173A	*glnE* (AT:D173A) in pND707	Mc Loughlin (1999)
pRJ009:D175A	*glnE* (AT:D175A) in pND707	Mc Loughlin (1999)
pRJ009:D173AD175A	*glnE* (AT:D173AD175A) in pND707	Mc Loughlin (1999)
pRJ009:W694G	*glnE* (AT:W694G) in pND707	Mc Loughlin (1999)
pRJ009:G697N	*glnE* (AT:G697N) in pBluescript II	Mc Loughlin (1999)
pRJ009:W694GG697N	*glnE* (AT:W694GG697N) in pND707	Mc Loughlin (1999)
pRJ009:D701E	*glnE* (AT:D701E) in pND707	Mc Loughlin (1999)
pRJ009:D703E	*glnE* (AT:D703E) in pND707	Mc Loughlin (1999)
pRJ009:D701ED703E	*glnE* (AT:D701ED703E) in pND707	Mc Loughlin (1999)
pRJ009:D701N	*glnE* (AT:D701N) in pND707	Mc Loughlin (1999)
pRJ009:D703N	*glnE* (AT:D703N) in pND707	Mc Loughlin (1999)
pRJ009:D701ND703N	*glnE* (AT:D701ND703N) in pND707	Mc Loughlin (1999)
pRJ009:RQ2	*glnE* (AT:RQ2) in pETDW2	this work
pRJ009:W452P	*glnE* (AT:W452P) in pND707	this work
pRJ009:W456A	*glnE* (AT:W456A) in pND707	this work
pDW1:N169G	*glnE* (AT-N_{440}:N169G) in pND707	this work

2.1.7 Oligonucleotides

2.1.7.1 PCR and sequencing primers

Primer	Sequence (5'-3')
PII FP	AATGAATTCGCGTTATGT
PII RP	AATGCTTTGGCCCGCAT
Primer 9	GGCAGCATTCAAAGCAG
M13 universal	TGTAAAACGACGGCCAGT
AT-C 464 FP	GGAATTCCATATGGAAGATGACACTACGCCA
AT Q2 RP	CCCCGGTACCTTATAGCGTACCGGCGATATCCGC
pET T7 FP	TAATACGACTCACTATAGGG
pET T7 RP	CTCAGCTTCCTTTCGGGCTT
AT-N RP1	AGCCGCTGCCCCATGCGGGT
AT-N FP2	TGCGATGCTGCGCCCGTTTG
AT-N FP3	CGCATCGCCTGGGCGCAA

2.1.7.2 Primers for site directed mutagenesis

Mutation	Primer sequence
PII:ATP-binding cleft entrance mutants	
PII:G24A	CATGCCGGYAATASCGACTTCGGC
PII:G24AT26A	CATGCCGGYAATASCGACTTCGGC
PII:G24D	CATGCCGGYAATASCGACTTCGGC
PII:T26A	CATGCCGGYAATASCGACTTCGGC
PII:T-loop mutants	
PII:H42N	GCTCGGTATTGCCTTTCT
PII:T43A	GTACAGCTCGGCATGGCC
PII:Y46F	GCCGCGGAACAGCTCGGT
PII:Y51F	ATCCACCATAAACTCCGC
PII:Y51S	ATCCACCATAGACTCCGC
PII:ATP-binding cleft mutants	
PII:V64AP66S	GTCGTCCGSTACGRCAATCTCAAT
PII:V64AP66T	GTCGTCCGSTACGRCAATCTCAAT
PII:K90N	GAAGATGTTACCGTCACC
PII:R103D	CTCTTCACCGGYASSGATSYGAATGACCCG
PII:R103CT104A	CTCTTCACCGGYASSGATSYGAATGACCCG
PII:R103HT104A	CTCTTCACCGGYASSGATSYGAATGACCCG
PII:T104A	CTCTTCACCGGYASSGATSYGAATGACCCG
PII:E106A	GTCCTCGCACCGGTACG
PII:salt-bridge mutant	
PII:K3LD5T	CAAGGAAATCATATGAAACTGATTACCGCGATTATAAAA
ATase:Activity reversal mutant	
AT-N_{440}:N169G	GGTGGGGAGCTGGGTTTCTCCTCTGATATC-S GATATCAGAGGAGAAACCCAGCTCCCCACC-N
ATase:Q1 linker mutants	
AT:W452P	CTGTCGGAACAGCCGCGTGAGCTGTGGCAGG-S CCTGCCACAGCTCACGCGGCTGTTCCGACAG-N
AT:W456A	CGTGAGCTGGCGCAGGATGCGTTGCAGGAAG-S CTTCCTGCAACGCATCCTGCGCCAGCTCACG-N

2.1.8 Cell culture lines

Cell line	Origin	Reference
Sp2/0-Ag14 (Sp2/0)	Cross between mouse lines p3-X63 Ag8 and BALB/c	Kohler and Milstein (1975) Schulman *et al., (*1978)
Mouse sarcoma 180 cells	BALB/c	Tikasingh *et al., (*1965)

2.1.9 Hybridoma culture media

Sp2/0 medium: DMEM medium, calf serum (20%), L-glutamine (4mM), amphotericin ($2.5\mu gmL^{-1}$), penicillin G ($100UmL^{-1}$), streptomycin ($100UmL^{-1}$), gentamicin ($0.05mgmL^{-1}$). All the components were added aseptically to the DMEM medium.

Fusion medium: DMEM medium, L-glutamine (4mM), amphotericin (2.5μgmL^{-1}), penicillin G (100UmL^{-1}), streptomycin (100UmL^{-1}), gentamicin (0.05mgmL^{-1}), non-essential amino acids (1x), HEPES (pH 7.2, 20mM), β-mercaptoethanol (10μM), sodium bicarbonate (2.4μgmL^{-1}). All the components were added aseptically to the DMEM medium.

Hybridoma medium: DMEM medium, calf serum (20%), L-glutamine (4mM), amphotericin (2.5μgmL^{-1}), penicillin G (100UmL^{-1}), streptomycin (100UmL^{-1}), gentamicin (0.05mgmL^{-1}), non-essential amino acids (1x), HEPES (pH 7.2, 20mM), β-mercaptoethanol (10μM), sodium bicarbonate (2.4μgmL^{-1}). All the components were added aseptically to the DMEM medium.

HAT selective hybridoma medium: 5mL of HAT (100x) solution (2.1.3.1) and 5mL of OPI (100x) solution (Sigma) was added to 500mL of hybridoma medium.

HT selective hybridoma medium: 5mL of HT (100x) solution (2.1.3.1) was added to 500mL of hybridoma medium.

Cloning medium: 5mL of OPI (100x) solution (Sigma) was added to 500mL of hybridoma medium.

2.2 METHODS

2.2.1 Microbiological methods

2.2.1.1 Growth of *E. coli* cultures on solid media in plates

A sterile wire loop was used to streak a single bacterial colony, or a glass spreader was used to streak broth culture, onto LB/LBA plates (2.1.5). Where the cells contained heat inducible protein expression vectors, the culture was incubated at 30^{o}C to avoid premature protein induction, otherwise cultures were grown at 37^{o}C.

2.2.1.2 Growth of *E. coli* cultures in liquid media

A small volume (generally 2mL) of LB/LBA medium (2.1.5) was inoculated with a single bacterial colony removed from a plate with a sterile wire loop. The culture was

grown overnight at the same temperature as the inoculating plate. The resulting stationary phase culture was diluted 1 in 100 to inoculate larger cultures (20-50mL) of LB/LBA medium (2.1.5). All liquid cultures were grown with aeration in a shaking waterbath at 220rpm.

2.2.1.3 Preparation of competent *E. coli* cells

Preparation of competent cells followed the method of Sambrook *et al.*, (1989). The required *E. coli* strain was streaked onto a LB plate (2.1.5) and incubated overnight at 37°C. A single colony from that plate was then used to inoculate 2mL LB medium (2.1.5), which was cultured overnight at 37°C, with shaking (starter culture). A 50mL LB culture was inoculated using 500μL of starter culture and grown for several hours at 37°C, with shaking until an OD_{595} of 0.5-0.6 was attained.

Initially the culture was chilled on ice for 30min. The chilled cells were pelleted by centrifugation (6,000rpm, 10min, 4°C), and resuspended in 50mL of chilled 100mM $MgSO_4$. The cells were pelleted again (6,000rpm, 10min, 4°C), and resuspended in 25mL of chilled 100mM $CaCl_2$, then chilled on ice for 30min. The cells were pelleted once more (6,000rpm, 10min, 4°C), and resuspended in 5mL of chilled 100mM $CaCl_2$, then chilled on ice for another 30min. Chilled sterile glycerol (1.2mL, 80% v/v) was added to the competent cells dropwise, with gentle stirring. The competent cells were stored at –70°C in 200μL aliquots.

2.2.1.4 Transformation of competent *E. coli* cells

Previously prepared competent cells (see section 2.2.1.3) were transformed using the method of Sambrook *et al.*, (1989). The competent cells (200μL glycerol stock) and plasmid stock were thawed on ice. Plasmid (1μL) or ligation mix (10μL) were added to the competent cells and incubated for 30min on ice. The mixture was "heat shocked" for 1min (30°C for heat inducible vectors and 37°C for the others), then placed on ice again for 5min. Prewarmed LB media (2.1.5) (1mL) was added to the transformation mix and the mixture was incubated for 1-2h at the heat shock temperature. During this time β-

lactamase is transcribed from the *bla* gene in the plasmid conferring ampicillin resistance to the successfully transformed cells.

Transformed cells were spread onto selective LBA plates (2.1.5) (10μL for plasmid and 50μL for ligation mix). The remaining cells were pelleted with centrifugation (6,000rpm, 10min, room temperature) and also spread onto selective LBA plates (2.1.5). The plates were incubated overnight at the temperature appropriate to the plasmid (30^{o}C for heat inducible vectors and 37^{o}C for the others).

Successful transformants were assessed using small-scale plasmid preparations (see sections 2.2.2.1 and 2).

2.2.1.5 Storage of *E. coli* cells in DMSO

A 2mL culture was prepared (see section 2.2.1.2) and grown overnight. The culture was split into 2x1mL aliquots and 77μL of sterile DMSO added to each. The cells were stored at –70^{o}C.

2.2.2 Nucleic acid manipulations

2.2.2.1 Small-scale plasmid preparation: CTAB method

Individual, discrete colonies grown on LBA plates (2.1.5), were streaked onto LBA sector plates (2.1.5). The plates were incubated overnight at the appropriate temperature (30^{o}C for heat inducible vectors and 37^{o}C for the others). The cells from each sector were lifted from the plate using a sterile wire loop (which was dipped in the STET buffer first) and added to a microfuge tube containing 200μL of STET buffer (2.1.3.2).

The small-scale plasmid preparation was produced following the method of De Sal *et al.*, (1988). Chicken egg white lysozyme (1mgmL^{-1}) was added to the cell suspension to disrupt the bacterial cell wall and release the plasmid. The suspension was incubated for 5min at room temperature, then boiled for 45s. Cellular debris was pelleted with

centrifugation (13,200rpm, 10min, room temperature) and removed with a sterile toothpick. The plasmid DNA was precipitated with 8μL of CTAB buffer (2.1.3.2) at room temperature for 5min. The DNA was pelleted by centrifugation (13,200rpm, 10min, room temperature) and the supernatant removed by vacuum aspiration.

The DNA pellet was resuspended in 300μL of 1.2M NaCl solution with vigorous vortexing and precipitated again with 750μL of 100% ethanol (-70^{o}C). The DNA was pelleted again by centrifugation (13,200rpm, 10min, room temperature) and the supernatant removed by vacuum aspiration. The DNA pellet was washed with 750μL of 70% ethanol (-70^{o}C) and pelleted as before. The residual supernatant was removed with vacuum drying for 2-5min (Savant Speed Vac SC100). The pellet was resuspended in 50μL of TE buffer pH 8.0 (2.1.3.2) with RNase (0.4mgmL^{-1}) added, and incubated for 1h at 37^{o}C to digest any contaminating RNA.

Analysis of the plasmid was performed using restriction digests (see section 2.2.2.3) and agarose gel electrophoresis (see section 2.2.3.1). Typical plasmid yields ranged from 2-5μg.

2.2.2.2 Small/medium-scale plasmid preparation: CONCERT kit method

The kits were used to produce high-grade plasmid DNA. The CONCERT kit (Gibco) utilises the alkaline-SDS lysis method of Sambrook *et al.*, (1989), followed by ion exchange separation on a filter membrane. The small-scale kits used up to 4mL of culture, and were used to produce DNA for sequencing. The medium-scale kits used up to 25mL of culture, and were used to produce DNA for cloning work. Analysis of the product was performed using agarose gel electrophoresis (see section 2.2.3.1).

2.2.2.3 DNA digestion with restriction enzymes

Restriction digests were carried out in the 10x reaction buffers specified by the manufacturer, or in OPA buffer (One Phor All, Pharmacia) when two incompatible enzymes were used in a double digest. The basic components of a 20μL digest were

DNA (2μg), enzyme (5U) and reaction buffer (1x). Twenty μL (check digest) and 50μL (cloning digest) reactions were generally used. The reaction was incubated for 1h at the temperature recommended by the manufacturer for the specific enzyme, then the enzyme was inactivated following the manufacturer's guidelines. Analysis of the product was performed using agarose gel electrophoresis (see section 2.2.3.1).

2.2.2.4 Ligation with T4 DNA ligase

The ligation reaction used T4 DNA ligase (Promega) and the 10x reaction buffer supplied by the manufacturer. The molar ratio of vector DNA to insert DNA was 1:10 in a 20μL reaction. The ligation mixture was incubated overnight at 14^{o}C and transformed the next day into competent *E. coli* cells (see section 2.2.1.4).

2.2.2.5 Site-directed mutagenesis

All the PII mutant recombinant vectors were produced previously essentially following the methods described in Sambrook *et al.*, (1989). Oligonucleotide directed mutagenesis of the pRJ001 plasmid (2.1.6.2), was performed using the primers listed in Table 2.1.7.2. The Eckstein method was carried out using phosphorothioate nucleotides (Taylor *et al.*, 1985; Sayers *et al.*, 1992). Several modifications to the method outlined in the manufacturer's manual (Amersham) were also introduced. Single-stranded phagemid DNA was produced following the methods of Vieira and Messing (1987). Hybridisation was used to screen for mutations and Sanger dideoxy chain termination sequencing (Sanger *et al.*, 1977) was used to confirm the presence of the correct mutation. Sequencing using the PII FP and PII RP primers (2.1.7.1) also confirmed no other mutations had been introduced into the *glnB* gene insert.

2.2.3 Agarose gel electrophoresis for separation of DNA

2.2.3.1 DNA separation

Analysis and isolation of plasmid DNA, DNA fragments and PCR products was performed following the methods of Sambrook *et al.*, (1989). Agarose (0.7-1.0% w/v) was dissolved in TAE buffer (2.1.3.2) with boiling and allowed to cool to 60^{o}C, before the intercalating agent: ethidium bromide (0.16μgmL^{-1}) was added. The gel was cast into a tray (MiniSub DNA electrophoresis unit, BioRad) then run for 30-40min at 70V in TAE buffer (2.1.3.2) to separate the DNA. The individual DNA bands were visualised with UV light using a 312nm transilluminator and the image recorded by the Gel Cam Documentation system (Bresatec). Biorad's 1kB ruler was used as the size marker.

2.2.3.2 Isolation and purification of DNA: CONCERT extraction kit

The fragments of linearised DNA or PCR product were visualised with UV light and cut out of the agarose gel with a scalpel blade. Exposure to the UV light was kept to a minimum to minimise damaging the DNA. The excised fragment was processed following the manufacturer's instructions.

2.2.3.3 Concentration of DNA fragments: ethanol precipitation

Three molar Na acetate (1/10 DNA volume) and absolute ethanol (2x the DNA volume, -70^{o}C) were added to the DNA and incubated at –70^{o}C for 30min. The DNA was pelleted using centrifugation (30,000rpm, 10min, 4^{o}C) and the supernatant removed by careful aspiration. The DNA pellet was washed with 70% ethanol (1x the DNA volume, -70^{o}C) and pelleted as before. The residual supernatant was removed with vacuum drying for 2-5min (Savant Speed Vac SC100). The pellet was resuspended in 50μL of TE buffer pH 8.0 (2.1.3.2). Analysis of the product was performed using agarose gel electrophoresis (see section 2.2.3.1).

2.2.4 Polymerase chain reaction (PCR) for nucleic acid amplification

The polymerase chain reaction (Chien *et al.*, 1976) was used to amplify various DNA fragments using the appropriate templates and oligonucleotide primers in a thermal cycler (Peltier PTC200, MJ Research). Reactions were carried out in the buffer system specified by the manufacturer.

2.2.4.1 DNA fragments for cloning

These reactions used the high fidelity supermix system (Gibco) and were set up following the manufacturer's instructions. The primers were engineered to introduce restriction digest sites into the PCR product (see section 2.1.7.1 for primers). Analysis of the product was performed using agarose gel electrophoresis (see section 2.2.3.1).

Thermocycler conditions were:

Reaction step	Temp (^{o}C)	Time (s)	# cycles
pre-amplification	94	120	1
denaturation	94	60	30
annealing and extension	50	60	30
extension	72	120	30
final extension	72	600	1

2.2.4.2 Site-directed mutagenesis

These reactions used *pfu* turbo DNA polymerase (Stratagene). The protocol used was based upon the Quick Change Site-Directed mutagenesis system (Stratagene method manual, 1999). Mutagenesis reactions (50μL) were set up following the manufacturer's instructions. The complementary primers were engineered to introduce a point mutation into the insert within the plasmid (see section 2.1.7.2 for primers). The *pfu* turbo DNA polymerase was added to the reaction mix 2min into the first cycle (hot start) to improve the enzyme's performance. Analysis of the product was performed using agarose gel electrophoresis (see section 2.2.3.1).

Thermocycler conditions were:

Reaction step	Temp (^{o}C)	Time (s)	# cycles
pre-amplification	95	180	1
denaturation	95	60	18
annealing and extension	55	60	18
extension	68	900	18

Parent DNA in the sample was digested with 0.7μL of *DpnI* (14U in 50μL reaction) for 60min at 37^{o}C. The PCR amplified plasmid was transformed into the appropriate competent *E. coli* cells (see section 2.2.1.4).

2.2.4.3 Automated sequencing

These reactions (10μL) used the Big Dye terminator system (Amersham) following the manufacturer's instructions. Depending on the situation internal or external primers were used (see section 2.1.7.1 for primers).

Thermocycler conditions were:

Reaction step	Temp (^{o}C)	Time (s)	# cycles
denaturation	96	30	35
annealing and extension	50	15	35
extension	60	240	35

The samples were cleaned up following the manufacturer recommended method. Forty μL of sequencing cleanup mix (2.1.3.2) was added to each sequencing reaction. The reaction was vortexed and incubated for 30min at room temperature. The DNA was pelleted by centrifugation (13,200rpm, 10min, room temperature) and the supernatant removed with careful aspiration. A further 250μL of 70% ethanol was added with mixing. The DNA was re-pelleted by centrifugation (13,200rpm, 10min, room temperature) and the supernatant removed. The residual supernatant was removed with vacuum drying for 2-5min (Savant Speed Vac SC100). The sample was wrapped in foil and stored at 4^{o}C until processed on the ABI 310 automatic sequencer (Perkin Elmer).

2.2.4.4 Screening with colony PCR for positive transformants

Bacteria were removed from the centre of each isolated colony using a tip (200μL) and transferred to 10μL of ddH_2O and boiled for 2min. One μL of boiled sample was added to each 10μL reaction. These reactions used *Taq* DNA polymerase (Promega) and were set up following the manufacturer's instructions. Primers were chosen to demonstrate the presence of an insert within a freshly produced recombinant vector (see section 2.1.7.1 for primers). Analysis of the product was performed using agarose gel electrophoresis (see section 2.2.3.1).

Thermocycler conditions were:

Reaction step	Temp (^oC)	Time (s)	# cycles
pre-amplification	94	180	1
denaturation	94	60	35
annealing and extension	50	60	35
extension	72	105	35
final extension	72	600	1

2.2.5 Protein production

2.2.5.1 Thermal induction of protein over-expression

Plasmids, which contained the strong tandem λ promoters P_R and P_L, were used to produce many of the proteins used in this work (pND707 derived recombinant vectors) (see section 2.1.6.2 for vectors). Transcription from the two λ promoters is repressed at 30^oC by the thermolabile repressor protein expressed from the *cI857* gene in *E. coli*. When the temperature is shifted rapidly to 42^oC (OD_{595} 0.5-0.6) the repressor protein no longer functions and the insert gene is transcribed giving rise to protein over-expression (Elvin *et al.*, 1990; Lilley *et al.*, 1993; Love *et al.*, 1996). SDS PAGE was used to monitor protein over-expression (see section 2.2.6.1).

2.2.5.2 IPTG induction of protein over-expression

Another group of proteins were over-expressed from pET derived recombinant vectors (see section 2.1.6.2 for vectors) using IPTG induction (0.4mM at OD_{595} 0.5-0.6). In this system T7 RNA polymerase transcribes the target DNA in the recombinant vector. These plasmids were transformed into BL21 (DE3) recA plysS. This strain contains the DE3 lysogen (the IPTG induces production of T7 RNA polymerase), *plysS* plasmid (expresses T7 lysozyme to inhibit basal level T7 RNA polymerase activity prior to induction) and recA (absence of this enzyme prevents recombination of vector and chromosomal DNA). These cells need chloramphenicol ($25\mu gmL^{-1}$) in their culture media to retain the *plysS* plasmid. This system was generally used for proteins and truncations, which showed poor solubility when expressed in the thermal system of the pND707 vector. With this system the induction temperature can be lowered to 18^oC to potentially improve protein solubility. SDS PAGE was used to monitor protein over-expression (see section 2.2.6.1).

The remaining group of proteins were over-expressed from pBluescript derived recombinant vectors (see section 2.1.6.2 for vectors) using IPTG induction (0.4mM at OD_{595} 0.5-0.6). These vectors contain the *lac* promoter.

2.2.5.3 Small-scale protein induction and freeze/thaw lysis

The appropriate strain/plasmid was grown in 50mL culture (see section 2.2.1.1 and 2) and induced by the corresponding induction method (see section 2.2.5.1 and 2). Cells containing pND707 derived plasmids were grown for 3-4h post-induction at 42^oC and harvested, cells containing the pET derived plasmids were grown overnight at 18^oC and harvested, and cells containing the pBluescript derived plasmids were grown overnight at 37^oC and harvested. A 1mL aliquot was removed from the culture just prior to induction (pre-induction sample) and just prior to harvesting the cells (post-induction sample). These samples were processed (see section 2.2.6.1.2) and analysed for protein over-expression using SDS PAGE (see section 2.2.6.1).

The cells were harvested by centrifugation (6,000rpm, 10min, 4°C) and resuspended in resuspension buffer (2.1.3.3) with a protease inhibitor cocktail added (7.2mM β-mercaptoethanol, 2μM PMSF, 4μM pepstatin, 1μM leupeptin) to an OD_{595} of 100. Chicken egg white lysozyme (0.1mgmL^{-1}) was added to the cell suspension to disrupt the bacterial cell wall and release the proteins. The cell suspension was incubated on ice for 30min, then underwent 3 freeze/thaw cycles where the sample was dipped in liquid nitrogen until frozen, followed by thawing at room temperature until liquid again. Increasing viscosity of the cell suspension indicated successful cell lysis. The extract was clarified by centrifugation (40,000rpm, 30min, 4°C). A small aliquot was removed from the cell suspension prior to addition of the lysozyme (pre-lysing sample), and also from the clarified supernatant (post-lysing sample) for analysis in SDS PAGE (see section 2.2.6.1). These cell free extracts were used for all the assays where cell lysates were used.

2.2.5.4 Solubility of expressed proteins

The solubility of various over-expressed proteins was analysed following the methods of Grisshammer and Nagai (1995) (see section 2.2.5.3). The pre-lysing and post-lysing samples were analysed for protein solubility using SDS PAGE western blotting (see section 2.2.6.5).

2.2.5.5 Large-scale protein induction

The appropriate strain/plasmid was grown in 5L LBA culture (see section 2.2.1.1 and 2) using a 5L Biolab CP fermentor (Braun) and induced by the corresponding induction method (see section 2.2.5.1 and 2). The cells were grown for 3-4h post-induction at 42°C and harvested (pND707 derived) or 37°C overnight (pWVH57). A 1mL aliquot was removed from the culture just prior to induction (pre-induction sample) and just prior to harvesting the cells (post-induction sample). These samples were processed (see section 2.2.6.1.2) and analysed for protein over-expression using SDS PAGE (see section 2.2.6.1).

The cells were harvested by centrifugation (6,000rpm, 10min, 4^{o}C) and resuspended in 50mL DEAE buffer A corresponding to the over-expressed protein (2.1.3.3). The cell suspension was snap frozen and stored at –70^{o}C until processed further.

2.2.5.6 Uridylylation of PII/GlnK effector-proteins for deadenylylation assays

Uridylylation of the effector-protein PII/GlnK was performed following the methods of Rhee *et al.*, (1989) to produce PII/GlnK protein with covalently bound UMP groups for deadenylylation assays (see section 2.2.10.2.2) The large-scale preparations were also used in SPR (see section 2.2.11).

2.2.5.6.1 Large-scale uridylylation of purified protein

Each reaction was 2mL. Purified PII/GlnK (4mg) (see section 2.2.7.1-4) and partly purified UTase (200μL of ~80% purity) (see section 2.2.7.5) were added to the uridylylation reaction mix (2.1.3.8). The reaction was incubated at 30^{o}C for 30min, then passed through a size exclusion PD-10 column (Pharmacia) to separate the PII/GlnK-UMP from the other reaction constituents. A small aliquot was removed before and after addition of UTase for analysis in native PAGE (see section 2.2.6.2).

One reaction was usually enough for GlnK to become fully uridylylated. To produce fully uridylylated PII the reaction had to be repeated with fresh reaction constituents.

2.2.5.6.2 Small-scale uridylylation of partly purified protein

Each reaction was 200μL. Partly purified PII/GlnK/PII mutant (~100μg) (see section 2.2.7.3) and partly purified UTase (2.2μL of ~0.83mgmL^{-1}) (see section 2.2.7.3) were added to the uridylylation reaction mix (2.1.3.8). The reaction was incubated at 30^{o}C for 30min, then placed at –20^{o}C until used in the deadenylylation assay (see section 2.2.10.2.2). A small aliquot was removed before and after addition of UTase for analysis in native PAGE (see section 2.2.6.2).

2.2.6 Protein separation-polyacrylamide gel electrophoresis (PAGE)

The PAGE gels were prepared following the methods of Laemmli (1970). The gels were cast and run using the Mini-PROTEAN II electrophoresis system at 200V for 30-40min (until the bromophenol blue dye front reached the bottom of the gel) in the appropriate running buffer (2.1.3.3.1 & 2). The gel mixture was not degassed as suggested in the original method.

2.2.6.1 SDS PAGE preparation

2.2.6.1.1 Gel preparation

The acrylamide concentration for the resolving gel was determined by the molecular weight of the proteins of interest.

Resolving gel constituents:

Constituents	Component volumes (mL) for 2 gels			
	8%	10%	12%	15%
ddH_2O	3.5	3.0	2.5	1.75
Tris-HCl (1.5M, pH 8.8)	1.875	1.875	1.875	1.875
SDS (10% w/v)	0.075	0.075	0.075	0.075
Acrylamide/bis (30% v/v of 37.5:1)	2.0	2.5	3.0	3.75
Ammonium persulphate (10% w/v)	0.03	0.03	0.03	0.03
TEMED	0.003	0.003	0.003	0.003

Stacking gel constituents:

Constituents	Volume (mL)
ddH_2O	1.75
Tris-HCl (0.5M, pH 6.8)	0.75
SDS (10% w/v)	0.03
Acrylamide/bis (30% v/v of 37.5:1)	0.45
Ammonium persulphate (10% w/v)	0.025
TEMED	0.003

2.2.6.1.2 Sample preparation

The cells from the pre-induction sample and post-induction sample (1mL) (see sections 2.2.5.3-5) were pelleted by centrifugation (8,000rpm, 10min, room temperature) and resuspended in SDS PAGE sample loading buffer (2.1.3.3.1) to an OD_{595} of 10. This buffer denatures the proteins, reduces disulphide bonds and enables visualisation of the samples progress through the gel. The sample was vortexed, boiled for 2min and vortexed again. The sample was then clarified by centrifugation (13,200rpm, 10min, room temperature) to remove contaminating, denatured chromosomal DNA. The sample was then ready for loading onto the gel.

Small aliquots removed from protein samples throughout the purification process were combined 1:1 with SDS PAGE sample loading buffer (2.1.3.3.1) and boiled for 2min. The sample was then ready for loading onto the gel.

2.2.6.1.3 Molecular weight markers

SDS PAGE gels were routinely run with a low molecular weight standard (BioRad). The standard was diluted 1/20 in SDS PAGE sample loading buffer (2.1.3.3.1), boiled for 2min and stored at –20^{o}C ready for loading onto the gel.

2.2.6.2 Native PAGE preparation

2.2.6.2.1 Gel preparation

The acrylamide concentration for the resolving gel was determined by the molecular weight of the proteins of interest and their surface charge distribution. The gels constituents were essentially the same as for SDS PAGE (see section 2.2.6.1.1) except no SDS was added, and NP40 was added instead (minimise protein aggregation). For the resolving gel 18.5µL of 10% v/v NP40 was added, and for the stacking gel 7.5µL of 10% v/v NP40 was added.

2.2.6.2.2 Sample preparation

Small aliquots removed from purified protein samples before and after uridylylation (see section 2.2.5.6) were combined 1:1 with Native PAGE sample loading buffer (2.1.3.3.2) and were then ready for loading onto the gel.

2.2.6.3 Coomassie staining/destaining of PAGE gels

The PAGE gels (see section 2.2.6) were stained for 30min in Coomassie staining solution (2.1.3.3.1) then destained with destaining solution (2.1.3.3.1) until the gel background was clear. This usually involved several changes of the destaining solution and the whole process was performed at room temperature.

2.2.6.4 Drying Coomassie stained gels

The stained PAGE gel (see section 2.2.6.3) was soaked in a 20% v/v methanol solution for 20min at room temperature to minimise cracking in the drying process. The gel was then rinsed in ddH_2O and placed between 2 sheets of cellulose acetate film (pre-soaked in ddH_2O) supported in a drying frame. The gels were placed in a fumehood to air dry overnight.

2.2.6.5 Western blot analysis of PAGE gels

Western blot analysis was performed following the methods of Towbin *et al.*, (1979).

2.2.6.5.1 Protein transfer to nitrocellulose membrane

Nitrocellulose membrane (BioRad) was soaked in the appropriate transfer buffer (2.1.3.4), then placed in a Mini Trans-Blot module (BioRad) with the electrophoresed gel (see section 2.2.6). The separated proteins were transferred from the gel to the membrane for 1h at 80V in the appropriate transfer buffer (2.1.3.4). The membrane was then rinsed in TBS buffer (2.1.3.4) (2x, 5min), and blocked with MTBS buffer (2.1.3.4) for 30min at room temperature.

2.2.6.5.2 Immunoblotting the nitrocellulose membrane

The membrane was probed with primary antibody (test bleed eluate, hybridoma supernatant, crude monoclonal/polyclonal ascitic fluid or purified monoclonal/polyclonal ascitic fluid) diluted in MTTBS (2.1.3.4) at room temperature for 1h (or overnight), with gentle shaking. The membrane was then rinsed with TTBS (2.1.3.4) (4x, 5min). The membrane was probed further with secondary antibody conjugated to alkaline phosphatase (2.1.2.3) diluted in MTTBS (2.1.3.4) at room temperature for 1h, with gentle shaking. The membrane was then rinsed with TTBS (2.1.3.4) (2x, 5min) and TBS (2.1.3.4) (2x, 5min), drained and soaked for 10min in alkaline phosphatase buffer (2.1.3.4). Colour development followed addition of the chromagenic substrates NBT (0.03%w/v) and BCIP (0.016% w/v) with gentle rocking for ~10min. EDTA (20mM) was added to stop colour development, by chelating free Mg^{2+} ions and arresting phosphatase activity. The membrane was rinsed with TBS (2.1.3.4) (2x, 5min) and ddH_2O (2x, 5min), drained and dried between chromatography paper sheets (Whatman). The membranes were stored in the dark between chromatography paper (Whatman) and plastic film.

2.2.7 Protein purification

2.2.7.1 French press cell lysis

The cell suspension (see section 2.2.5.5) was thawed and pressed twice under 16,000 psi pressure using a FRENCH Pressure cell press (SIM AMINCO). Part way through the study the method was changed to include a protease inhibitor cocktail (7.2mM β-mercaptoethanol, 2μM PMSF, 4μM pepstatin, 1μM leupeptin), which was added to the cells suspension prior to and after lysing the cells. The cellular debris was removed from the preparation by centrifugation (18,000rpm, 30min, 4^{o}C). A small aliquot was removed from the clarified supernatant for analysis in SDS PAGE (see section 2.2.6.1).

2.2.7.2 DNA precipitation

DNA was removed from the clarified cell free extract (see section 2.2.7.1 and 2.2.5.3) by streptomycin sulphate (1.5% w/v) precipitation. The solution was stirred or shaken at 4^{o}C for 15min then the precipitated, contaminating DNA removed by centrifugation (18,000rpm for large-scale and 13,200rpm for small-scale, 30min, 4^{o}C). A small aliquot was removed from the clarified supernatant for analysis in SDS PAGE (see section 2.2.6.1).

2.2.7.3 Protein precipitation

Ammonium sulphate (144mgmL^{-1}) was slowly added to the DNA-free supernatant (see section 2.2.7.2) with stirring at 4^{o}C. The solution was stirred or shaken for 30min at 4^{o}C. The precipitated, contaminating, cellular protein was removed by centrifugation (18,000rpm for large-scale and 13,200rpm for small-scale, 30min, 4^{o}C). A small aliquot was removed from the clarified supernatant for analysis in SDS PAGE (see section 2.2.6.1).

Further ammonium sulphate (64-256mgmL^{-1}) was slowly added to the supernatant with stirring at 4^{o}C. The solution was stirred or shaken for 30min at 4^{o}C. The precipitated

protein was removed by centrifugation (18,000rpm for large-scale and 13,200rpm for small-scale, 30min, 4^{o}C), and resuspended in the appropriate chilled DEAE buffer A (2.1.3.3) (original supernatant volume). A small aliquot was removed from the resuspended pellet and supernatant waste for analysis in SDS PAGE (see section 2.2.6.1). The small-scale protein solutions processed this way were used for all the *in vitro* assays where partly purified cell lysates were used.

2.2.7.4 DEAE Fractogel chromatography

The partly purified large-scale protein solution (see section 2.2.7.3) was purified further using anion exchange chromatography in the low-pressure chromatography EconoSystem (BioRad).

Initially, the protein solution was dialysed against three changes of the appropriate chilled DEAE buffer A (2.1.3.3) at 4^{o}C, with stirring to remove the residual ammonium sulphate. The [protein] of the sample was roughly determined by measuring the OD_{280} (OD_{280} of 1=~1mgmL^{-1}), then diluted in appropriate DEAE buffer A (2.1.3.3) to ~5mgmL^{-1}. The diluted sample was sterilised through a 0.22μm syringe filter to ensure all particulate matter was removed before application to the Fractogel TSK DEAE-650 matrix (Merck), which was pre-equilibrated with the appropriate DEAE buffer A (2.1.3.3).

All the chromatography was performed at 4^{o}C with a flow rate of 2mLmin^{-1}. The column was rinsed with the appropriate DEAE buffer A (2.1.3.3) (3 column volumes) to remove unbound proteins. The bound proteins were eluted over a linear gradient from 0 to 1M NaCl. The column was cleaned with the appropriate DEAE buffer B (2.1.3.3) (3 column volumes) to remove contaminating bound proteins, then re-equilibrated with the appropriate DEAE buffer A (2.1.3.3) (5 column volumes). Protein elution was detected with an UV monitor at λ 280nm. A small aliquot was removed from the eluted fractions of interest for analysis in SDS PAGE (see section 2.2.6.1). Fractions which contained the protein of interest were pooled, then diluted for reapplication to the column. In the second pass through the matrix, isocratic steps were introduced to separate peaks

containing contaminating proteins close to the target protein peak in the first chromatographic step. A small aliquot was removed from the eluted fractions of interest for analysis in SDS PAGE (see section 2.2.6.1). Fractions which contained the purified, target protein, were pooled.

The purified protein was concentrated, and the buffer exchanged back to the appropriate DEAE buffer A (2.1.3.3), by removing the NaCl using an Ultrafree 15mL concentrator (Millipore). The concentration of the purified protein was determined using the Bradford method (see section 2.2.8.1), and the concentrated protein stored in aliquots (200μL) at –70^{o}C.

2.2.7.5 Purification of UTase protein for uridylylation assays

AN1459 cells (2.1.4) containing the pNV101 plasmid (2.1.6.2) were used to express UTase protein. Large-scale cultures were used for protein over-expression (see section 2.2.5.5). Purification of this protein followed sections 2.2.7.1-4. This protein was prone to proteolysis in the initial dialysing step, so the protease inhibitor cocktail was included in the lysis step (see section 2.2.7.1). The second ammonium sulphate precipitation was 256mgmL^{-1} (see section 2.2.7.3).

2.2.7.6 Purification of ATase/AT-C_{518}/AT-N_{440} proteins for adenylylation and deadenylylation assays

JM109 cells (2.1.4) containing the pRJ009, pDW4 and pDW1 plasmids (2.1.6.2) were used to express ATase, AT-C_{518} and AT-N_{440} proteins, respectively. Large-scale cultures were used for protein over-expression (see section 2.2.5.5). Purification of these proteins followed sections 2.2.7.1-4. The second ammonium sulphate precipitation was 256mgmL^{-1} (see section 2.2.7.3).

2.2.7.7 Purification of PII protein for adenylylation assays

RB9040 (*glnD*$^-$) cells (2.1.4) containing the pRJ001 plasmid (2.1.6.2) were used to express PII protein (with no UTase present these cells could not uridylylate the over-expressed PII protein). Large-scale cultures were used for protein over-expression (see section 2.2.5.5). Purification of these proteins followed sections 2.2.7.1, 3 and 4. The streptomycin sulphate precipitation step (see section 2.2.7.2) was replaced with a β-mercaptoethanol precipitation step (Vasudevan *et al.*, 1994), after the ammonium sulphate precipitation step (only one precipitation of 400mgmL^{-1}) (see section 2.2.7.3).

β-mercaptoethanol (26%) was added at room temperature (fumehood) with stirring. The solution was stirred for a further 20min, and the contaminating, precipitated protein removed by centrifugation (18,000rpm, 30min, 4^{o}C). A small aliquot was removed from the clarified supernatant for analysis in SDS PAGE (see section 2.2.6.1). This solution was then processed by DEAE anion exchange chromatography (see section 2.2.7.4).

2.2.7.8 Purification of GlnK protein for adenylylation assays

RB9040 (*glnD*$^-$) cells (2.1.4) containing the pNV103 plasmid (2.1.6.2) were used to express GlnK protein (with no UTase present these cells could not uridylylate the over-expressed GlnK protein). Large-scale cultures were used for protein over-expression (see section 2.2.5.5). Purification of these proteins followed section 2.2.7.7.

The GlnK protein solution (see section 2.2.7.7) received one more purification step using cybacron blue matrix (binds nucleotide binding proteins) in the low-pressure chromatography EconoSystem (BioRad). The method used was the same as section 2.2.7.4, except that the matrix was cybacron blue-agarose and there was only the initial pass through the matrix (no isocratic steps).

2.2.7.9 Purification of GS/GS-AMP proteins for aden/deadenylylation assays

RB9017 (*glnE*$^-$) cells (2.1.4) containing the pWVH57 or pJRV001 plasmid (2.1.6.2) were used to express GS protein (with no ATase present these cells could not adenylylate the over-expressed GS protein). DH5α cells containing the pWVH57 plasmid (2.1.6.2) grown under high nitrogen conditions (NH_4Cl at 0.5%, w/v, in growth medium) were used to produce the covalently modified form of GS; GS-AMP (n~11, where n represents the average state of adenylylation of GS monomers from 1-12; see section 2.2.10.2.3). Large-scale cultures were used for protein over-expression (see section 2.2.5.5).

Purification followed the methods of Shapiro and Stadtman, (1970) and was not the same as the purification methods used for the other proteins used in this work. The methods were the same up to the removal of the chromosomal DNA (see section 2.2.7.2).

The pH of the DNA-free supernatant was adjusted to pH 5.2 (1M acetic acid) and the solution was stirred for 15min at 4^{o}C. Contaminating, precipitated protein was removed by centrifugation (18,000rpm, 30min, 4^{o}C). A small aliquot was removed from the clarified supernatant for analysis in SDS PAGE (see section 2.2.6.1).

Ammonium sulphate (176mgmL^{-1}) was slowly added to the supernatant with stirring at 4^{o}C, and the pH of the solution was adjusted to pH 4.6 (1M acetic acid). The solution was stirred for 1h at 4^{o}C, then the pH was readjusted to pH 4.6 and the solution stirred a further 1h at 4^{o}C (or overnight at 4^{o}C). The precipitated protein was removed by centrifugation (18,000rpm, 30min, 4^{o}C), and resuspended in 50mL chilled GS buffer (2.1.3.3)/5L of original bacterial culture. A small aliquot was removed from the resuspended pellet and supernatant waste for analysis by SDS PAGE (see section 2.2.6.1).

The pH of the resuspended pellet was adjusted to pH 5.7 (1M NH_4OH). The solution was stirred for 1h at 4°C, the pH was readjusted to pH 5.7, and the solution stirred for a further 1h at 4°C. Contaminating, precipitated protein was removed by centrifugation (18,000rpm, 30min, 4°C). A small aliquot was removed from the clarified supernatant for analysis in SDS PAGE (see section 2.2.6.1).

The temperature of the supernatant was raised to 63°C with constant swirling for 10min and then cooled for 5min on ice with constant swirling. The denatured, contaminating protein was removed by centrifugation (18,000rpm, 30min, 4°C). A small aliquot was removed from the clarified supernatant for analysis in SDS PAGE (see section 2.2.6.1). Ammonium sulphate (176mgmL^{-1}) was slowly added to the supernatant with stirring at 4°C, the pH of the solution was then adjusted to pH 4.4 (1M acetic acid). The solution was stirred for 1h at 4°C and the pH of the solution was then readjusted to pH 4.4 and stirred for a further 1h at 4°C (or overnight at 4°C). The precipitated protein was removed by centrifugation (18,000rpm, 30min, 4°C), and resuspended in 15mL chilled GS buffer (2.1.3.3)/5L of original bacterial culture. A small aliquot was removed from the resuspended pellet and supernatant waste for analysis by SDS PAGE (see section 2.2.6.1).

The pH of the resuspended pellet was adjusted to pH 5.7 (1M NH_4OH). The solution was stirred for 1h at 4°C and the pH of the solution was then readjusted to pH 5.7 and stirred a further 1h at 4°C. Contaminating, precipitated protein was removed by centrifugation (18,000rpm, 30min, 4°C). A small aliquot was removed from the clarified supernatant for analysis in SDS PAGE (see section 2.2.6.1). The resulting protein preparations were ~95-99% pure.

The purified protein was concentrated using an Ultrafree 15mL concentrator (Millipore). The concentration of the purified protein was determined using the Bradford method (see section 2.2.8.1), and the concentrated protein stored in aliquots (200μL) at –70°C. The purified GS was used in the adenylylation assay (see section 2.2.10.2.1) and the purified GS-AMP was used in the deadenylylation assay (see section 2.2.10.2.2).

2.2.8 Protein quantification

2.2.8.1 Total solution: Bradford assay

The concentration of proteins in solution was measured following the method of Bradford (1976) using Coomassie Blue G-250 protein assay dye (BioRad). A series of standards (2, 3, 4, 5, 6, 7, 8 and 9 μg of BSA) were added to 800μL of ddH_2O, and various dilutions of the unknown sample were also diluted this way. Two hundred μL of dye reagent was added to each protein dilution and the reaction was incubated at room temperature for 30min and transferred to a 96 well "U" bottom plate (Sarstedt). The optical density was measured at λ 595nm. The OD_{595} values ("y" axis) were plotted against the amount of protein standard ("x" axis). A standard curve was generated by linear regression using Microsoft Excel. The unknown sample concentration was determined by substituting the measured OD_{595} for the "y" value in the equation for the standard curve.

2.2.8.2 Individual bands on gel: known standards

The [target protein] in the cell lysates (see section 2.2.5.3) and partly purified cell lysates (see section 2.2.7.3) was determined by visual comparison with known standards in a SDS PAGE gel. Bradford assays could not be used due to the low purity of the protein preparations and differing levels of over-expression between the various proteins.

Two 15% SDS PAGE gels (see section 2.2.6.1) were run with purified PII protein (see section 2.2.7.7). A 10-well comb (0.5, 1, 1.5, 2, 2.5, 3, 3.5 and 4μg) and a 15-well comb (0.25, 0.5, 1, 1.5, 2, 2.5, 3, 3.5, 4, 4.5, 5, 5.5 and 6μg) were used. Two of each gel were run, so one could be Coomassie stained (see section 2.2.6.3) and dried (see section 2.2.6.4), and one could be visualised by Western blot (see section 2.2.6.5). The same procedure was repeated with AT-C_{522} (see section 2.2.7.6) using 12% SDS PAGE gels (see section 2.2.6.1). These gels became the standard curves. From the standard curves the range of protein bands which can be visually distinguished is 0.5-3μg. The protein

preparations were diluted and run in the appropriate SDS PAGE gels (see section 2.2.6.1), aiming for a 1.5μg band for visual comparison with the standard curve.

2.2.9 Production of monoclonal antibodies

2.2.9.1 Myeloma (Sp2/0) cell line culture

The Sp2/0 myeloma cells (Schulman *et al.*, 1978) were cultured in Sp2/0 media (2.1.9) and grown at 37^{o}C, in a humidified, CO_2 (5%) environment. The cells were maintained in 50mL of medium in 75cm^2 flasks. They were passaged every 3-4d by aspiration with a sterile, plugged pasteur pipette, and a 1 in 4 split with pre-warmed media (37^{o}C).

2.2.9.2 Mouse sarcoma cell line culture

The mouse sarcoma 180 cells (Tikasingh *et al*., 1965) were cultured in BALB/c mice. The mice were inoculated IP with 400μL of sarcoma 180 cells. The abdomens of the mice started to show distension after 10 days, at which time they were euthenased with CO_2 gas, and the ascitic fluid harvested aseptically. The ascitic fluid was mixed with sterile calf serum (50%) then aliquoted (1mL) into cryotubes (Nunc) and stored in liquid nitrogen.

2.2.9.3 Immunisation of mice

Groups of 10 BALB/c mice (same sex), 8-10wk old were regularly inoculated (intraperitoneally, IP) with 50μg of Ag (protein) and monitored by ELISA (see section 2.2.10.4) for Ab responses. A double emulsion in Freund's complete adjuvant (2.1.1) was given as the primary inoculum, and the ensuing boosts used Freund's incomplete adjuvant (2.1.1). Both monoclonal and polyclonal Ab preparations were produced from mice immunised this way.

2.2.9.3.1 Preparation of the inoculum

A double emulsion preparation of the Ag (protein) was prepared following the method of Goding (1983). Initially the protein was diluted to 200μgmL^{-1} in PBS (2.1.3.1) and then combined 1:1 with Freund's adjuvant (2.1.1). Repeated aspiration with a needle (18 gauge) and syringe was used to emulsify the two phases. When the Ag was thoroughly dispersed throughout the adjuvant the solution went white and was very viscous. An equal volume of double emulsion solution (2.1.3.1) was added to the adjuvant mixture and the emulsion aspirated again. The mice were injected with 200μL of emulsion IP using a 25-gauge needle and syringe.

2.2.9.3.2 Immunisation schedule

The inoculation schedules were different for mice producing monoclonal and polyclonal Ab preparations.

Day	Monoclonal	Polyclonal
0	Primary	Primary
7		Boost 1
14		Boost 2
21		Boost 3
28	Boost 1	Boost 4
35		Boost 5
42	Boost 2	Boost 6
46		Sarcoma cells
49		Boost 7 (IV also)
56	Boost 3	Harvest
	Boost (IV also)/ harvest spleens as needed	

2.2.9.3.3 Tail bleeding of mice

The Ab responses in the mice were constantly monitored using ELISA (see section 2.2.10.4). The ELISA used a small amount of serum (10μL), which was extracted from the mouse by a tail bleed (Harlow and Lane, 1988). The mice were bled 4d after each boost, and prior to the primary inoculation and harvest.

The serum was collected on filter paper discs (TropBio) from a scalpel nick in the tail vein. The discs were air-dried then stored at –20^{o}C in a sealed bag until needed.

The Abs were eluted from the paper disc at 4^{o}C overnight in 500µL of TEN-T-C (2.1.3.5). This solution was essentially a 1/50 dilution of the antiserum and was titrated in ELISA (see section 2.2.10.4) to assess the level of Ab response. The eluate was stored at –20^{o}C until needed.

2.2.9.3.4 Pre-harvest inoculation

To maximise the immune response at the time of harvest (spleen for monoclonal preparation and ascitic fluid for polyclonal preparation), an extra 10µL inoculation of protein diluted to 200µgmL^{-1} in PBS (2.1.3.1) was inoculated intravenously (30 gauge needle) into the tail vein. This extra boost was given 4d before harvest.

2.2.9.4 Production of ascitic fluid

2.2.9.4.1 Monoclonal antibody

Production of mAbs as ascitic fluid in mice was carried out following the method of Goding (1983). At least one week prior to inoculating the mice with hybridoma cells the mice were inoculated IP with pristane (200µL/mouse). Hybridoma cell lines, which had been cloned by limiting dilution (at least twice) (see section 2.2.9.6.3), were cultured into 6x75cm^{2} culture flasks to produce confluent monolayers. The cells were harvested by centrifugation (1,000rpm, 10min, room temperature) and resuspended in DMEM media (Gibco). The cells were inoculated IP into 8x BALB/c mice. When the abdomens of the mice started to show distension they were euthenased with CO_2 gas, and the ascitic fluid harvested.

The ascitic fluid was removed from the body cavity using an 18-gauge needle and syringe. PMSF (1µM) was added to the ascitic fluid to inhibit protease activity. The serum was clarified by centrifugation (3,000rpm, 15min, 4^{o}C) and more PMSF (1µM)

was added to the supernatant. The mAb preparation was stored in aliquots at –20^{o}C until needed. The mAb preparation was titrated in ELISA (see section 2.2.10.4) to determine the titre.

2.2.9.4.2 Polyclonal antibody

High titre polyclonal antiserum was produced from ascitic fluid by the method of Tikasingh *et al.*, (1965). Mice were inoculated following the schedule in section 2.2.9.3.2. The abdomens of the mice (inoculated with 400µL of sarcoma 180 cells IP) started to show distension after 10 days, at which time they were euthenased with CO_2 gas, and the ascitic fluid harvested.

The procedure for clarifying and storing the polyclonal Ab preparation was the same as the method for the mAb preparation (see section 2.2.9.4.1).

2.2.9.5 Fusion of splenocytes and myeloma cells

Fusion of the immunised mouse splenocytes to the myeloma cells (Sp2/0) was performed following the method of Harlow and Lane, (1988).

2.2.9.5.1 Preparation of the myeloma cells

The day before the fusion the Sp2/0 cells were aspirated from the surface of a 50mL culture flask and counted in a haemocytometer (stained trypan blue 0.14%). The cells were pelleted by centrifugation (1,000rpm, 10min, room temperature) and the cell concentration adjusted to 5 x 10^5 cellmL^{-1} with fresh Sp2/0 medium (2.1.9). The cells were then placed back into the original "conditioned" culture flask.

The next day, prior to the fusion the cells were again aspirated from the surface of the flask, 10mL of the cell suspension was added to 10mL of fusion medium (2.1.9) supplemented with calf serum (20%) and OPI (2%). This 20mL suspension of Sp2/0 cells was used in the fusion.

2.2.9.5.2 Preparation of the spleen cells

On the fourth day after the final boost (IP & IV) the mouse was euthenased and the spleen removed aseptically and placed in 20mL of fusion medium (2.1.9) (37^{o}C). To minimise the chances of contamination, the spleen was transferred to another laminar flow cabinet where the fusion was performed.

The splenocyte suspension was prepared in a petri dish using a needle (25 gauge) and syringe (10mL). Medium was repeatedly injected into the spleen using the needle and syringe until the spleen became transparent. A pair of bent needles (18 gauge); were used to massage the remaining connective tissue capsule to further dislodge splenocytes still inside the spleen capsule. The connective tissue remnants were discarded and the cell suspension was drawn through the needle several more times to break up cell clumps. The splenocyte suspension was transferred to a 50mL centrifuge tube ready for the fusion. The petri dish was rinsed with a further 10mL of fusion medium (2.1.9) (37^{o}C) and the rinse was added to the 50mL centrifuge tube also.

2.2.9.5.3 Fusion by stirring

The fusion procedure was based on the original techniques of Galfre *et al.*, (1977), and the adaptations by Harlow and Lane, (1988).

The splenocytes were pelleted by centrifugation (400g, 5min, room temperature) and resuspended in 20mL of fusion medium (2.1.9) (37^{o}C). Then both the splenocyte suspension and the Sp2/0 suspension were pelleted by centrifugation (400g, 5min, room temperature) and resuspended in 20mL of fusion medium (2.1.9) (37^{o}C) for a further rinse. Both the cells were pelleted as before then resuspended in 10mL of fusion medium (2.1.9) (37^{o}C) and combined. The mixed cell suspension was pelleted by centrifugation (800g, 5min, room temperature) and the supernatant discarded.

The cells were fused with a 50% PEG_{1500} solution (Sigma). One mL of the PEG solution was added dropwise to the mixed cell pellet with stirring over 1min with a

sterile, plugged pasteur pipette, stirring continued for a further minute. Then 1mL of fusion media (2.1.9) (37^{o}C) was added dropwise with stirring over 1min from a 10mL pipette, followed by 9mL of fusion medium (2.1.9) (37^{o}C) with stirring over 2min, using the same pipette.

The fused cells were pelleted by centrifugation (400g, 5min, room temperature) and resuspended in 200mL of HAT selective hybridoma medium (2.1.9) (37^{o}C) then plated out into 96 well plates (100μLwell^{-1}). A further 100μLwell^{-1} of HAT selective hybridoma medium (2.1.9) (37^{o}C) was added to the plates 4-5d and 8-10d later. The plates were grown at 37^{o}C in a humidified, CO_2 (5%) environment.

2.2.9.6 Hybridoma cell line culture

The hybridoma cells were always grown in a 37^{o}C, humidified, CO_2 (5%) environment. All the stages of hybridoma culture were checked for growth under the inverted microscope every 3-4d. Cell culture supernatant from the hybridomas was also routinely screened in ELISA (see section 2.2.10.4) at all stages to ensure that time was not wasted culturing cells which no longer secreted Ab.

2.2.9.6.1 Preliminary hybridoma cell line culture

Examination of the wells in the 96 well plates by inverted microscope started at ~10d. The hybridomas appeared as large, round, luminous cells. When the fastest growing cells reached about 80% confluency of the well, the culture supernatants from all the wells on the 96 well plates were screened for Ab secretion by ELISA (see section 2.2.10.4). Wells which housed positive Ab secreting hybridomas were noted and cultured further.

2.2.9.6.2 Subsequent hybridoma cell line culture

Passaging of all the hybridomas at all the stages was carried out aseptically in a laminar flow cabinet. Cells were dislodged from plastic surfaces by aspiration with sterile,

plugged pasteur pipettes and cultured at ~80-90% confluency. Whenever a cell line was passaged up to the next level it was still maintained in the original source. For example when cells were taken from 96 well to 24 well culture, a portion of the cells were left behind in the 96 well plate, and topped up with fresh medium to continue growing. Newly formed hybridoma cells often die when transferred to a fresh "unconditioned" plastic surface.

Cells transferred from 96 well to 24 well culture were cultured in HT selective hybridoma medium (2.1.9) (37^{o}C). Cells transferred from 24 well to 25cm^{2} flask culture were cultured in hybridoma medium (2.1.9) (37^{o}C), and all ensuing passages from this point used hybridoma medium (2.1.9) (37^{o}C).

2.2.9.6.3 Single cell cloning by limiting dilution

Once the hybridoma cell line had undergone cryopreservation (see section 2.2.9.6.4) and thawing (see section 2.2.6.9.6.5), if it was still secreting Abs it could be cloned by limiting dilution following the method of Goding (1983). The cells were counted and diluted in cloning medium (2.1.9) (37^{o}C) to 20cellsmL^{-1}, then added to a plate divided into 4 sections with 4, 2, 1 and 0.5 cellswell^{-1} in each section. Each well was topped up with cloning medium (2.1.9) (37^{o}C) to 200μL.

The cloning plates were assessed and passaged in the same manner as the fusion plates (see sections 2.2.9.6.1 and 2), except there is no HAT or HT to be omitted from the medium with subsequent passages, only OPI.

For a cell line to be considered monoclonal there were two criteria to be fulfilled:

1. All the wells on the cloning plate with cells must have activity in ELISA (see section 2.2.10.4) for two successive cloning runs.
2. Titration of the cell culture supernatant from cryopreserved (see section 2.2.9.6.4) cloned cell lines must produce the same curves in ELISA (see section 2.2.10.4) for two successive cloning runs.

2.2.9.6.4 Cryopreservation of hybridoma cell lines

Hybridoma/Sp2/0 cell lines were stored in liquid nitrogen. Cells from 25cm^2 flasks were pelleted by centrifugation (1,000rpm, 10min, room temperature) and resuspended in 800µL hybridoma/Sp2/0 medium (2.1.9) (37^{o}C). The cell suspension was transferred to a 1mL cryotube (NUNC), which already contained 100µL of DMSO. The cells were quickly mixed into the DMSO, then the tube was placed in a cryocane and stored at –70^{o}C overnight, before being shifted to liquid nitrogen storage.

The supernatant from the pelleted hybridomas was retained. Na azide was added (0.1%) to the supernatant to inhibit growth of any contaminating organisms with subsequent use. The supernatant was stored at 4^{o}C. This supernatant was used for all the isotyping assays (see section 2.2.9.7). It was also used for all the screening ELISAs (see section 2.2.10.4) using different point mutations of the PII protein and truncations of the ATase protein.

2.2.9.6.5 Thawing cell lines from liquid nitrogen

The cryotube containing the cells, which had been stored in liquid nitrogen (see section 2.2.9.6.4), was placed in hot tap water until the cell suspension was liquid. The cells were then transferred to 10mL of hybridoma/Sp2/0 medium (2.1.9) (37^{o}C). The diluted cells were pelleted by centrifugation (1,000rpm, 10min, room temperature) and resuspended in 10mL hybridoma/Sp2/0 medium (2.1.9) (37^{o}C) and transferred to a 25cm^2 flask for culture.

2.2.9.7 Isotyping monoclonal antibodies

Supernatant from hybridoma cell culture (see section 2.2.9.6.4) was used to determine the isotype of the Abs being secreted by the various hybridoma cell lines. The isotyping method was adapted from the basic ELISA (see section 2.2.10.4). The GαM-HRPO conjugated secondary antibody step (step 5) was replaced with the following steps:

5a. GαM-isotype antibody diluted in TEN-T-C (2.1.3.5) was added to the plate (50μLwell^{-1}) and incubated at room temperature for 1h.

5b. The plate was washed 4 times with TEN-T (2.1.3.5) and the plates tapped dry on paper towelling.

5c. RαG-HRPO conjugated secondary antibody diluted in TEN-T-C (2.1.3.5) was added to the plate (50μLwell^{-1}) and incubated at room temperature for 1h.

2.2.9.8 Purification of antibodies using protein A agarose chromatography

The Ab solution (see section 2.2.9.4) was purified further using protein A agarose chromatography and the MAPS II purification system (BioRad) (2.1.1) in the low-pressure chromatography EconoSystem (BioRad).

Initially, the Ab solution was diluted 1:1 in the MAPS II binding buffer (BioRad) (2.1.1). The diluted sample was sterilised through a 0.22μm syringe filter to ensure all particulate matter was removed before application to the protein A agarose matrix (BioRad) (2.1.1). The matrix was pre-equilibrated with the MAPS II binding buffer (BioRad) (2.1.1).

All the chromatography was performed at 4^{o}C with a flow rate of 2mLmin^{-1}. The sample flow through was reapplied to the column at least 5 times. The column was rinsed with the MAPS II binding buffer (BioRad) (2.1.1) (3 column volumes) to remove unbound proteins. The bound Ab was eluted with MAPS II elution buffer (BioRad) (2.1.1) (5 column volumes). The column was cleaned with the MAPS II regeneration buffer (BioRad) (2.1.1) (5 column volumes) to remove contaminating bound proteins then re-equilibrated with the MAPS II binding buffer (BioRad) (2.1.1) (3 column volumes). Protein elution was detected with an UV monitor at λ 280nm. There was only one elution peak. The fractions were pooled and a small aliquot was removed for analysis in SDS PAGE (see section 2.2.6.1) and ELISA (see section 2.2.10.4).

The purified Ab was concentrated and the buffer exchanged back to the MAPS II binding buffer (BioRad) (2.1.1) using an Ultrafree 15mL concentrator (Millipore). The

concentration of the purified protein (mAb) was determined using the Bradford method (see section 2.2.8.1), and the concentrated purified mAb stored in aliquots (200µL) at –70^{o}C.

2.2.10 *In vitro* assays

2.2.10.1 Uridylylation assay

2.2.10.1.1 Steady state assay

This assay monitors the degree of uridylylation of PII/GlnK/PII mutants by measuring the incorporation of UMP [^{3}H]. The method essentially follows that of Rhee *et al*., (1989).

Each reaction was 1mL. Purified PII/GlnK/PII mutant (4.3µM) (see sections 2.2.7.7 and 8) was added to the uridylylation reaction mix (2.1.3.8) to which UTP [^{3}H] (2µCi) was also added. Pre-warmed (30^{o}C) partly purified UTase (100µL of ~80% purity) (see section 2.2.7.5) was added to initiate the reaction. The reaction mix was also pre-warmed at 30^{o}C. The reaction was carried out in a 30^{o}C waterbath.

At various time points (0, 1, 2, 5, 10, 20, 60, 90 and 120min) a 100µL aliquot was removed from the reaction and added to a microfuge tube on ice containing 500µL of BSA (0.1mgmL^{-1}). The proteins were precipitated by addition of 500µL of chilled 20% w/v TCA solution, and incubation on ice for at least 30min (Ausubel *et al.*, 1994).

The precipitated protein was pelleted by centrifugation (13,200rpm, 10min, 4^{o}C) and rinsed 8 times with chilled TCA solution (5% w/v). The residual TCA was removed by aspiration and 100µL of ddH_2O added to the protein pellet. The sample was vortexed (30s), sonicated (10min) and vortexed (30s) before adding 1mL of Ecolite scintillation fluid (ICN). The radioactivity level of the samples was read with 1min exposure times on the 1410 liquid scintillation counter (Wallac).

2.2.10.1.2 Initial rate assay

This assay was the same as the steady state assay (see section 2.2.10.1.1), except the time points were 0, 1, 2, 5, 10, 15 and 20min, and the amount of partly purified UTase (~80% purity) (see section 2.2.7.5) added was reduced. The UTase (12μL) was made up to 100μL for addition to the assay with 20mM HEPES pH7.5.

2.2.10.1.3 Conversion of DPM values to [bound radio-ligand]

The conversion of the DPM to the concentration of bound radio-ligand followed the method of Hulme (1990).

Measured DPMs were converted to μM bound radioactive effector using the equation:

$$RL\ (nM) = \frac{B\ (DPM)}{\text{Volume (mL)} \times \text{Specific activity (Cimmol}^{-1}) \times 2220 \times \text{dilution factor}}$$

Curves were generated in Microsoft Excel by plotting [bound radio-ligand] ("y" axis) against time ("x" axis). Linear regressions were generated from the initial rate assays using Microsoft Excel.

2.2.10.2 GS activity assays

The activities of ATase were monitored in a coupled assay. The first step involves ATase adenylylating GS or deadenylylating GS-AMP. The second step utilises the γ-glutamyl transferase activity of GS using ammonium hydroxide as a substrate. The γ-glutamylhydroxamate (γ-GH) produced by GS can be detected at OD_{492}. Adenylylation of GS impacts on this activity, so the degree of adenylylation can be determined (Stadtman *et al.*, 1979). These assays were carried out in 96 well "U" bottom plates (Sarstedt) at 30^{o}C following the method of van Heeswijk et al., (1996).

2.2.10.2.1 Adenylylation assay

Adenylylation assay mix (2.1.3.7) (for the purposes of this work the concentrations used in 2.1.3.7 will be called standard conditions) with various combinations of proteins and small effector-molecules (150μL) was added to row A of the plate (in duplicate). ATase/truncations/mutants were diluted in BSA (1mgmL^{-1}) with PEG_{6000} (10% w/v) and added to row B (100μL) in duplicate. One hundred μLwell^{-1} γ-glutamyl transferase assay mix B (2.1.3.7) was added to the rest of the plate. One hundred μL of assay mix was removed from row A and added to row B to initiate the reaction. Ten μL of reaction mix was removed from row B, and added to the secondary assay mix at various time points (0, 1, 2, 3, 4, 5, 10, 16, 23, 30, 36, 47, 61 and 90min), following initiation of the reaction. The second reaction was incubated for 30min and stopped with addition of 200μL of GS assay stop mix (2.1.3.7). Colour development was measured as absorbance at OD_{492} and curves were generated in Microsoft Excel by plotting [γ-GH] ("y" axis) against time ("x" axis).

2.2.10.2.2 Deadenylylation assay

The deadenylylation assay was the same as the adenylylation assay (see section 2.2.10.2.1), except deadenylylation assay mix (2.1.3.7) (for the purposes of this work the concentrations used in 2.1.3.7 will be called standard conditions) was used in row A instead of adenylylation assay mix.

2.2.10.2.3 Determination of GS adenylylation state

Ten μL of purified GS/GS-AMP (2.2.7.9) was added to 100μL each of γ-glutamyl transferase assay mix A, B, C and D (2.1.3.7) and incubated in a plate for 30min at 30^{o}C. The reactions were stopped by addition of 200μL of GS assay stop mix (2.1.3.7). Colour development was measured as absorbance at OD_{492}. The mean state of adenylylation (n) was determined using the following equation:

$$n= 12-12\ (((OD_{492}\ B)-(OD_{492}\ A))/((OD_{492}\ D)-(OD_{492}\ C))).$$

2.2.10.2.4 Initial rate assay

This assay was the same as the above assays (see sections 2.2.10.2.1 and 2). Except the time points were only 0, 1, 2, 3, 4, and 5min. Colour development was measured as absorbance at OD_{492} and curves were generated in Microsoft Excel by plotting [γ-GH] ("y" axis) against time ("x" axis). Linear regressions were generated from the curves using Microsoft Excel.

2.2.10.3 Direct binding of radiolabelled small effector-molecules

The direct binding of small effector-molecules was measured following the method of Kamberov *et al.*, (1995b). This is a very simple method utilising radio-labelled forms of the small effector-molecules e.g. ATP [^{14}C], α-kg [^{14}C] and gln [^{14}C], and determining the difference between radioactivity of the reaction mix before and after passing through a microconcentrator. The complexed protein+small-effector molecules are retained and the unbound radiolabelled small effector-molecules pass through the membrane.

Proteins were diluted (10μM) in small effector binding assay buffer (2.1.3.9) with the radiolabelled small effector-molecule and any companion small effector-molecules if necessary, and incubated for 30min at room temperature. Ten μL of reaction mix was removed from the reaction and added to 1mL of Ecolite scintillation fluid (ICN). The rest of the reaction mix was loaded into a 5,000nwt microconcentrator (Millipore) and centrifuged at 2,000rpm (room temperature) until half the reaction mix had passed through the membrane. Ten μL of the filtrate was added to 1mL of Ecolite scintillation fluid (ICN). The radioactivity level of both the samples was read with 1min exposure times on the 1410 liquid scintillation counter (Wallac). The DPM were then converted to [bound radio-ligand] (see section 2.2.10.1.3).

2.2.10.4 ELISA

All the ELISA's were carried out in 96 well "U" bottom plates (Sarstedt), utilising a fairly standard format as follows:

1. The plate was coated (100μLwell^{-1}) overnight at room temperature with purified Ag (protein) diluted in coating buffer (2.1.3.5).

2. The Ag solution was flicked out and the plates tapped dry on paper towelling.

3. Primary Ab (test-bleed eluate, hybridoma supernatant, crude monoclonal/polyclonal ascitic fluid or purified monoclonal/polyclonal ascitic fluid) diluted in TEN-T-C (2.1.3.5) was added to the plate (50μLwell^{-1}) and incubated at room temperature for 1h.

4. The plate was washed 4 times with TEN-T (2.1.3.5) and the plates tapped dry on paper towelling.

5. HRPO conjugated secondary Ab diluted in TEN-T-C (2.1.3.5) was added to the plate (50μLwell^{-1}) and incubated at room temperature for 1h.

6. The plate was washed 6 times with TEN-T (2.1.3.5) and the plates tapped dry on paper towelling.

7. ELISA buffer (2.1.3.5) was added to the plate (100μLwell^{-1}) and incubated at room temperature for 1h.

8. Colour development was measured as absorbance at OD_{405}.

9. A positive secreting hybridoma produced an OD_{405} at least 2x background. For titre determination the values for OD_{405} ("y" axis) were plotted against antibody dilution ("x" axis) using Microsoft Excel.

2.2.11 Surface plasmon resonance (SPR) analysis

All the SPR experiments were run on the BIAcore X system (BIAcore AB). The experiments were run with a constant flow rate of 5μLmin^{-1} at 25^{o}C.

2.2.11.1 Protein immobilisation on SPR chip

All the protein-ligated chips used in this work were amine coupled by the manufacturer's recommended protocol using purified protein (at least 95% purity) to CM5 carboxy-methyldextran chips (BIAcore AB). The method was as follows:

1. Activate chip surface with 35μL of 1:1 NHS (0.1M) and EDC (0.4M)

2. Inject protein to be ligated (0.1mgmL^{-1}) 20μL at a time, until the desired amount of protein has been attached to the matrix.
3. Cap unligated active matrix with 35μL of ethanolamine HCl pH8.5 (1M).
4. Regenerate the chip surface with 10μL of 100mM H_3PO_4 and wash, several times.
5. Equilibrate chip with HBS running buffer (2.1.3.6) overnight.

The first channel on each chip was used as a negative control. The surface underwent the amine coupling procedure with no protein. The second channel had the ligated protein.

2.2.11.2 SPR binding experiments and data analysis

Various combinations of small effector-molecules and proteins diluted in HBS running buffer (2.1.3.6) were used as the analyte. Interactions between the analyte protein and the immobilised protein were monitored by the change in SPR angle with time. The change in SPR response (resonance units) plotted against time is called a sensorgram. The protocol that generated the sensorgrams reported in this work was as follows:

1. Equilibrate chip with HBS running buffer (2.1.3.6) for 7min.
2. Inject 20μL of analyte solution.
3. HBS running buffer (2.1.3.6) for 2min.
4. Wash.
5. Regenerate chip surface with 10μL of 100mM H_3PO_4.

At least three replicates were performed for each condition. Within each cycle the solutions passed over the negative control channel then the ligated protein channel. Most of the small effector-molecules used in these experiments bind to both the analyte protein and the ligated protein, so each condition was also run with no protein in the analyte, just the small effector-molecules as another negative control.

As a general rule the amount of bound analyte (RU) is expressed as the difference between the baseline SPR signal and the signal at 1min post injection, i.e. 1min into the disassociation phase.

2.2.11.3 Kinetic analysis

The sensorgrams for each condition were analysed using BIAEvaluation 3.0 software. For the conditions where there were no small effector-molecules (only protein), the negative control sensorgram was subtracted from the ligated protein sensorgram to remove any signal due to non-specific interactions with the matrix. For the sensorgram of the conditions where small effectors were included, the sensorgram generated from small effector-molecules alone passing over the ligated protein surface was subtracted to remove any signal due to the small effector-molecules interacting with the ligated protein. The two sets of subtracted curves were used in the kinetic analysis.

Each curve was analysed using global analysis and non-linear curve fitting for the whole sensorgram. Two models were used. The first was the two-state model, where there is a 1:1 interaction of the analyte protein and ligated protein followed by a conformational change in the complex. The second model was the bivalent model, where there is a major binding event at one point followed closely by a second minor binding event at another point. This model was developed from antibody-antigen binding studies (BIAEvaluation software handbook, 1997).

The goodness of fit between the curve generated from the mathematical models and the actual sensorgram is described by the chi^2 value. This value is the average squared residual per data point and the smaller this value the closer the mathematical model is to the actual curve (BIAEvaluation software handbook, 1997).

CHAPTER 3 Production and Characterisation of Monoclonal Antibodies to PII and ATase

3.1 INTRODUCTION

The adenylylation cascade in *E. coli* is the mechanism which the bacterium utilises to regulate gln production by GS. ATase reversibly inactivates GS by covalent addition or removal of an AMP group to each monomer. The N status of the cell is signalled by the uridylylation state of the two proteins PII and GlnK, which stimulate ATase to either adenylylate GS when they are not uridylylated or deadenylylate GS-AMP when they are uridylylated. Although this is a well-studied system with 3D structures determined for PII (Carr *et al.*, 1996), GlnK (Xu *et al.*, 1998) and the N-terminal deadenylylation domain of ATase (Xu *et al.*, 2004), the molecular details of the interaction between the two signalling proteins and ATase are still undetermined.

Attempts to crystallise PII/ATase complexes to study the nature of the interaction of the two proteins have proved unsuccessful, so with this in mind a different approach was adopted. A panel of monoclonal antibodies (mAbs), truncation constructs and point mutants of these proteins were used as tools to address questions of structure and function (Yi *et al.*, 2002).

Antibodies (Abs) are high affinity serum proteins produced by the host organism in response to invasion by foreign material. In a normal immune response a whole repertoire of Abs (polyclonal) are produced that bind to different parts of the antigen (Ag). Each Ab in this population binds to a single epitope (Ep) (a grouping of 3-5 amino acids) and is derived from a single B cell (Roitt, 1988).

The laboratory fusion of individual B cells from a hyperimmunised mouse with mouse myeloma cells to form hybridomas (hybrid cells) that can be selected and cloned by limiting dilution, allowed for the production of Ab preparations that contain only one Ab. The phenomenal power of this laboratory procedure is the ability to select and maintain a hybridoma cell line that continuosly produces an extremely specific

homogeneous Ab preparation against a single Ep (Kohler and Milstein, 1975). If the individual Ep or binding region is known, then any demonstrated inhibitory effect due to mAb binding can be narrowed down to the binding region of the mAb.

In this chapter several proteins from the nitrogen assimilation pathway of *E. coli* K12 have been used to produce mAbs in order to study the interactions of various proteins in the nitrogen signalling cascade. The proteins used in this study can be over-expressed from recombinant vectors, and established *in vitro* assays exist that can be used to assess functional interactions between them. Inhibitory mAbs (and in some instances non-inhibitory mAbs) can help shed light on the nature of the interaction being studied.

One of the main areas of focus for this study was the interaction between the receptor-protein ATase, the effector-proteins PII/GlnK and the central enzyme GS, which was investigated using the adenylylation assay (Stadtman *et al.*, 1979). The interaction between the receptor-protein ATase and the covalently modified forms of the other proteins was investigated using the deadenylylation assay (Stadtman *et al.*, 1979; Jaggi *et al.*, 1997).

One panel of mAbs was generated against the compact signalling effector-protein PII, which is capable of binding to at least three different receptor-proteins within the cascade by means of an exposed flexible T-loop (Jiang *et al.*, 1997a). The other panel of mAbs was produced against the receptor-protein ATase. The aim of this chapter was to produce and characterise a panel of mAbs against the PII and ATase proteins. The production and characterisation results are presented in this chapter. The impact of the ATase mAbs on the adenylylation and deadenylylation activities of the ATase protein, and the mapping of the PII/PII-UMP binding sites on ATase are dealt with in Chapter 6.

3.2 METHODS

3.2.1 Expression and purification of proteins

All the recombinant vectors were produced previously except for pRJ009:RQ2 (see Chapter 6) and pDW1:N169G (see Chapter 7), which were generated in this study. The vectors are listed in Table 2.1.6.2 and 3.1.

All strains were grown in LB medium and when appropriate supplemented with ampicillin (100μgmL^{-1}) and chloramphenicol (25μgmL^{-1}) (see section 2.2.1.1 and 2). The method of protein induction was dependent on the particular promoter used in the expression vector (see section 2.2.5.1 and 2). In this work plasmids derived from the pND707 vector (Love *et al.*, 1996) were thermally induced and those derived from the pET vector (Neylon *et al.*, 2000) under the control of the T7 promoter were induced with IPTG at 18^{o}C.

3.2.1.1 Purified PII/GlnK and PII mutants

The purified preparations of the PII/GlnK and PII mutants were over-expressed from the plasmids listed in Table 3.1. The RB9040 (2.1.4) strain was used as the host for over-expression to take advantage of its *glnD*$^{-}$ genotype, so as to prevent the over-expressed effector-proteins from becoming uridylylated by endogenous UTase.

Large-scale preparations (see section 2.2.5.5) were made for the effector-proteins using thermal induction (pND707-derived) (see section 2.2.5.1). These proteins were then purified (see sections 2.2.7.7 and 8) to at least 95% purity (except for the PII:Y51F protein, which was probably ~60% purity) as judged by SDS PAGE.

The purified PII/GlnK protein preparations (see section 2.2.7.7 and 8) were used to produce uridylylated effector-proteins (see section 2.2.5.6.1) for the ELISAs (see section 2.2.10.4).

Plasmid	Description	Source/Reference
pRJ001	*glnB* (PII) in pND707	Jaggi *et al.*, (1996)
pRJ001:G24A	*glnB* (PII:G24A) in pND707	Vasudevan lab unpublished work
pRJ001:G24AT26A	*glnB* (PII:G24AT26A) in pND707	Vasudevan lab unpublished work
pRJ001:G24D	*glnB* (PII:G24D) in pND707	Vasudevan lab unpublished work
pRJ001:T26A	*glnB* (PII:T26A) in pND707	Vasudevan lab unpublished work
pRJ001:H42N	*glnB* (PII:H42N) in pND707	Vasudevan lab unpublished work
pRJ001:T43A	*glnB* (PII:T43A) in pND707	Vasudevan lab unpublished work
pRJ001:Y46F	*glnB* (PII:Y46F) in pND707	Jaggi (1998)
pRJ001:Y51F	*glnB* (PII:Y51F) in pND707	Jaggi (1998)
pRJ001:Y51S	*glnB* (PII:Y51S) in pND707	Vasudevan lab unpublished work
pRJ001:V64AP66S	*glnB* (PII:V64AP66S) in pND707	Vasudevan lab unpublished work
pRJ001:V64AP66T	*glnB* (PII:V64AP66T) in pND707	Vasudevan lab unpublished work
pRJ001:K90N	*glnB* (PII:K90N) in pND707	Vasudevan lab unpublished work
pRJ001:R103D	*glnB* (PII:R103D) in pND707	Vasudevan lab unpublished work
pRJ001:R103CT104A	*glnB* (PII:R103CT104A) in pND707	Vasudevan lab unpublished work
pRJ001:R103HT104A	*glnB* (PII:R103HT104A) in pND707	Vasudevan lab unpublished work
pRJ001:T104A	*glnB* (PII:T104A) in pND707	Vasudevan lab unpublished work
pNV103	*glnK* (GlnK) in pND707	Vasudevan lab unpublished work
PRJ002	*glnE* (AT-C_{522}) in pND707	Jaggi *et al.*, (1997)
pRJ007	*glnE* (AT-N_{423}) in pND707	Jaggi *et al.*, (1997)
pRJ009	*glnE* (ATase) in pND707	Jaggi *et al.*, (1997)
pRJ0012	*glnE* (AT-N_{548}) in pND707	Jaggi (1998)
pRJ0013	*glnE* (AT-N_{501}) in pND707	Jaggi (1998)
pRJ0014	*glnE* (AT-C_{439}) in pND707	Jaggi (1998)
pRJ0015	*glnE* (AT-C_{396}) in pND707	Jaggi (1998)
pDW1	*glnE* (AT-N_{440}) in pND707	Wen (2000)
pDW2	*glnE* (AT-C_{481}) in pND707	Wen (2000)
pDW3	*glnE* (AT-N_{467}) in pND707	Wen (2000)
pDW4	*glnE* (AT-C_{518}) in pND707	Wen (2000)
pDW7	*glnE* (AT-C_{340}) in pETDW2	Wen (2000)
pDW8+glnB	*glnE* (AT-C_{305})+*glnB* in pETDW2	Wen (2000)
p235+glnB	*glnE* (AT-C_{235})+*glnB* in pETDW2	Vasudevan lab unpublished work
pET AT:ΔR	*glnE* (AT:ΔR) in pETDW2	O'Donnell (2000)
pRJ009:N169G	*glnE* (AT:N169G) in pBluescript II	Mc Loughlin (1999)
pRJ009:D173A	*glnE* (AT:D173A) in pND707	Mc Loughlin (1999)
pRJ009:D175A	*glnE* (AT:D175A) in pND707	Mc Loughlin (1999)
pRJ009:D173AD175A	*glnE* (AT:D173AD175A) in pND707	Mc Loughlin (1999)
pRJ009:W694G	*glnE* (AT:W694G) in pND707	Mc Loughlin (1999)
pRJ009:G697N	*glnE* (AT:G697N) in pBluescript II	Mc Loughlin (1999)
pRJ009:W694GG697N	*glnE* (AT:W694GG697N) in pND707	Mc Loughlin (1999)
pRJ009:D701E	*glnE* (AT:D701E) in pND707	Mc Loughlin (1999)
pRJ009:D703E	*glnE* (AT:D703E) in pND707	Mc Loughlin (1999)
pRJ009:D701ED703E	*glnE* (AT:D701ED703E) in pND707	Mc Loughlin (1999)
pRJ009:D701N	*glnE* (AT:D701N) in pND707	Mc Loughlin (1999)
pRJ009:D703N	*glnE* (AT:D703N) in pND707	Mc Loughlin (1999)
pRJ009:D701ND703N	*glnE* (AT:D701ND703N) in pND707	Mc Loughlin (1999)
pRJ009:RQ2	*glnE* (AT:RQ2) in pETDW2	this work
pDW1:N169G	*glnE* (AT-N_{440}:N169G) in pND707	this work

Table 3.1 ***Recombinant proteins.*** List of the plasmids encoding the recombinant proteins used in this chapter including the plasmid name and source.

3.2.1.2 Purified ATase and truncation constructs

Large-scale preparations (see section 2.2.5.5) were made for ATase, AT-N_{548} and AT-C_{522}. These proteins were then purified (see section 2.2.7.6) to at least 85-95% purity as judged by SDS PAGE.

3.2.1.3 ATase, truncation constructs and mutants cell lysates

For the comparative studies the following proteins: ATase, AT-N_{423}, AT-N_{440}, AT-N_{467}, AT-N_{501}, AT-N_{548}, AT-C_{522}, AT-C_{518}, AT-C_{481}, AT-C_{439}, AT-C_{396}, AT-N_{440}:N169G, AT:N169G, AT:D173A, AT:D175A, AT:D173AD175A, AT:W694G, AT:G697N, AT:W694GG697N, AT:D701E, AT:D703E, AT:D701ED703E, AT:D701N, AT:D703N and AT:D701ND703N (pND707-derived) (Table 3.1), were all expressed in JM109 cells (2.1.4) and cell extracts were made as described in section 2.2.5.3. The five remaining constructs: AT-C_{340}, AT-C_{305}, AT-C_{235}, AT:ΔR and AT:RQ2 (pET-derived) (Table 3.1) were all expressed in BL21 (DE3) recA cells (2.1.4) and cell extracts were similarly produced. The approximate individual target protein concentration was estimated by comparison with a known standard in SDS PAGE (see section 2.2.8.2).

3.2.2 Production and characterisation of hybridomas

Mice were immunised for hybridoma production using purified PII protein (see section 3.2.1.1) or purified ATase protein (see section 3.2.1.2) using the immunisation schedule for mAb production outlined in section 2.2.9.3.2. Splenocytes from the primed mouse and myeloma cells (Sp2/0) were fused using PEG (see section 2.2.9.5) to form hybridomas (see Figure 3.1).

Hybrid cells formed from the correct partners were selected using HAT selective hybridoma medium (see section 2.2.9.5.3). Hybridoma cells secreting antibodies were selected using ELISA (see sections 2.2.9.6.1 and 2.2.10.4). Propagation and maintenance of the positive Ab secreting hybridomas was performed following the methods outlined in section 2.2.9.6.

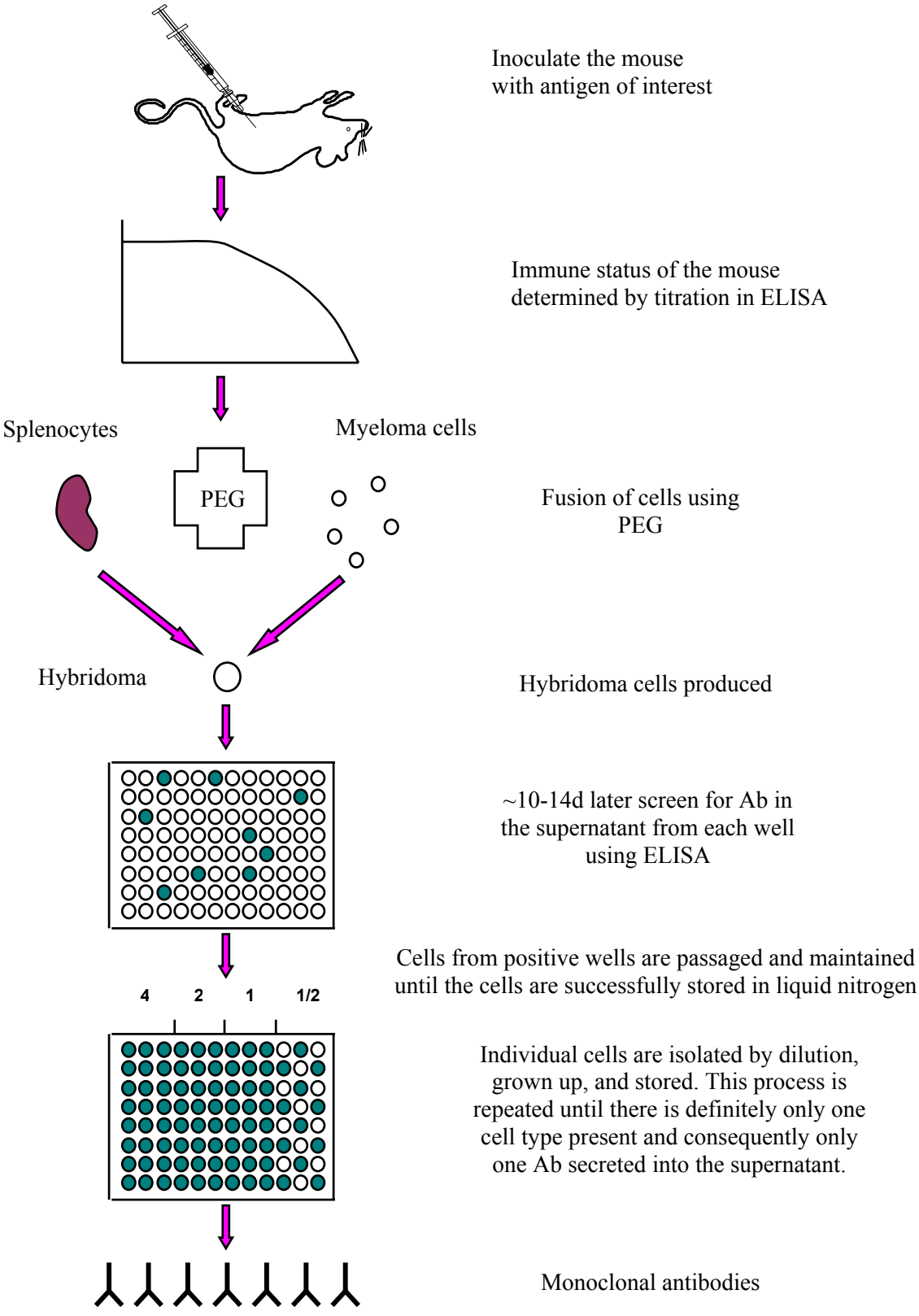

Figure 3.1 ***Monoclonal antibody production.*** Schematic diagram of the process of producing murine hybridomas and monoclonal antibodies.

The ATase mAbs were cloned by the limiting dilution method (see section 2.2.9.6.3), and ascitic fluid produced (see section 2.2.9.4.1).

3.2.2.1 ELISA

Purified PII (see section 3.2.1.1) or purified ATase, and ATase truncation constructs AT-C_{522} and AT-N_{548} (see section 3.2.1.2) were used to coat the initial screening ELISA plates at 4μgmL^{-1}. Hybridoma supernatant from each well of the 96 well culture plate (50μL) was also used in the initial screening ELISA (see section 2.2.10.4), such that PII mAbs were screened against the PII protein and ATase mAbs were screened against the three ATase protein derivatives (ATase, AT-C_{522} and AT-N_{548}).

The hybridoma cell-lines were constantly monitored for continued Ab secretion at all levels of passage (newly formed hybridomas are very fragile and frequently die or stop secreting Ab) (Goding, 1983). The monitoring ELISA used PII or ATase.

At the final level of passage the supernatant was retained from cryopreservation of the hybridoma cell-lines (see section 2.2.9.6.4) and used in the further characterisation of mAb binding by ELISA.

3.2.2.2 Western blotting

Protein preparations produced as described in section 3.2.1.3 were separated by 12% SDS PAGE (see section 2.2.6.1), transferred to nitrocellulose membrane (see section 2.2.6.5.1) and immunoblotted with ATase mAb (see section 2.2.6.5.2). Five mAbs were chosen from the results of the initial screening ELISA (Table 3.6). There was one N-terminal domain mAb 6B5, two central R domain (i.e. the overlapping region of the two domain constructs AT-N_{548} and AT-C_{522}) mAbs 5A7 and 39G11, and two C-terminal domain mAbs 6A3 and 27D7. All the mAbs except 39G11 were purified using protein A agarose (see section 3.2.3).

3.2.3 Isotyping and purification of monoclonal antibodies

All of the mAbs produced were isotyped (see section 2.2.9.7). None of them were IgM (Tables 3.2 and 3.6); this meant protein A agarose could be used to purify the crude Ab preparations.

Four of the five ATase mAb ascitic fluids 6B5, 5A7, 6A3 and 27D7 (see section 2.2.9.4.1) were purified using protein A agarose chromatography (see section 2.2.9.8). One PII mAb 19G4 was purified from hybridoma supernatant using the same method. The resulting purified Ab preparations were at least 90-95% pure (as judged by SDS PAGE) and were checked in ELISA (see section 3.2.2.1) to ensure that they still had activity. The PII mAb was no longer active (data not shown).

3.3 RESULTS

3.3.1 PII mAb binding to the PII mutant proteins using ELISA

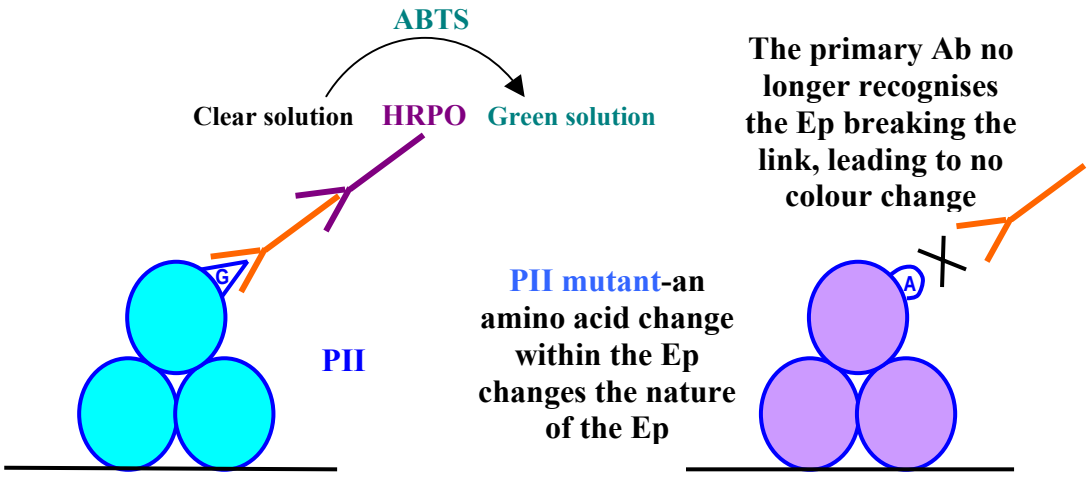

Figure 3.2 ***Indirect ELISA for screening mAb binding to PII and mutants.*** Schematic diagram of the principles behind the indirect ELISA used to characterise PII_{wt}, PII mutants and GlnK.

The structure of wild-type *E. coli* PII and GlnK and their ATP complexes have been resolved (see Chapter 1). The prominent features of PII and PII-like proteins are the ATP-binding cleft, the flexible T-loop region, the B-loop region and the structural core

composed of three 8-stranded β-sheets surrounded by α-helices. The results of the indirect ELISA (Figure 3.2) with PII_{wt}, PII mutants and GlnK are presented in Tables 3.2-3.5. The proteins were all coated to the plate at $4\mu gmL^{-1}$ to standardise the ELISAs and the supernatants were collected from hybridomas of a similar confluency prior to cryopreservation, so the Abs added to the ELISA should have been in excess.

Of the 32 mAbs produced against PII, there were 21 mAbs from the IgG_1, antibody subclass, 9 mAbs from the IgG_{2b} antibody subclass and two from the IgG_{2a} antibody subclass (Table 3.2). All of the ATase mAbs were of the IgG_1 subclass (Table 3.6).

The first question addressed was whether any of the mAbs recognised the T-loop of PII. For this the binding of mAbs in ELISA to PII_{wt} and the PII mutants of this region PII:H42N, PII:T43A, PII:Y46F, PII:Y51S and PII:Y51F were compared (Table 3.2). The tabulated results imply that none of the mutations in the T-loop can completely disrupt the binding of the various mAbs. Absorbance values for the T-loop mutants were of a similar magnitude to wild type (only 2-3 fold difference observed and all absorbance values are above the threshold that was set at 0.1). The PII:H42N mutant from this panel generally had lower absorbance values than the others.

The second region of interest is the ATP-binding cleft, which is found in all PII-like proteins. To determine if any of the mAbs bound to the ATP-binding cleft the PII mutants PII:K90N, PII:R103D, PII:R103CT104A, PII:R103HT104A and PII:T104A were compared to PII_{wt} in ELISA (Table 3.3). The PII mutants that contained the V64A mutation are also found in the ATP-binding cleft, but they have been presented in Table 3.5 with GlnK because residue 64 is Ala in GlnK.

As with the T-loop there are no mutations in the ATP-binding cleft that can completely disrupt the binding of the various mAbs. The PII:T104A mutant from this panel generally had lower absorbance values than the others.

Monoclonal antibody	Antibody Isotype	Protein					
		PII_{wt}	PII:H42N	PII:T43A	PII:Y46F	PII:Y51S	PII:Y51F
33H12	IgG_1	1.326	0.560	1.493	1.696	1.287	2.469
20G10	IgG_1	1.217	0.423	1.121	1.954	1.606	2.628
13E12	IgG_{2b}	2.919	1.996	2.665	3.001	2.503	2.794
4A6	IgG_{2a}	1.473	0.821	1.706	2.742	1.559	2.989
36E6	IgG_1	1.999	0.885	1.712	2.736	1.723	3.047
9A9	IgG_1	1.931	1.117	2.558	2.791	2.143	2.715
7G11	IgG_1	1.293	0.913	2.059	2.531	1.293	3.044
1A4	IgG_1	1.207	0.926	1.844	2.737	1.221	2.772
14C9	IgG_{2b}	2.352	1.406	2.475	3.214	2.361	2.867
19G4	IgG_1	2.350	1.308	2.311	2.705	2.379	2.678
2A5	IgG_{2b}	1.350	0.615	1.628	2.461	1.478	3.172
35H10	IgG_{2b}	1.710	0.908	2.045	2.542	2.028	3.132
19D2	IgG_{2b}	1.642	0.841	2.091	2.215	1.531	2.922
39E5	IgG_1	1.170	0.586	1.728	2.275	1.217	2.467
10E11	IgG_1	1.284	0.709	2.204	2.550	1.678	2.757
29B12	IgG_1	1.281	0.612	1.483	2.256	1.271	2.873
21F7	IgG_1	1.446	0.903	1.356	2.210	2.000	2.685
21H7	IgG_1	2.022	1.063	1.979	1.897	2.090	2.869
18E6	IgG_1	1.242	0.695	1.843	2.426	1.265	2.709
12H4	IgG_{2b}	1.854	0.964	2.717	3.074	2.682	3.215
24H2	IgG_{2a}	3.237	2.175	2.668	2.968	2.896	2.849
9D3	IgG_1	2.045	1.155	2.412	2.792	2.126	3.038
20G9	IgG_1	2.225	1.256	2.308	2.569	2.348	2.870
18E1	IgG_{2b}	2.154	1.198	2.297	2.600	2.112	2.978
27A5	IgG_1	1.895	1.009	2.130	2.709	1.887	2.948
2H2	IgG_1	1.602	0.690	1.681	2.377	1.891	2.826
36D3	IgG_1	1.660	0.648	1.573	2.320	1.624	2.731
6G3	IgG_1	1.194	0.624	1.776	2.417	1.170	2.871
17C5	IgG_1	2.019	0.906	2.066	2.477	1.752	2.776
21G3	IgG_{2b}	0.738	0.651	2.070	2.554	1.566	2.745
5C3	IgG_{2b}	0.992	0.458	2.205	2.139	1.097	2.809
13C3	IgG_1	0.700	0.286	1.392	1.207	0.838	1.756

Table 3.2 ***Binding patterns for PII monoclonal antibodies against PII, and the PII T-loop mutants.*** All the mAbs were characterised in an indirect ELISA format (see section 3.2.2.1) using undiluted hybridoma culture supernatant with purified protein ($4\mu gmL^{-1}$) coated directly to the plate and the optical density read at λ 405. Antibody isotyping was performed using the Sigma isotyping kit modified to the same indirect ELISA format (see section 2.2.9.7). The results have been colour coded for easier interpretation. 0.101-0.500:red, 0.501-1.000:blue, 1.001-2.000:purple and >2.000:green.

Monoclonal antibody	Protein					
	PII_{wt}	PII:K90N	PII:R103D	PII:R103C T104A	PII:R103H T104A	PII:T104A
33H12	1.326	2.041	1.320	1.034	1.146	0.667
20G10	1.217	1.719	1.056	0.968	1.105	0.412
13E12	2.919	3.052	3.091	2.363	1.871	0.174
4A6	1.473	2.578	1.889	1.387	1.217	0.106
36E6	1.999	2.362	1.667	1.340	1.652	1.261
9A9	1.931	3.174	2.472	1.599	1.963	1.786
7G11	1.293	1.930	1.920	0.881	1.008	0.649
1A4	1.207	1.665	1.225	1.099	1.034	0.454
14C9	2.352	3.218	2.293	2.116	2.238	1.402
19G4	2.350	2.623	1.651	1.607	1.652	1.108
2A5	1.350	2.049	1.646	1.292	1.663	0.889
35H10	1.710	2.546	1.896	1.716	1.736	1.087
19D2	1.642	2.537	1.502	1.206	1.306	0.618
39E5	1.170	2.308	1.591	1.177	1.272	0.829
10E11	1.284	2.880	2.188	1.231	1.489	1.576
29B12	1.281	2.102	1.399	1.180	1.421	0.585
21F7	1.446	2.086	1.546	1.213	1.635	0.809
21H7	2.022	2.789	2.129	1.702	1.904	0.982
18E6	1.242	2.065	1.146	0.920	1.100	0.584
12H4	1.854	3.335	2.963	2.062	2.443	1.246
24H2	3.237	3.494	3.232	3.320	3.292	2.127
9D3	2.045	3.233	2.289	1.943	2.000	2.657
20G9	2.225	2.640	2.276	1.844	2.072	0.859
18E1	2.154	3.067	2.777	1.668	1.993	1.238
27A5	1.895	2.574	1.865	1.538	2.238	1.067
2H2	1.602	2.235	1.500	1.295	1.286	0.735
36D3	1.660	2.150	1.615	1.263	1.264	0.792
6G3	1.194	2.134	1.479	1.107	1.253	0.809
17C5	2.019	2.507	1.527	1.219	1.861	0.943
21G3	0.738	2.460	1.905	1.366	1.373	0.755
5C3	0.992	2.236	1.697	1.111	1.072	0.523
13C3	0.700	1.727	0.827	0.559	0.802	0.488

Table 3.3 ***Binding patterns for PII monoclonal antibodies against PII, and PII ATP-binding cleft mutants.*** All the mAbs were characterised in an indirect ELISA format (see section 3.2.2.1) using undiluted hybridoma culture supernatant, with purified protein (4μgmL^{-1}) coated directly to the plate and the optical density read at λ 405. The results have been colour coded for easier interpretation. 0.101-0.500:red, 0.501-1.000:blue, 1.001-2.000:purple and >2.000:green.

Monoclonal antibody	Protein			
	PII_{wt}	PII:G24A	PII:G24D	PII:T26A
33H12	1.326	1.298	1.005	1.127
20G10	1.217	1.411	0.679	0.927
13E12	2.919	2.255	2.487	1.183
4A6	1.473	2.734	1.412	0.788
36E6	1.999	2.292	1.261	1.598
9A9	1.931	1.132	1.302	0.967
7G11	1.293	1.028	0.942	0.453
1A4	1.207	1.216	0.839	0.274
14C9	2.352	1.727	0.927	0.836
19G4	2.350	1.383	0.960	0.669
2A5	1.350	1.364	0.985	0.773
35H10	1.710	1.364	1.020	0.655
19D2	1.642	0.841	0.703	0.305
39E5	1.170	0.846	1.237	0.608
10E11	1.284	1.791	1.016	0.435
29B12	1.281	1.203	1.002	0.408
21F7	1.446	1.088	0.526	0.815
21H7	2.022	0.805	0.271	1.621
18E6	1.242	0.928	0.195	0.331
12H4	1.854	0.766	0.968	0.694
24H2	3.237	0.636	0.100	2.394
9D3	2.045	1.390	0.117	1.107
20G9	2.225	1.548	0.045	1.002
18E1	2.154	0.591	0.020	0.689
27A5	1.895	1.529	0.044	0.797
2H2	1.602	0.821	0.068	0.604
36D3	1.660	0.513	0.003	0.547
6G3	1.194	0.751	0.050	0.340
17C5	2.019	1.122	0.036	0.590
21G3	0.738	1.922	1.172	0.049
5C3	0.992	0.877	0.763	0.077
13C3	0.700	0.154	0.034	0.116

Table 3.4 ***Binding patterns for PII monoclonal antibodies against PII and ATP-binding cleft entrance mutants.*** All the mAbs were characterised in an indirect ELISA format (see section 3.2.2.1) using undiluted hybridoma culture supernatant, with purified protein (4μgmL^{-1}) coated directly to the plate and the optical density read at λ 405. The results have been colour coded for easier interpretation. 0.00-0.100:black with aqua background, 0.101-0.500:red, 0.501-1.000:blue, 1.001-2.000:purple and >2.000:green.

Monoclonal antibody	Protein					
	PII_{wt}	PII-UMP	GlnK	GlnK-UMP	PII:V64A P66S	PII:V64A P66T
33H12	1.326	0.758	0.837	1.797	0.994	1.140
20G10	1.217	0.589	0.839	1.589	0.710	0.784
13E12	2.919	2.533	1.453	1.427	2.320	2.646
4A6	1.473	2.367	0.674	0.721	2.738	1.212
36E6	1.999	1.482	1.298	2.020	0.918	0.990
9A9	1.931	1.335	0.181	0.429	0.183	0.336
7G11	1.293	1.526	1.615	1.042	0.141	0.170
1A4	1.207	1.379	1.361	0.655	0.173	0.137
14C9	2.352	1.926	0.904	0.994	0.103	0.015
19G4	2.350	1.450	1.474	1.301	0.063	0.011
2A5	1.350	2.633	1.245	1.213	0.061	0.018
35H10	1.710	2.002	0.875	0.840	0.065	0.016
19D2	1.642	1.351	0.635	0.657	0.024	0.027
39E5	1.170	1.515	0.058	0.168	0.053	0.017
10E11	1.284	1.728	0.079	0.205	0.054	0.039
29B12	1.281	1.897	0.086	0.182	0.030	0.018
21F7	1.446	1.352	0.030	0.095	0.043	0.011
21H7	2.022	0.884	0.058	0.056	0.020	0.038
18E6	1.242	0.831	0.084	0.112	0.026	0.008
12H4	1.854	0.723	0.023	0.064	0.654	1.263
24H2	3.237	2.605	0.041	0.044	0.141	0.098
9D3	2.045	1.601	0.028	0.053	0.046	0.019
20G9	2.225	1.339	0.026	0.033	0.063	0.003
18E1	2.154	1.751	0.012	0.028	0.016	0.016
27A5	1.895	1.565	0.003	0.033	0.031	0.012
2H2	1.602	0.709	0.044	0.022	0.026	0.026
36D3	1.660	0.908	0.053	0.030	0.023	0.004
6G3	1.194	1.172	0.028	0.091	0.032	0.004
17C5	2.019	1.836	0.065	0.150	0.055	0.003
21G3	0.738	0.719	0.275	0.495	0.104	0.023
5C3	0.992	0.680	0.059	0.089	0.020	0.031
13C3	0.700	0.354	0.021	0.081	0.008	0.010

Table 3.5 ***Binding patterns for PII monoclonal antibodies against PII, GlnK, PII-UMP, GlnK-UMP and PII to GlnK at Val64 mutants.*** All the mAbs were characterised in an indirect ELISA format (see section 3.2.2.1) using undiluted hybridoma culture supernatant, with purified protein ($4\mu gmL^{-1}$) coated directly to the plate and the optical density read at λ 405. The results have been colour coded for easier interpretation. 0.00-0.100:black with aqua background, 0.101-0.500:red, 0.501-1.000:blue, 1.001-2.000:purple and >2.000:green.

The entrance to the ATP-binding cleft contains the Gly24 and Thr26 residues. The Thr26 residue undergoes a conformational shift when ATP is bound to the protein (Xu *et al.*, 1998). In Table 3.4 the ELISA results for PII_{wt} have been compared with the PII:G24A, PII:G24D and PII:T26A mutants. There are 2 mAbs that no longer recognise their Ep when there is an Ala at position 26 in the place of the Thr. Mutating residue Gly24 to Asp rather than an Ala had a far more dramatic effect on mAb binding. There were 8 mAbs that no longer bound to the PII protein when this mutation was introduced.

The panel of PII mAbs were also screened in ELISA against PII_{wt}, GlnK and their fully uridylylated forms (the uridylylation status was checked by native PAGE-data not shown) along with two mutants where the Val64 residue is swapped to the Ala of GlnK (Table 3.5).

Uridylylation of the T-loop of PII did not change the mAb binding profile. All the Abs still recognised the covalently modified form PII-UMP. The same also applied for GlnK, the mAb binding pattern for GlnK and the covalently modified form GlnK-UMP were effectively the same (Table 3.5).

There was quite a distinct difference between PII and GlnK, 18 of the 32 mAbs did not recognise GlnK. The PII:V64AP66S/T double mutants both had very similar mAb binding profiles and there were only 5 mAbs that truly recognised these mutant proteins (Table 3.5).

One of the main aims of producing the panel of mAbs against PII was to develop a tool that could distinguish between the two very similar forms of the signalling protein present within *E. coli* i.e PII and GlnK. Two mAbs 19G4 (binds to both PII and GlnK) and 24H2 (PII specific) (Table 3.5) were chosen for further work where PII and GlnK needed to be distinguished. van Heeswijk *et al.,* (2000) grew several *E. coli* strains on a poor N source (arginine) to study *in vivo* formation of heterotrimers between PII and GlnK (Figure 3.3).

Figure 3.3 ***PII/GlnK heterotrimers form in vivo.*** Native gel (see section 2.2.6.2) of extracts from wild type *E. coli* (YMC10) and a PII deficient (RB9060) and GlnK deficient *E. coli* strain (WCH30) probed with mAb 19G4 (PII/GlnK) lanes 1-3, and mAb 24H2 (PII specific) lanes 4-6. van Heeswijk *et al*., (2000) *PNAS* **97**:3942-3947.

The residue Val64 or Pro66 of PII is in the most antigenic part of the protein, with the mutation of Val64 to Ala or Pro66 to Ser/Thr reducing the number of mAbs which bound well to the double mutant proteins down from 32 to 5 (Table 3.5). The Val64 residue is involved in the interaction with ATP in PII (Xu, *et al.*, 2001) and also with ATP in GlnK as an Ala (Xu, *et al.*, 1998). The PII mutants, which showed the closest mAb binding profile to GlnK and its uridylylated form GlnK-UMP, were the two double V64AP66S/T mutants.

The three/four most antigenic residues of PII all map to the same region of the protein as seen by the red region in the surface diagram of PII (Figure 3.4).

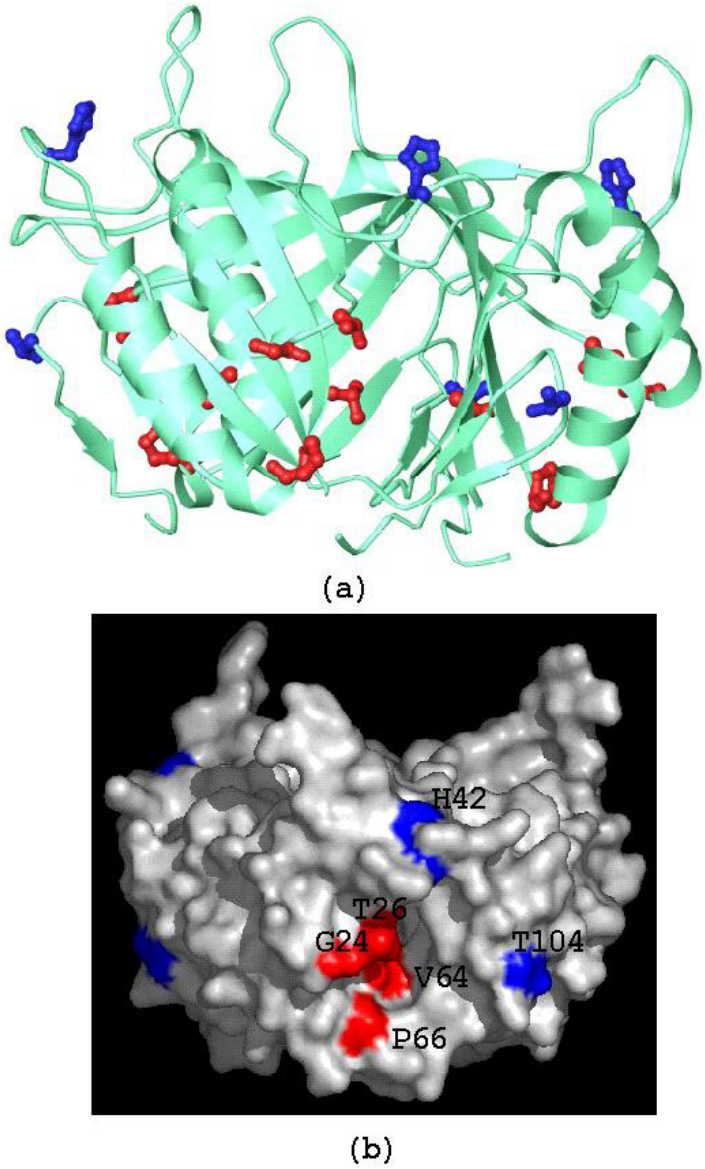

Figure 3.4 ***Antigenic residues of the PII protein.*** The antigenic residues determined from the comprehensive ELISA screens (Tables 3.2-3.5) have been highlighted in (a) ribbon diagram and (b) a surface diagram of the PII protein (Xu *et al.*, 1998). The three or four residues which showed a reduction in mAb binding are highlighted in red and the two residues which still bound to all the mAbs but at a lower level are highlighted in blue.

3.3.2 Initial ATase monoclonal antibody binding to the AT-C_{522} and AT-N_{440} constructs using ELISA

The ATase mAb hybridoma supernatants were screened (see section 3.2.2.1) at the outset with the entire ATase protein and two truncated forms (AT-C_{522} and AT-N_{548}) that encompassed either activity domain (see Chapter 6), to give an early indication of where they were binding on ATase. In this case the mAbs were produced to use as tools

to investigate the intramolecular signalling between the domains of ATase. The results of the initial screening ELISA for ATase are shown in Table 3.6.

Monoclonal antibody	Antibody isotype	Protein		
		AT_{wt}	$AT\text{-}C_{522}$	$AT\text{-}N_{548}$
5A7	IgG_1	+	+	+
6A3	IgG_1	+	+	-
6B5	IgG_1	+	-	+
27D7	IgG_1	+	+	-
27G2	IgG_1	+	+	+
28A9	IgG_1	+	+	+
39G11	IgG_1	+	+	+
6D6	IgG_1	+	+	-
10C2	IgG_1	+	+	-
23B8	IgG_1	+	+	-

Table 3.6 ***Initial screening of the ATase mAbs against ATase and the truncation constructs $AT\text{-}C_{522}$ and $AT\text{-}N_{548}$.*** All the mAbs were run in an indirect ELISA format (see section 3.2.2.1) using undiluted hybridoma culture supernatant titrated across the plate, with purified protein ($4\mu gmL^{-1}$) coated directly to the plate and the optical density read at λ 405. Antibody isotyping was performed using the Sigma isotyping kit modified to the same indirect ELISA format (see section 2.2.9.7). (+) denotes activity in ELISA (-) no activity in ELISA.

Based on the constructs ($AT\text{-}N_{548}$ and $AT\text{-}C_{522}$) used to initially screen the panel of ATase mAbs the results in Table 3.6 show there was 1 ATase mAb that bound exclusively to the AT-N domain (deadenylylation domain) of ATase (6B5). Four ATase mAbs bound to the putative R domain of ATase (5A7, 27G2, 28A9, 39G11) and 5 ATase mAbs bound exclusively to the AT-C domain (adenylylation domain) of ATase (6A3, 27D7, 6D6, 10C2, 23B8).

3.3.3 ATase mAb binding to all the ATase truncation constructs and ATase mutants using Western blotting

Truncation construct	Amino acids	Domains	M Wt (kDa)	Source
ATase	1-946	N-Q1-R-Q2-C	108	Jaggi *et al.*, (1997)
AT-N_{311}	1-311	Part N	36	Vasudevan lab unpublished work
AT-N_{423}	1-423	Part N	48	Jaggi (1998)
AT-N_{440}	1-440	N	50	Wen (2000)
AT-N_{467}	1-467	N-Q1	54	Jaggi (1998)
AT-N_{501}	1-501	N-Q1-part R	58	Jaggi (1998)
AT-N_{548}	1-548	N-Q1-part R	64	Jaggi *et al.*, (1997)
AT:RQ2	463-627	R-Q2	18	This work (Chapter 6)
AT-C_{522}	425-946	Part N-Q1-R-Q2-C	60	Jaggi *et al.*, (1997)
AT-C_{518}	429-946	Part N-Q1-R-Q2-C	59	Wen (2000)
AT-C_{481}	466-946	R-Q2-C	55	Wen (2000)
AT-C_{439}	508-946	Part R-Q2-C	50	Jaggi (1998)
AT-C_{396}	551-946	Part R-Q2-C	46	Jaggi (1998)
AT-C_{341}	606-946	Q2-C	39	Wen (2000)
AT-C_{305}	642-946	C	35	Wen (2000)
AT-C_{235}	712-946	Part C	27	Vasudevan lab unpublished work

Table 3.7 ***ATase truncation constructs.*** List of the ATase truncation constructs used in this chapter including the region of the ATase protein the construct derives from, the domains it encompasses, calculated molecular weight and source. ATase domain organisation can be represented as N-Q1-R-Q2-C; where N is the amino terminal deadenylylation domain, Q1 and Q2 are flexible linker regions, R is the central regulatory domain and C the carboxy terminal adenylylation domain (see Chapter 6).

In addition to the truncation constructs of ATase used in the initial ELISA screen, the complete panel of ATase truncation constructs created at James Cook University were also tested for mAb binding in this work using Western blotting. Details of all the truncation constructs used in this Chapter are presented in Table 3.7.

Cell lysates were used for all the western blotting characterisation (see section 3.2.1.3) because several constructs are insoluble (see Chapter 6 for details).

3.3.3.1 R domain mAbs

All of the ATase truncation constructs and the entire ATase protein cell lysates (see section 3.2.1.3) (Table 3.7) were separated by 12% SDS PAGE and immunoblotted with purified (see section 2.2.9.8) mAb 5A7 (Figure 3.5a) and crude mAb 39G11 (Figure 3.5b). These two mAbs bound in the overlapping region of AT-N_{548} and AT-C_{522} from the initial screening ELISA (Table 3.6).

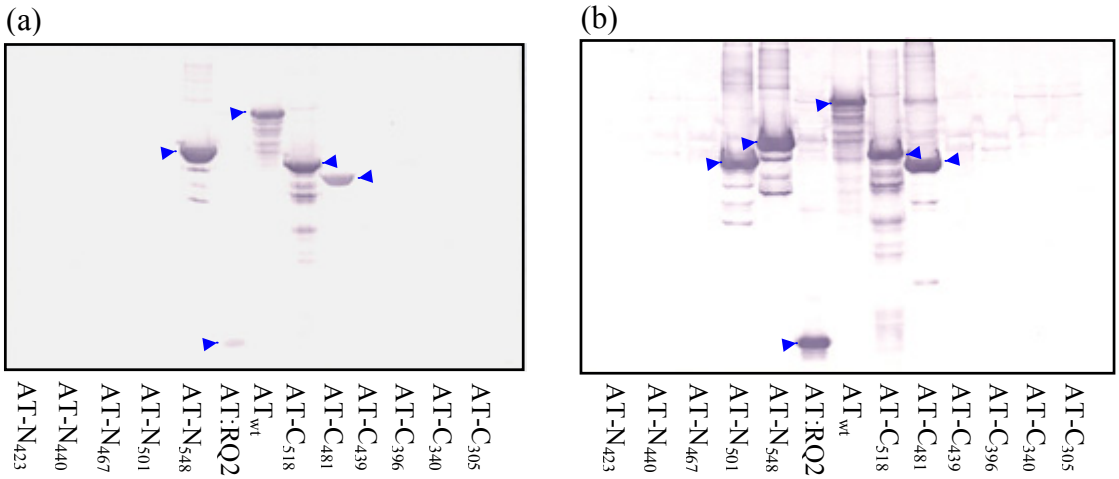

Figure 3.5 ***R domain mAb binding to ATase and truncation constructs.*** Western blot of 12% SDS PAGE (see section 2.2.6.5) of whole cell extracts for the ATase protein and various ATase truncation constructs (Table 3.7) using (a) mAb 5A7 as purified ascitic fluid (see section 2.2.9.8) and (b) mAb 39G11 as crude ascitic fluid. The bands indicating the appropriate induced proteins are marked with arrows.

Visual inspection of Figure 3.5 shows that both ATase mAb 5A7 and 39G11 are binding somewhere in the central region of ATase from the end of Q1 to the end of Q2, because they bound to the AT:RQ2 construct that is described in detail in Chapter 6.

The other three constructs that the ATase mAb 5A7 bound to were AT-N_{548}, AT-C_{518} and AT-C_{481} (Table 3.7). The overlap region of the AT-N_{548} and AT-C_{481} truncation constructs is from residues 466 to 548 of ATase, but the AT-N_{501} truncation construct does not bind to mAb 5A7; therefore the region where this mAb is binding to ATase must be from residues 502 to 548.

The ATase mAb 39G11 bound to the following truncation constructs: AT-N_{501}, AT-N_{548}, AT-C_{518} and AT-C_{481} (Table 3.7). The overlap region of the AT-N_{501} and AT-C_{481} truncation constructs is from residues 466 to 501. From this result it is possible to narrow down the binding site for the mAb 39G11 on ATase to the region between residues 466-501.

3.3.3.2 C domain mAbs

Two mAbs were chosen from the initial screening ELISA (Table 3.6) that only bound to AT-C_{522} and not AT-N_{548}. Both ATase mAbs 6A3 and 27D7 were used as purified ascitic fluid (see section 2.2.9.8) and denoted the C domain mAbs. All of the ATase truncation constructs and the entire ATase protein cell lysates (see section 3.2.1.3) (Table 3.7) were separated by 12% SDS PAGE and immunoblotted with purified (see section 2.2.9.8) ATase C domain mAbs 6A3 (Figure 3.6a) and 27D7 (Figure 3.6b). In this western blot analysis the extracts from ATase mutants (see Chapter 7) within the adenylylation domain β polymerase motif were also included.

Visual inspection of Figure 3.6 shows the 6A3 and 27D7 mAbs bind in the C-terminal region of ATase after the Q2 region, since they do not bind to AT:RQ2 or any of the N-terminal truncation constructs. The smallest C-terminal truncation construct to demonstrate binding to both the mAbs was AT-C_{305}. Another smaller C-terminal truncation construct AT-C_{235}, which had the putative catalytic site determined by a sequence alignment with rat DNA polymerase β (Holm and Sander, 1995) removed did not bind to the the mAbs (data not shown). Therefore both the mAbs are binding to the ATase protein in the region between the residues 642 and 711 i.e. the adenylylation catalytic site.

Several point mutations were made in the putative C domain catalytic site of ATase at residues Trp694, Gly697, Asp701 and Asp703. None of the mutations at these residues disrupted the binding of either mAb to the ATase protein; therefore the mAbs are probably binding somewhere in the region of residues 641 to 694 or 703 to 711.

In fact based on the binding patterns in Figure 3.6 it appears the two C domain mAbs are binding in the same region of ATase. Assessment of these two mAbs in conjunction with activity assays could define more precisely where their binding sites may be located (see Chapter 6).

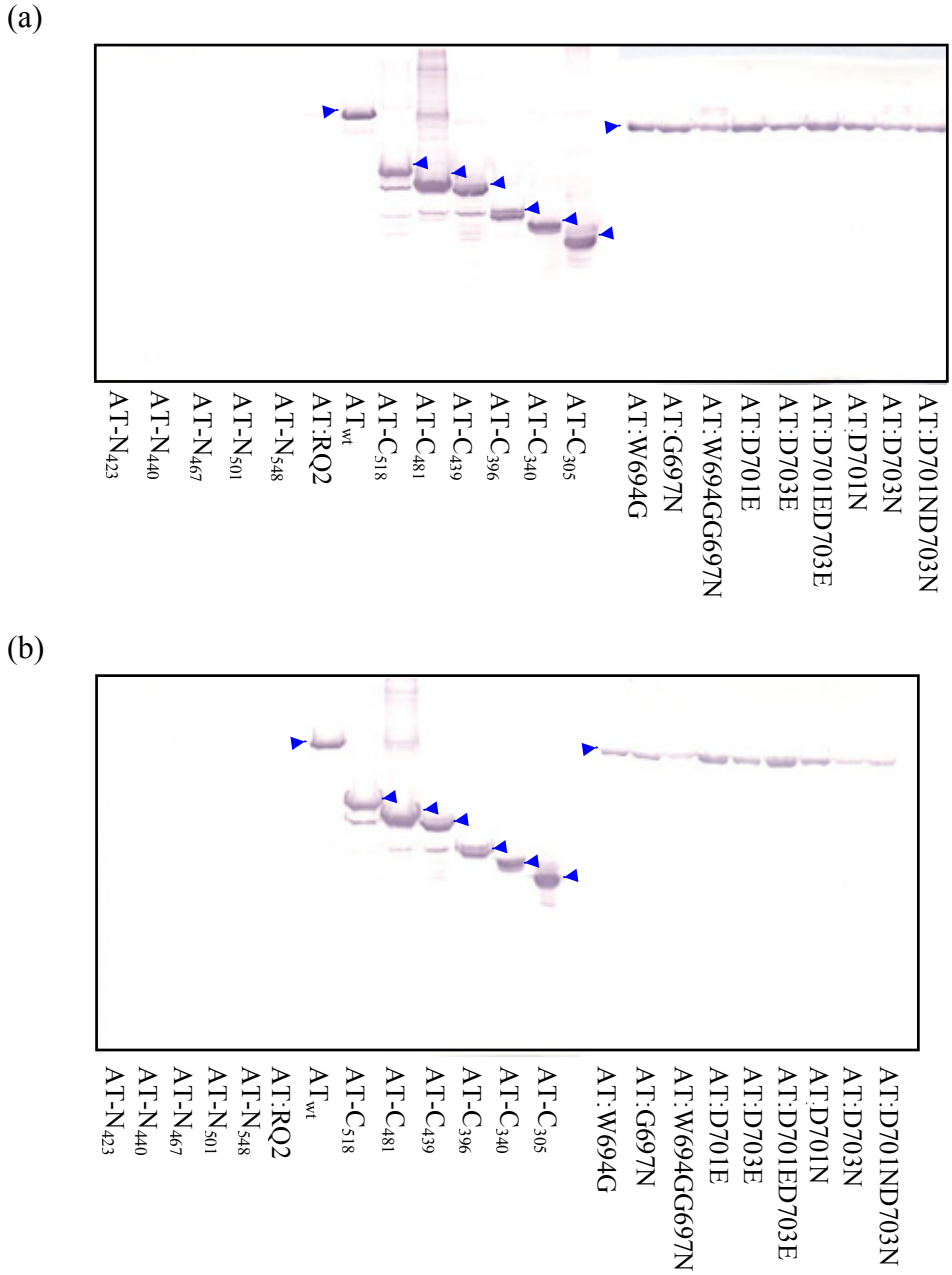

Figure 3.6 ***C domain mAbs binding to ATase, truncation constructs and mutants.*** Western blot of 12% SDS PAGE (see section 2.2.6.5) of whole cell extracts for the ATase protein, various ATase truncation constructs (Table 3.7) and ATase mutants using the C domain mAbs (a) 6A3 and (b) 27D7 as purified ascitic fluid (see section 2.2.9.8). The bands indicating the appropriate induced proteins are marked with arrows.

3.3.3.3 N domain mAb

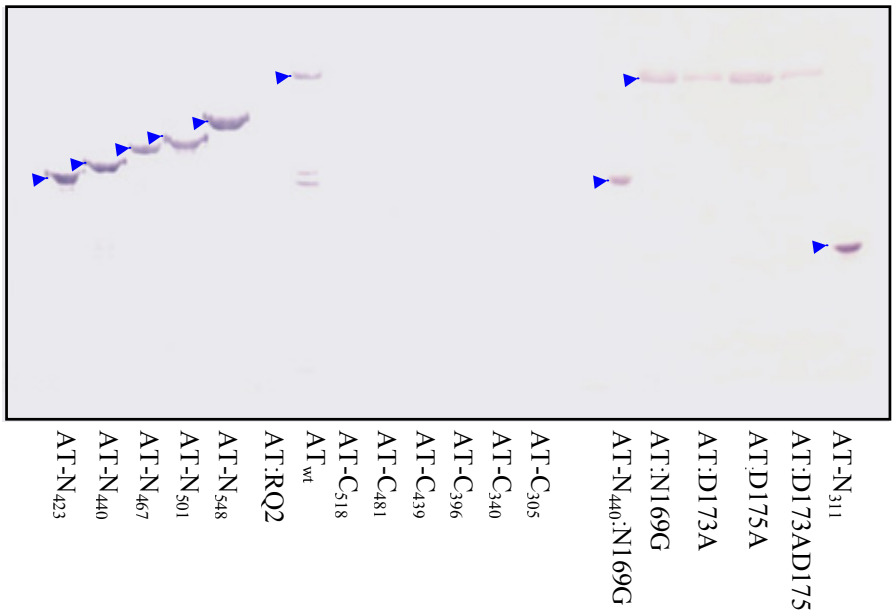

Figure 3.7 ***N domain mAb binding to ATase, truncation constructs and mutants.*** Western blot of 12% SDS PAGE gel (see section 2.2.6.5) of whole cell extracts for the ATase protein, various ATase truncation constructs and ATase mutant proteins using the N domain mAb 6B5 as purified ascitic fluid (see section 2.2.9.8). The bands indicating the appropriate induced proteins are marked with arrows.

The ATase mAb 6B5 was chosen from the initial screening ELISA (Table 3.6) because it only bound to AT-N_{548} and not AT-C_{522} and was denoted the N domain mAb. In order to locate the binding site for this mAb all of the ATase truncation constructs and the entire ATase protein cell lysates (see section 3.2.1.3) (Table 3.7) were separated by 12% SDS PAGE and immunoblotted with purified mAb (see section 2.2.9.8) (Figure 3.7). In this Western blot analysis the extracts from ATase mutants (see Chapter 7) within the deadenylylation domain β polymerase motif were also included.

Visual inspection of Figure 3.7 shows the 6B5 mAb binds in the N-terminal region of the ATase protein, it does not bind to AT:RQ2 or any of the C-terminal truncation constructs. The smallest N-terminal truncation construct to demonstrate binding to the 6B5 mAb was AT-N_{311} (first 311 N-terminal residues). Therefore the mAb 6B5 is binding to ATase in the region between the residues 1 and 311 (Figure 3.8). The

truncation construct AT-N_{311}, includes the putative catalytic site determined by sequence alignment with rat DNA polymerase β (Holm and Sander, 1995).

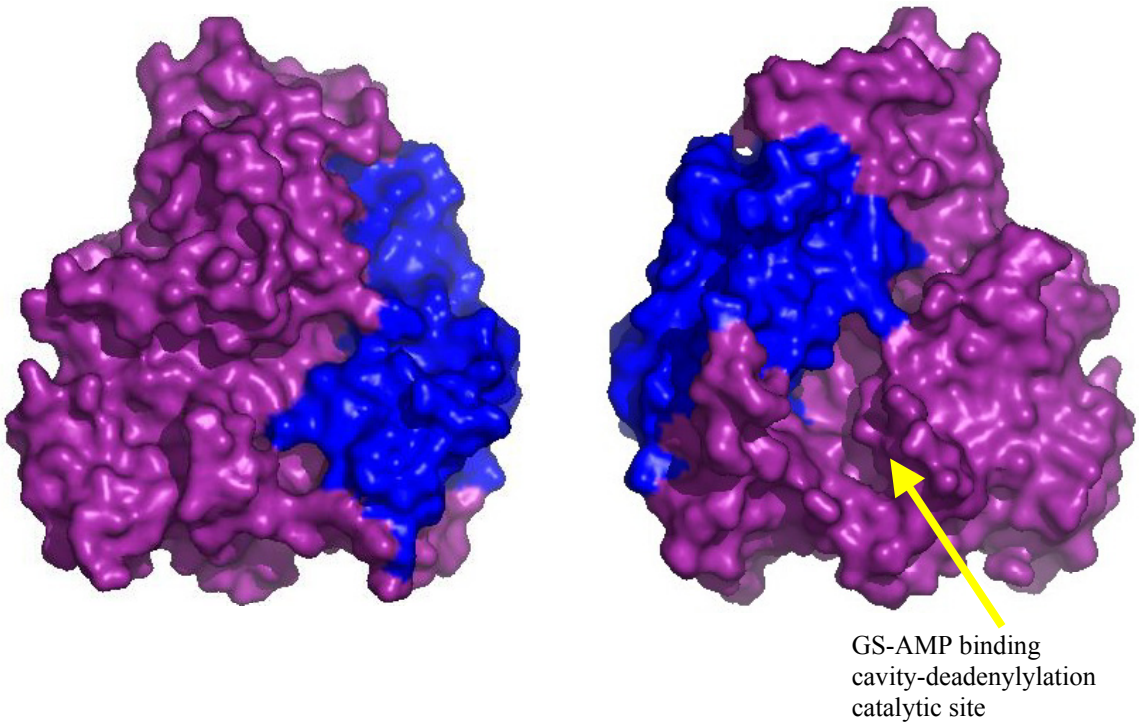

Figure 3.8 ***Binding region of N domain mAb.*** Surface diagram of AT-N_{440} (Xu *et al.*, 2004) the deadenylylation domain of ATase. The purple region is the first 311 residues of the protein where the 6B5 mAb binds. Also shown on the diagram is the binding cavity for the GS-AMP protein.

Several point mutations were made in the putative N domain catalytic site of ATase at residues Asn169, Asp173 and Asp175. None of the mutations at these residues disrupted the binding of mAb 6B5 to ATase; therefore the mAb binds somewhere in the region of residues 1 to 169 or 176 to 311. The enzyme inhibition studies carried out in Chapter 6 suggest the likely binding region is the one encompassing residues 1 to 169.

The panel of truncation constructs (Table 3.7) proved to be a valuable tool in determining the binding regions for the ATase mAbs. The more detailed Western blot investigation of the mAb binding patterns using all the ATase truncation constructs and ATase mutant proteins produced in this laboratory (Figures 3.5-7) allowed the generation of the following schematic diagram, which shows the regions of the ATase

protein where the mAbs are binding (Figure 3.9). All of these mAbs are against primary Eps.

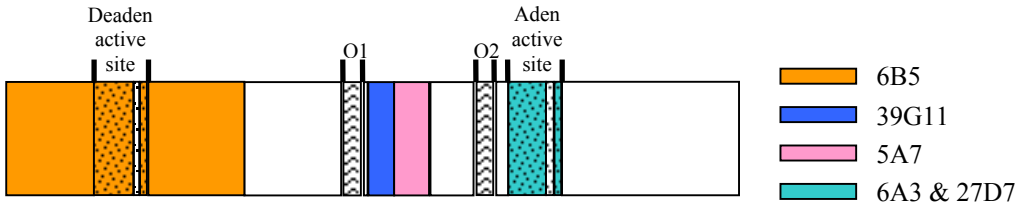

Figure 3.9 ***Monoclonal antibody binding regions of the ATase protein.*** This diagram shows the regions of the ATase protein where the mAbs are binding derived from the Western blotting data using all the ATase truncation constructs and ATase mutant proteins (see section 3.3.3). Also shown in the diagram are the putative active sites (Holm and Sander, 1995) and the two putative Q-linkers (Wooton and Drummond, 1989).

3.4 DISCUSSION

Modification of the T-loop of PII, whether by point mutation or uridylylation did not change the PII mAb binding profile (Table 3.2). This means the T-loop was not very antigenic, because none of the mAbs were binding to this region of the protein. This result is a bit surprising considering that the T-loop is implicated in the interaction of the PII protein and three different receptor-proteins (ATase, NRII and UTase) (Jiang *et al.*, 1997a). A further interaction with the GS protein mediated through the T-loop has also been proposed in the course of this work (Chapter 5). The T-loop is highly flexible and exposed on the surface of the protein (Carr *et al.*, 1996), increasing its chance of being antigenic (Tainer and Russell, 1994).

The most antigenic region of PII determined from this suite of mutants, was the area encompassing residues Gly24, Thr26 and Val64/Pro66 (Figure 3.4). This was confirmed by the reduced binding between the mutants and the mAb panel. This suggests that these residues are exposed and mobile in the entire protein (Tainer and Russell, 1994). The alignment of the ATP-binding cleft entrance residue, Thr26, is dependent on T-loop conformation (Xu *et al.*, 2001); therefore if the T-loop is highly mobile, Thr26 would be likewise.

There were two different mutations of the residue Gly24 of PII; one was a change to Ala and the other was a change to Asp. The change to Asp had a far more dramatic effect than changing to Ala, reducing the number of mAbs that bound to the mutated PII:G24D protein. This suggests that changing the Gly24 residue of the protein to Asp causes a significant change in the conformation of this region of the protein, which binds to a number of mAbs.

Residues Val64 or Pro66 of PII are in the most antigenic part of the PII protein, with the mutation of Val64 to Ala or Pro66 to Ser/Thr reducing the number of mAbs which bound well to the double mutants down from 32 to 5 (Table 3.5). The Val64 residue is involved in the interaction with ATP in the PII protein (Xu *et al.*, 2001) and also with ATP in the GlnK protein as an Ala (Xu *et al.*, 1998). The PII mutants, which showed the closest mAb binding profile to GlnK and its uridylylated form GlnK-UMP, were the two double V64AP66S/T mutants.

Differences between the two effector-proteins PII and GlnK/GlnK-UMP in the T-loop did not impact on mAb binding, but there were 14 mAbs which did not bind to GlnK/ GlnK-UMP (Table 3.5). Two of the PII mAbs (24H2 and 19G4) were used in further work to distinguish between PII and GlnK monomers incorporated into heterotrimers produced *in vivo* in *E. coli* (van Heeswijk *et al.*, 2000). Both of these mAbs recognise conformational Eps, which means they recognise residues next to each other spatially when the protein is folded rather than consecutive residues in the primary sequence (primary Ep).

In SPR, when GlnK was bound to the ligated ATase protein, the mAb 24H2 (which did not bind to the free protein) was able to bind to complexed GlnK (data not shown). This suggests that this mAb is binding in a region of the protein (including the residues Gly24 and Val64 or Pro66) which undergoes a conformational shift upon binding to the ATase protein to make GlnK more like PII and able to bind to the mAb.

The 19G4 mAb was purified using protein A agarose from hybridoma cell culture supernatant. The mAb lost its activity after this process. Sometimes the drop in pH

which is used to elute the bound mAb from the matrix can cause inactivation of the mAb (Goding, 1983).

The panel of mAbs and mutants for ATase is not as broad as that for PII. However, the ATase protein also has a large panel of truncated constructs available for investigation. The mAbs were produced against the whole protein, but when they were initially screened in ELISA (directly from the hybridoma culture plate) they were screened against the entire protein, the AT-N_{548} construct and the AT-C_{522} construct (Table 3.6). From these early screens five mAbs were chosen for further investigation; one against the N-terminal deadenylylation domain (6B5), two against the central R domain (5A7 and 39G11), and two against the C-terminal adenylylation domain (6A3 and 27D7). All these ATase mAbs were cloned and produced as ascitic fluid, and all except 39G11 were purified using protein A agarose.

These AT mAbs were used to investigate the binding sites for the effector-proteins PII, PII-UMP, GlnK and GlnK-UMP by assessing their impact on ATase activity in adenylylation and deadenylylation assays (see Chapter 6).

In conclusion, the work described in this chapter resulted in the production of a PII specific mAb (24H2) and PII/GlnK specific mAb (19G4) that were the key tools used to demonstrate the *in vivo* formation of heterotrimers between PII and GlnK in *E. coli* when the N status was low (van Heeswijk *et al.*, 2000). It is possible that other PII mAbs could be useful for mapping interactions with the various receptors of PII. The two PII mAbs 13E12 and 4A6 (bound poorly to the ATP-binding cleft mutant PII:T104A) could possibly help determine the contribution of that region of the protein to interactions with receptor-proteins. The 13C3 mAb bound poorly in the ATP-binding cleft entrance of PII. This mAb could possibly be useful in further investigations of α-kg binding and its impact on adenylylation activity of ATase (see Chapter 7). The mAbs against ATase were selected based on their binding to the different functional domains of ATase and the value of these in mapping the PII binding site on ATase will be demonstrated in the work reported in Chapter 6.

CHAPTER 4 Investigation of Structure and Function of PII by Site-directed Mutagenesis and its Functional Characterisation in the Adenylylation Cascade

4.1 INTRODUCTION

Many PII and PII-like proteins have been found across 11 bacterial families, and several lower and higher-plant families. In some instances a single organism can have several PII-like proteins (van Heeswijk *et al.*, 1995; Arcondeguy *et al.*, 2001) and these PII-like proteins can potentially form heterotrimers (Forchhammer *et al.*, 1999; van Heeswijk *et al.*, 2000). All of the PII-like signalling proteins characterised so far are involved in nitrogen assimilation. They have been grouped in terms of the 3rd and 5th residue of the monomer into GlnB-like or GlnK-like. The GlnB-like proteins have a Lys at residue 3 and a Glu or Asp at residue 5, whereas the GlnK-like proteins have a hydrophobic residue (Leu, Ile, Met or Phe) at position 3, and Ile, Thr or Met at position 5. The other feature that classifies the proteins as GlnK-like is the existence of a relationship between the *glnK*-like gene and the *amtB* gene (Arcondeguy *et al.*, 2001).

A sequence alignment of the PII-like and GlnK-like proteins demonstrates some highly conserved features (Figure 4.1). The functional T-loop (residues 37-55) is fairly highly conserved in a substantial proportion of the proteins and it is this part of the protein that is thought to make the multiple interactions with various receptor-proteins. However, the most conserved region of the proteins is surprisingly the ATP-binding cleft, rather than the residues that maintain structural integrity (Xu *et al.*, 1998). In Figure 4.1, 14 representative amino acid sequences have been aligned highlighting the key elements of the proteins.

```
           1                                                          60
glnB_ecoli MKKIDAIIKP FKLDDVREAL AEVGITGMTV TEVKGFGRQK GHTELYRGAE YMVDFLPKVK
glnB_klepn MKKIDAIIKP FKLDDVREAL AEVGITGMTV TEVKGFGRQK GHTELYRGAE YMVDFLPKVK
glnB_haein MKKIEAMIKP FKLDDVRESL SDIGISGMTI TEVRGFGRQK GHTELYRGAE YMVDFLPKVK
glnB_braja MKKIEAIIKP FKLDEVR.SL SGVGLQGITV TEAKGFGRQK GHTDLYRGAE YIVDFLPKVK
glnB_azobr MKKIEAIIKP FKLDEVKEAL HEVGIKGITV TEAKGFGRQK GHTELYRGAE YVVDFLPKVK
glnB_rhime MKKIEAIIKP FKLDEVKEAL QEVGLQGITV TEAKGFGRQK GHTELYRGAE YVVDFLPKVK
glnB_rhoru MKKIEAIIKP FKLDEVKEAL HEIGLQGITV TEAKGFGRQK GHTELYRGAE YVVDFLPKVK
glnB_rhoca MKKVEAIIKP FKLDEVKEAL QEAGIQGLSV IEVKGFGRQK GHTELYRGAE YVVDFLPKVK
glnK_ecoli MKLVTVIIKP FKLEDVREAL SSIGIQGLTV TEVKGFGRQK GHAELYRGAE YSVNFLPKVK
glnB_rhilv MKKIEAIIKP FKLDEVRSPS G.VGLQGITV TEAKGFGRQK GHTELYRGAE YVVDFLPKVK
glnB_synp7 MKKIEAIIRP FKLDEVKIAL VNAGIVGMTV SEVRGFGRQK GQTERYRGSE YTVEFLQKLK
glnB_porpu MKKIEAIIRP FKLNEVKIAL VKGGIGGMTV VKVSGFGRQK GQTERYKGSE YSIDIIDKIK
nrgB_bacsu MFKVEIVTRP ANFEKLKQEL GKIGVTSLTF SNVHGCGLQK AHTELYRGVK IESNVYERLK
glnL_metmp MKMIRAVVRP SKAEEVVDAL AESGCLALTK MDVIGRGKQK G....IKIDQ IYYDELPKTM
           ----------  ----------  ----------                  ----------
                β-1         α-A         β-2                        β-3

          61                                                        112 %identity
glnB_ecoli IEIVVPDDIV DTCVDTIIRT AQTGKIGDGK IFVFDVARVI RIRTGEEDDA AI     100
glnB_klepn IEIVVTDDIV DTCVDTIIRT AQTGKIGDGK IFVFDVARVI RIRTGEEDDA AI      99
glnB_haein LEVVVPDELV DQCIEAIIET AQTGKIGDGK IFVYHVERAI RIRTGEENED AI      78
glnB_braja IEIVIGDDLV ERAIDAIRRA AQTGRIGDGK IFVSNIEEAI RIRTGESGLD AI      71
glnB_azobr IEVVMEDSLV ERAIEAIQQA AHTGRIGDGK IFVTPVEEVV RIRTGEKGGD AI      71
glnB_rhime VEVVLADENA EAVIEAIRNA AQTGRIGDGK IFVSNVEEVI RIRTGETGLD AI      70
glnB_rhoru IELVIEDALV ERAIEAIQQA AQTGRIGDGK IFVYAIEEAI RIRTGERGGD AI      69
glnB_rhoca IEMVLPDEMV DIAIEAIVGA ARTEKIGDGK IFVSSIEQAI RIRTGETGED AV      68
glnK_ecoli IDVAIADDQL DEVIDIVSKA AYTGKIGDGK IFVAELQRVI RIRTGEADEA AL      68
glnB_rhilv VEVVLADENA EAVIEAIRKA AQTGRIGDGK IFVSNVEEVI RIRTGETGID AI      68
glnB_synp7 LEIVVEDAQV DTVIDKIVAA ARTGEIGDGK IFVSPVDQTI RIRTGEKNAD AI      65
glnB_porpu IEIIVSDDKV NSITEIIIKT AKTGEIGDGK IFISDVEQVI RIRTNDLNSA AL      60
nrgB_bacsu IEIVVSKVPV DQVTETAKRV LKTGSPGDGK IFVYEISNTI NIRTGEEGPE AL      41
glnL_metmp LMLVVEDDTA ENVIELITKT AYTGSFGYGK IFVSPVDEAY TVRTRS.... ..      40
           ----------  ----------  ----------  ----------  ----------
                           α-B         β-4         β-5         β-6
```

Figure 4.1 ***Sequence alignment of several representative PII-like proteins.*** Sequences for 14 PII homologue proteins from different species recovered from the SWISS-prot data bank have been aligned. Residues highlighted in red were conserved in all of the 50 sequences retrieved. Residues highlighted in blue represent 1-3 changes out of the 50 sequences retrieved: Leu20 had 1 change, Tyr51 had 2 changes, Lys58 had 1 change, Thr83 had 3 changes, Asp88 had 1 change and Phe92 had 2 changes. Comparative sequence identities with the *E. coli* PII protein are given as a percentage. Secondary structural elements are designated according to Carr *et al.*, (1996). Abbreviations and references are as follows: glnB_ecoli (*E. coli*; Vasudevan *et al.*, 1991), glnB_klepn (*Klebsiella pneumoniae*; Holtel and Merrick, 1988), glnB_haein (*Haemophilus influenzae*; Fleischmann, 1995), glnB_braja (*Bradyrhizobium japonicum*; Martin *et al.*, 1989), glnB_azobr (*Azospirillum brasilense*; De Zamarockzy *et al.*, 1990), glnB_rhime (*Rhizobium meliloti*; Arcondeguy *et al.*, 1996), glnB_rhoru (*Rhodospirillum rubrum*; Johansson and Nordlund, 1996), glnB_rhoca (*Rhodobacter capsulatus*; Kranz *et al.*, 1990), glnK_ecoli (*E. coli* GlnK; van Heeswijk *et al.*, 1995), glnB_rhilv (*Rhizobium leguminosarum*; Colonna-Romano *et al.*, 1987), glnB_synp7 (*Synechococcus* sp. PCC 7942; Tsinoremas *et al.*, 1991), glnB_porpu (*Porphyra purpurea*; Reith and Munholland, 1993), nrgb_bacsu (*Bacillus subtilis*; Wray *et al.*, 1994) and gln1_metmp (*Methanococcus maripaludis*; Kessler *et al.*, 1998).

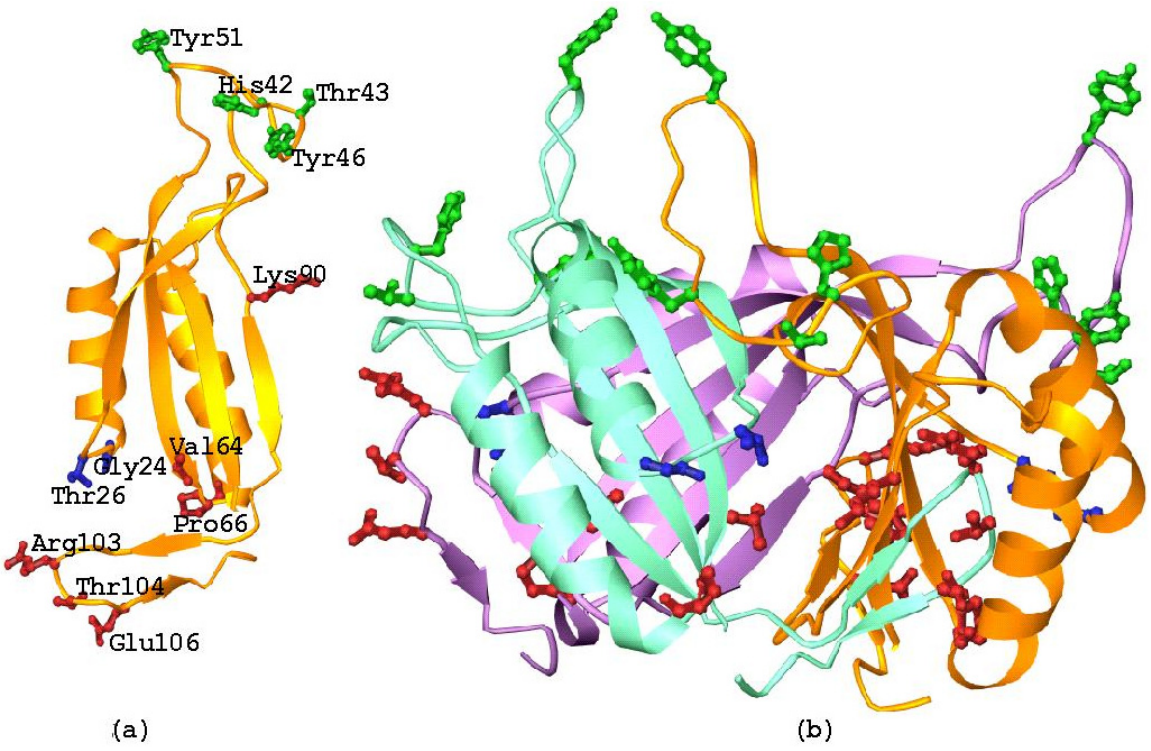

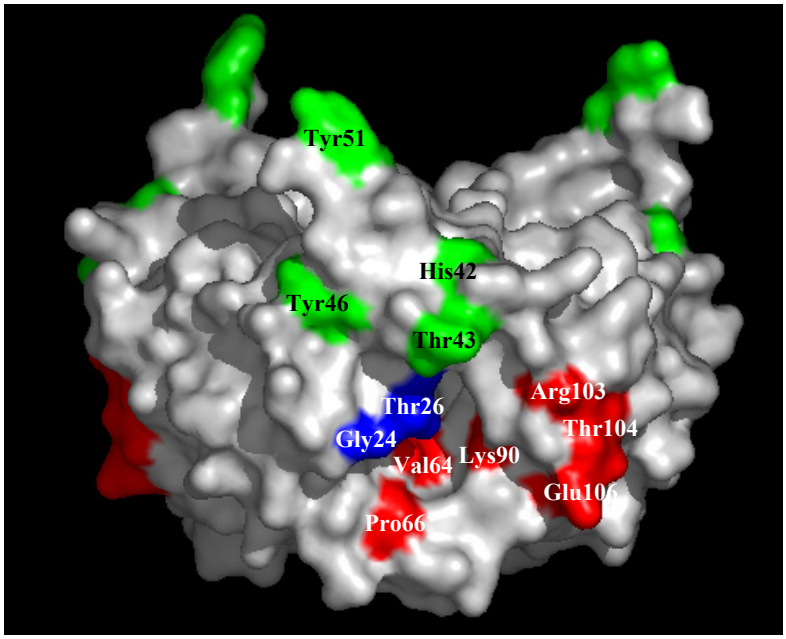

(c)

Figure 4.2 ***Location of mutated residues within the 3D model of the PII protein.*** In this diagram the mutated residues have been highlighted in the (a) monomer, (b) trimer and (c) trimer surface of the *E. coli* PII protein. The residues have been assigned to the important regions of the protein, such that green sidechains are T-loop mutants, blue sidechains are ATP-binding cleft entrance mutants, and red sidechains are ATP-binding cleft mutants.

As introduced in Chapter 1, the 3-dimensional structures have been determined by X-ray crystallography for PII (Carr *et al.*, 1996) and GlnK (Xu *et al.*, 1998) from *E. coli*

and they are both trimeric with 3 exposed T-loops and ATP-binding clefts. The structure of a PII-like protein from another proteobacterium *Herbaspirillum seropedicae* has recently been resolved and it also has a similar structure to *E. coli* PII (Benelli *et al.*, 2002).

Two new structures of PII-like proteins from cyanobacteria *Synechococcus sp* and *Synechocystis sp* have also been determined by X-ray crystallography. Both of these proteins have the same trimeric structure as the two *E. coli* structures comprised from ~12kD monomers. They also have T-loops and ATP-binding clefts (Xu *et al.*, 2003) and the PII from *Synechococcus sp* shows a divalent metal binding site that appears to have stabilised the structure.

All of these PII proteins differ in their T-loops and their consequent functions and receptor-proteins they interact with. The two cyanobacterial PII-like proteins are more similar to plant derived PII proteins (Smith *et al.*, 2003) and are functionally distinct from the proteobacterial *E. coli* PII. Although these two PII-like proteins have the conserved Tyr51 residue, in the cell they are phosphorylated at residue Ser49 on the T-loop of the protein, rather than uridylylated at the Tyr51 residue like its proteobacterial counterparts. It is this modification which determines the different interactions of the cyanobacterial PII-like proteins and their receptor-proteins. The cyanobacterial PII can be uridylylated, but the uridylylated protein does not impact on the activities of GS-AMP (Forchhammer, 2003).

A previous study by Jiang *et al.*, (1997a) produced a series of point mutations in the PII protein (*E. coli*), including a T-loop deletion mutant (Δ47-53) to investigate the functional importance of some of the highly conserved residues. This study suggested the exposed T-loop (which includes Tyr51, the site of reversible uridylylation) was not necessary for small effector-molecule binding, but was needed for the interaction of the PII protein with the three receptor-proteins ATase, UTase and NRII. Mutations in the B-loop of the PII protein, which lines the highly conserved ATP-binding cleft affected interactions with both small molecule-effectors and receptor-proteins. These results supported the structural predictions that the T-loop and ATP-binding cleft formed at the

monomer interfaces of the PII protein were important regulatory sites. Further work by Jiang *et al.*, (1997b) investigated the properties of the PII mutant that had no T-loop (Δ47-53) by producing heterotrimers, which contained a single wild-type subunit and two mutant subunits. This protein was able to carry out all the normal PII functions and interactions; this suggests only one T-loop is necessary for PII to perform effectively.

In this chapter another panel of PII (*E. coli*) mutants generated previously in this laboratory has been investigated. In Figure 4.2, the residues chosen for mutation in the PII protein have been highlighted to show their position within the monomer and trimer. These PII mutants were used in adenylylation and uridylylation assays and assessed for ATP and α-kg binding. Several of the PII mutants were also examined further using SPR.

4.2 METHODS

4.2.1 Expression and purification of the proteins

Plasmid	Description	Source/Reference
pRJ001	*glnB* (PII) in pND707	Jaggi *et al.*, (1996)
pRJ001:G24A	*glnB* (PII:G24A) in pND707	Vasudevan lab unpublished work
pRJ001:G24AT26A	*glnB* (PII:G24AT26A) in pND707	Vasudevan lab unpublished work
pRJ001:G24D	*glnB* (PII:G24D) in pND707	Vasudevan lab unpublished work
pRJ001:T26A	*glnB* (PII:T26A) in pND707	Vasudevan lab unpublished work
pRJ001:H42N	*glnB* (PII:H42N) in pND707	Vasudevan lab unpublished work
pRJ001:T43A	*glnB* (PII:T43A) in pND707	Vasudevan lab unpublished work
pRJ001:Y46F	*glnB* (PII:Y46F) in pND707	Jaggi (1998)
pRJ001:Y51F	*glnB* (PII:Y51F) in pND707	Jaggi (1998)
pRJ001:Y51S	*glnB* (PII:Y51S) in pND707	Vasudevan lab unpublished work
pRJ001:V64AP66S	*glnB* (PII:V64AP66S) in pND707	Vasudevan lab unpublished work
pRJ001:V64AP66T	*glnB* (PII:V64AP66T) in pND707	Vasudevan lab unpublished work
pRJ001:K90N	*glnB* (PII:K90N) in pND707	Vasudevan lab unpublished work
pRJ001:R103D	*glnB* (PII:R103D) in pND707	Vasudevan lab unpublished work
pRJ001:R103CT104A	*glnB* (PII:R103CT104A) in pND707	Vasudevan lab unpublished work
pRJ001:R103HT104A	*glnB* (PII:R103HT104A) in pND707	Vasudevan lab unpublished work
pRJ001:T104A	*glnB* (PII:T104A) in pND707	Vasudevan lab unpublished work
pWVH57	*glnA* (GS) in pBluescript II KS+	van Heeswijk *et al.*, (1996)
pJRV001	*glnA* (GS) in pND707	Vasudevan lab unpublished work
pRJ009	*glnE* (ATase) in pND707	Jaggi *et al.*, (1997)
pNV101	*glnD* (UTase) in pND707	Jaggi *et al.*, (1996)

Table 4.1 ***Recombinant proteins.*** List of the plasmids encoding the recombinant proteins used in this chapter including the plasmid name and source.

All the PII mutant recombinant vectors were produced previously in the Vasudevan laboratory using oligonucleotide directed mutagenesis of the pRJ001 plasmid (2.1.6.2) (see section 2.2.2.5).

The purified preparations of PII/PII mutants were over-expressed from the plasmids listed in Table 2.1.6.2 and 4.1. The RB9040 (2.1.4) strain was used for over-expression. This strain is *glnD*$^{-}$, which meant the over-expressed effector-proteins would not be uridylylated by endogenous UTase. The cells were grown in LB medium and when appropriate supplemented with ampicillin (100μgmL^{-1}) (see section 2.2.1.1 and 2).

Large-scale preparations (see section 2.2.5.5) were made for the effector-proteins using thermal induction (pND707-derived) (see section 2.2.6.1). These proteins were then purified (see sections 2.2.7.7) to at least 95% purity (except for PII:Y51F, which was estimated to be ~60% pure) as judged by SDS PAGE.

4.2.2 Direct small effector-molecule binding assay

Purified PII and PII mutant proteins (see section 4.2.1) were used in these assays (see section 2.2.10.3). Control experiments in the absence of PII showed no partitioning of small effector-molecules under these ultrafiltration conditions.

4.2.3 Adenylylation assays

The adenylylation assays were performed with standard conditions (see section 2.2.10.2.1), and additional α-kg (10μM and 1mM) using the purified PII and PII mutants (see section 4.2.1) as the effector-proteins.

4.2.4 SPR binding studies

A CM5 dextran chip was ligated with approximately 86 fmolmm^{-3} of purified ATase (see section 2.2.7.6) using amine coupling (see section 2.2.11.2). The binding experiments were run following the methods in section 2.2.11.3 using purified PII and

PII mutant proteins (see section 4.2.1), with various combinations of the small effector-molecules ATP and α-kg. The small effector-molecule combinations were chosen so they were relevant to the adenylylation assay conditions (see section 2.2.10.2.1).

4.2.5 Uridylylation assay

The uridylylation assays were run as steady state (see section 2.2.10.1.1) and initial rate (see section 2.2.10.1.2) assays for the purified PII and PII mutant proteins (see section 4.2.1).

4.3 RESULTS

4.3.1 Direct ATP binding to PII and PII mutants

The PII and PII mutants were assessed for their ability to bind ATP in the presence and absence of α-kg at pH 6.0 and 7.5 (see section 4.2.2). The comparative ATP binding capacities of all the PII mutants are shown in Table 4.2. The binding of ATP has been expressed as a proportion of PII_{wt} ATP binding at pH 7.5.

Most of the PII mutants bound less ATP than PII_{wt} at pH 7.5 (varying from 0.95-0.13 compared to PII_{wt}, which is expressed as 1). The PII:Y51F protein bound the same amount of ATP as PII_{wt}, and PII:G24D bound appreciably more ATP than the PII_{wt} (Table 4.2). Of the mutants that bound less ATP the PII:T104A mutant showed the greatest reduction and hardly bound any ATP (<5% of total ATP present compared to PII_{wt}, which bound 36.6±0.6%).

In the absence of α-kg the ATP binding to PII_{wt} doubled at pH 6.0 when compared with the amount of binding at pH 7.5. In most of the mutants the ATP binding at pH 6.0 was higher than at pH 7.5 with the exception of PII:T26A, PII:Y51F and PII:E106A, which showed no changes. Interestingly the T-loop mutants PII:H42N, PII:T43A and PII:Y46F show a doubling in the amount of ATP bound, which translates to nearly 75%

of available ATP. By comparison the ATP-binding cleft mutants showed only small increases in ATP binding with the shift in pH.

When α-kg was present, PII_{wt} bound nearly 92% of available ATP at pH 7.5 and ~98% at pH 6.0. The addition of α-kg restored the ATP binding of many of the mutants to the wild type protein levels at either pH (Table 4.2).

Protein	no α-kg		α-kg	
	pH 7.5	pH 6.0	pH 7.5	pH 6.0
PII_{wt}	1.00 ± 0.02 (927.5 ± 15.9)	1.95 ± 0.16	2.51 ± 0.00	2.61 ± 0.01
ATP-binding cleft entrance mutant				
PII:G24A	0.87 ± 0.09	2.10 ± 0.15	2.56 ± 0.00	2.63 ± 0.01
PII:G24AT26A	0.84 ± 0.02	1.58 ± 0.09	2.50 ± 0.02	2.53 ± 0.03
PII:G24D	1.39 ± 0.06	1.85 ± 0.04	1.77 ± 0.05	2.35 ± 0.07
PII:T26A	0.95 ± 0.07	1.00 ± 0.03	2.10 ± 0.02	1.94 ± 0.09
T-loop mutant				
PII:H42N	0.70 ± 0.00	2.23 ± 0.02	2.11 ± 0.04	2.41 ± 0.01
PII:T43A	0.93 ± 0.01	2.23 ± 0.03	2.41 ± 0.01	2.60 ± 0.00
PII:Y46F	0.85 ± 0.04	2.05 ± 0.09	2.58 ± 0.01	2.63 ± 0.00
PII:Y51F	1.03 ± 0.08	0.99 ± 0.05	2.60 ± 0.02	2.21 ± 0.08
PII:Y51S	0.84 ± 0.05	1.33 ± 0.08	2.61 ± 0.00	2.58 ± 0.01
ATP-binding cleft mutant				
PII:V64AP66S	0.63 ± 0.03	0.89 ± 0.04	1.92 ± 0.00	1.96 ± 0.01
PII:V64AP66T	0.71 ± 0.17	0.84 ± 0.01	1.70 ± 0.01	1.88 ± 0.03
PII:K90N	0.42 ± 0.00	0.60 ± 0.02	0.61 ± 0.02	0.33 ± 0.01
PII:R103D	0.48 ± 0.03	0.34 ± 0.02	1.48 ± 0.11	1.10 ± 0.01
PII:R103CT104A	0.64 ± 0.03	0.87 ± 0.07	1.47 ± 0.10	2.16 ± 0.02
PII:R103HT104A	0.51 ± 0.01	1.00 ± 0.03	0.67 ± 0.01	1.05 ± 0.07
PII:T104A	0.13 ± 0.00	0.70 ± 0.03	0.40 ± 0.02	1.17 ± 0.11
PII:E106A	0.88 ± 0.07	0.91 ± 0.04	1.46 ± 0.00	1.59 ± 0.12

Table 4.2 ***Binding of ATP to PII and PII mutants.*** This table shows binding of ^{14}C labelled ATP (2μM) to PII_{wt} (*E. coli*) and mutant PII proteins (10μM), ± α-kg (1mM) at pH 7.5 and 6.0 (see section 4.2.2). All assays were performed in duplicate and with PII_{wt} as a reference, essentially according to Jiang *et al.*, (1997a) so that a direct comparison can be made with mutants described in their work. The amount of binding has been expressed as a proportion of PII_{wt} binding with no α-kg at pH 7.5 (927.5 ± 15.9 DPM). At pH 7.5 and pH 6.0 PII_{wt} protein bound 36.6%±0.6% and 72.8%±5.8% of the total ATP present in the assay, respectively. When 1mM α-kg was added to the assay the amount of ATP bound rose to 91.9%±0.1% and 97.6%±0.4% of total ATP present in the assay, respectively.

Significantly, when α-kg was present the pH had little effect on ATP binding for most of the T-loop and ATP-binding cleft entrance mutants. However when there was no α-

kg present most of these mutants bound more ATP at pH 6.0 implying that the drop in pH and the presence of α-kg have a similar impact on the ATP binding property of PII (Table 4.2).

The ATP-binding cleft mutants bound much less ATP than the wild type protein. Addition of α-kg improved ATP binding to differing degrees and in most cases ATP binding was improved at the lower pH. The PII:R103D mutant bound less ATP at pH 6 than the wild type protein (Table 4.2).

4.3.2 Direct α-kg binding to PII and PII mutants

The PII and PII mutants were assessed for their ability to bind α-kg in the presence and absence of ATase at pH 7.5 with ATP (see section 4.2.2). The comparative α-kg binding capacities of all the PII mutants are shown in Table 4.3.

The binding of α-kg has been expressed as a proportion of PII_{wt} α-kg binding without ATase present. The assay was also performed at pH 6.0. Under these conditions the proteins were precipitating out, so the results have not been reported.

All the ATP-binding cleft mutants had reduced α-kg binding. Several T-loop and ATP-binding cleft entrance mutants also had reduced α-kg binding. The residues involved were Gly24 (mutation to Asp dropped binding more than the mutation to Ala), Thr26, His42, Thr43 and Tyr51 (mutation to Ser had no effect on α-kg binding, but mutation to Phe caused α-kg binding to drop) (Table 4.3).

Some of the mutants showed an increase in α-kg binding when ATase was present. The degree of increase was similar and only ~10% higher than when ATase was absent.

Protein	no ATase	ATase
PII_{wt}	1.00 ± 0.00 (1850.1 ± 5.8)	1.14 ± 0.01
ATP-binding cleft entrance mutant		
PII:G24A	0.78 ± 0.04	0.82 ± 0.01
PII:G24AT26A	0.99 ± 0.01	1.14 ± 0.00
PII:G24D	0.28 ± 0.02	0.30 ± 0.02
PII:T26A	0.64 ± 0.00	0.81 ± 0.01
T-loop mutant		
PII:H42N	0.58 ± 0.04	0.82 ± 0.00
PII:T43A	0.87 ± 0.00	0.98 ± 0.02
PII:Y46F	1.02 ± 0.01	1.16 ± 0.01
PII:Y51F	0.80 ± 0.01	0.79 ± 0.00
PII:Y51S	1.14 ± 0.01	1.12 ± 0.00
ATP-binding cleft mutant		
PII:V64AP66S	0.92 ± 0.01	1.05 ± 0.02
PII:V64AP66T	0.94 ± 0.01	1.00 ± 0.00
PII:K90N	0.29 ± 0.02	0.69 ± 0.01
PII:R103D	0.36 ± 0.02	0.33 ± 0.03
PII:R103CT104A	0.54 ± 0.04	0.57 ± 0.00
PII:R103HT104A	0.23 ± 0.02	0.22 ± 0.01
PII:T104A	0.38 ± 0.04	0.32 ± 0.01
PII:E106A	0.41 ± 0.00	0.77 ± 0.04

Table 4.3 ***Binding of α-kg to PII and PII mutants.*** This table shows binding of ^{14}C labelled α-kg (5μM) to PII_{wt} (*E. coli*) and mutant PII proteins (10μM) with ATP (2mM), ± ATase protein (10μM) at pH 7.5 (see section 4.2.2). The assay was also performed at pH 6.0. Under these conditions the proteins were precipitating out, so the results have not been reported. All assays were performed in duplicate and with PII_{wt} as a reference. The amount of binding has been expressed as a proportion of PII_{wt} binding. PII_{wt} alone bound 64.5%±0.2% of the total α-kg present in the assay, and when 10μM ATase was added the amount of α-kg bound rose to 73.5%±0.3% of the total α-kg present in the assay.

4.3.3 Adenylylation activity stimulated by PII and PII mutants

α-Ketoglutarate has two effects on adenylylation activity. Addition of a small amount of α-kg (10μM) stimulates adenylylation activity and addition of a large amount of α-kg (>10mM) depresses adenylylation activity (Jiang *et al.*, 1998b). The PII protein also binds to α-kg co-operatively with ATP (Kamberov *et al.*, 1995). In this series of adenylylation assays the impact of α-kg binding to PII_{wt} and the PII mutants was investigated.

Standard initial rate adenylylation assays (see section 4.2.3) were run for all the mutant effector-proteins and wild type PII with α-kg at the two concentrations 10μM and 1mM, and without α-kg. The rates were compared back to the PII_{wt} rate without α-kg present (Figure 4.3c). Several representative steady state curves (Figure 4.3a) and initial rate curves (Figure 4.3b) have been included.

Firstly the result in Figure 4c confirms previous studies that the low concentration of α-kg further stimulates adenylylation by PII_{wt} and that the higher concentration inhibits the reaction. The adenylylation activity stimulated by the various PII mutants in the absence of α-kg remained the same as PII_{wt} or was reduced. Two mutants, PII:R103D and PII:H42N deviated from the norm and showed an increase of ~20% in the initial adenylylation rate when no α-kg was present. This result indicated these two mutants were more effective at stimulating ATase than PII_{wt} under the standard adenylylation conditions used. The PII:G24AT26A, PII:T26A, PII:V64AP66T and PII:Y46F mutants were all the same as PII_{wt} and all the remaining mutants were less effective at stimulating adenylylation activity in ATase.

Addition of 10μM α-kg improved the adenylylation activity stimulated by all the mutants except PII:Y51S, PII:R103HT104A and PII:T104A (Figure 4.3c).

Addition of 1mM α-kg caused a drop in stimulated adenylylation activity for most of the T-loop and ATP-binding cleft entrance mutants except for PII:H42N and PII:Y51F, which stimulated the same level of activity. All the ATP-binding cleft mutants, except PII:E106A, PII:V64AP66S/T and PII:T104A showed an increase in the adenylylation activity they stimulated when 1mM α-kg was present in the assay. The PII:E106A and PII:V64AP66S/T mutants showed a drop in stimulated adenylylation activity under these conditions and PII:T104A showed no change in stimulated activity (Figure 4.3c).

(a)

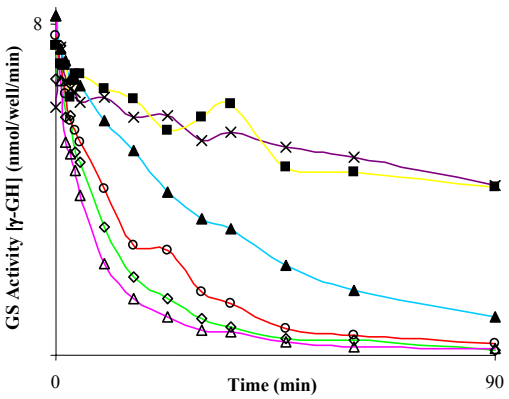

(b)

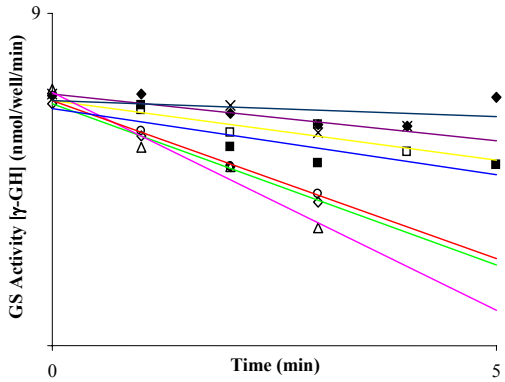

(c)

Protein	no α-kg	10μM α-kg	1mM α-kg
PII_{wt}	1.00	1.90	0.18
ATP-binding cleft entrance mutant			
PII:G24A	0.59	1.13	0.34
PII:G24AT26A	1.07	1.96	0.56
PII:G24D	0.61	1.46	0.53
PII:T26A	1.03	1.98	0.27
T-loop mutant			
PII:H42N	1.22	2.55	1.28
PII:T43A	0.82	1.94	0.64
PII:Y46F	1.05	2.06	0.37
PII:Y51F	0.45	1.15	0.49
PII:Y51S	0.25	0.25	0.15
ATP-binding cleft mutant			
PII:V64AP66S	0.67	1.22	0.34
PII:V64AP66T	1.08	2.02	0.48
PII:K90N	0.73	0.98	1.83
PII:R103D	1.35	1.70	2.21
PII:R103CT104A	0.26	1.28	0.46
PII:R103HT104A	0.29	0.30	0.50
PII:T104A	0.26	0.26	0.29
PII:E106A	0.72	1.89	0.57

Figure 4.3 ***Adenylylation assays for PII and PII mutants.*** The representative curves (a & b) show adenylylation of the GS protein stimulated by several of the mutants and PII_{wt} protein. In (a) the assay has reached a steady state and in (b) only the first 5min are examined. Standard adenylylation conditions (see section 2.2.10.2.1) were used except that the GS concentration used was 25nM (half the normal concentration). The assays were also run with high α-kg (1mM) and low α-kg (10μM). All assays were performed in duplicate and with PII_{wt} as a reference. The initial rate curves were fitted with a linear regression using Microsoft Excel. For each of the mutants that had activity in the assay the R^2 coefficient for the linear regression was >94%, often 99% (except for T43A, which was 90% and E106A, which was 91%). PII_{wt} (open diamond), PII:Y51S (closed square), PII:G24D (closed triangle), PII:R103D (open triangle), PII:T104A (X), PII:K90N (open circle), no AT (closed diamond) and no PII (open square). The ATase protein has a small amount of activity when there is no PII protein present stimulated by gln alone (using half the normal concentration of GS protein minimised this activity). (c) Initial rates for all the mutant PII proteins expressed as a proportion of wild type activity without α-kg.

4.3.4 Direct binding of PII and several PII mutants to ATase using surface plasmon resonance

This series of experiments was designed to investigate the impact of the small effector-molecules, ATP and α-kg on the binding of the ligated ATase protein to PII_{wt} and several PII mutants. The PII:Y51S T-loop mutant bound more α-kg and less ATP than PII_{wt} (Tables 4.2 and 4.3). The PII:R103D and PII:T104A ATP-binding cleft mutants both bound less α-kg and ATP than PII_{wt} (Tables 4.2 and 4.3). These mutants were chosen for the SPR experiment to investigate the impact of impaired ATP and α-kg binding on the interaction of the PII and ATase proteins.

Sensorgrams were produced from 20μL of various mixtures of effector-proteins with and without small effector-molecules being injected across ligated ATase at $5\mu L min^{-1}$. The disassociation phase was demonstrated by 2 min of buffer only passing across the ATase protein. The reported RU measurement was taken at 1 min into the disassociation phase. The sensorgrams for the various conditions with the four effector-proteins are shown in Figure 4.4.

The sensorgrams show that PII_{wt} demonstrated the highest binding to ATase under all conditions. The PII:Y51S mutant showed the poorest binding with negligible amounts of protein still being bound to ATase after 1min of buffer running over the ligated chip surface. The two ATP-binding cleft mutants demonstrated intermediate binding with more PII:R103D binding to ATase than PII:T104A (Figure 4.5).

Addition of a small amount of α-kg to the adenylylation assay dramatically improved the adenylylation rate for PII_{wt}, but hardly affected the binding of PII_{wt} to ATase. Increasing the amount of α-kg in the assay dramatically reduced the adenylylation activity, but as with the lower amount of α-kg there was minimal impact on binding to ATase (Figure 4.5).

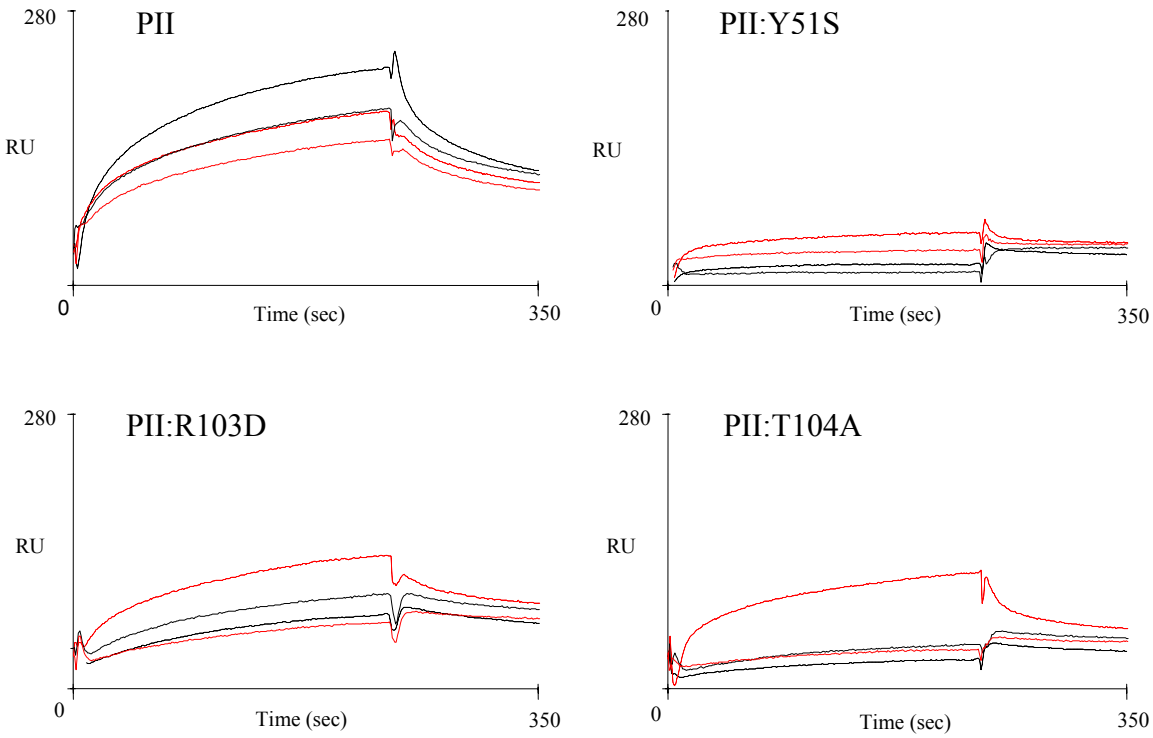

Figure 4.4 ***Surface Plasmon Resonance sensorgrams for PII and mutants interacting with ATase.*** This figure shows the sensorgrams for PII_{wt} (15μM) and several mutants interacting with ligated ATase in SPR using the Biacore X (see section 4.2.4). A CM5 dextran chip was ligated with approximately 86 $fmolmm^{-3}$ purified ATase using amine coupling. For a negative control the various small effector mixes with no protein were run across the ligated chip and the resulting curves subtracted from the runs where protein had been included. The subtracted curves were used for the analyses. Protein alone (black dashed), protein+1mM ATP+2mM Mg^{2+} (red dashed), protein+1mM ATP+2mM Mg^{2+}+2uM α-kg (solid black) and protein+1mM ATP+2mM Mg^{2+}+1mM α-kg (solid red).

The PII:Y51S mutant showed very poor binding to ATase under all conditions and had no activity under all conditions. This mutant bound more α-kg (~10%) and less ATP (~15%) than PII_{wt} (Tables 4.2 and 4.3). In this instance the inability of PII:Y51S to effectively bind to ATase and not changes in small effector-molecule binding to the mutant effector-protein appear to be the important factor in the behaviour of PII:Y51S in the adenylylation assay (Figure 4.5).

By contrast, small effector-molecule binding does appear to affect the behaviour of PII:T104A in the adenylylation assay. This mutant binds ATP half as well as PII_{wt}, and α-kg only binds very poorly (Tables 4.2 and 4.3). Increasing the concentration of α-kg had little effect on the binding of PII:T104A to ATase. This result is in keeping with the wild type protein, except a higher concentration of α-kg was necessary to achieve the same effect due to PII:T104A's poorer binding to α-kg. A similar effect was seen with

PII:R103D (also binds α-kg poorly) at the higher concentration of α-kg i.e. the higher concentration of α-kg improved the performance of PII:R103D in the adenylylation assay without affecting its binding to ATase (Figure 4.5).

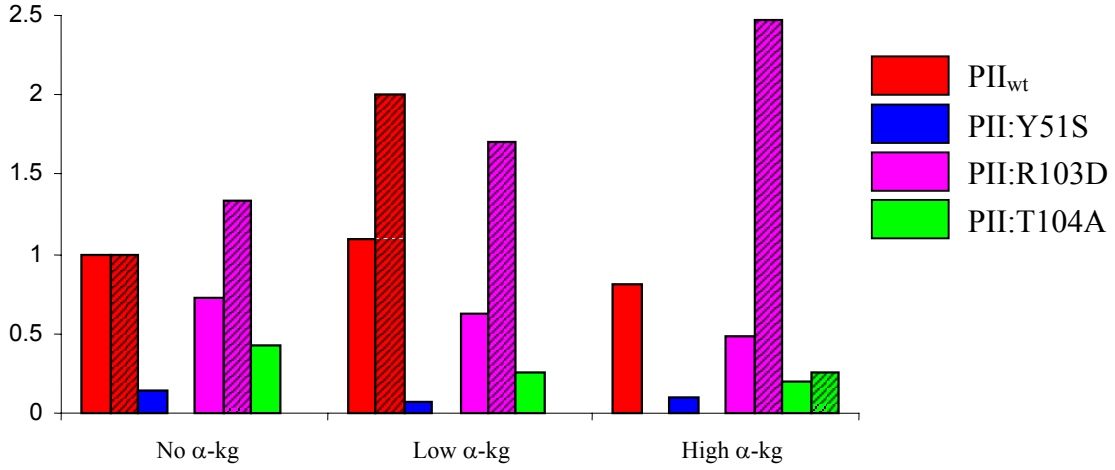

Figure 4.5 ***Comparative adenylylation rates and direct binding of PII and several PII mutants to ATase.*** This figure shows the amount of PII_{wt} or PII mutant protein bound to the ligated ATase protein 1min post addition of analyte protein (RU) derived from Figure 4.4 presented as a proportion of PII_{wt} binding with no α-kg (solid colour). Also included in this figure are the adenylylation rates for these conditions (see section 4.2.3) presented as a proportion of PII_{wt} activity with no α-kg (diagonal stripe). All assays were performed in duplicate and with PII_{wt} protein as a reference. The initial rate curves were fitted with a linear regression using Microsoft Excel. For each of the mutant proteins that had activity in the assay the R^2 coefficient for the linear regression was >94%, often 99%. ATase has a small amount of adenylylation activity when there is no PII present stimulated by gln alone, this activity has been subtracted from the adenylylation rates. In both assays high α-kg was 1mM, but in SPR and adenylylation low α-kg was 2μM and 10μM, respectively.

The ATP-binding cleft mutant PII:R103D is approximately half as effective as PII_{wt} at binding ATP (Table 4.2), yet 1.35x as effective at stimulating adenylylation (Table 4.3). As seen in Figure 4.6 the exposed negatively charged region of the complexed ATP molecule is adjacent to the exposed region of the Arg residue at position 103 (Xu *et al.*, 2001).

(a)

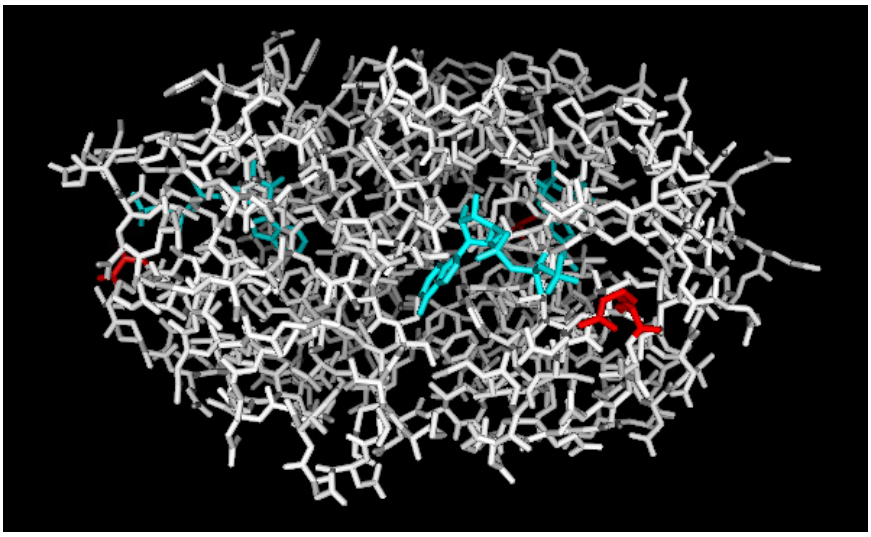

(b)

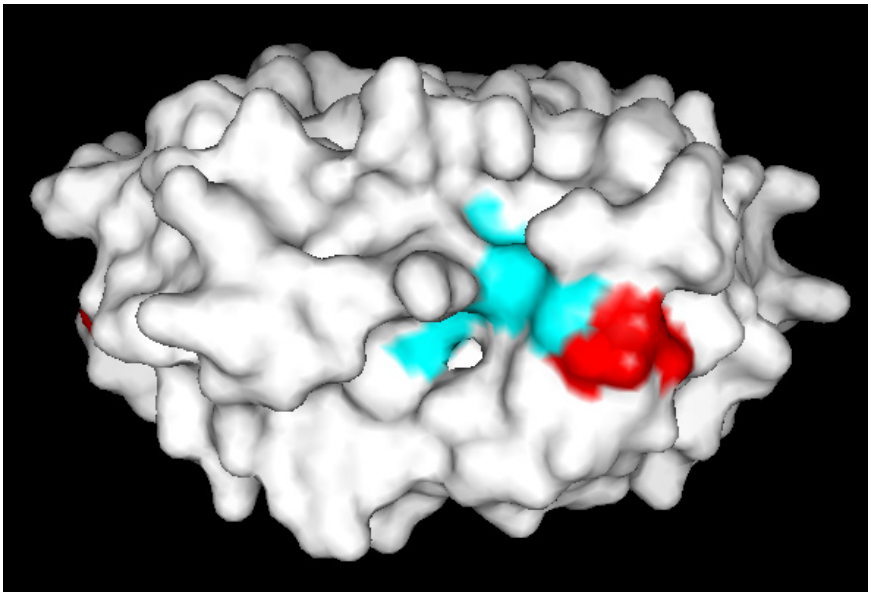

Figure 4.6 ***3D model of PII complexed to ATP.*** (Xu *et al.*, 2001) In this (a) stick diagram and (b) surface diagram of the PII trimer (*E. coli*) the R103D residue has been highlighted in red and the complexed ATP molecule in cyan. Note the exposed section of the Asp at position 103 is adjacent to the exposed portion of the ATP molecule on the surface of the protein. In this crystal of PII the T-loop was disordered, so the structure of that region of the protein could not be resolved.

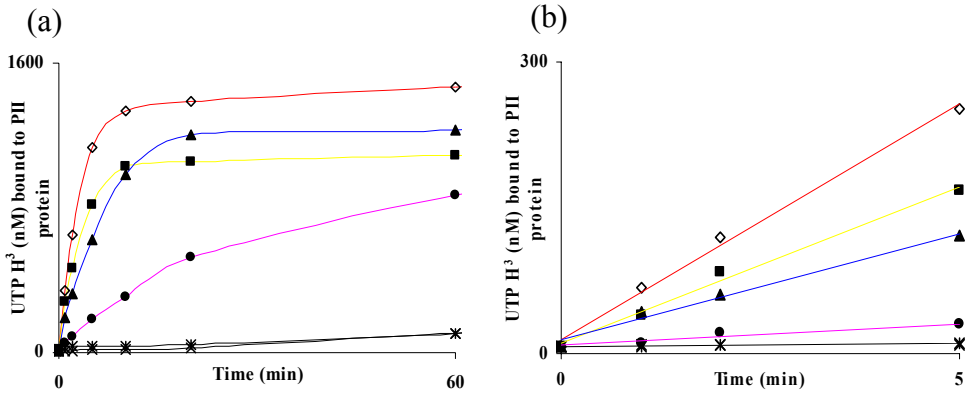

(c)

Protein	
PII_{wt}	1.00
ATP-binding cleft entrance mutant	
PII:G24A	0.97
PII:G24AT26A	0.66
PII:G24D	0.45
PII:T26A	1.10
T-loop mutant	
PII:H42N	0.03
PII:T43A	1.07
PII:Y46F	0.38
PII:Y51F	0.02
PII:Y51S	0.00
ATP-binding cleft mutant	
PII:V64AP66S	0.61
PII:V64AP66T	0.73
PII:K90N	0.23
PII:R103D	0.40
PII:R103CT104A	0.01
PII:R103HT104A	0.00
PII:T104A	0.00
PII:E106A	0.12

Figure 4.7 ***Uridylylation assays for PII and PII mutants.*** The representative curves (a & b) show uridylylation of several of the PII mutants and PII_{wt} (*E. coli*). In (a) the assay has reached a steady state and in (b) only the first 5min are examined. Standard uridylylation conditions were used (see section 4.2.5). All assays were performed in duplicate and with PII_{wt} as a reference. The initial rate curves have been fitted with a linear regression using Microsoft Excel. For each of the PII mutants that showed activity in the assay the R^2 coefficient for the linear regression was >94%, often 99% (except for R103D, which was 90%). PII_{wt} (open diamond), PII:G24AT26A (closed square), PII:G24D (closed triangle), PII:Y51F (asterisk), PII:T104A (X), PII:E106A (closed circle). (c) Initial rates for all the PII mutants expressed as a proportion of wild type activity.

.

4.3.5 Uridylylation of PII and PII mutants

Wild type PII and the PII mutants were assessed by their ability to be uridylylated by UTase. Standard initial rate uridylylation assays (see section 4.2.5) were run for all the mutant effector-proteins and wild type PII protein. The rates were compared back to the wild type PII rate (Figure 4.7c). Several representative steady state curves (Figure 4.7a) and initial rate curves over a 5min period (Figure 4.7b) have been included.

All of the mutants except PII:G24A, PII:T26A and PII:T43A showed a drop in the rate of uridylylation. The PII:G24A mutant had the same rate as the PII_{wt}. The PII:T26A and PII:T43A mutants had slightly higher rates of uridylylation than PII_{wt}. The PII:H42N, PII:Y51S/F, PII:R103C/HT104A and PII:T104A mutants were not uridylylated at all (Figure 4.7c).

4.4 DISCUSSION

Both the small effector-molecules ATP and α-kg bind to the PII protein in a co-operative manner (Kamberov *et al.*, 1995). Most of the T-loop and ATP-binding cleft entrance mutants showed improved ATP binding with the addition of α-kg (1mM) bringing the amount of ATP bound to the proteins back to the wild type level (Table 4.2). Two of the T-loop mutants PII:H42N and PII:T43A, and two of the ATP-binding cleft entrance mutants PII:G24D and PII:T26A, all showed reduced α-kg binding (Table 4.3) and a reduced response to α-kg in improving ATP binding at pH 7.5 (Table 4.2).

α-Ketoglutarate is potentially binding to the PII protein in the T-loop (Xu *et al.*, 1998). The reduced response to α-kg in improving ATP binding for the two T-loop mutants PII:H42N and PII:T43A was probably a direct result of the mutated proteins impaired capacity to bind α-kg. The PII:Y51F mutant also had diminished α-kg binding, but PII:Y51S did not. In this case the non-polar nature of the Phe residue may have disrupted α-kg binding by changing the hydrophobicity of the environment near the α-kg binding site, alternatively the OH group of Ser or the native Tyr at position 51 may form an interaction that stabilises the α-kg binding site.

The conformation of the T-loop can affect the positioning of Thr26 and either allow ATP to enter the cleft or partially block its entry (Xu, *et al.*, 2001). It's possible that mutating Thr26 to Ala impacted on the T-loop conformation, reducing α-kg binding. Mutating Gly24 to Ala had no effect, but mutating it to Asp produced the PII mutant with the least capacity to bind α-kg. Introducing a larger charged side chain into that region of the protein may also have caused a shift in the T-loop conformation reducing its capacity to bind α-kg. A similar result was demonstrated with mAb binding (see Chapter 3), where the Ala mutation had little effect on the mAb binding profile, but the Asp mutation caused 8 out of the 32 PII mAbs to no longer bind to the PII protein. This indicates that the Asp mutation is affecting the conformation or the surface charge of this region, which could in turn affect the T-loop conformation. The repulsion by the negative charge of the Asp side chain may also be another reason for the lower binding of α-kg (also negatively charged). Interestingly the adenylylation data in Figure 4.3 may support the suggestion that PII has two α-kg binding sites, a high affinity site that stimulates ATase activity at low α-kg concentration and a low affinity α-kg site that inhibits ATase activity at high α-kg concentrations (see Chapter 7).

All the ATP-binding cleft mutants showed diminished ATP binding. All these mutants also showed reduced α-kg binding probably as a direct result of their poorer ATP binding. The pH effect that is observed in the data presented in Table 4.2 suggests that the twofold increase in ATP binding at the lower pH may be the result of protonation of a PII side chain that consequently results in a conformational change in the protein. Interestingly based on the ATP binding data it appears that the binding of α-kg may result in the same conformational change at the higher pH and lowering the pH does not result in any further increase in ATP binding. The effect of pH reduction is less for the mutants PII:T26A and PII:Y51F. One possible explanation is that the hydroxyl group in the Thr26 side-chain must be making an important contact when a protonation/conformational change occurs somewhere in PII at pH 6.0 (a situation similar to α-kg binding). Similarly the OH group in Tyr51 may also play a role in stabilising the ATP binding since the PII:Y51S mutant appears to show a significant pH dependent shift compared with PII:Y51F. Obviously the pH effect for these two mutants is subtle since the addition of α-kg restores ATP binding to wild type levels.

Most of the mutants showed an increase in α-kg binding to a similar degree when ATase was present (Table 4.3), possibly due to α-kg binding directly to the ATase protein (ATase α-kg binding compared with PII was 0.16 ±0.05). However there were several mutants that showed no increase in α-kg binding, challenging the validity of the proposition. The PII:Y51S mutant does not bind to ATase (Figure 4.5), however the level of α-kg binding is close to the level observed for PII_{wt} in the presence of ATase (Table 4.3). With respect to α-kg binding, the mutants that were examined in this chapter appear to imply that α-kg binding occurs around Thr26 (compare the binding for PII:G24A, PII:G24D and PII:G24AT26A) with contributions from the T-loop residues, especially His42.

From structural alignment data, Benelli *et al.*, (2002) predicted that α-kg may bind in the lateral region of the ATP-binding cleft in the vicinity of residues Lys90 and Arg101, and although both ATP and α-kg could bind in the cleft their binding sites were not superimposed. The α-kg binding results derived in this chapter support this notion. Inspection of the position of Thr26 in the two surface diagrams of PII with and without ATP bound (Figures 4.2c and 4.6), show that this residue is at the lateral end of the cleft and binding of α-kg in this region would not superimpose over ATP.

Most of the ATP-binding cleft mutants were not as effective as PII_{wt} at stimulating adenylylation activity in ATase, with the exception of the PII:R103D mutant, which was better. All the PII:T104A mutant proteins had no activity (similar to the activity level when PII is omitted from the assay). These results support the notion that ATP is an absolute requirement for the binding activities of PII and that in the absence of bound ATP, PII does not adopt the best T-loop conformation for interacting with its various receptors. The Arg103 to Asp mutation is indeed interesting. The PII:R103D mutants ATP binding is low in the absence or presence of α-kg compared with PII_{wt}, and yet its ability to stimulate adenylylation by ATase is better than PII_{wt} and mutants such as PII:E106A that have a similar ATP binding profile. This result appears to suggest that the negative charge at Asp103 may mimic the negative charge of the ATP molecule when bound to PII_{wt}. The crystal structure of PII bound to ATP does support this notion because the negative charges on the phosphate group in ATP are exposed when bound

in the ATP-binding cleft and are capable of interacting with other proteins (Figure 4.6b).

The Gly24 residue in the ATP-binding cleft entrance region and Tyr51 residue in the T-loop seem to play an important part in stimulating adenylylation, both mutants that contained a mutated Gly24 residue had diminished activity as did the two Tyr51 mutants.

Nearly all the mutants showed some increase in adenylylation activity with the addition of 10μM α-kg. The mutants which showed no improvement were PII:Y51S, PII:T104A and PII:R103HT104A. For the two PII:T104A mutants it was probably due to poor ATP binding leading to poor α-kg binding, but for the PII:Y51S mutant that would not be the case, because it had wild type ATP and α-kg binding. For the PII:Y51S mutant it was probably because it bound very poorly to ATase. In SPR the PII:Y51S mutant bound poorly to the ligated ATase protein under all effector conditions (Figure 4.5). Mutating Tyr51 to Phe did not cause such a dramatic drop in adenylylation activity as the Ser mutation. From previous SPR studies (Jaggi, 1998), the ligated ATase bound more of the Phe mutant than the Ser mutant; this further supports the idea that in the case of the PII:Y51S mutant the interaction with the ATase protein itself was impaired.

Addition of 1mM α-kg caused inhibition of stimulated adenylylation activity by most mutants, though rarely to the degree of that shown by the wild type PII protein. The adenylylation activity stimulated by PII:H42N was greater than that of PII_{wt} with low α-kg, but interestingly the level of activity was still appreciable when 1mM α-kg was present. In most ATP-binding cleft mutants, an increase in stimulated adenylylation activity was actually observed. The PII:K90N and PII:R103D mutants had significant increases in stimulated adenylylation activity when 1mM α-kg was added to the assay. It is possible that the poorer α-kg binding capacity of these mutants means they need a higher concentration of α-kg to enable sufficient α-kg to bind to the protein to improve adenylylation activity. Consequently, the improvement seen in the interaction between PII and GS when 10μM α-kg is added to the adenylylation assay with PII_{wt} (see Chapter 5), is seen at a higher concentration of α-kg with these mutants.

Most of the mutations had a negative impact on uridylylation, except the Gly24 to Ala, Thr26 to Ala and Thr43 to Ala mutations. In a previous study by Jiang *et al.*, (1997a), using mutations also made in the PII T-loop and B-loop, which comprises one side of the ATP-binding cleft, similar results to this present study were obtained. All the mutants produced in that study were not uridylylated as well as PII_{wt} either. This further highlights the importance of the T-loop and the ATP-binding cleft for the functions of the PII protein, particularly in the interaction with UTase.

This study has added to the detailed pool of knowledge of the contributions made by individual residues within the functionally important T-loop and ATP-binding cleft to the activities of PII within the adenylylation cascade. In particular it appears that α-kg may be binding to PII in the vicinity of residue Thr26 and that changing the Gly24 residue to Asp dramatically affects the conformation of the protein in this region, diminishing α-kg binding. Another mutation of particular interest was the Arg103 to Asp mutation, which strongly suggests that the exposed negatively charged region of the ATP molecule complexed to PII is important in the adenylylation reaction.

CHAPTER 5 Investigation of the Functional Differences of PII and GlnK in the Adenylylation Cascade

5.1 INTRODUCTION

The X-ray crystallographic structures have been determined for both the PII protein (Cheah *et al.*, 1994; Carr *et al.*, 1996) and the GlnK protein (Xu *et al.*, 1998) of *E. coli*. The two proteins have superimposable squat "barrel-like" cores, which are approximately 50Å wide and 30Å high. Both proteins are trimeric and each 112 amino acid monomer (12.2 and 12.4kD, respectively) is comprised of 4 β-sheets and 2 α-helices. The monomers are arranged so the α-helices are positioned on the outside of the core. In Figure 5.1a and b, the 3D models for PII and GlnK have been superimposed to highlight their structural similarity.

The two proteins differ at the C-terminus and the loops (Xu *et al.*, 1998). The conformations of the T-, B- and C-loops of the two proteins are quite distinct. The Tyr51 residue, which is the site of reversible uridylylation (Son *et al.*, 1987, Jaggi *et al.*, 1996) within the T-loop is positioned ~13Å above the core in PII (Carr *et al.*, 1996) and ~8Å above the core in GlnK (Xu *et al.*, 1998). GlnK has a 3_{10} helix in the middle of its T-loop when stabilised in a crystal lattice (Xu *et al.*, 1998). A similar structure has been found in the thirteen residue flexible loop of another signalling protein, interferon γ when it is complexed with its receptor-protein. The 3_{10} helix makes intimate contact with its receptor-protein (Walter *et al.*, 1995). The 3_{10} helix in the GlnK protein may function in a similar way when binding to receptor-proteins (Xu *et al.*, 1998).

Another major difference between the two paralogues is found in the ATP-binding cleft. GlnK has an anion binding site (not present in PII) in amongst the highly conserved ATP-binding cleft (Xu *et al.*, 1998). It has been proposed competition between anions (PO_3^{4-} and SO_4^{2-}) and ATP in binding to GlnK could be a possible mechanism for coupling N regulation with the level of sulphate or possibly phosphate. The difference in their ATP binding sites may be linked to differences in the functions of the two proteins within the organism (Xu *et al.*, 1998).

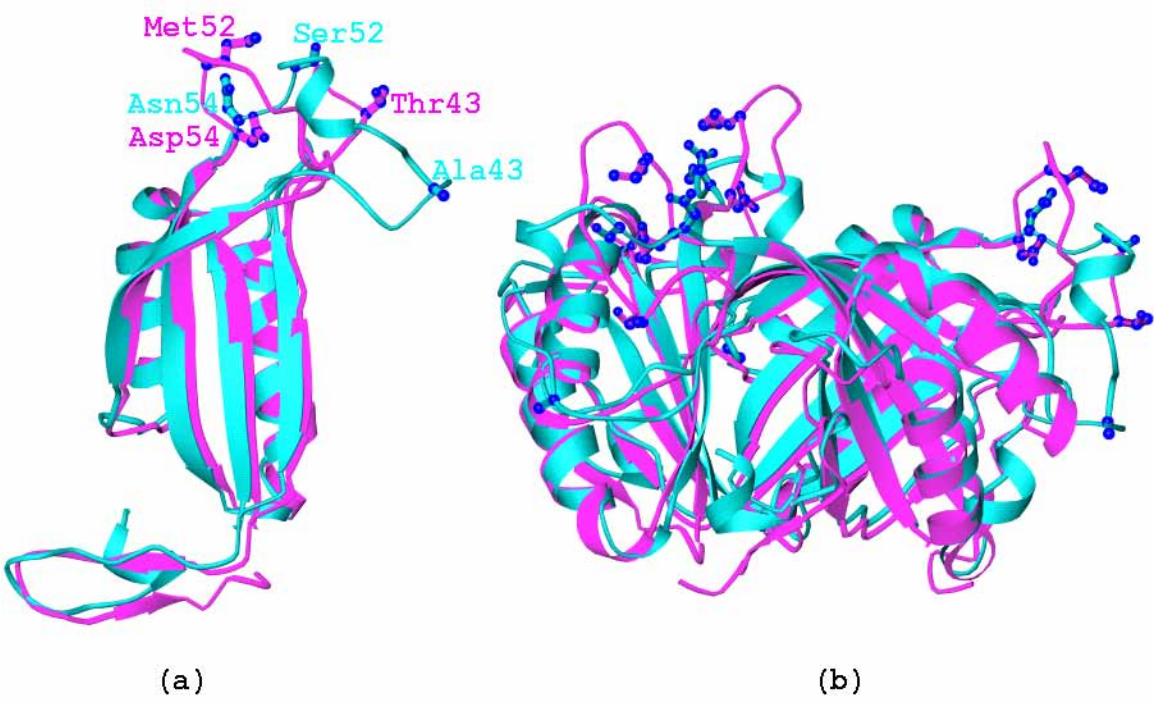


```
PII   MKKIDAIIKPFKLDDVREALAEVGITGMTVTEVKGFGRQKGHTELYRGAEYMVDF
GlnK  MKLVTVIIKPFKLEDVREALSSIGIQGLTVTEVKGFGRQKGHAELYRGAEYSVNF
PII   LPKVKIEIVVPDDIVDTCVDTIIRTAQTGKIGDGKIFVFDVARVIRIRTGEEDDAAI
GlnK  LPKVKIDVAIADDQLDEVIDIVSKAAYTGKJGDGKIFVAELQRVIRIRTGEADEAAL
```

(c)

Figure 5.1 ***Structure of the nitrogen signalling proteins PII and GlnK of E. coli.*** X-ray crystal structure of the PII (pink) (Carr *et al.*, 1996) and GlnK (cyan) (Xu *et al.*, 1998) proteins from *E. coli* have been overlaid to demonstrate their structural similarities. In (a) the monomer is depicted and in (b) the trimer is depicted. The three residues that differ in the T-loop have also been highlighted. (c) The 112 residues from the monomers of both proteins have been aligned. Non-conserved residues are highlighted in blue, and the highly conserved T-loop is highlighted in red. The three non-conserved residues within the T-loop: T43A, M52S and D54N are highlighted in purple.

Early experiments by Senior (1975) demonstrated a correlation between the regulation of the GS adenylylation state and the concentrations of the key stimuli gln and α-kg. The intracellular gln concentration signals N status, and the intracellular α-kg concentration signals C status. The α-kg molecule binds to the PII protein synergistically with ATP (Kamberov *et al.*, 1995) and gln binds to ATase and UTase (Jiang *et al.*, 1998a). Measurements for the *in vivo* concentration range for α-kg (*E. coli*) have been determined as 0.1-0.9mM (Senior, 1975), and for gln (*Salmonella typhimurium*) as ~0.3 to ~2-3mM (Ikeda *et al.*, 1996).

A recent review of PII signal transduction proteins by Atkinson and Ninfa (2000) proposed that when there was no α-kg present, PII adopted a conformation which did not allow the protein to interact with ATase or NRII. If the concentration of α-kg was ~5μM, one molecule of α-kg bound to PII allowing it to interact with ATase and NRII. If the concentration of α-kg rose to ~150μM, all three sites on the PII molecule were occupied by α-kg and the PII protein could no longer interact with ATase or NRII (see Figure 5.2).

Figure 5.2 ***Regulation of PII conformation.*** The main C signal is α-kg. Trimeric PII has three α-kg binding sites and three uridylylation sites. The binding of α-kg influences the ability of PII to interact with ATase and NRII, both of which are involved in N regulation. At low α-kg concentrations, the conformation of PII is such that it is able to interact with ATase and NRII. At high α-kg concentrations, the conformation of PII is such that it cannot interact with ATase or NRII. Additionally, uridylylation reduces the negative co-operativity in α-kg binding. Ovals, circles and triangles are used to represent the three different conformations of PII. Small black dots represent bound molecules of α-kg (Diagram reproduced from Ninfa and Atkinson, 2000).

The first aim of this chapter was to investigate the binding of PII, GlnK and their uridylylated forms to ATase under various small effector-molecule conditions using SPR. Previous studies have used adenylylation/deadenylylation activity assays, which provide information on the outcomes of complex interactions between several proteins rather than direct binding data for individual interactions. Surface plasmon resonance provides a means to study individual protein-protein interactions, and measure the direct

impact of small effector-molecule (ATP, gln and α-kg) binding on these interactions. In conjunction with direct binding studies, adenylylation and deadenylylation assays were also carried out with various conditions (in terms of effector-proteins and small effector-molecules).

The binding constants determined previously for α-kg and ATP (with and without α-kg) binding to PII, are 5.62±0.40μM, 0.24±0.03μM and 1.49±0.08μM, respectively (Kamberov *et al.*, 1995). The second aim of this chapter was to compare small effector-molecule binding for PII and GlnK.

A previous study by Atkinson and Ninfa (1999) investigated differences between PII, GlnK and several GlnK mutants using assays for NRI phosphorylation, adenylylation of GS, and uridylylation/deuridylylation by UTase. They found that both proteins could activate the phosphatase activity of NRII, stimulate adenylylation, and become uridylylated by UTase. However GlnK-UMP was not readily deuridylylated by UTase, unlike PII-UMP. PII was more effective at stimulating adenylylation (~40x) and GlnK did not show the low α-kg response in adenylylation (Jiang *et al.*, 1998b). The third aim of this chapter was to compare the capacity of the two effector-proteins to be uridylylated.

The two proteins share 67% sequence homology over the entire protein, but within the T-loop they share 85% sequence homology. In Figure 5.1c the amino acid sequences of PII and GlnK have been aligned with non-conserved residues highlighted in blue and the T-loop region highlighted in red (non-conserved residues within the T-loop are highlighted in purple). Evidence strongly suggests the T-loop is flexible in solution and that the sequence conservation, which doesn't have a matching structural conservation, is actually to confer flexibility on the loop, allowing it to interact with several different receptor-molecules (Xu *et al.*, 1998). Within the T-loop there are only three residues out of twenty (residues 36-55) where the two proteins differ (residues 43, 52, and 54), and this gives rise to the difference in T-loop structure.

Previous studies by Jiang *et al.*, (1997a) highlighted the importance of the highly conserved T-loop in the interaction of PII with its receptor-proteins. All their T-loop mutants had an impaired interaction with at least one receptor-protein. The PII mutants R38H, G41A and E50Q had a defective interaction with UTase predominantly. The A49P mutant only had a defective interaction with NRII. These results suggested that changes in the T-loop conformation could determine different specific interactions with the various receptor-proteins.

With this in mind Arcondeguy *et al.*, (2000) produced a range of PII mutants where all the non-conserved residues of the T-loop were mutated to the equivalent GlnK protein residues singly, doubly and as a triplet, such that the PII protein T-loop became the GlnK protein T-loop. The authors of that study examined the capacity of these PII mutants to regulate the interaction between *K. pneumoniae NifL* and *NifA*. Under normal circumstances only GlnK is involved in this interaction. The Asp to Asn mutation at position 54 in the T-loop enabled PII mutants carrying this mutation to partly substitute for GlnK, and if the T43A mutation was also included the PII mutant could completely substitute for GlnK.

The fourth and final aim of this chapter was to use the above-mentioned swapped PII T-loop mutants (Arcondeguy, *et al.*, 2000) in the adenylylation, deadenylylation and uridylylation assays to see if these interactions were also distinguished by a specific residue in the T-loop. Also included in this comparison was the PII salt-bridge mutant PII:K3LD5T produced previously by Canyon (1998), where the two distinguishing residues at positions 3 and 5 were swapped to GlnK residues.

5.2 METHODS

5.2.1 Expression and purification of the proteins

The purified preparations of PII and GlnK were over-expressed from the pRJ001 and pNV103 plasmids, respectively (Table 2.1.6.2 and 5.1). The RB9040 (2.1.4) strain was used for over-expression. This strain is *glnD*$^-$, which meant the expressed effector-proteins would not be uridylylated by endogenous UTase. The cells were grown in LB

medium and when appropriate supplemented with ampicillin (100μgmL^{-1}) (see section 2.2.1.1 and 2).

Plasmid	Description	Source/Reference
pRJ001	*glnB* (PII) in pND707	Jaggi *et al.*, (1996)
pNV103	*glnK* (GlnK) in pND707	Vasudevan lab unpublished
pTA52	*glnB* (PII:T43A) in pBluescript II KS+	Arcondeguy *et al.*, (2000)
pTA53	*glnB* (PII:M52S) in pBluescript II KS+	Arcondeguy *et al.*, (2000)
pTA54	*glnB* (PII:D54N) in pBluescript II KS+	Arcondeguy *et al.*, (2000)
pTA55	*glnB* (PII:D54NM52S) in pBluescript II KS+	Arcondeguy *et al.*, (2000)
pTA56	*glnB* (PII:D54NT43A) in pBluescript II KS+	Arcondeguy *et al.*, (2000)
pTA57	*glnB* (PII:D54NM52ST43A) in pBluescript II KS+	Arcondeguy *et al.*, (2000)
pTA58	*glnB* (PII:M52ST43A) in pBluescript II KS+	Arcondeguy *et al.*, (2000)
pSC003	*glnB* (PII:K3LD5T) in pND707	Canyon (1998)
pWVH57	*glnA* (GS) in pBluescript II KS+	van Heeswijk *et al.*, (1996)
pJRV001	*glnA* (GS) in pND707	Vasudevan lab unpublished work
pRJ009	*glnE* (ATase) in pND707	Jaggi *et al.*, (1997)
pNV101	*glnD* (UTase) in pND707	Jaggi *et al.*, (1996)

Table 5.1 ***Recombinant proteins.*** List of the plasmids encoding the recombinant proteins used in this chapter including the plasmid name and source.

Large-scale preparations (see section 2.2.5.5) were made for the PII/GlnK protein using thermal induction (pND707-derived) (see section 2.2.6.1). These proteins were then purified (see sections 2.2.7.7 and 8, respectively) to at least 95% purity as judged by SDS PAGE.

All the swapped T-loop mutant recombinant vectors were produced previously (Arcondeguy *et al.*, 2000).

The partly purified preparations of the PII, GlnK and swapped PII mutants were over-expressed from their various plasmids listed in Table 2.1.6.2 and 5.1. The RB9065 (2.1.4) strain was used for over-expression. This strain is *glnD*$^-$ and *glnB*$^-$, which meant the expressed effector-proteins would not be uridylylated by endogenous UTase and there would be no contaminating endogenous PII. The cells were grown in LB medium and when appropriate supplemented with ampicillin (100μgmL^{-1}) and gln (14mM) (see section 2.2.1.1 and 2).

The PII, GlnK and PII:K3LD5T proteins were thermally induced (see section 2.2.5.1) and the swapped PII T-loop mutants were induced with IPTG (see section 2.2.5.2).

These protein preparations were produced from small-scale cultures (see section 2.2.5.3) and partly purified (see section 2.2.7.3). The approximate individual target protein concentration was determined by comparison with bands of known concentration in SDS PAGE (see section 2.2.8.2).

5.2.2 SPR binding studies

A CM5 dextran chip was ligated with approximately 86 $fmolmm^{-3}$ of purified ATase (see section 2.2.7.6) using amine coupling (see section 2.2.11.2). The binding experiments were run following the methods in section 2.2.11.3 using purified PII/GlnK protein (see section 5.2.1), and uridylylated purified PII/GlnK protein (see section 2.2.5.6.1) with various small effector-molecule combinations. The small effector-molecule combinations were chosen, so they were consistent with the adenylylation and deadenylylation conditions (see section 2.2.10.2).

5.2.3 Adenylylation and deadenylylation assays

The adenylylation and deadenylylation assays (see section 2.2.10.2) were performed with many different combinations of small effector-molecules using the different PII/GlnK and swapped PII T-loop mutant effector-proteins.

5.2.4 Direct small effector-molecule binding assay

Purified PII/GlnK proteins derived from large-scale induction of their respective expression vectors (Table 5.1) in RB9040 strain (see section 5.2.1) were used in these assays (see section 2.2.10.3).

5.2.5 Uridylylation assay

The uridylylation assays were run as steady state (see section 2.2.10.1.1) and initial rate (see section 2.2.10.1.2) assays using purified PII and GlnK (5.2.1).

5.2.6 Uridylylation of the partly purified effector-proteins

The partly purified small-scale protein preparations derived from induction of their respective expression vectors (Table 5.1) in RB9065 strain (see section 5.2.1) were used to produce uridylylated effector-proteins (see section 2.2.5.6.2) for the deadenylylation assays (see section 2.2.10.2.2).

5.3 RESULTS

5.3.1 ATase binding constants using surface plasmon resonance

This series of experiments was designed to investigate the impact of the three small effector-molecules ATP, gln and α-kg on the binding of ATase to the four effector-proteins PII, PII-UMP, GlnK and GlnK-UMP. These small molecules and proteins are all necessary components of the adenylylation and deadenylylation assays (see section 5.2.3). Without them, ATase cannot regulate the activity of GS. It should be noted that the concentrations for the small effector-molecules were chosen to emulate various *in vitro* assay conditions.

Table 5.2 shows the disassociation constants for the PII, PII-UMP, GlnK and GlnK-UMP effector-proteins binding to ligated ATase derived from SPR studies (see section 5.2.2). The binding constants (K_D) for PII binding to ligated ATase with various small effector-molecule mixes were very similar ranging from 7.6μM to 14.7μM (Table 5.2). The K_D range variations for GlnK, PII-UMP and GlnK-UMP binding to ATase under the different conditions studied were 6.1nM to 3μM, 220nM to 1.39mM, and 3.5nM to 11.1μM, respectively (Table 5.2).

Addition of ATP (1mM) and Mg^{2+} (2mM) (condition 2, Table 5.2) to GlnK and GlnK-UMP improved their binding to ATase, but had little effect on the binding interaction of PII and PII-UMP. A further addition of 2μM α-kg (condition 3, Table 5.2) reduced the binding of GlnK and GlnK-UMP to ATase slightly, but had no effect on the binding of PII and PII-UMP to ATase. Increasing the concentration of α-kg to 1mM (condition 4,

Table 5.2) improved the binding of PII-UMP to ATase, but had little effect on the binding of the other three effector-proteins to ATase.

Condition	PII	GlnK	PII-UMP	GlnK-UMP
1. Protein (0.5mgmL^{-1})	11.5μM (2.32)	3.0μM (5.14)	13.7μM (1.18)	11.1μM (0.241)
2. ATP(1mM)+Mg^{2+} (2mM)	9.0μM (0.466)	17.7nM (1.23)	23.0μM (1.8)	425.5nM (1.78)
3. ATP+ Mg^{2+}+α-kg (2μM)	14.7μM (0.836)	97.1nM (3.62)	15.7μM (0.328)	10.0μM (3.06)
4. ATP+ Mg^{2+}+α-kg (1mM)	7.6μM (0.913)	31.6nM (1.75)	220nM (0.487)	8.7μM (1.62)
5. ATP+ Mg^{2+}+gln (2mM)	10.0μM (0.972)	18.0nM (0.944)	1.39mM (4.76)	3.5nM (2.63)
6. ATP+ Mg^{2+}+α-kg (2μM)+gln	11.9μM (1.08)	1.1μM (4.18)	8.0μM (0.459)	7.5μM (1.34)
7. ATP+ Mg^{2+}+α-kg (1mM)+gln	7.6μM (0.34)	6.1nM (1.2)	4.7μM (0.573)	6.7μM (2.05)

Table 5.2 ***Binding affinities of PII and GlnK to ATase under various small effector-molecule conditions, using surface plasmon resonance.*** This table shows the K_D values for the PII, GlnK, PII-UMP and GlnK-UMP effector-proteins interacting with the ligated ATase protein in SPR using the Biacore X (see section 2.2.11). A CM5 dextran chip was ligated with approximately 86 fmolmm^{-3} of purified ATase (see section 2.2.7.6) using amine coupling (see section 2.2.11.2). The disassociation constants were derived using Biaevaluation 3.0 software (see section 2.2.11.3). The chi^2 for each condition is shown in parentheses below the binding constants. For the protein alone condition the analyte solution was also passed over a blank chip, which had been activated and capped, but no protein ligated. This blank chip was used as the negative control. For the conditions that included small effector-molecules, the blank was set up as follows. The various small effector-molecule mixes with no protein were run across the ligated chip and the resulting curves subtracted from the runs where protein had been included. The subtracted curves were used for the analyses. Each condition had at least three replicates.

Addition of gln (2mM) to the ATP (1mM) + Mg^{2+} (2mM) condition (condition 5, Table 5.2) had no effect on PII or GlnK binding to ATase. Under this condition the binding of PII-UMP to ATase dropped and the binding of GlnK-UMP improved, both quite dramatically. However when 2μM α-kg (condition 6, Table 5.2) was included to conditions in 5, the binding of GlnK and GlnK-UMP to ATase was reduced, whereas the binding of PII-UMP improved. Further increasing the concentration of additional α-kg to 1mM (condition 7, Table 5.2) only had an impact on GlnK, improving its binding to ATase.

5.3.2 Adenylylation and deadenylylation assays

The results presented in Table 5.2 indicated there were several conditions where the effector-proteins PII and GlnK or PII-UMP and GlnK-UMP behaved differently when binding to ATase. In order to gain a better insight into the data obtained from SPR studies, further adenylylation/deadenylylation assays (see section 5.2.3) were carried out with the various conditions.

5.3.2.1 Standard adenylylation condition with and without α-kg (10μM)

Condition 5 [ATP (1mM) + Mg^{2+} (2mM) + g1n (2mM)] from the SPR studies (Table 5.2) matches closest to standard adenylylation conditions (Figure 5.3a) (see section 5.2.3). The K_D's for the PII and GlnK proteins binding to the ligated ATase protein under these conditions were 10μM and 18nM, respectively (Table 5.2). Therefore GlnK binds more tightly to ATase under these conditions. When 25nM GlnK was added (PII concentration in standard adenylylation assay) to the assay, the rate of γGH formation was only slightly higher than when it was omitted (Figure 5.3a). However when the GlnK concentration in the assay was raised to 250nM, the rate of γGH formation improved to almost the same level as for the assay with 25nM PII (Figure 5.3a).

Condition 6 [ATP (1mM) + Mg^{2+} (2mM) + gln (2mM) + α-kg (2μM)] used for the SPR experiment (Table 5.2) matches closest to standard adenylylation conditions + 10μM α-kg (Figure 5.3b). The K_D's for the PII and GlnK proteins binding to the ligated ATase protein under these conditions were 11.9μM and 1.1μM, respectively (Table 5.2). Therefore PII and GlnK bind with a similar strength to ATase under these conditions. Addition of 10μM α-kg to the adenylylation assay had no impact on the behaviour of GlnK (25, 125, 250nM) (Figure 5.3b). In contrast PII responded strongly (fast initial rate) to the addition of 10μM α-kg to the standard adenylylation assay (Figure 5.3b).

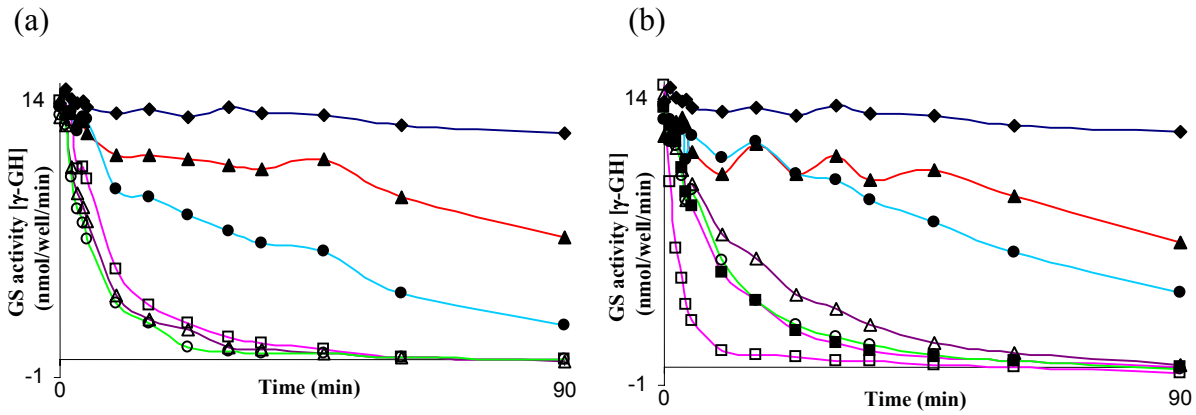

Figure 5.3 ***Adenylylation assay using the effector-proteins PII and GlnK.*** This assay shows the improvement in activity of the ATase protein with increasing concentrations of the GlnK protein by measuring the production of γ-glutamyl hydroxamate by GS. Both (a) standard assay conditions (see section 5.2.3) & (b) standard assay conditions + 10μM α-kg were used. No AT (♦), 0.025μM PII (□), no PII or GlnK (▲), 0.025μM GlnK (●), 0.125μM GlnK (Δ), 0.25μM GlnK (○). For (b) only 0.025μM PII (no α-kg) (■). All assays were performed in duplicate and with PII_{wt} as a reference. Error bars have not been shown on the curves as they hinder visual inspection. The standard error range for all the curves is generally <0.4.

The results from Figure 5.3 and Table 5.2 suggest that the interaction of PII and GlnK with ATase are not the sole determinants of the observed differences in stimulated activity (see later).

5.3.2.2 Standard deadenylylation condition

Condition 4 of the SPR experiment [ATP (1mM) + Mg^{2+} (2mM) + α-kg (1mM)] (Table 5.2) matches closest to standard deadenylylation conditions (Figure 5.4) (see section 5.2.3). The K_D's for PII-UMP and GlnK-UMP binding to ligated ATase under these conditions were 220nM and 8.7μM, respectively (Table 5.2). Therefore PII-UMP appears to bind ~40-fold more tightly to ATase under these conditions.

In order to examine if the binding of GlnK-UMP to ATase impacts on the difference between PII-UMP and GlnK-UMP in deadenylylation, GlnK-UMP was also used in the assay at 1μM (40 fold) and 2μM (80 fold). The results depicted in Figure 5.4 show that GlnK-UMP was able to stimulate deadenylylation by ATase albeit at a lower rate than PII-UMP. One direct conclusion that may be drawn from this not withstanding the *in vivo* situation is that, unlike the adenylylation situation discussed earlier it is probable

that the difference in behaviour between PII-UMP and GlnK-UMP in the deadenylylation assay could be attributed to the differences in their binding to ATase.

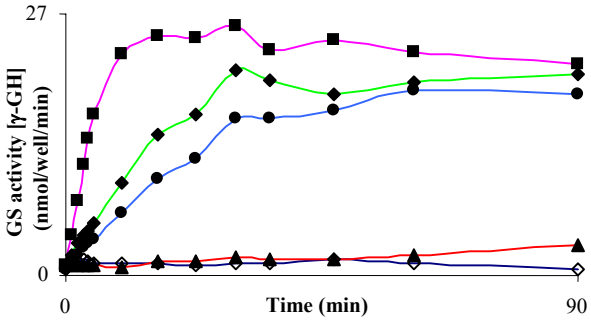

Figure 5.4 ***Deadenylylation assay using the effector-proteins PII-UMP and GlnK-UMP.*** This assay (see section 5.2.3) shows the improvement in deadenylylation activity of the ATase protein with increasing concentrations of the GlnK-UMP effector-protein by measuring the production of γ-glutamyl hydroxamate by GS-AMP. No AT (◊), 0.025μM PII-UMP (■), 0.025μM GlnK-UMP (▲), 1μM GlnK-UMP (●), 2μM GlnK-UMP (♦). All assays were performed in duplicate and with PII_{wt} as a reference. Error bars have not been shown on the curves as they hinder visual inspection. The standard error range for all the curves is generally <0.4.

5.3.2.3 Glutamine effect on deadenylylation with no α-kg present

Addition of gln (condition 7, Table 5.2) to the standard deadenylylation condition (condition 4, Table 5.2) caused a reduction in PII-UMP binding to ATase (K_D 220nM to 4.7μM), but did not affect GlnK-UMP binding to ATase (K_D 8.7μM to 6.7μM). This result is consistent with the knowledge that gln activates the adenylylation activity of ATase and is also an allosteric inhibitor of deadenylylation activity.

When there is no α-kg present (condition 2, Table 5.2) PII-UMP still shows a reduction in binding to ATase when gln is added (condition 5, Table 5.2) (K_D 23μM to 1.39mM), however GlnK-UMP shows an improvement in binding to ATase (K_D 425.5nM to 3.5nM) (Table 5.2) under these conditions. To further investigate the impact of gln binding to ATase in the deadenylylation of GS-AMP, the activity assay was run without α-kg present. In this assay any demonstrated shift in activity due to gln binding could only be due to disruption of the interaction between the uridylylated effector-protein and ATase (Figure 5.5). The concentrations of GS-AMP and the uridylylated effector-

protein added to the assay were double standard conditions to ensure there was clearly discernible deadenylylation activity when there was no α-kg present (α-kg is required for deadenylylation activity).

Under these conditions, inclusion of gln in the deadenylylation assay (no α-kg) completely wiped out the residual activity due to PII-UMP, but had no effect on the residual activity stimulated by GlnK-UMP (Figure 5.5). Therefore inhibition of deadenylylation activity under these conditions was probably due to gln complexed ATase protein not binding to PII-UMP. This result implies that the reduction in PII-UMP binding to ATase when gln is present is probably associated with a conformational change in ATase that inhibits PII-UMP binding.

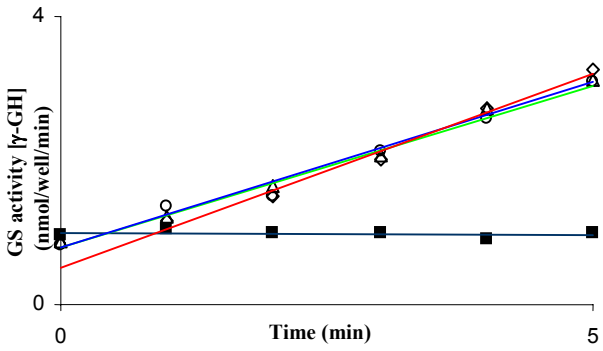

Figure 5.5 ***Glutamine effect on PII-UMP and GlnK-UMP stimulation in deadenylylation with no α-kg present.*** This deadenylylation assay (see section 5.2.3) measured the amount of γ-glutamyl hydroxamate produced by GS-AMP, when the assay used twice as much GS-AMP and uridylylated effector-proteins as standard conditions (see section 5.2.3), no α-kg and with/without gln (20mM). The initial rate curves have been fitted with a linear regression using Microsoft Excel. 50nM PII-UMP, no kg (◊), 50nM PII-UMP, no kg, gln (20mM) (■), 4μM GlnK-UMP, no kg (Δ), 4μM GlnK-UMP, no kg, gln (20mM) (○). All assays were performed in duplicate and with PII_{wt} as a reference. Error bars have not been shown on the curves as they hinder visual inspection. The standard error range for all the curves is generally <0.4.

5.3.2.4 Interplay between effector-proteins within the assays

The PII, GlnK, PII-UMP and GlnK-UMP proteins are potentially binding at the same site or very close to each other in the ATase protein (see chapter 6). Therefore in instances where the K_Ds are different and the stimulated adenylylation and

deadenylylation activities are different it may be possible to demonstrate inhibition between the effector-proteins if they are binding at the same site.

5.3.2.4.1 Adenylylation

The standard adenylylation condition (condition 5, Table 5.2) shows a dramatic difference between PII and PII-UMP binding to ATase. The K_D's for PII and PII-UMP binding to ATase under these conditions were 10μM and 1.39mM, respectively (Table 5.2). Under these conditions there is also a difference in binding to ATase between PII and GlnK, and PII and GlnK-UMP; the respective K_Ds were 10μM compared to 18nM, and 10μM compared to 3.5nM (Table 5.2). In order to measure the impact of the simultaneous presence of PII and the other effector-proteins, PII-UMP, GlnK or GlnK-UMP were added to the standard adenylylation assay containing PII (25nM; see Figure 5.6).

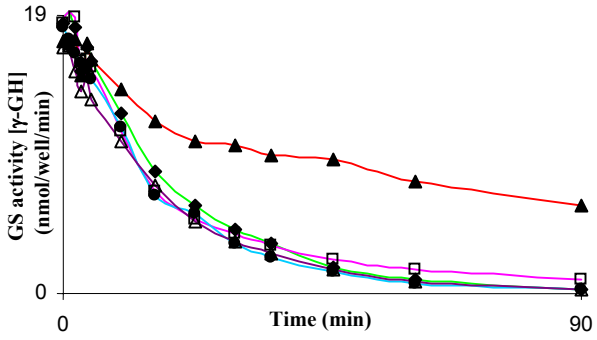

Figure 5.6 ***PII mediated adenylylation effector-protein inhibition assay.*** This curve shows the changes in activity of ATase stimulated by PII with additional effector-proteins added to the adenylylation assay. Activity is measured by the production of γ-glutamyl hydroxamate by GS. Standard assay conditions (see section 5.2.3) were used. PII (25nM) only (♦), PII (25nM) + PII-UMP (25nM) (□), PII (25nM + PII-UMP (500nM) (▲), PII (25nM) + GlnK (25nM) (○), PII (25nM) + GlnK-UMP (25nM) (Δ). All assays were performed in duplicate and with PII_{wt} as a reference. Error bars have not been shown on the curves as they hinder visual inspection. The standard error range for all the curves is generally <0.4.

Addition of the effector-protein PII and its uridylylated form, PII-UMP to the adenylylation assay (at the same molar concentration) did not change the stimulated activity of ATase. However, when PII-UMP was added in molar excess (20 fold), the stimulated activity of ATase dropped quite dramatically (Figure 5.6). This implies that

PII and PII-UMP may bind at the same site. Like PII-UMP, when GlnK or GlnK-UMP is added to the standard assay at the same molar concentration, there is no effect on the adenylylation activity of ATase stimulated by PII (Figure 5.6).

5.3.2.4.2 Deadenylylation

The standard deadenylylation condition (condition 4, Table 5.2) shows a difference between PII-UMP and PII binding to ligated ATase. The K_D's for PII-UMP and PII binding to ATase under these conditions, were 220nM and 7.6μM, respectively (Table 5.2). Under these conditions there is also a difference between PII-UMP and GlnK-UMP binding to ligated ATase. The K_D's for PII-UMP and GlnK-UMP binding to ATase under these conditions, were 220nM and 8.7μM, respectively (Table 5.2). The standard deadenylylation assay using PII-UMP as the effector-protein with various additional effector-proteins is shown in Figure 5.7.

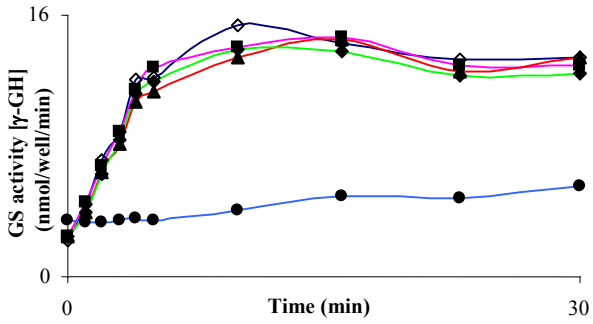

Figure 5.7 ***PII-UMP mediated deadenylylation effector-protein inhibition assay.*** This assay shows the changes in activity of the ATase protein stimulated by the PII-UMP protein with additional effector-proteins added to the deadenylylation assay. Activity is measured by the production of γ-glutamyl hydroxamate by GS-AMP. Standard assay conditions (see section 5.2.3) were used. PII-UMP (25nM) only (◊), PII-UMP (25nM) + PII (25nM) (■), PII-UMP (25nM) + PII (125nM) (▲), PII-UMP (25nM) + PII (5μM) (●), PII-UMP (25nM) + GlnK-UMP (250nM) (♦). All assays were performed in duplicate and with PII_{wt} as a reference. Error bars have not been shown on the curves as they hinder visual inspection. The standard error range for all the curves is generally <0.4.

Addition of the effector-protein PII-UMP and its non-uridylylated form PII to the deadenylylation assay (at the same molar concentration and at 5 times the molar concentration) did not change the ATase protein's stimulated activity. However, when molar concentration of PII was increased to 200 times that of PII-UMP the stimulated

activity of ATase dropped dramatically (Figure 5.7). When added to the standard assay at the same molar concentration the GlnK-UMP effector-protein had no impact on the deadenylylation activity of ATase stimulated by PII-UMP (Figure 5.7).

5.3.3 ATP binding to PII and GlnK

The PII and GlnK proteins (10μM) were assessed for their ability to bind ATP in the presence and absence of α-kg (1mM) over a concentration range of 0-50μM ATP^{14}C (see section 5.2.4) the raw DPM have been converted to μM ATP^{14}C (see section 2.2.10.1.3) (Figure 5.8). Unfortunately the concentration of effector-protein used in the assay was too high to produce a saturated curve for Scatchard plot analysis. The binding constants for ATP binding to PII with and without α-kg determined previously by Kamberov *et al.*, (1995) were 0.24±0.03μM and 1.49±0.08μM, respectively.

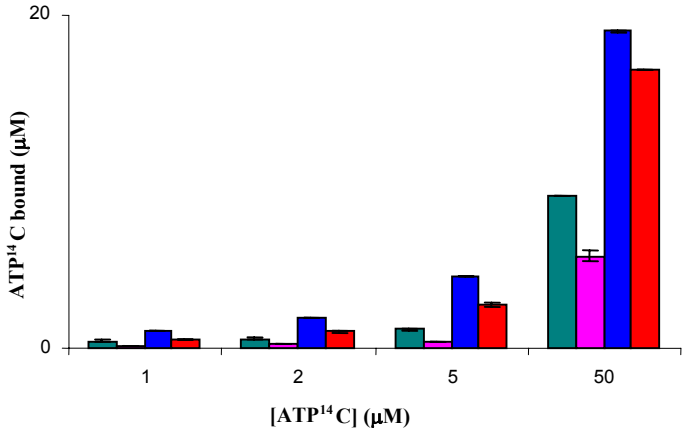

Figure 5.8 ***ATP binding to PII and GlnK.*** PII and GlnK (10μM) were assessed for ATP binding (see section 5.2.4) using radio-labelled ^{14}C ATP with and without α-kg (1mM). PII (teal), GlnK (pink), PII+1mM kg (blue) and GlnK+1mM kg (red).

Both the PII and GlnK proteins bound ATP and showed improved ATP binding when 1mM α-kg was included in the reaction. PII bound more ATP than GlnK with and without α-kg (Figure 5.8).

5.3.4 α-kg binding to PII and GlnK

The PII and GlnK proteins (10μM) were assessed for their ability to bind α-kg in the presence of ATP over a concentration range of 0-10μM α-kg ^{14}C (see section 5.2.4) the raw DPM have been converted to μM α-kg ^{14}C (see section 2.2.10.1.3) (Figure 5.9). Unfortunately the concentration of effector-protein used in the assay was too high to produce a saturated curve for Scatchard plot analysis. The binding constant for α-kg binding to PII determined previously by Kamberov *et al.*, (1995) was 5.62±0.4μM.

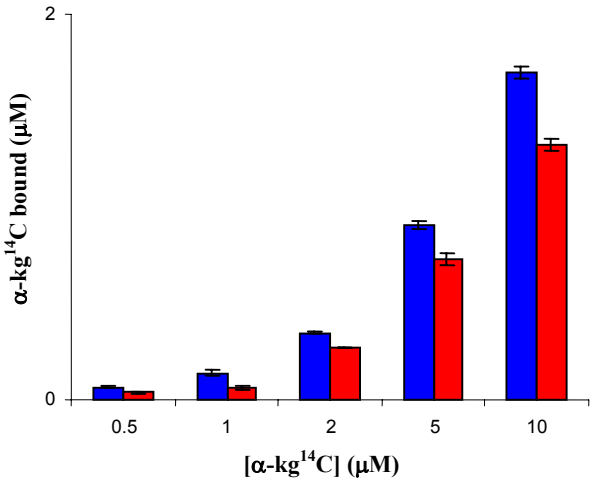

Figure 5.9 ***α-Ketoglutarate binding to PII and GlnK.*** PII and GlnK (10μM) were assessed for α-kg binding (see section 5.2.4) using radio-labelled ^{14}C α-kg in the presence of ATP (2mM). PII (blue) and GlnK (red).

Both PII and GlnK bound to α-kg with PII binding more than GlnK (Figure 5.9).

5.3.5 Uridylylation assay

The two effector-proteins were assessed for their ability to be uridylylated by UTase (see section 5.2.5). The incorporation of UTP ^{3}H was measured for both the purified PII and GlnK proteins (see section 5.2.1) (Figure 5.10).

The initial rate of incorporation of UTP ^{3}H for GlnK was 1.66 fold faster than PII (Figure 5.10). This means the interaction between the GlnK and UTase proteins was more effective than the interaction between the PII and UTase proteins.

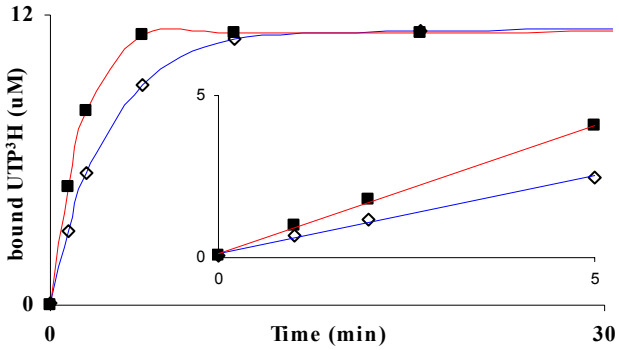

Figure 5.10 ***Uridylylation assay for purified PII and GlnK.*** These curves show the steady state assay (see section 2.2.10.1.1) and the initial rate assay in the inset (see section 2.2.10.1.2). The initial rate curves were fitted with a linear regression using Microsoft Excel. The rates of incorporation of $UTP^{3}H$ for PII and GlnK were 0.48 $\mu Mmin^{-1}$ and 0.79 $\mu Mmin^{-1}$, respectively.

5.3.6 Comparison of swapped PII to GlnK mutants

The T-loop of the PII and GlnK proteins is very important for interactions with various receptor-proteins in the N assimilation pathway in *E. coli,* and a high proportion of residues are conserved between the two paralogues. However, three residues in the T-loop of PII and GlnK are different (Figure 5.1c) and a series of PII mutants carrying the GlnK residues were produced by Arcondeguy, *et al.*, (2000) and tested for interaction with NifA. The three residues involved were Thr43, Met52 and Asp54, and they were mutated to Ala, Ser and Asn, respectively (either individually, as double mutants or the triple mutant).

The differences between PII and GlnK at residues 3 and 5 are used for classification purposes (Arcondeguy *et al.*, 2001). The PII:K3LD5T mutant produced previously by Canyon (1998) was also included in this study to compare their function in the adenylylation cascade.

The above mentioned mutants were used in adenylylation and deadenylylation assays to assess the role of the T-loop in distinguishing between the activities of PII and GlnK. The PII mutants were also uridylylated to see what effect the mutations might have on presentation of the T-loop to UTase, and the role of the different residues in distinguishing between PII and GlnK.

5.3.6.1 Adenylylation assay

There are two distinct differences between PII and GlnK in the adenylylation assay. The first is their capacity to stimulate the adenylylation activity of ATase under standard conditions (see section 5.3.2.1). GlnK is not as effective as PII at stimulating the activity of ATase (Figure 5.3a) when used in the same molar concentration. Secondly, as shown previously, GlnK does not respond the addition of α-kg (10μM) in the standard adenylylation assay, whereas the activities of PII are increased (Figure 5.3b). The PII, GlnK and swapped PII T-loop mutants were only partly purified (see section 5.2.1) and their concentration was determined by comparison with a SDS-PAGE protein standard (see section 2.2.8.2). Since the protein concentrations were only approximately determined the mutants were compared in terms of the difference between stimulated ATase activity with and without α-kg (10μM) (Figure 5.11).

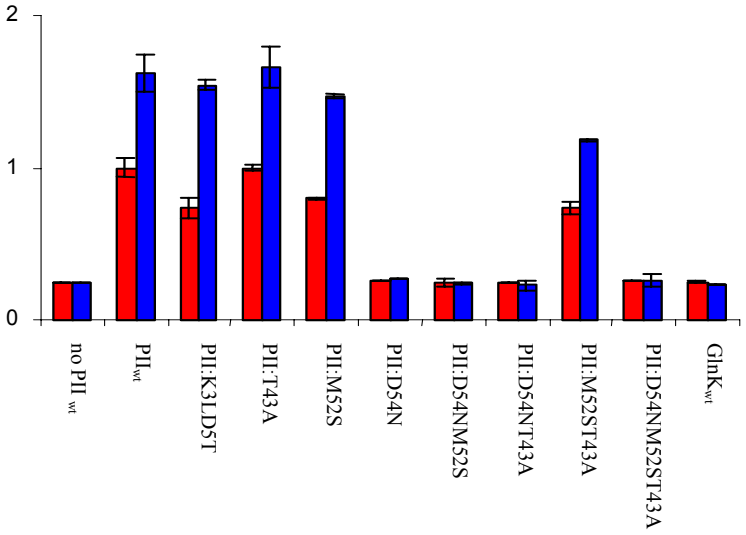

Figure 5.11 Comparative adenylylation rates for PII, GlnK and PII swapped mutants. The assay was performed with standard conditions (see section 5.2.3) (red) and standard conditions+10uM α-kg (blue). The activity of ATase was measured by the production of γ-glutamyl hydroxamate by GS. All assays were performed in duplicate and with PII_{wt} protein as a reference. The initial rate curves were fitted with a linear regression using Microsoft Excel. The initial rates for all the mutants have been expressed as a proportion of PII_{wt} protein standard activity.

All the PII mutants that contained the D54N mutation stimulated adenylylation rates in ATase to a level equivalent to that of the ATase protein when no effector-protein was

present (with and without 10uM α-kg). These mutants had the same behaviour as GlnK in the assay (Figure 5.11).

The result shown in Figure 5.11 depicts the dramatic effect of the Asp54 to Asn mutation on PII activity, including the double and triple mutants that carried this change. The PII protein normally stimulated by 10μM α-kg behaves identically to GlnK in the adenylylation assay when just one residue is changed.

5.3.6.2 Deadenylylation assay

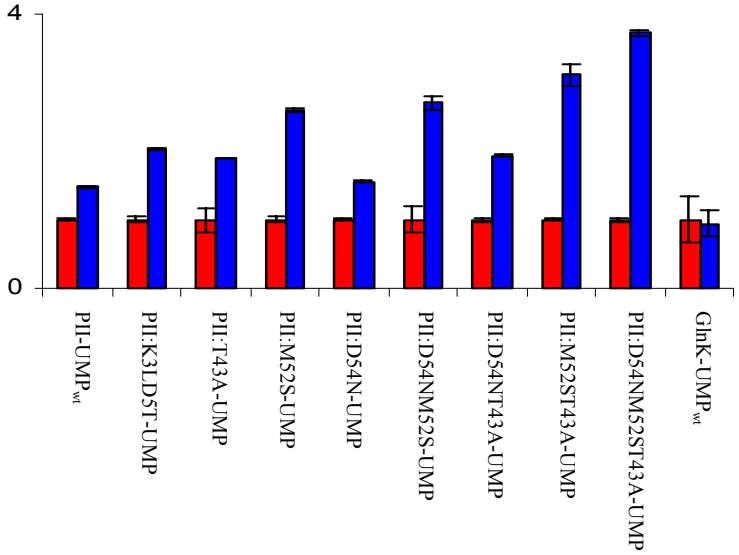

Figure 5.12 Comparative deadenylylation rates for uridylylated PII, GlnK and swapped PII T-loop mutants. Standard assay conditions were used (see section 5.2.3) (red). The assay was also run with PII-UMP, GlnK-UMP and uridylylated mutant proteins at 5x standard concentration (blue). The activity of ATase was measured by the production of γ-glutamyl hydroxamate by GS-AMP. All assays were performed in duplicate and with PII_{wt} protein as a reference. The initial rate curves were fitted with a linear regression using Microsoft Excel. The initial rates for all the proteins have been expressed as a proportion of their individual standard activity.

The difference between the stimulated deadenylylation activity by the uridylylated forms of the PII and GlnK proteins is quite marked (Figure 5.4), and it takes a 40 fold increase in the concentration of GlnK-UMP for it to stimulate ATase effectively. In this case the approximate effector-protein concentration was accurate enough to compare the effector-proteins by merely raising their concentration in the assay. The deadenylylation

assays were run with standard conditions (see section 5.2.3) and 5 times effector-protein for PII, GlnK and each of the swapped PII mutants (Figure 5.12).

None of the uridylylated PII mutants behaved like GlnK-UMP in deadenylylation. Increasing the concentration of each uridylylated mutant 5 fold gave rise to an improvement in the deadenylylation activity of ATase, like the stimulated activity due to wild type PII-UMP (Figure 5.12).

5.3.6.3 Uridylylation

UTase is 1.66 fold more efficient at uridylylating GlnK than PII (see section 5.3.5). Because the proteins were only partly purified (see section 5.2.1) the uridylylation assay utilising radio-labelled UTP was not used (see section 5.2.5), in case of non-specific incorporation.

Each of the effector-proteins was uridylylated by UTase for 20min in the standard reaction (see section 5.2.6) and separated on a 9% non-denaturing PAGE gel (see section 2.2.6.2) (Figure 5.13).

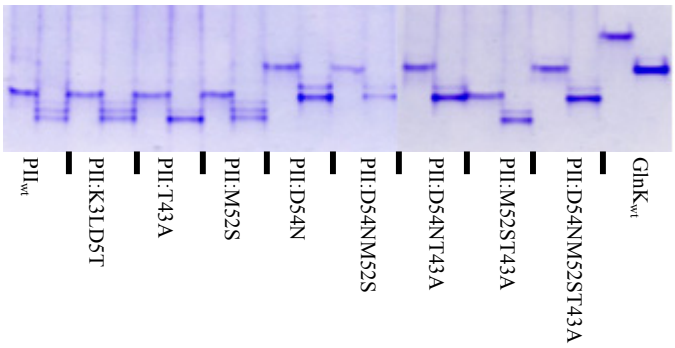

Figure 5.13 Uridylylation of partly purified PII, GlnK and swapped PII T-loop mutants. This non-denaturing PAGE gel (9% acrylamide) shows the degree of uridylylation of all the proteins after 20min in the standard uridylylation reaction (see section 5.2.6). The first lane for each protein is the protein prior to uridylylation. The second lane for each protein is the uridylylated protein. The lower band is fully uridylylated protein and the bands in between are partly uridylylated protein.

Visual inspection of Figure 5.13 shows most of the swapped PII T-loop mutants exhibited a greater degree of uridylylation than PII_{wt} after 20min. The two mutants, PII:K3LD5T and PII:M52S were uridylylated to a similar level as the PII_{wt} protein. These mutants had bands corresponding to the three different forms of the protein i.e. one, two and three uridylylated monomers present (Figure 5.13).

Under the same conditions, the GlnK protein was almost completely uridylylated to GlnK-UMP_3. By comparison, all the mutants carrying the D54N or T43A mutation were uridylylated to the same intermediate degree, somewhere in between the PII_{wt} and $GlnK_{wt}$ proteins, with stronger bands in the double-uridylylated monomer position than GlnK (Figure 5.13). Although not as pronounced as the results shown for the adenylylation assay the above result does indicate that the PII mutants carrying the GlnK T-loop residues at positions 43 and 54 are more efficiently uridylylated than PII, or the PII:K3LD5T and PII:M52S mutants.

5.4 DISCUSSION

The GlnK protein appears to have a much lower K_D for ATase under standard adenylylation conditions compared to PII (condition 5, Table 5.2), yet it is much less effective than PII at stimulating adenylylation activity in ATase (Figure 5.3a). One possible explanation is that another additional interaction may be affecting the behaviour of ATase, especially since increasing the amount of GlnK in the assay improves the adenylylation activity of ATase. The other partner in the assay is GS; possibly the better performance of PII (compared to GlnK) is due to a stronger interaction with GS within the catalytic complex, especially, when one considers that the 12 subunits of GS could be more efficiently adenylylated or deadenylylated if ATase was tethered to GS (similar to processive and non-processive polymerase activity of various DNA polymerases).

Addition of various small effector-molecules had little impact on the interaction of PII and ATase (all the K_D's fall within a range of 7.6μM to 14.7μM) (Table 5.2). The K_D's for standard adenylylation conditions and standard adenylylation conditions + 10μM α-

kg, are 10μM and 11.9μM (conditions 5 and 6, Table 5.2), respectively. However, in the assay, addition of 10μM α-kg improves the activity of ATase when PII is present (Figure 5.3b). Alternatively addition of 10μM α-kg when GlnK is the effector-protein leads to no change in the adenylylation activity of ATase, and in this case the K_D's for standard adenylylation conditions and standard adenylylation conditions + 10μM α-kg are 18nM and 1.1μM (conditions 5 and 6, Table 5.2), respectively. Again the difference between the impact of PII and GlnK (both PII and GlnK can bind to α-kg; see Figure 5.9) on the adenylylation activity of ATase when 10μM α-kg is present is probably due to differences in their interaction with GS.

In adenylylation, one T-loop residue clearly stood out (Figure 5.11). Changing the residue Asp54 in the T-loop of PII to Asn totally changed the behaviour of the protein from PII-like to GlnK-like, regardless of any other residue changes in the T-loop. This supports the notion that the structure of the PII protein is suited to multifunctional interactions and that a single residue in the T-loop may facilitate the strong interaction with a specific receptor-protein and modulate its activity. The study by Jiang *et al.*, (1997a) showed that the interaction of PII with NRII for example could be mapped to the T-loop residue Ala49. Interestingly, the D54N mutation was the single most important amino acid for determining the difference in behaviour of the PII and GlnK proteins with respect to NifA activity in *K. pneumoniae* (Arcondeguy *et al.*, 2000). However, in that case the T43A mutation was also needed to bring the activity of the mutated PII up to the level of GlnK.

There was a 40 fold difference between the K_D's of PII-UMP and GlnK-UMP for ATase in SPR under standard deadenylylation conditions (condition 4, Table 5.2). When the concentration of GlnK-UMP in the assay was increased (40 fold and 80 fold) GlnK-UMP was able to stimulate the activity of ATase in deadenylylation (Figure 5.4). A 160 fold increase in the concentration of GlnK-UMP brought the deadenylylation activity of ATase up to the level induced by PII-UMP (data not shown). It appears that the poorer performance of GlnK-UMP in the assay may be due to poorer binding to ATase under these conditions. However, it is possible that in the *in vivo* context this weak binding may be compensated for by the formation of heterotrimers between PII

and GlnK (Forchhammer *et al.*, 1999; van Heeswijk *et al.*, 2000). Wen (2000) demonstrated that uridylylated heterotrimers stimulated ATase adenylylation activity *in vitro* to a level between that of PII-UMP and GlnK-UMP.

Unlike adenylylation there was no distinguishing T-loop residue for deadenylylation; all the uridylylated swapped PII T-loop mutants behaved like PII-UMP (Figure 5.12). The triple mutant, PII:D54NM52ST43A has a GlnK T-loop, yet it still behaved like PII_{wt}. This suggests that the main body of PII-UMP is more important in interacting with ATase than the uridylylated T-loop. This result was in accordance with the results of Jiang *et al.*, (1998a). These workers found that modification of the Tyr51 residue of PII with different groups other than UMP (AMP and CMP) did not change the performance of ATase in the deadenylylation assay. The core of the two uridylylated effector-proteins (rather than the T-loop) may be the region of the two proteins that leads to the difference in their performance in binding to ATase, and subsequent different performances in deadenylylation. Maybe uridylylation of the T-loop is more important in disrupting the interaction with GS or improving the interaction with GS-AMP than in the interaction with ATase.

When the deadenylylation assay was run without α-kg and the concentrations of GS-AMP and effector-protein were doubled, ATase showed discernible activity (Figure 5.5). If gln was added to the assay when PII-UMP was the effector-protein the activity was abolished, but if GlnK-UMP was the effector-protein then the activity remained unchanged. This ties in nicely with the SPR data (Table 5.2) for condition 5 [ATP+Mg^{2+}+gln], where the K_Ds for the uridylylated effector-proteins, PII-UMP and GlnK-UMP binding to ATase were 1.39mM and 3.5nM, respectively (Table 5.2). The inhibition of deadenylylation activity under these circumstances by gln is probably due to the reduced binding of PII-UMP to ATase. Glutamine is an allosteric inhibitor of deadenylylation activity, so the inhibition mechanism may be due to conformational changes resulting from gln binding within the C-terminal adenylylation domain of ATase (Jaggi *et al.*, 1997). The conformational change in ATase due to gln binding may reduce the binding of PII-UMP.

The UTase protein initially uridylylates GlnK 1.66 times faster than PII (Figure 5.10). Uridylylation of PII and GlnK occurs at the residue Tyr51 (Son and Rhee, 1987), which is at the apex of the T-loop of each monomer (Cheah *et al.*, 1994; Carr *et al.*, 1996, Xu et *al.*, 1998). Consequently, the T-loop is very important in the interaction between PII/GlnK and UTase. The Met52 residue in PII, which is Ser in GlnK, does not appear to play any part in the interaction (Figure 5.13). The two salt-bridge residues in PII, Lys3 and Asp5, which don't form a salt bridge in GlnK (Leu3 & Thr5), don't appear to play any part in the interaction of PII and UTase either.

The two residues that affected the degree of swapped PII T-loop mutant uridylylation were T43A and D54N. When the Thr43 or Asp54 residues of PII were mutated to the GlnK protein's Ala43 or Asn54, the resulting mutant behaved more like GlnK, i.e. becoming uridylylated faster (Figure 5.13). These two residues must be important in distinguishing the interaction between PII/GlnK and UTase. The mutants were not being uridylylated as quickly as GlnK, so there may still be other regions of GlnK that play a part in the interaction with UTase to make it faster than PII. As noted previously these two residues were also important for stimulating NifA inhibition of *nifL* determined by Arcondeguy *et al.*, (2000).

The PII and GlnK proteins both bound ATP and α-kg (Figures 5.8 and 5.9), but in both instances PII was more effective. Just how these differences impact on differing behaviour in the various assays studied in this chapter is not clear. The total lack of response from GlnK when α-kg (10μM) is added to the adenylylation assay (Figure 5.3b) cannot be explained by the α-kg binding, because GlnK still bound α-kg, albeit not as well as PII.

The main conclusions that can be drawn from this chapter are as follows: (1) the effector-proteins may interact with GS in the adenylylation catalytic complex, with PII being more efficient than GlnK, (2) the poorer binding of GlnK-UMP to ATase may account for its poorer performance in deadenylylation assays, and (3) residue 54 determines the difference in behaviour of the two paralogues in adenylylation, and in

conjunction with residue 43 largely determines the different behaviour of the two proteins in uridylylation as well.

CHAPTER 6 The Bifunctional Enzyme ATase has a Central Domain Flanked by the Two Activity Possessing Domains

6.1 INTRODUCTION

Adenylyl transferase is the bifunctional effector enzyme responsible for regulating the enzymatic activity of GS in *E. coli* by the reversible adenylylation of each of the twelve monomers of the GS protein. Sequence alignment with rat DNA polymerase β and kanamycin nucleotidyl transferase (Holm and Sander, 1995) demonstrated the presence of two nucleotidyl transferase signature motifs within ATase: the first site spanning residues 117-184 and the second site spanning residues 644-712. The two antagonistic activities of ATase reside in separate domains (AT-N_{423}: residues 1-423 and AT-C_{522}: residues 425-946) at either end of the protein (Jaggi, *et al.*, 1997).

Further examination of the sequence of the ATase protein showed the presence of two Q-linkers. A Q-linker is defined as a region containing mainly hydrophilic residues (gln, glu, arg, ser and pro) that does not possess a secondary structure and acts as a tether between two domains (Wooton and Drummond, 1989). The first Q-linker, Q1 spans residues 441-462 and the second Q-linker, Q2 spans residues 606-627. The discovery of these two putative Q-linkers within the primary sequence of the protein suggested that there may be three domains within ATase, and that the two terminal domains encompassing the putative active sites may flank a central domain, which may act as a regulatory domain (R). An example of another protein with this kind of arrangement is aspartokinase-homoserine dehydrogenase I (AK-HDH I) also found in *E. coli* (James and Viola, 2002). This protein comprises the N-terminal aspartokinase domain (catalysing the first reaction in the pathway the phosphorylation of aspartate), a central regulatory domain and the C-terminal homoserine dehydrogenase domain, which catalyses the third reaction in the pathway, the reduction of the aldehyde intermediate to produce homoserine.

Solubility of truncated proteins is a good guide to determining natural domain delineation (Severinova, *et al.*, 1996). Accordingly the AT-N_{423} truncation construct

(Jaggi *et al.*, 1997) showed poor solubility, but extending the construct by 17 residues to the first Q-linker (AT-N_{440}) produced a completely soluble construct (Wen, 2000; Xu *et al.*, 2004). The original AT-C_{522} truncation construct was prone to proteolytic cleavage, production of another construct AT-C_{518} eliminated this problem (Wen, 2000).

A series of N- and C-terminal truncation constructs were produced previously in the Vasudevan laboratory at James Cook University using the position of the predicted active sites and Q-linkers as a guide for truncation positions (see Chapter 1). A program designed to predict secondary structure (Predictprotein) (Rost and Sander, 1993) was also used to help explain the solubility of the various ATase truncation constructs.

Entire ATase and the truncation constructs AT-N_{440}, AT-N_{501}, AT-N_{548} and AT-C_{522} were all fully soluble. The AT-C_{396} truncation construct showed a slight drop in solubility and the remaining constructs AT-N_{423}, AT-C_{439} and AT-C_{481} showed a major drop in solubility. With the addition of 17 amino acids the poorly soluble AT-N_{423} truncation construct became the completely soluble AT-N_{440} construct. This suggests that the N-terminal domain boundary may be at the start of Q1, which correlates well with the secondary structure prediction (Wen, 2000; Xu *et al.*, 2004). The structure of the AT-N_{440} truncation construct has now been solved with X-ray crystallography, and the AT-N_{423} construct truncation was terminated in the centre of an α-helix as predicted, destabilising the construct (Xu *et al.*, 2004). Termination of the truncation within an α-helix would account for the poor solubility of the AT-N_{423} construct.

The truncation constructs AT-N_{501} and AT-N_{548} demonstrated good solubility, indicating correct folding and that these polypeptides contain at least one completely folded domain. The properties of the remaining parts of these polypeptides (from residue 441 onwards) did not appear to destabilise their folding.

Removal of the Q1 linker from the AT-C_{522} truncation construct gave rise to the AT-C_{481} construct, which by analogy with AT-N_{440} would have been expected to be fully soluble. A possible explanation for the poor solubility of AT-C_{481} came from the predicted nature of the Q1 linker. Using a helical wheel projection (Schiffer and

Edmundson, 1967) (see Chapter 1) the Q1 linker is predicted to contain an amphipathic α-helix, where one face is predominantly hydrophobic whilst the other is predominantly hydrophilic containing all the charged residues and gln residues. Removal of the Q1 linker may have exposed hydrophobic areas of the C-terminal domain, which are normally stabilised by contact with the Q1 linker thereby reducing the solubility of the AT-C_{481} construct.

Like AT-N_{423} the AT-C_{439} truncation spans a predicted helix, which may be the reason for its poor solubility also. The AT-C_{396} truncation is more soluble than AT-C_{481} or AT-C_{439}, suggesting that a third central domain (Q1 to Q2) may be present that becomes destabilised in the latter two longer constructs. However, two smaller C-terminal truncation constructs AT-C_{340} (Q2-C domain) and AT-C_{305} (C domain) formed completely insoluble inclusion bodies when expressed from pND707-derived plasmids (Wen, 2000).

A further ATase truncation construct was produced by Ryan O'Donnell (2000) which had the putative central domain removed (designated AT:ΔR). The AT:ΔR construct (N domain-Q1-Q2-C domain) also formed completely insoluble inclusion bodies when expressed from a pND707-derived plasmid at 42^{o}C (O'Donnell, 2000).

The first aim of the work in this chapter is to provide evidence for the presence of a central domain by producing an appropriate truncation construct, to complete the already existing suite of truncation constructs, and to assess the solubility of the expressed truncation construct. Based on the hypothesis that protein solubility can be taken as an indication of domain integrity, the demonstration of a soluble R domain truncation construct would support the concept that the region of the protein between the two Q-linkers is a distinct domain. The second aim of this chapter is to investigate the function of the putative central domain by studying the enzyme activity of various truncation constructs.

Monoclonal antibodies and truncation constructs can be used as tools to address questions of enzyme structure and function (Yi *et al.*, 2002). The third aim of studies

reported in this chapter is to investigate intramolecular signalling and the role of the R domain within ATase by investigating inhibition of enzyme activity using ATase mAbs that bound to the three regions of ATase (see Chapter 3).

6.2 METHODS

6.2.1 Expression and purification of proteins

Plasmid	Description	Source/Reference
PRJ002	*glnE* (AT-C_{522}) in pND707	Jaggi *et al.*, (1997)
pRJ007	*glnE* (AT-N_{423}) in pND707	Jaggi *et al.*, (1997)
pRJ009	*glnE* (ATase) in pND707	Jaggi *et al.*, (1997)
pRJ0012	*glnE* (AT-N_{548}) in pND707	Jaggi (1998)
pRJ0013	*glnE* (AT-N_{501}) in pND707	Jaggi (1998)
pRJ0014	*glnE* (AT-C_{439}) in pND707	Jaggi (1998)
pRJ0015	*glnE* (AT-C_{396}) in pND707	Jaggi (1998)
pDW1	*glnE* (AT-N_{440}) in pND707	Wen (2000)
pDW2	*glnE* (AT-C_{481}) in pND707	Wen (2000)
pDW3	*glnE* (AT-N_{467}) in pND707	Wen (2000)
pDW4	*glnE* (AT-C_{518}) in pND707	Wen (2000)
pDW7	*glnE* (AT-C_{340}) in pETDW2	Wen (2000)
pDW8+glnB	*glnE* (AT-C_{305})+*glnB* in pETDW2	Wen (2000)
p235+glnB	*glnE* (AT-C_{235})+*glnB* in pETDW2	Vasudevan lab unpublished work
pAT:ΔR	*glnE* (AT:ΔR) in pET	O'Donnell (2000)
pRJ009:RQ2	*glnE* (AT:RQ2) in pETDW2	this work
pRJ001	*glnB* (PII) in pND707	Jaggi *et al.*, (1996)
pWVH57	*glnA* (GS) in pBluescript II KS+	van Heeswijk *et al.*, (1996)
pJRV001	*glnA* (GS) in pND707	Vasudevan lab unpublished work

Table 6.1 ***Recombinant proteins.*** List of the plasmids encoding the recombinant proteins used in this chapter including the plasmid name and source.

All the recombinant vectors produced previously were generated following the methods described in Vasudevan *et al.*, (1991). Detailed descriptions of their construction can be found in the individual references listed in Tables 2.1.6.2 and 6.1.

All strains were grown in LB medium and when appropriate supplemented with ampicillin (100μgmL^{-1}) and chloramphenicol (25μgmL^{-1}) (see section 2.2.1.1 and 2). The following proteins: ATase, AT-N_{423}, AT-N_{440}, AT-N_{467}, AT-N_{501}, AT-N_{548}, AT-C_{522}, AT-C_{518}, AT-C_{481}, AT-C_{439} and AT-C_{396} (pND707-derived) (Table 6.1), were all expressed in JM109 cells (2.1.4). The five remaining constructs: AT-C_{340}, AT-C_{305}, AT-C_{235}, AT:ΔR and AT:RQ2 (pET-derived) (Table 6.1) were all expressed in BL21 (DE3)

recA cells (2.1.4). The method of protein induction was determined by the plasmid (see section 2.2.5.1 and 2). Plasmids derived from the pND707 vector were thermally induced and those derived from the pET vector were induced with IPTG at 18^{o}C.

Large-scale preparations (see section 2.2.5.5) were made for ATase, AT-N_{440}, AT-N_{501}, AT-N_{548}, AT-C_{481}, AT-C_{518} and AT-C_{522}. These proteins were then purified (see section 2.2.7.6) to at least 85-95% purity as judged by SDS PAGE. The remaining protein preparations were produced from small-scale cultures (see section 2.2.5.3) and not purified. The approximate individual target protein concentration was determined by comparison with bands of known concentration in SDS PAGE (see section 2.2.8.2).

6.2.2 Construction of the R domain truncation construct

The R domain truncation construct was generated using standard methods outlined in Chapter 2. The two gene-specific primers, AT-C 484 FP and AT Q2 RP (2.1.7.1) were used to PCR amplify the R-Q2 region of the *glnE* gene from the pRJ009 plasmid (2.1.6.2 and 6.1) (see section 2.2.4.1). The two restriction enzymes, *NdeI* and *SmaI* were used to digest the insert and pETDW2 vector (2.1.6.2) (see section 2.2.2.3) prior to ligation (see section 2.2.2.4). The resulting plasmid was transformed into DH5-α cells (2.1.4) (see section 2.2.1.4). The sequence of the RQ2 insert was verified by automatic sequencing of a PCR product generated from the two sequencing primers pET T7 FP and pET T7 RP (2.1.7.1) and the above plasmid (see section 2.2.4.3).

6.2.3 Solubility of the R domain truncation construct

The newly constructed RQ2 plasmid was transformed into competent BL21 (DE3) recA cells (2.1.4) (see section 2.2.1.4) for protein induction. A small-scale induction was performed (see section 2.2.5.3) and the solubility of the expressed protein assessed (see section 2.2.5.4) at several induction temperatures (18^{o}C, 30^{o}C, 37^{o}C).

6.2.4 Production of monoclonal and polyclonal antibodies to ATase

The production and characterisation of the ATase mAbs has been covered in detail in Chapter 3.

Polyclonal Abs were raised in mice (see section 2.2.9.4.2) against purified ATase, AT-N_{548} and AT-C_{522}. The AT-N_{548} and AT-C_{522} antisera were combined 1:1 and purified using protein-A agarose chromatography (see section 2.2.9.8).

6.2.5 Adenylylation and deadenylylation assays

The adenylylation and deadenylylation assays (see section 2.2.10.2) were performed with many different combinations of effector-molecules using ATase and various ATase truncation constructs, both as crude cell lysates and purified proteins (see section 6.2.1). The assays were also run with the different ATase mAbs (see section 6.2.4) pre-incubated with ATase for at least 30min.

6.3 RESULTS

The domain organisation of ATase has been investigated in detail at the Vasudevan Laboratory, James Cook University. Truncations of the ATase protein (946 residues long) were designated AT-N or AT-C depending on their location in the linear polypeptide chain and the number of amino acid residues contained in each truncation construct is indicated by a subscripted number (eg. AT-N_{440} refers to the N-terminal 440 residues of ATase) (Figure 6.1).

Two Q-linkers (Wooton and Drummond, 1989) have been noted in ATase (Jaggi, 1998; Xu *et al.*, 2004), and between them resides the putative R domain. The entire ATase protein can be represented as N-Q1-R-Q2-C.

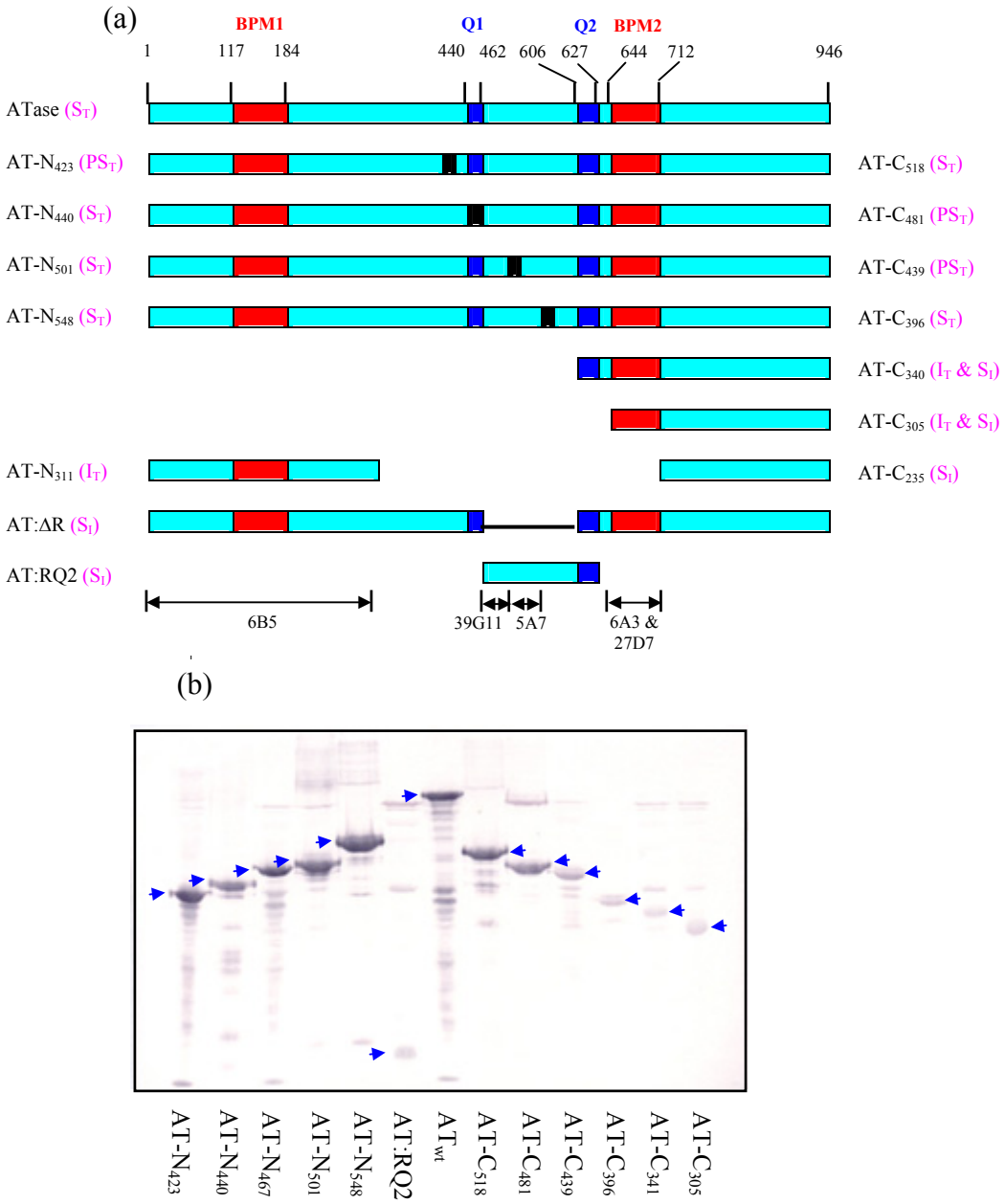

Figure 6.1 ***Schematic representation of the truncation constructs of ATase.*** (a) Truncations of the ATase protein (946 residues long) were designated AT-N or AT-C depending on their location in the linear polypeptide chain and the number of amino acid residues contained in each truncation construct is indicated by a subscripted figure (eg. AT-N_{440} refers to the N-terminal 440 residues of ATase). Also indicated on the diagram are the positions of the two predicted β-polymerase motifs (BPM1 & BPM2) (Holm and Sander, 1995), the two Q-linkers (Q1 & Q2) (Wooton and Drummond, 1989), and the binding regions of the ATase mAbs (see Chapter 3). The solubility of the constructs is shown in pink. Soluble (S), partly soluble (PS), Insoluble (I), thermal induction ($_T$), and IPTG induction at low temperature ($_I$). (b) Western blot analysis of 12% SDS PAGE gel (see section 2.2.6.5) of whole cell extracts for the various truncation constructs using a purified mix of AT-N_{548} and AT-C_{522} polyclonal Ab ascitic fluid for detection (see section 6.2.4). The bands indicating the appropriate induced proteins are marked with arrows.

The 3D structure of entire ATase is yet to be elucidated and attempts to obtain crystals have not been successful. So we sought to understand the structure, function and regulation of ATase by producing truncated proteins and testing these polypeptides for their solubility and enzyme activity (Jaggi, 1998; O'Donnell, 2000; Wen, 2000).

This study characterised the various ATase truncation constructs produced by others in the Vasudevan laboratory (Jaggi, 1998; O'Donnell, 2000; Wen, 2000) and produced the central R domain truncation construct AT:RQ2 (see below). A schematic representation of the ATase truncation constructs is shown in Figure 6.1a and a Western blot of a 12% SDS PAGE gel using most the truncation constructs is shown in Figure 6.1b.

6.3.1 Construction of the R domain truncation construct

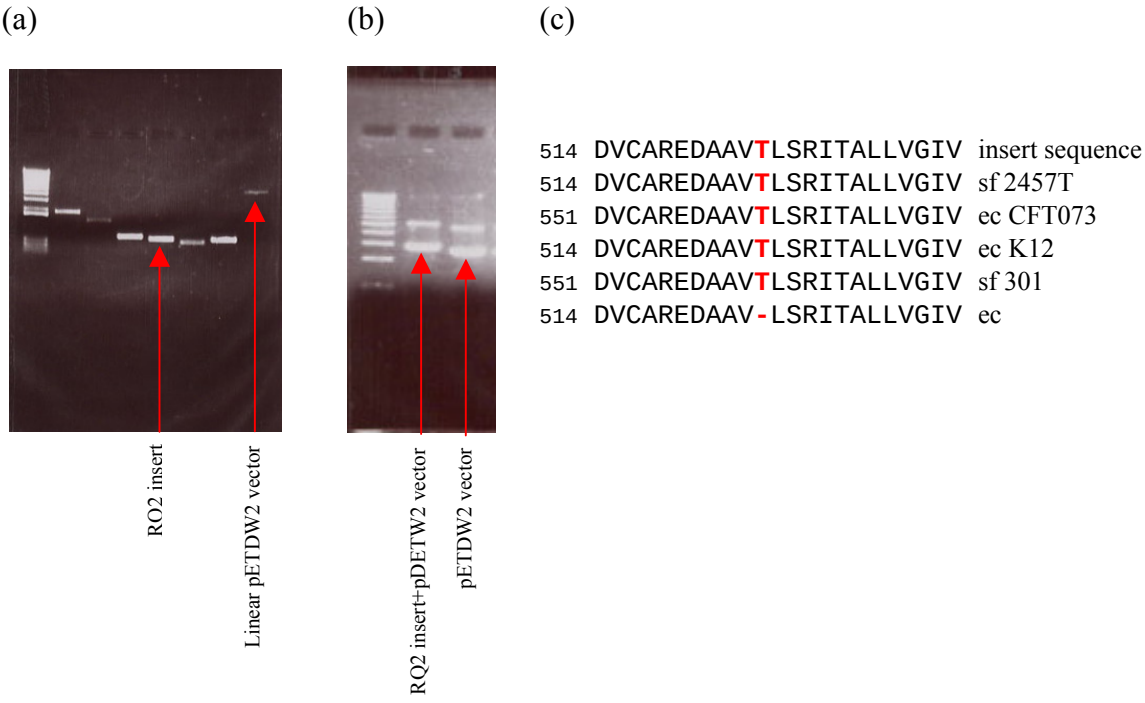

Figure 6.2 ***Generation of the R domain truncation construct.*** (a) PCR product (see section 6.2.2) and (b) ligated plasmid (see section 6.2.2) visualised by agarose gel electrophoresis (see section 2.2.3.1). (c) BLAST search of the NCBI database using sequence derived from R domain vector (see section 6.2.2). Abbreviations and references are as follows: sf 2457T (*Shigella flexneri* 2a; Wei *et al.*, 2003), ec CFT073 (*E. coli*; Welch *et al.*, 2002), ec K12 (*E. coli*; Blattner *et al.*, 1997), sf 301 (*S. flexneri* 2a; Jin *et al.*, 2002), and ec (*E. coli*; van Heeswijk *et al.*, 1993).

A PCR product (~0.49kB, Figure 6.2a) was generated from pRJ009 using the gene-specific primers AT-C 464 FP and AT Q2 RP (2.1.7.1). The pRJ009 plasmid is

pND707-derived and contains the *glnE* gene (Jaggi *et al.*, 1997). The fragment was ligated into the pETDW2 (2.1.6.2) vector, a pETMCS II (Neylon *et al.*, 2000) derivative, which utilises the T7 promoter system (see section 2.2.5.2). The plasmid DNA was of the correct size as judged by comparison with the DNA ladder and the pDW2 vector in agarose gel electrophoresis (Figure 6.2b).

Sequence analysis of the insert from both directions using the pET T7 FP and pET T7 RP primers (2.1.7.1) showed the correct fragment was amplified (Figure 6.2c). Previous work from the Vasudevan laboratory had used the early van Heeswijk sequence for ATase (van Heeswijk *et al.*, 1993), which is missing the Thr highlighted in red. The insert derived from this work concurred with subsequent published sequences for ATase (Figure 6.2c).

6.3.2 Solubility of the R domain truncation construct

The plasmid encoding the AT:RQ2 truncation construct was used to transform competent BL21 (DE3) recA cells (2.1.4) for small-scale protein induction (see section 6.2.3). This construct was expressed at a low level constantly, like AT-C_{235} (data not shown) and there was no increase in expression with the addition of IPTG (Figure 6.3a). Both of these plasmids were constructed from pETDW2 (Wen, 2000).

Based on studies which showed that the solubility of truncated proteins (domains) of a normally water soluble multi-domain protein were a good indicator of correct folding and natural domain boundaries (Severinova *et al.*, 1996), the AT:RQ2 truncation was subjected to a rapid solubility test (see section 6.2.3). The solubility of the AT:RQ2 truncation construct is shown in Figure 6.3b. The cells were harvested at an OD_{595} of 0.9 from each induction temperature. Equal volumes (10μL of OD_{595} 100) of whole cell extract and cell-free lysate for each temperature were separated by 15% SDS PAGE (see section 2.2.6.1), transferred to nitrocellulose membrane and detected (see section 2.2.6.5) with purified mAb 5A7 (see section 2.2.9.4.2).

Soluble proteins have bands of similar intensity for both whole cell extract and the cell-free lysate; whereas proteins with reduced solubility have a band with reduced intensity in the cell-free lysate. From a visual inspection of Figure 6.3b the AT:RQ2 polypeptide expressed at 37°C was insoluble, the polypeptide expressed at 30°C was fairly soluble, and the polypeptide expressed at 18°C was fully soluble. Hence lowering the induction temperature and slowing down the folding of the polypeptide improved the solubility of the AT:RQ2 truncation construct.

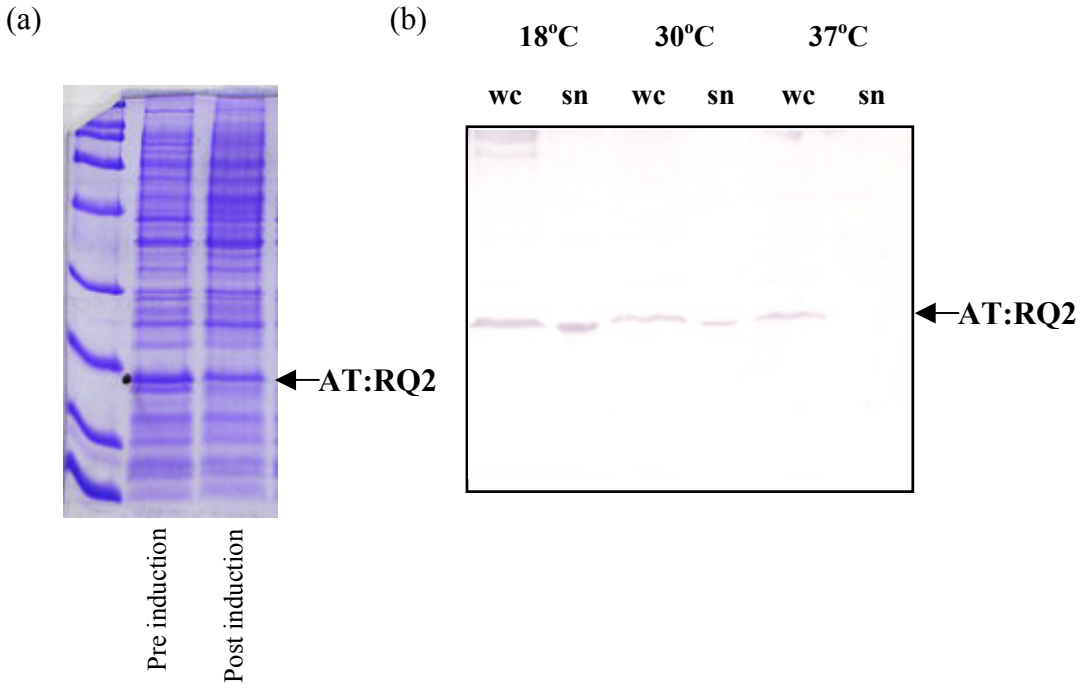

Figure 6.3 ***Over-expression and solubility test for the R domain construct.*** (a) Coomassie stained 15% PAGE gel showing expression of IPTG induced AT:RQ2 in BL21 (DE3) RecA cells (2.1.4) (see section 6.2.3). (b) Solubility analysis of the constantly expressed truncation construct AT:RQ2 at 18°C, 30°C and 37°C. Western blot of 15% SDS PAGE gel (see section 2.2.6.5) of whole cell extracts (wc) and cell-free lysates (sn) using purified mAb 5A7 (see section 2.2.9.4.2).

6.3.3 Solubility of further truncated constructs of ATase

6.3.3.1 AT-N_{311}

Another truncation construct designated AT:ΔQ2 (the second Q-linker removed) (O'Donnell, 2000) produced a high level of totally insoluble protein (~36kD), which was too small to be the predicted construct (105.6kD). In order to investigate this

further, the 5' end of the insert DNA in this construct was sequenced by automated sequencing (see section 2.2.4.3) using ATN FP3 primer (2.1.7.1). The result indicated a missing base pair at position 927, which led to early termination of translation of this construct. The 311 amino acid protein being produced had a predicted size of 35.69kD. This construct was not used for any assays (AT-N_{311} from Figure 6.1), but it was valuable for narrowing down the binding region of the N-terminal mAb 6B5.

6.3.3.2 AT-C_{235}

Another construct designated AT-C_{235} was expressed from a synthetic operon consisting of the AT-C_{235} minigene and *glnB* (D. Wen and S.G. Vasudevan, unpublished). This construct was constantly expressed at a low level, and addition of IPTG had no effect on expression. Expression at 18^{o}C led to a fully soluble product (data not shown). This construct was not used for any assays, but it was very useful in narrowing down the binding region of the C-terminal mAbs 6A3 and 27D7.

6.3.4 Enzymatic activities of the truncated constructs of ATase

Several of the truncated constructs of the ATase protein were examined for enzyme activity in the adenylylation and deadenylylation assays (see section 6.2.5). Some of the truncation constructs were used as purified protein (see section 6.2.1) and others were used as cell lysates (see section 6.2.1).

6.3.4.1 The adenylylation activity of C-terminal truncation constructs and their dependence on PII and gln

The C-terminal truncation constructs were examined for their ability to carry out adenylylation of the GS protein. It was previously demonstrated that the AT-C_{522} truncation construct adenylylation activity was independent of PII (Jaggi *et al.*, 1997). The various adenylylation activity levels of ATase, AT-C_{518}, AT-C_{396}, AT-C_{340} and AT:ΔR are shown in Figure 6.4.

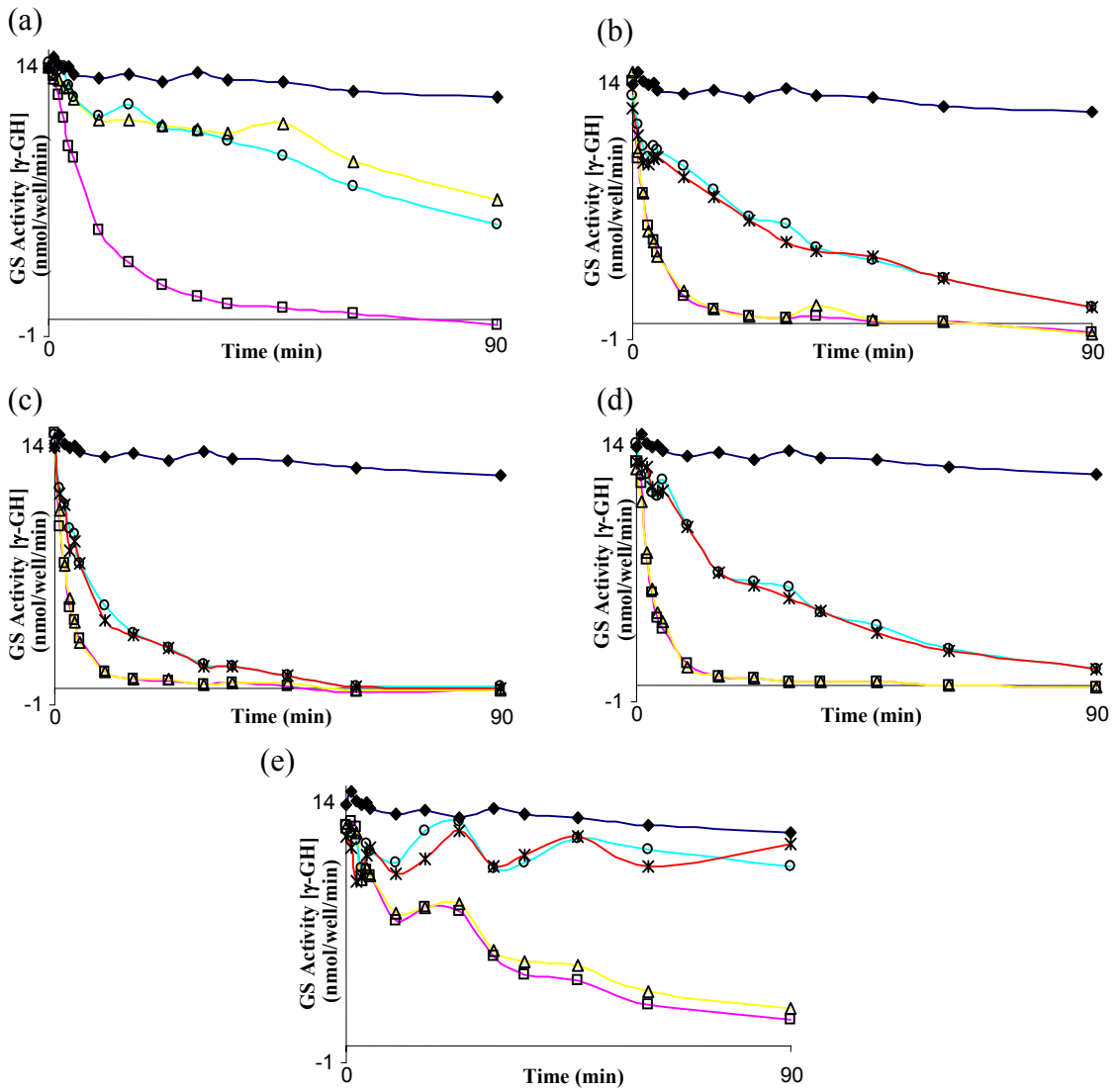

(f)

Condition	Protein				
	AT_{wt} (0.025μM)	AT-C_{518} (0.6μM)	AT-C_{396} (0.6μM)	AT-C_{340} (~0.6μM)	AT:ΔR (~0.2μM)
+PII+gln	1.00	1.00	1.00	1.00	1.00
-PII+gln	0.28	0.99	0.98	1.05	0.91
+PII-gln	0.39	0.35	0.49	0.30	0.15
-PII-gln	0.06	0.34	0.49	0.28	0.17

Figure 6.4 ***Adenylylation assays using ATase and C domain truncation constructs.*** These assays show the changes in activity of (a) ATase (purified), (b) AT-C_{518} (purified), (c) AT-C_{396} (purified), (d) AT-C_{340} (cell lysate) and (e) AT:ΔR (cell lysate) (see section 6.2.1) under various conditions. Activity was assessed by determining the adenylylation state of GS by measuring the production of γ-glutamyl hydroxamate with various combinations of effector-molecules present in the assay. Standard assay conditions were used (see section 6.2.5). No AT/construct+PII+gln (♦), AT/construct+PII+gln (□), AT/construct-PII+gln (Δ), AT/construct+PII-gln (○), and AT/construct-PII-gln (*). All assays were performed in duplicate and with AT_{wt} as a reference. Error bars have not been shown on the curves as they hinder visual inspection. The standard error range for all the curves is generally <0.4. (f) The first 5min were fitted with a linear regression using Microsoft Excel. The R^2 coefficients for these curves are usually >0.9. The initial rates for all the proteins have been expressed as a proportion of their standard activity.

All the C-terminal truncation constructs were used in the assay at 0.6μM rather than 0.025μM (entire ATase) to give similar activity levels to entire ATase (see section 6.3.3.3). The AT:ΔR truncation construct expressed poorly and was not purified. To avoid interference from the potentially more active endogenous ATase (the expression strain was not *gln E*$^-$) this construct was used at ~0.2μM in the assay (see below).

Intact ATase needs both PII and gln present to stimulate full adenylylation activity. Removal of either effector causes a drop in activity (Figure 6.4a). If PII is omitted from the adenylylation assay there is a ~70% drop in activity, and if gln is omitted from the assay there is a ~60% drop in activity (Figure 6.4f). Omission of both PII and gln virtually abolishes activity (Figure 6.4f). By contrast the adenylylation activity for each of the C-terminal truncation constructs and AT:ΔR is independent of PII (Figures 6.4b-e) since their activity level is the same whether the PII effector-protein is present or not.

From Figure 6.4f all the C-terminal truncation constructs had ~100% (91-105%) adenylylation activity when PII was omitted from the assay. All the C-terminal truncation constructs were dependent on gln for full activity (Figures 6.4b-e), because the removal of gln from the assay resulted in a drop in adenylylation activity ranging from ~50-85% (Figure 6.4f). When gln was omitted from the assay further removal of PII still had no effect on the activity of the truncated C-terminal proteins.

These results suggest that the C-terminal truncation constructs have the same conformation as PII bound ATase with regards to adenylylation activity, however the specific activity of the truncated C-terminal domain appears to be lower than that of the same domain in the intact protein (see later).

6.3.4.2 Characterisation of the AT-N_{440} construct in deadenylylation activity assay

The N domain truncation construct, AT-N_{440} was examined for its ability to carry out deadenylylation of the GS-AMP protein. It was previously demonstrated that the enzyme activity of the AT-N_{423} truncation construct was dependent on the effector-

protein PII-UMP and independent of α-kg in deadenylylation (Jaggi *et al.*, 1997). The various activity levels of ATase and AT-N_{440} are shown in Figure 6.5.

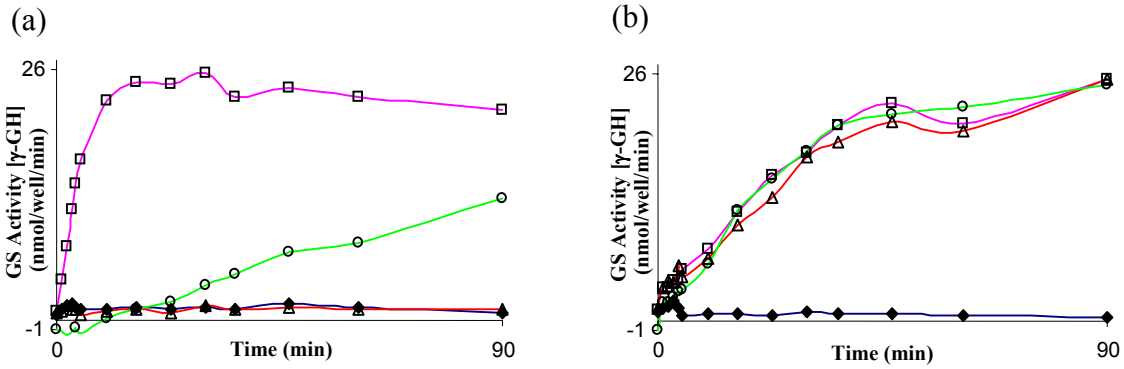

(c)

Condition	Protein	
	AT_{wt} (0.025μM)	AT-N_{440} (15μM)
+PII-UMP+α-kg	1.00	1.00
-PII-UMP+α-kg	0.00	0.98
+PII-UMP- α-kg	0.04	0.97
-PII-UMP- α-kg	0.00	0.95

Figure 6.5 ***Deadenylylation assays using ATase and the AT-N_{440} truncation construct.*** These assays show the changes in activity of (a) ATase (purified) and (b) N-terminal truncation construct AT-N_{440} (purified) (see section 6.2.1) under various conditions. Activity was assessed by determining the deadenylylation state of GS-AMP by measuring the production of γ-glutamyl hydroxamate with various combinations of effector-molecules present in the assay. Standard assay conditions were used (see section 6.2.5). No AT/construct+PII-UMP+α-kg (♦), AT/construct+PII-UMP+α-kg (□), AT/construct-PII-UMP+α-kg (Δ), and AT/construct+PII-UMP-α-kg (○). All assays were performed in duplicate and with AT_{wt} as a reference. Error bars have not been shown on the curves as they hinder visual inspection. The standard error range for all the curves is generally <0.4. (c) The first 5min were fitted with a linear regression using Microsoft Excel. The R^2 coefficients for these curves are usually >0.9. The initial rates for all the proteins have been expressed as a proportion of their standard activity.

ATase needs both PII-UMP and α-kg present to stimulate full deadenylylation activity (Figure 6.5a). If PII-UMP is omitted from the deadenylylation assay there is a 100% drop in activity, and if α-kg is omitted from the assay there is a ~95% drop in activity (Figure 6.5c). In contrast the deadenylylation activity for the N domain truncation construct, AT-N_{440} is independent of both PII-UMP and α-kg (Figure 6.5b). The activity level of this truncation construct is unchanged whether the PII-UMP protein or α-kg is present or not (Figure 6.5c).

The AT-N_{440} truncation construct was purified (see section 6.2.1), consequently it could be added to the deadenylylation assay to give a final concentration of 15μM to give a discernible level of activity in the assay (Table 6.2). However, the AT:ΔR truncation construct expressed poorly and was not purified. This meant to add this construct to the assay at 15μM was not possible and at ~0.2μM there was no discernible activity (data not shown).

6.3.4.3 Comparison of activity levels of ATase and truncated constructs

The comparative activity levels of ATase and the truncation constructs, AT-N_{440} and AT-C_{518} were assessed over a range of concentrations in the initial rate assay (see section 6.2.5). The comparative rates expressed as the rate per μM are shown in Table 6.2.

Adenylylation			Deadenylylation		
Protein	**Rate** (nmol/well/min/min)	**RateμM^{-1}**	**Protein**	**Rate** (nmol/well/min/min)	**RateμM^{-1}**
0.025μM AT_{wt}	-1.2449 (0.9810)	-49.80	**0.025μM AT_{wt}**	1.4061 (0.9552)	56.24
	-1.4569 (0.9696)	-58.28		1.4289 (0.9260)	57.16
				1.2378 (0.9166)	49.51
				1.6835 (0.8802)	67.34
Average		**-54.04**			**57.56**
0.1μM AT-C_{518}	-0.2276 (0.9640)	-2.276	**2μM AT-N_{440}**	0.1102 (0.9962)	0.0551
0.125μM AT-C_{518}	-0.2769 (0.9422)	-2.215	**2.5μM AT-N_{440}**	0.1266 (0.9751)	0.0506
0.15μM AT-C_{518}	-0.4449 (0.9509)	-2.966	**3μM AT-N_{440}**	0.1623 (0.9723)	0.0541
0.2μM AT-C_{518}	-0.5263 (0.9700)	-2.632	**3.5μM AT-N_{440}**	0.2012 (0.9946)	0.0575
0.6μM AT-C_{518}	-1.2792 (0.9994)	-2.132			
Average		**-2.444**			**0.0543**

Table 6.2 ***Relative activity levels for ATase, and the truncation constructs AT-C_{518} and AT-N_{440}.*** This table shows the relative adenylylation/deadenylylation activity levels under standard conditions (see section 6.2.5) of the truncation constructs AT-C_{518} and AT-N_{440}, and full length ATase expressed as the activity rate per μM. The assays were run for 5min and the curves were fitted with a linear regression using Microsoft Excel. The R^2 coefficient for each curve is shown in brackets.

The activity of $ATase_{wt}$ in adenylylation was ~22 times higher than that of the AT-C_{518} construct. On the other hand the activity of $ATase_{wt}$ in deadenylylation was three orders of magnitude higher than that of the AT-N_{440} construct (Table 6.2). These relative rates

were used to determine the concentration of the truncation constructs used in the assays. ATase was used at 0.025μM in both the assays. The N-terminal truncation constructs were used at 15μM in deadenylylation (where possible) (see section 6.2.5), and the C-terminal truncation constructs were used at 0.6μM in adenylylation (where possible) (see section 6.2.5).

6.3.5 Probing the activities of ATase using monoclonal antibodies

Specific mAbs can be useful tools to address signalling within the ATase molecule as exemplified by similar studies in other systems (eg. Yi *et al.*, 2002). In the first instance, the mAbs (see Chapter 3) were screened with two of the truncation constructs (AT-N_{548} and AT-C_{522}) to distinguish mAbs that bound to either the N-terminal deadenylylation domain or the C-terminal adenylylation domain.

Further investigation using Western blotting with all the ATase truncation constructs and mutants (see Chapter 3) showed the N domain mAb 6B5 was binding somewhere in the first 311 residues of the ATase protein. The two R domain mAbs were shown to bind to two different regions. The 39G11 mAb binds somewhere between residues 466 and 501, and the 5A7 mAb binds somewhere between residues 502 and 548. The two C domain mAbs were probably not binding to the same site, but they were both binding somewhere between residues 642 and 711. The binding regions of the five mAbs are summarised in Figure 6.1a.

Various adenylylation and deadenylylation assays (see section 6.2.5) were run in the presence of the different mAbs to investigate their impact on the enzyme activity of ATase and to probe the mechanism of the enzymatic activity.

6.3.5.1 Effect of N domain mAb on ATase activity

When the purified N domain mAb 6B5 (see section 6.2.4) was added to either assay at a molar ratio of 1:1 it had no effect on the activity of ATase (purified; see section 6.2.1) (Figure 6.6). To ensure that the lack of inhibition was not due to the mAbs lower

affinity for the protein, the assays were also run with 10 times more 6B5, and there was still no inhibition (data not shown).

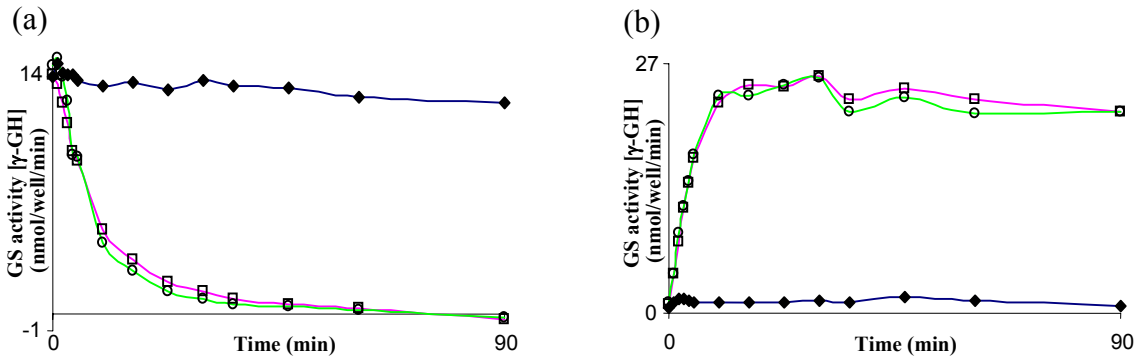

Figure 6.6 ***Inhibition of adenylylation and deadenylylation activity in ATase by N domain mAb 6B5.*** These assays show the changes in activity of ATase by measuring the production of γ-glutamyl hydroxamate by GS/GS-AMP when the 6B5 mAb is present in the (a) adenylylation and (b) deadenylylation assays. Standard assay conditions were used (see section 6.2.5). The purified mAb (see section 6.2.4) was preincubated with ATase (1:1) for 30min at room temperature. No AT+PII-UMP+α-kg (♦), AT+PII-UMP+α-kg (□), and AT+PII-UMP+α-kg+6B5 (○). All assays were performed in duplicate and with AT_{wt} as a reference. Error bars have not been shown on the curves as they hinder visual inspection. The standard error range for all the curves is generally <0.4.

The deadenylylation activity of the truncation construct AT-N_{440} was also not affected by addition of the N domain mAb 6B5 to the deadenylylation assay (see section 6.2.5) (data not shown). This implies that the 6B5 mAb binds away from the deadenylylation active site within the N domain of ATase.

6.3.5.2 Effect of R domain mAbs on ATase activity

6.3.5.2.1 Inhibition of PII binding in adenylylation

The two R domain mAbs 39G11 (crude ascitic fluid; see section 6.2.4) and 5A7 (purified; see section 6.2.4) were used in adenylylation assays (see section 6.2.5) with ATase and AT-C_{518} (both purified; see section 6.2.1) to investigate the impact of these mAbs on adenylylation activity (Figure 6.7). Entire ATase and the PII independent truncated construct, AT-C_{518} (R-Q2-C) were chosen for these assays because they were shown to bind these mAbs (Figure 6.1). The two poorly soluble C-terminal truncation

constructs, which also bind to these mAbs, were not used in this series of adenylylation assays.

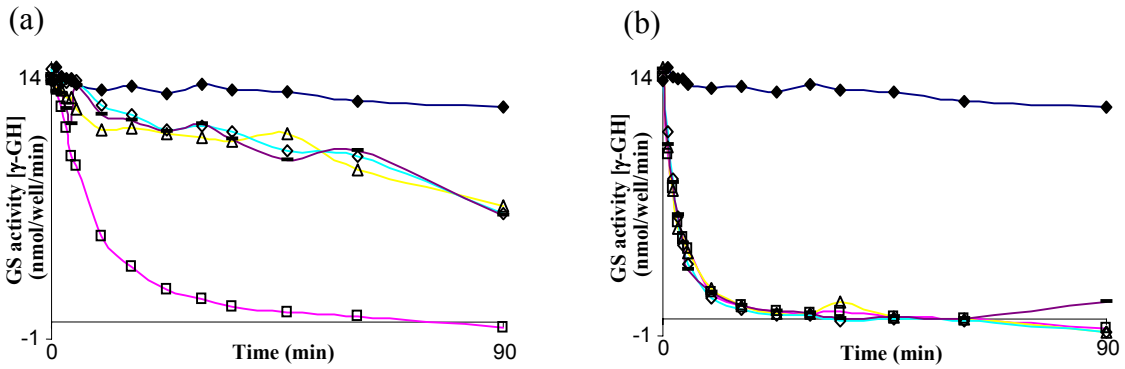

Figure 6.7 ***Inhibition of adenylylation activity in ATase and AT-C_{518} by R domain mAbs 5A7 and 39G11.*** These assays show the changes in activity of (a) ATase and (b) the C-terminal truncation construct AT-C_{518} in adenylylation by measuring the production of γ-glutamyl hydroxamate by GS with R domain mAbs 5A7 and 39G11 present. Standard assay conditions (see section 6.2.5) were used and the mAbs (see section 6.2.4) were preincubated with AT/AT-C_{518} (1:1) for 30min at room temperature. No AT/AT-C_{518}+PII+gln (♦), AT/AT-C_{518}+PII+gln (□), AT/AT-C_{518}-PII+gln (Δ), AT/AT-C_{518}+PII+gln+5A7 (◊), and AT/AT-C_{518}+PII+gln+39G11 (-). All assays were performed in duplicate and with AT_{wt} as a reference. Error bars have not been shown on the curves as they hinder visual inspection. The standard error range for all the curves is generally <0.4.

Pre-incubation of the two R domain mAbs, 5A7 and 39G11 in the adenylylation assay with ATase had the effect of reducing the activity of ATase (Figure 6.7a), but both these mAbs had no impact on the adenylylation activity of the AT-C_{518} truncation construct (Figure 6.7b). This result implies that the adenylylation activity of ATase is inhibited by mAbs 5A7 and 39G11. The level of inhibited activity resembled that seen when PII was omitted from the adenylylation assay, suggesting that these mAbs can block the binding of PII to ATase. The fact that the two R domain mAbs did not inhibit the adenylylation activity of the PII independent AT-C_{518} construct further supports the idea that these two mAbs inhibit PII binding to ATase.

6.3.5.2.2 Inhibition of PII-UMP binding in deadenylylation

The two R domain mAbs 39G11 (crude ascitic fluid; see section 6.2.4) and 5A7 (purified; see section 6.2.4) were used in the deadenylylation assay (see section 6.2.5) with ATase (purified; see section 6.2.1), in order to investigate the impact of these

mAbs on deadenylylation activity. The deadenylylation assay result for mAb 5A7 is shown in Figure 6.8.

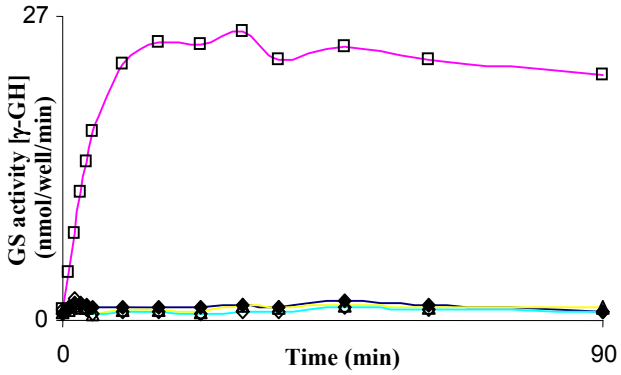

Figure 6.8 ***Inhibition of deadenylylation activity in ATase by R domain mAb 5A7.*** This assay shows the change in activity of ATase in deadenylylation by measuring the production of γ-glutamyl hydroxamate by GS-AMP with R domain mAb 5A7 present. Standard assay conditions (see section 6.2.5) were used and the mAb (see section 6.2.4) was preincubated with AT (1:1) for 30min at room temperature. No AT+PII+gln (♦), AT+PII-UMP+α-kg (□), AT+PII-UMP+α-kg (Δ), and AT+PII-UMP+α-kg+5A7 (◊). All assays were performed in duplicate and with AT_{wt} as a reference. Error bars have not been shown on the curves as they hinder visual inspection. The standard error range for all the curves is generally <0.4.

The R domain mAb 5A7 completely eliminated the deadenylylation activity of ATase (Figure 6.8). The effect of the R domain mAb 39G11 on deadenylylation activity was determined using the initial rate assay (see section 6.2.5) (data not shown). This mAb also eliminated all deadenylylation activity in ATase.

Both the R domain mAbs completely inhibited deadenylylation activity in ATase. Removing PII-UMP from the assay has the same effect (Figure 6.8), suggesting that the mode of inhibition was by prevention of PII-UMP binding. To investigate this idea further, a different initial rate deadenylylation assay (see section 6.2.5) was used with the two R domain mAbs. The standard conditions were modified so that no α-kg was added and twice as much GS-AMP and PII-UMP protein were added to the assay. Under these conditions, PII-UMP was the only effector responsible for the stimulated deadenylylation activity and both of the mAbs completely inhibited the activity (Table 6.3). Therefore the two R domain mAbs also inhibit PII-UMP binding.

Condition	Deadenylylation rate (nmol of γ-GH produced/well/min/min)
GS-AMP+AT+PII-UMP+αkg	3.1192 (0.9971)
2xGS-AMP+AT+2xPII-UMP-αkg	0.5392 (0.9874)
2xGS-AMP+AT+2xPII-UMP-αkg+5A7	0.00
2xGS-AMP+AT+2xPII-UMP-αkg+39G11	0.00

Table 6.3 ***Inhibition of PII-UMP binding by R domain mAbs 5A7 and 39G11.*** This table shows the initial deadenylylation activity of ATase stimulated only by PII-UMP in the presence and absence of the R domain mAbs, 5A7 and 39G11(see section 6.2.4). The activity was determined using initial rate assays, which measured the production of γ-glutamyl hydroxamate by GS-AMP (see section 6.2.5). The curves were fitted with a linear regression using Microsoft Excel and the resulting rates are shown here. The R^2 coefficient for each curve is shown in brackets.

6.3.5.3 Effect of C domain mAbs on ATase activity

When the purified C domain mAbs, 6A3 and 27D7 (see section 6.2.4) were added to the deadenylylation assay (see section 6.2.5) at a molar ratio of 1:1 they had no effect on the activity of ATase (purified; see section 6.2.1) (Figure 6.9). To ensure that the lack of inhibition was not due to the mAb's lower affinity for the protein, the assays were also run with 10 times more 6A3 and 27D7, and there was still no inhibition (data not shown).

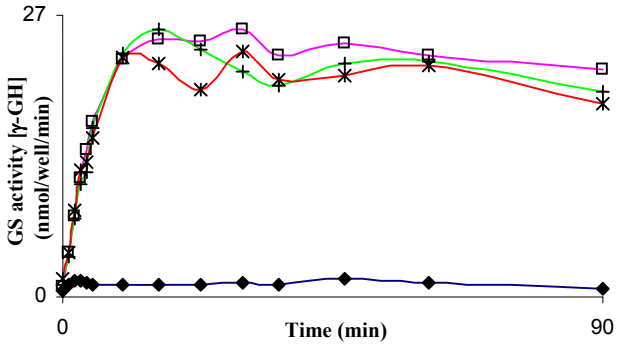

Figure 6.9 ***Deadenylylation activity of ATase in the presence of C domain mAbs 6A3 and 27D7.*** These assays show the changes in activity of ATase in deadenylylation by measuring the production of γ-glutamyl hydroxamate by GS-AMP with C domain mAbs 6A3 and 27D7 present. Standard assay conditions (see section 6.2.5) were used and the mAbs (see section 6.2.4) were preincubated with AT (1:1) for 30min at room temperature. No AT+PII-UMP+α-kg (♦), AT+PII-UMP+α-kg (□), AT+PII-UMP+α-kg+6A3 (+), and AT+PII-UMP+α-kg+27D7 (*). All assays were performed in duplicate and with AT_{wt} as a reference. Error bars have not been shown on the curves as they hinder visual inspection. The standard error range for all the curves is generally <0.4.

The two purified C domain mAbs, 6A3 and 27D7 (see section 6.2.4) were also used in adenylylation assays (see section 6.2.5) with ATase and AT-C_{518} (both purified, see section 6.2.1) to investigate the impact of these mAbs on adenylylation activity (Figure 6.10). Entire ATase and the PII independent C-terminal truncation construct, AT-C_{518} were chosen for these assays because they were demonstrated to bind with the mAbs (Figure 6.1) and had been used to assess the R domain mAb effects (Figure 6.7).

Both ATase and AT-C_{518} exhibited partial inhibition of adenylylation activity when either of the C domain mAbs was present in the assay (Figure 6.10). Because the mAbs partly inhibited the activity of the truncated construct, AT-C_{518} as well as intact ATase, it was probably not due to the inhibition of PII binding like the R domain mAbs.

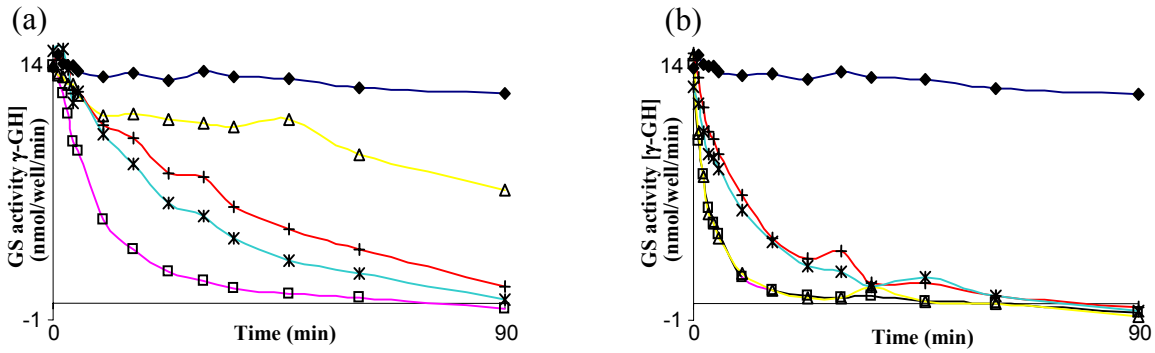

Figure 6.10 Adenylylation activity of ATase and AT-C_{518} in the presence of C domain mAbs 6A3 and 27D7. These assays show the changes in activity of (a) ATase and (b) the C-terminal truncation construct AT-C_{518} in adenylylation by measuring the production of γ-glutamyl hydroxamate by GS with C domain mAbs 6A3 and 27D7 present. Standard assay conditions (see section 6.2.5) were used and the mAbs (see section 6.2.4) were preincubated with AT/AT-C_{518} (1:1) for 30min at room temperature. No AT/AT-C_{518}+PII+gln (♦), AT/AT-C_{518}+PII+gln (□), AT/AT-C_{518}-PII+gln (Δ), AT/AT-C_{518}+PII+gln+6A3 (+), and AT/AT-C_{518}+PII+gln+27D7 (*). All assays were performed in duplicate and with AT_{wt} as a reference. Error bars have not been shown on the curves as they hinder visual inspection. The standard error range for all the curves is generally <0.6.

The partial inhibition of adenylylation activity by the C domain mAbs could be caused by inhibition of gln binding or partial inhibition of ATase and AT-C_{518} binding to GS. To address this question a series of adenylylation assays (see section 6.2.5) were run with the PII independent C-terminal truncation constructs, AT-C_{518}, AT-C_{396} (purified; see section 6.2.1) and AT-C_{340} (cell lysate; see section 6.2.1). The impact of the C domain mAbs on the activity of the C-terminal truncation constructs was investigated in the absence of gln (Figure 6.11). If the mAbs inhibited the activity of the C-terminal

truncation constructs under these conditions then the mAbs were directly interfering with the interaction between the ATase and GS proteins.

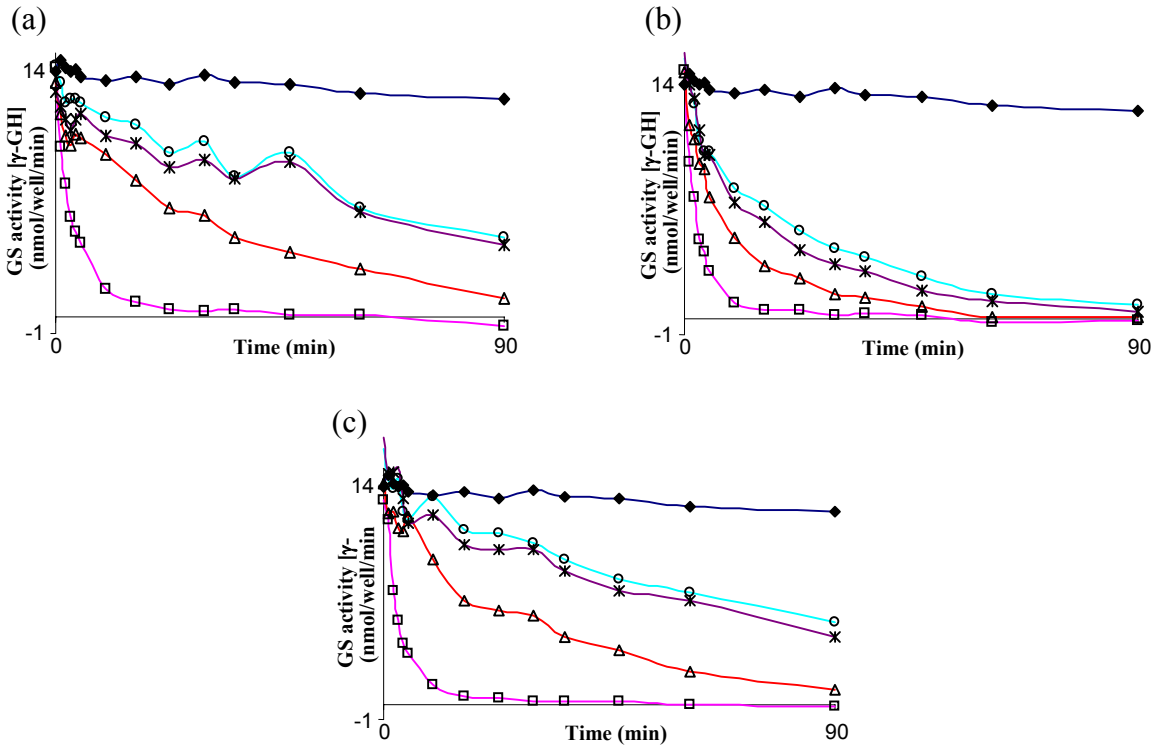

Figure 6.11 ***Inhibition of C-terminal truncation construct activity by C domain mAbs 6A3 and 27D7 in adenylylation with no glutamine.*** These assays show the changes in activity of the C-terminal truncation constructs (a) AT-C_{518} (purified; see section 6.2.1), (b) AT-C_{396} (purified; see section 6.2.1), and (c) AT-C_{340} (cell lysate; see section 6.2.1) in adenylylation with no gln. Activity was measured by the production of γ-glutamyl hydroxamate by GS with C domain mAbs 6A3 and 27D7 present. Standard assay conditions (see section 6.2.5) were used and the mAbs (see section 6.2.4) were preincubated with the constructs (1:1) for 30min at room temperature. No construct+PII+gln (♦), construct+PII+gln (□), construct+PII-gln (Δ), construct+PII-gln+6A3 (○), and construct+PII-gln+27D7 (*). All assays were performed in duplicate and with AT_{wt} as a reference. Error bars have not been shown on the curves as they hinder visual inspection. The standard error range for all the curves is generally <0.4.

When there was no gln present in the adenylylation assay each of the C-terminal truncation constructs showed further inhibition of adenylylation activity when either of the C domain mAbs was included in the assay (Figure 6.11). Both of these mAbs are partly blocking the interaction of ATase and GS, and because the inhibition is consistently different (i.e., mAb 6A3 always inhibits slightly more than mAb 27D7), the mAbs are probably binding at different sites on the ATase protein.

6.3.5.4 Inhibition of GlnK stimulated ATase activity using mAbs

In this series of adenylylation and deadenylylation assays the ATase mAbs were used to inhibit the activity of ATase when PII, GlnK, PII-UMP and GlnK-UMP were used as the effector-proteins (Table 6.4).

Adenylylation			Deadenylylation		
Conditions	**PII (25nM)**	**GlnK (125nM)**	**Conditions**	**PII-UMP (25nM)**	**GlnK-UMP (2uM)**
gln (1mM)	1.00	1.00	**α-kg (20mM)**	1.00	1.00
no PII, gln	0.15	0.15	**no PII-UMP, α-kg**	0.04	0.04
5A7 (25nM)	0.15	0.16	**5A7**	0.00	0.00
39G11 (25nM)	0.15	0.17	**39G11**	0.00	0.00
6A3 (25nM)	0.27	0.26	**6A3**	1.00	0.97
27D7 (25nM)	0.48	0.51	**27D7**	1.02	1.00
6B5 (25nM)	1.00	1.01	**6B5**	0.98	1.00

Table 6.4 ***Inhibition of ATase activity stimulated by all the effector-proteins using monoclonal antibodies.*** Standard assay conditions were used where ATase activity is measured by the production of γ-glutamyl hydroxamate by GS/GS-AMP (see section 5.2.3) except the concentration of the GS/GS-AMP protein was 2x standard conditions. The mAb was preincubated with ATase (1:1) for 30min at room temperature. The 6B5, 5A7, 6A3 and 27D7 mAbs were purified and 39G11was used as crude ascitic fluid (see section 5.2.3). All assays were performed in duplicate and with PII_{wt} as a reference. The initial rate curves were fitted with a linear regression using Microsoft Excel. The R2 coefficient for the curves was generally >0.9. The initial rates for all the effector-proteins have been expressed as a proportion of their standard activity.

The R domain mAbs 5A7 and 39G11 both inhibit the activity of ATase in adenylylation (to the no PII level) and deadenylylation (to the no PII-UMP level) when either PII/PII-UMP or GlnK/GlnK-UMP are the effector-proteins. In adenylylation the C domain mAbs 6A3 and 27D7 both inhibit the stimulation of activity in ATase by either effector-protein to a similar degree. In deadenylylation the C domain mAbs have no impact on PII-UMP or GlnK-UMP mediated ATase activity. The N domain mAb 6B5 had no impact on any activity of ATase, regardless of the effector-protein (Table 6.4).

In other words PII and GlnK are probably binding to the same site (or very close to it) on ATase, and PII-UMP and GlnK-UMP are also probably binding to the same site (or very close to it) on ATase. Potentially all four effector-proteins are binding to the same site (or very close to it) on the ATase protein.

6.4 DISCUSSION

Previous work by Jaggi *et al.*, (1997) demonstrated that ATase had two activity domains at either end of the protein. The deadenylylation domain at the N-terminal end of the protein (including a β-polymerase motif; Holm and Sander, 1995), followed by a Q-linker (Wooton and Drummond, 1989) and the adenylylation domain at the C-terminal end of the protein (including a β-polymerase motif; Holm and Sander, 1995). Further investigation of the protein sequence suggested there were two Q-linkers (rather than one) separating the protein into three domains (rather than two).

The N-terminal region of ATase before the first Q-linker is fully soluble (AT-N_{440}), strongly suggesting that this region is a complete, natural domain (Wen, 2000). The construct containing the second Q-linker and the C-terminal domain is also soluble (AT-C_{340}) (Wen, 2000). The truncation construct where both these domains are connected by the two Q-linkers (with the putative R domain removed; AT:ΔR) is also soluble (O'Donnell, 2000). The solubility of these three constructs strongly supported the notion that ATase is a protein comprising three domains (N-Q1-R-Q2-C). The final proof came with the successful generation of the AT:RQ2 construct as a soluble polypeptide (Figure 6.3) in this work. Assay data using various truncation constructs produced in this laboratory indicated that this central domain acted as a regulatory domain with the help of the two effector-proteins PII and PII-UMP (see later).

Adenylylation activity in intact ATase is dependent on the presence of the effector-protein, PII and the small effector-molecule, gln working synergistically. Omission of either of these effectors results in a reduction in the adenylylation activity (Figure 6.4f). Similarly the deadenylylation activity is dependent on the uridylylated form of the effector-protein, PII-UMP and the small effector-molecule, α-kg for synergistic stimulation. There is hardly any deadenylylation activity when PII-UMP is the only effector present in the assay, and no activity when α-kg is the only effector present (Figure 6.5c).

The binding sites for PII and PII-UMP on ATase were determined from assays using the two R domain mAbs 5A7 and 39G11 (Figures 6.8, 6.9 and Table 6.3). These mAbs bind in the N-terminal region of the R domain (between residues 466 and 548, see Chapter 3) and blocked the binding of PII and PII-UMP to ATase. Therefore PII and PII-UMP must bind in or very near to the N-terminal region of the R domain between residues 466 and 548. The fact that the two effector-proteins are binding in the R domain further supports the notion that it has a regulatory role. The GlnK paralogue and its uridylylated form were also demonstrated to bind in this region of ATase (Table 6.4).

When the deadenylylation domain is removed from ATase, the resulting polypeptide (Q1-R-Q2-C) becomes independent of PII in adenylylation (Figure 6.4b). This suggests that the N-terminal domain is blocking the adenylylation activity in ATase when the PII effector-protein is not bound ("closed conformation" in Figure 6.12). Further removal of part or all of the central R domain has no impact on adenylylation activity; the resulting polypeptides (part R-Q2-C and Q2-C) behave the same way (Figures 6.4b&d). Removal of the R domain alone also results in a polypeptide (N-Q1-Q2-C) that is independent of PII in adenylylation (Figure 6.4e). These results suggest that the R domain regulates adenylylation activity by interacting with the N domain so that its position relative to the C domain blocks the adenylylation capacity of ATase.

Similarly, deadenylylation activity is also independent of its effector-protein PII-UMP, when the R and C domain are removed (Figure 6.5b). Therefore in the "closed conformation" (Figure 6.12) deadenylylation activity is also blocked. A similar phenomenon is seen in the enzyme activities present in the N-terminal domain of aspartokinase-homoserine dehydrogenase I (see section 6.1). Removal of either of the activity domains resulted in a decrease in the regulation of the activity of the remaining domain (James and Viola, 2002).

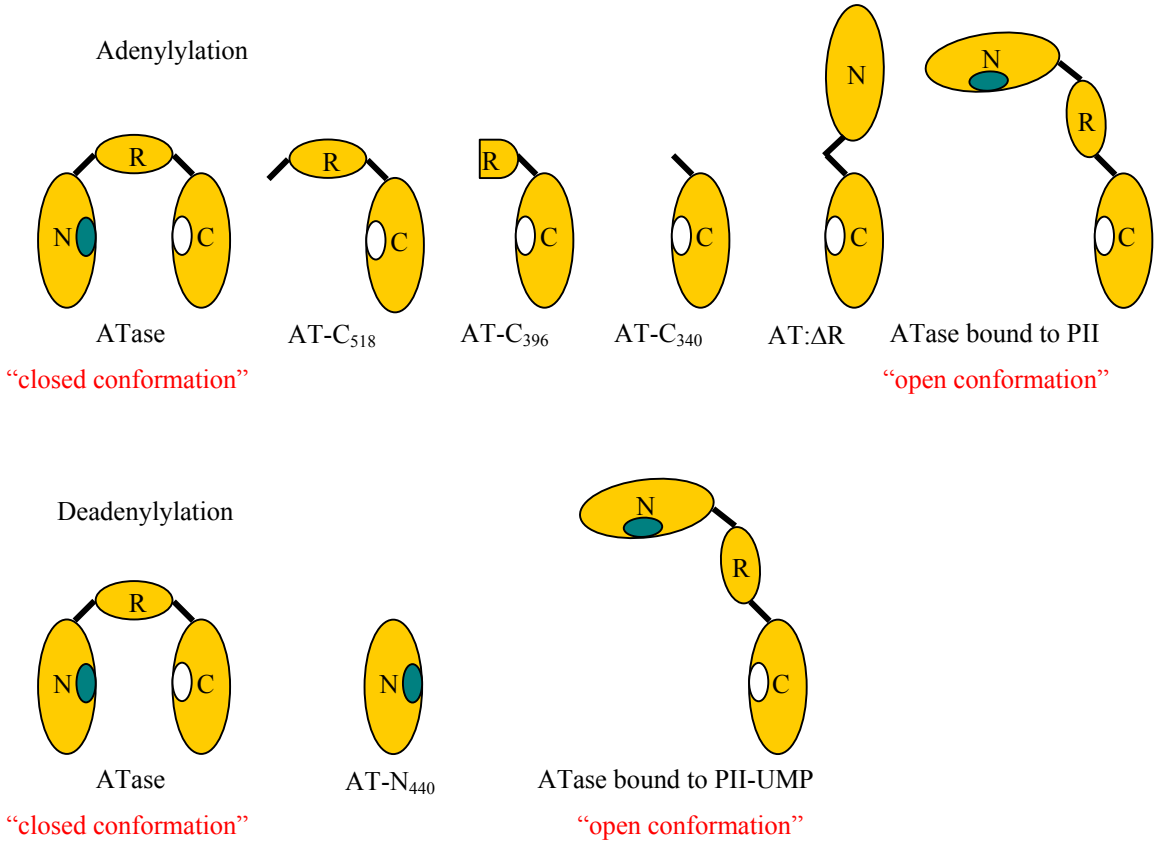

Figure 6.12 ***Schematic representation of the different conformations of ATase in adenylylation and deadenylylation.*** The activity results from the adenylylation and deadenylylation assays shown in Figures 6.4 and 6.5 have been summarised in this diagram. Uncomplexed ATase has a "closed" conformation (Jaggi, 1998) and has minimal activity in either assay. Removal of the N or R domains gives rise to polypeptides with similar adenylylation activity to PII complexed ATase and removal of the R+C domain gives rise to a polypeptide, which has activity independent of PII-UMP in deadenylylation. Addition of PII to the adenylylation assay or PII-UMP to the deadenylylation assay causes a shift in the position of the N domain relative to the C domain and ATase adopts the "open" conformation (Jaggi, 1998). The complexed ATase is then capable of adenylylating GS or deadenylylating GS-AMP, depending on the other effectors present in the assay. The adenylylation active site is shown in white and is accessible to GS in all the conformations except the uncomplexed "closed" conformation and the deadenylylation active site shown in cyan is accessible to GS-AMP in all conformations except the uncomplexed "closed" conformation.

The binding of PII or PII-UMP in the N-terminal region of the R domain may disrupt the interaction between the N and R domains, such that the steric hindrance by the two activity domains is alleviated and ATase adopts the "open conformation" (Figure 6.12). The "open conformation" allows adenylylation or deadenylylation to proceed depending on the effector-molecules present. As discussed in Chapter 1 the first Q-linker in ATase is amphipathic with a hydrophobic face down one side. It is possible that this hydrophobic face interacts with a hydrophobic patch in the N-terminal region of the R

domain and the binding of either effector-protein disrupts the interaction, so the N and R domains are separated to adopt the effector-protein complexed "open conformation" (Figure 6.12). The reduced solubility of the AT-C_{481} and AT-C_{439} truncation constructs (Figure 6.1) support the idea that there is a hydrophobic patch in the N-terminal region of the R domain, which is exposed when the first Q-linker is removed, reducing the solubility of the truncation constructs.

ATase is approximately 1060 times more active in deadenylylation than the N domain polypeptide (Table 6.2). This suggests that when the N domain is separated from the R domain by PII-UMP in the "open conformation" (Figure 6.12) the deadenylylation active site adopts a more suitable conformation for the deadenylylation reaction to proceed.

Jaggi (1998) proposed ATase functioned in a non-processive way when adenylylating the 12 Tyr397 residues of the dodecameric GS, which meant ATase would detach itself from GS with the addition of each individual AMP group. One of the free T-loops of PII, which was not involved in the adenylylation reaction, could bind to the next monomer on GS acting as an anchor enabling the PII/ATase complex to "walk" around the GS monomers adenylylating them. The "walking" model proposed by Jaggi (1998) for the PII/ATase protein complex adenylylating GS is not supported by these results, because the AT-C truncation constructs are PII independent and have an activity level similar to entire ATase (Table 6.2). If PII was necessary for "walking" around GS the C-terminal truncation constructs should behave more like the N-terminal domain construct, AT-N_{440}, which has dramatically reduced activity compared to the entire protein.

All of the ATase truncation constructs that included the C-terminal domain behaved as the wild type ATase protein with regards to their dependence on gln for full adenylylation activity (Figures 6.4b-e). Each construct showed a reduction in adenylylation activity when gln was removed from the assay. For entire ATase, further removal of PII from the assay virtually abolished activity (Figure 6.4f). These results suggest that the reduction in activity is not because PII can no longer bind without gln

present, but is due to some other factor. It is most likely that the presence or absence of gln impacts directly on the interaction between ATase and GS. This phenomenon is investigated further in Chapter 7.

The smallest C-terminal construct capable of adenylylation included the second Q-linker and the C domain (Wen, 2000). This means that gln is binding somewhere in this region of ATase. The binding sites for gln and α-kg within ATase and PII are investigated further in Chapter 7.

In summary, this chapter resolved the domain structure of the bi-functional ATase enzyme by providing compelling evidence for the presence of a central regulatory domain flanked by the two activity domains. This is based on both the production of a soluble peptide for the predicted central domain as well as evidence that mAbs that bind to this central region successfully block the binding of the effector-proteins PII, GlnK, PII-UMP and GlnK-UMP.

CHAPTER 7 Intramolecular signalling within ATase: Role of Glutamine and α-Ketoglutarate in the Adenylylation Cascade

7.1 INTRODUCTION

Adenylyl transferase is a multidomain enzyme that contains two DNA polymerase-β motifs (Holm and Sander, 1995) involved in the activation and inactivation of GS by deadenylylation and adenylylation, respectively. In the previous chapter the domain arrangement of ATase was examined and clear evidence was presented for the existence of a third central regulatory domain that controls the two activity domains. Each of the three domains N (AT-N_{440}: residues 1-440 in the intact ATase protein), R (AT-RQ2: residues 466-627) and C (AT-C_{305}: residues 642-946) were produced as soluble proteins and characterised enzymatically in the presence and absence of ATase mAbs (produced and characterised in Chapter 3).

Based on secondary structure prediction, and the relationship of truncation solubility and correct domain delineation, the N-terminal domain boundary was correctly predicted. The 3D structure of the new N-terminal truncation construct, AT-N_{440} (N-terminal deadenylylation domain of ATase) has now been solved with X-ray crystallography (Figure 7.1). Structural comparisons of AT-N_{440} with kanamycin nucleotidyl transferase and various eukaryotic DNA polymerase-β containing proteins confirm the prediction that the polymerase motif is highly conserved (Chapter 1).

Based on the similarities observed with eukaryotic DNA polymerase-β motifs, the highly conserved aspartate residues within the two β-polymerase motifs in ATase, (Asp173 and Asp175: deadenylylation, Asp701 and Asp703: adenylylation) were mutated to Ala, Glu or Asn individually, or in pairs. These mutations resulted in the complete inactivation of the respective active sites, even for such subtle changes as Asp to Glu, suggesting that active site confirmation is very important for either activity in ATase (McLoughlin, 1999).

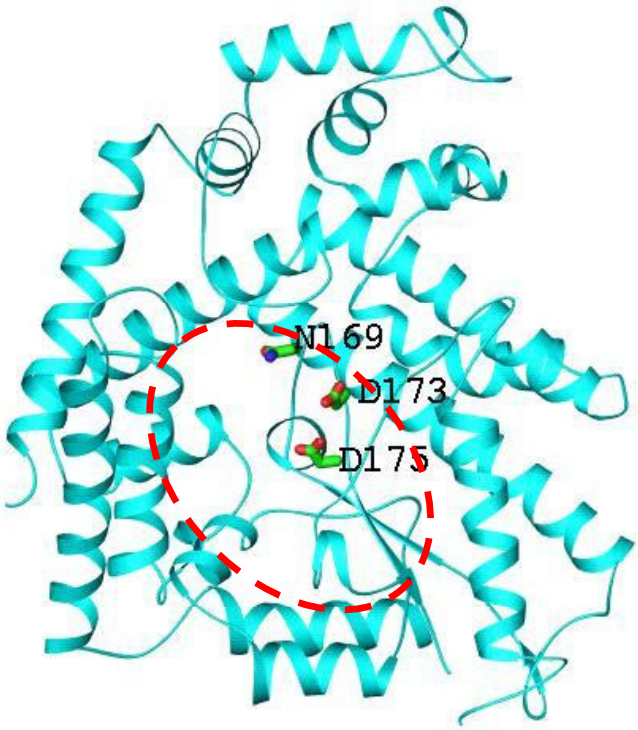

Figure 7.1 ***Structure of the deadenylylation domain of ATase.*** X-ray crystal structure of the AT-N_{440} truncation construct of the ATase protein from *E. coli*. (Xu *et al*., 2004). The three important residues from the McLoughlin (1999) suite of mutations have been highlighted. D173 and D175 hold the catalytic Mg^{2+} ion in position and N169 is probably involved in correct positioning of the phosphate group. These residues cluster in the probable GS-AMP binding site within the red ring.

The two highly conserved Asp173 and Asp175 residues within the deadenylylation active site are probably very important in holding the Mg^{2+} ion required for activity (Xu *et al.*, 2004). The equivalent conserved residues in rat DNA polymerase-β were shown to be important for holding the Mg^{2+} ion important for this protein's activity (Sawaya *et al.*, 1994; Davies *et al.*, 1994). Rat DNA polymerase-β is the protein to which the active sites of nucleotidyl transferases were compared (Holm and Sander, 1995).

The other important residue (from the McLoughlin (1999) suite of mutations) highlighted from solving the structure of the AT-N_{440} construct is the Asn169 residue. Asparagine 169 may be involved in positioning the phosphate group involved in the deadenylylation (phosphorylysis) reaction. The AT:N169G mutant also had drastically reduced activity in the deadenylylation assay (McLoughlin, 1999). The 3D structure of the N-terminal domain, AT-N_{440} also demonstrated a pocket at this site, where GS-AMP probably binds (Xu *et al.*, 2004) (Figure 7.1).

Mutations were also carried out to test if the opposing activities of ATase, which are not each other's microscopic reverse, could be artificially reversed by single site changes at positions Asn169, Trp694 and Gly697. Whilst no reversal was observed in entire ATase carrying the appropriate mutations, the W694G mutation produced an important mutant phenotype. The W694G mutation did not affect the adenylylation activity of ATase, but interestingly the adenylylation activity of this mutant is independent of gln, an allosteric activator of the adenylylation reaction. Further analysis indicated that the Trp694 residue may be the switch that signals gln presence to the adenylylation catalytic site (McLoughlin, 1999).

The first aim of studies reported in this chapter was to revisit the work of McLoughlin (1999) using the initial rate assay (see section 2.2.10.2.4) to give a more accurate comparison of mutant ATase activity. In connection with this a N169G mutation was introduced into the AT-N_{440} truncation construct to see if swapping this residue in the deadenylylation active site to the equivalent adenylylation active site residue, could produce a deadenylylation active site that could adenylylate GS. This step was taken because it was found that AT-N_{440} carried out its deadenylylation activity independently of PII-UMP and α-kg. With this in mind the hypothesis being tested was that if N169 is critical for binding the phosphate residues, which are thought to be essential for the phosphorylysis reaction, then mutation to a corresponding residue in the adenylylation motif could result in a role reversal. In this instance if the mutant polypeptide had no activity in adenylylation it would not be because of potential interference from the R and C domains of the entire ATase protein (McLoughlin, 1999).

As mentioned previously the GS adenylylation-state is regulated by the concentrations of the key small effector-molecules, gln and α-kg. The intracellular gln concentration signals N status, and the intracellular α-kg concentration signals C status. The α-kg molecule binds to PII synergistically with ATP (Kamberov *et al.*, 1995), and gln binds to ATase and UTase (Jiang *et al.*, 1998a). All the C-terminal truncation constructs are dependent on gln for full activity in adenylylation (see Chapter 6), so the second aim of this chapter was to try to determine the potential binding site for gln within the Q2-C region of ATase.

α-Ketoglutarate, the allosteric deadenylylation stimulator, has two effects on the *in vitro* adenylylation activity of ATase depending on the concentration added to the assay. A small amount of α-kg (10μM) stimulates adenylylation activity and a large amount of α-kg (>10mM) depresses adenylylation activity (Jiang *et al.*, 1998b). This response to α-kg in adenylylation suggests there is a high and low affinity-binding site within the adenylylation catalytic complex.

Kamberov *et al.*, (1995) demonstrated the existence of the high affinity binding site on the PII protein, which had a K_d for α-kg of 5.6±0.4 μM. The method these workers employed was only capable of determining K_d <25μM, so the low affinity site could not be assessed; however stoichiometry data did not rule out the possibility that the low affinity site could also be on the PII protein. Jiang *et al.*, (1998b) assessed the activity of the PII mutant, Q39E, which was defective for α-kg binding in the monocyclic reconstituted cascade system, and their data suggested PII was the sole α-kg binder.

However, preliminary data using the assays employed in this laboratory (see section 2.2.10.2) with ATase truncation constructs suggested the low affinity α-kg binding site could be situated on the ATase protein rather than PII. The fact that deadenylylation activity is stimulated in a dose dependent manner with increasing concentrations of α-kg also supported the preliminary findings. The third aim of this chapter was to carry out direct α-kg binding studies with ATase. Then use was made of all the ATase mutants and truncation constructs available in adenylylation and deadenylylation assays to investigate the possibility that the low affinity α-kg binding site may be situated on ATase within the Q1-R-Q2-C region rather than PII.

The final aim of this chapter was to investigate the role of the Q1 linker in intramolecular signalling. Removal of the Q1 linker from the fully soluble AT-C_{518} truncation construct dramatically reduced the solubility of the resulting truncation construct (AT-C_{481}). The possible reason for the drop in solubility was due to the amphipathic nature of the helical Q1 linker (Chapter 1). When the Q1 linker was removed, hydrophobic regions of the R domain within ATase may have become exposed reducing the solubility of the new construct (Jaggi, 1998). This suggests that

the Q1 linker in ATase is very closely associated with the R domain, and could possibly be involved in intramolecular signalling.

Several ATase mutants (AT:W452A and AT:E454A) and one truncation construct with two Q1 linkers (AT:$Q1^2$) were produced previously (O'Donnell, 2000). The Q1 linker mutants, AT:W452P and AT:W456A were produced in this work. The AT:W456P mutation was designed to dramatically change the structure of the Q1 linker of ATase. The W456P mutation was designed to introduce a turn into the middle of the hydrophobic side of the predicted amphipathic α helix within the Q-linker (Chapter 1). These mutants were assessed for changes in responses to the two allosteric effectors in both the adenylylation and deadenylylation assays.

7.2 METHODS

7.2.1 Expression and purification of proteins

Expression and purification of the ATase truncation constructs were covered in Chapter 6. The expression and purification of PII and GlnK were covered in Chapter 5.

The catalytic site ATase mutant recombinant vectors were produced previously. Complementary primers designed to introduce a point mutation within the gene insert in the plasmid were used in PCR (section 2.2.4.2). Detailed descriptions of their construction can be found in the individual reference McLoughlin, (1999). Several Q1 linker mutants, AT:W452A and AT:E454A were also produced previously by the same method (O'Donnell, 2000).

The AT-N_{440}:N169G, AT:W452P and AT:W456A mutants were produced in this work, also following the methods in section 2.2.4.2. The ATase protein expression vector pRJ009 (2.1.6.2) was used as the template and specific primers described in section 2.1.7.2 were used to introduce the point mutation.

All strains were grown in LB medium and when appropriate, supplemented with ampicillin (100μgmL^{-1}) (see section 2.2.1.1 and 2). All the ATase mutants (pND707-derived) (2.1.6.2), were expressed in JM109 cells (2.1.4). The method of protein induction was thermal induction (see section 2.2.5.1).

Plasmid	Description	Source/Reference
pRJ001	*glnB* (PII) in pND707	Jaggi *et al.*, (1996)
pNV101	*glnD* (UTase) in pND707	Jaggi *et al.*, (1996)
pNV103	*glnK* (GlnK) in pND707	Vasudevan lab unpublished
pWVH57	*glnA* (GS) in pBluescript II KS+	van Heeswijk *et al.*, (1996)
pJRV001	*glnA* (GS) in pND707	Vasudevan lab unpublished
pRJ009	*glnE* (ATase) in pND707	Jaggi *et al.*, (1997)
pRJ0012	*glnE* (AT-N_{548}) in pND707	Jaggi (1998)
pRJ0013	*glnE* (AT-N_{501}) in pND707	Jaggi (1998)
pRJ0015	*glnE* (AT-C_{396}) in pND707	Jaggi (1998)
pDW1	*glnE* (AT-N_{440}) in pND707	Wen (2000)
pDW2	*glnE* (AT-C_{481}) in pND707	Wen (2000)
pDW4	*glnE* (AT-C_{518}) in pND707	Wen (2000)
pDW7	*glnE* (AT-C_{340}) in pETDW2	Wen (2000)
pET AT:ΔR	*glnE* (AT:ΔR) in pETDW2	O'Donnell (2000)
pRJ009:$Q1^2$	*glnE* (AT:$Q1^2$) in pND707	O'Donnell (2000)
pRJ009:W452A	*glnE* (AT:W452A) in pND707	O'Donnell (2000)
pRJ009:E454A	*glnE* (AT:E454A) in pND707	O'Donnell (2000)
pRJ009:N169G	*glnE* (AT:N169G) in pBluescript II	Mc Loughlin (1999)
pRJ009:D173A	*glnE* (AT:D173A) in pND707	Mc Loughlin (1999)
pRJ009:D175A	*glnE* (AT:D175A) in pND707	Mc Loughlin (1999)
pRJ009:D173AD175A	*glnE* (AT:D173AD175A) in pND707	Mc Loughlin (1999)
pRJ009:W694G	*glnE* (AT:W694G) in pND707	Mc Loughlin (1999)
pRJ009:G697N	*glnE* (AT:G697N) in pBluescript II	Mc Loughlin (1999)
pRJ009:W694GG697N	*glnE* (AT:W694GG697N) in pND707	Mc Loughlin (1999)
pRJ009:D701E	*glnE* (AT:D701E) in pND707	Mc Loughlin (1999)
pRJ009:D703E	*glnE* (AT:D703E) in pND707	Mc Loughlin (1999)
pRJ009:D701ED703E	*glnE* (AT:D701ED703E) in pND707	Mc Loughlin (1999)
pRJ009:D701N	*glnE* (AT:D701N) in pND707	Mc Loughlin (1999)
pRJ009:D703N	*glnE* (AT:D703N) in pND707	Mc Loughlin (1999)
pRJ009:D701ND703N	*glnE* (AT:D701ND703N) in pND707	Mc Loughlin (1999)
pAT:ΔR	*glnE* (AT:ΔR) in pET	O'Donnell (2000)
pRJ009:RQ2	*glnE* (AT:RQ2) in pETDW2	this work (Chapter 6)
pRJ009:W452P	*glnE* (AT:W452P) in pND707	this work
pRJ009:W456A	*glnE* (AT:W456A) in pND707	this work
pDW1:N169G	*glnE* (AT-N_{440}:N169G) in pND707	this work

Table 7.1 ***Recombinant proteins.*** List of the plasmids encoding the recombinant proteins used in this chapter including the plasmid name and source.

The ATase mutant protein preparations were produced from small-scale cultures (see section 2.2.5.3) and not purified. The approximate individual target protein concentration was determined by comparison with a band of known concentration in SDS PAGE (see section 2.2.8.2).

7.2.2 Adenylylation and deadenylylation assays

The adenylylation and deadenylylation assays (see section 2.2.10.2) were performed using the different ATase mutants and truncation constructs with various combinations of small effector-molecules to study the roles of gln and α-kg. All the assays were performed as initial rate assays (see section 2.2.10.2.4).

7.2.3 Direct small effector-molecule binding assay

Purified PII and ATase protein derived from large-scale expression of vectors in RB9040 and JM109 strains, respectively (see section 5.2.1) were used in these assays (see section 2.2.10.3).

7.3 RESULTS

7.3.1 Generation of new ATase mutants

The PCR reactions generating the AT-N_{440}:N169G, AT:W452P and AT:W456A mutations (see section 7.2.1) all gave rise to a DNA fragment which was of the expected size when analysed by agarose gel electrophoresis (see section 2.2.3.1) (Figure 7.2a). The ligated DNA fragments+vector were successfully transformed into competent DH5α cells (2.1.4) giving rise to transformants that grew on the selective LBA plates (see section 2.2.1.4). Small-scale plasmid preparations were made for each of the newly formed plasmids (see section 2.2.2.2) and restriction digestion analysis with *NdeI* yielded correct sized DNA fragments (see section 2.2.2.3) (Figure 7.2b).

Automated sequence analysis of the mutated region of the inserts was performed (see section 2.2.4.3) using the AT N FP2 primer (2.1.7.1) for AT:W452P and AT:W456A, and the AT N RP1 primer (2.1.7.1) for AT-N_{440}:N169G. Each of the three mutations was successfully generated (Figure 7.3).

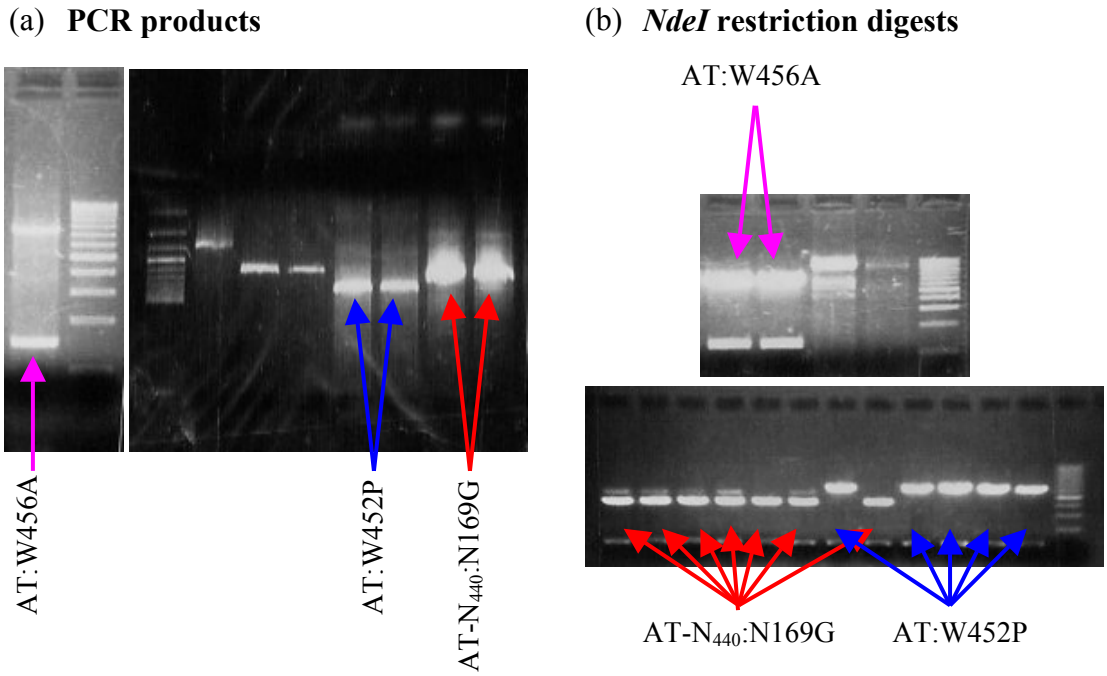

Figure 7.2 ***Generation of the new ATase mutants.*** (a) PCR product (see section 7.2.1) and (b) *Nde I* digested plasmid (see section 7.2.1) visualised by agarose gel electrophoresis (see section 2.2.3.1) for AT:W452P, AT:W456A and AT-N_{440}:N169G.

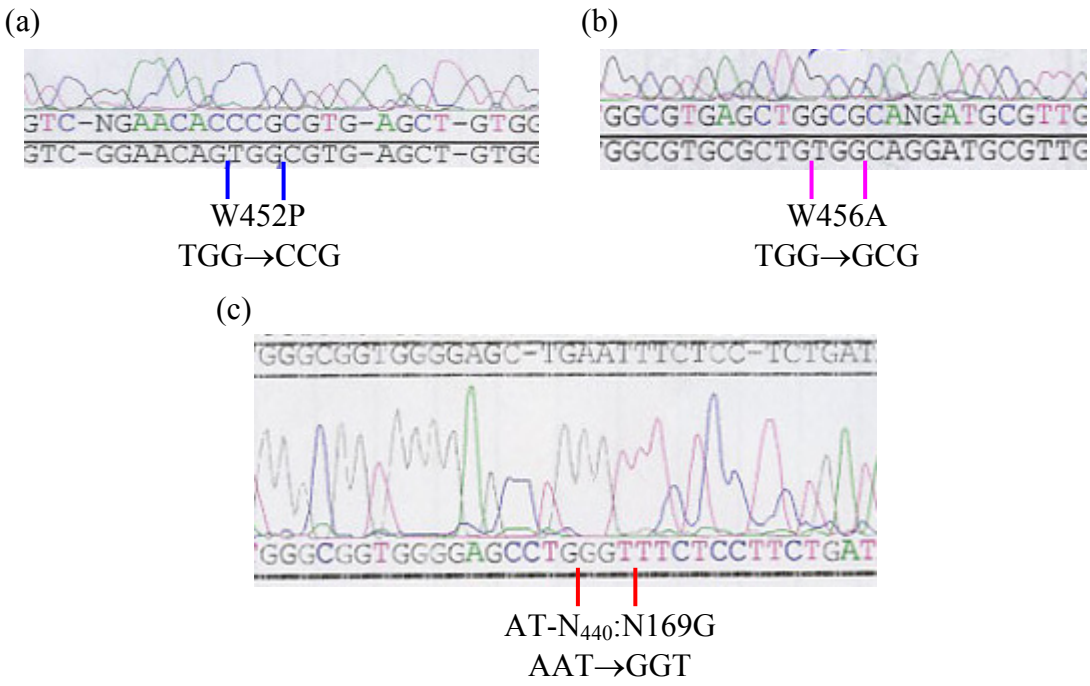

Figure 7.3 ***Mutated residue sequence data for new ATase mutants.*** Sequence data generated by automated sequencing (see section 2.2.4.3) for the (a) AT:W452P, (b) AT:W456A and (c) AT-N_{440}:N169G mutants. The original ATase *glnE* sequence is shown in black.

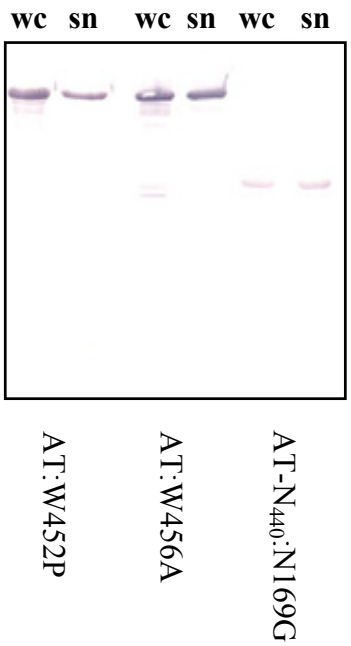

Figure 7.4 ***Over-expression and solubility test by Western blot analysis of the three new ATase mutants.*** Western blot of 12% SDS PAGE gel (see section 2.2.6.5) of whole cell extracts (wc) and cell-free lysates (sn) using a mixture of purified mAbs 5A7, 6B5 and 27D7 (see section 2.2.9.4.2).

Each of the newly formed plasmids was transformed into competent JM109 cells (2.1.4) for protein induction (see section 2.2.1.4), and a small-scale induction was performed (see section 2.2.5.3). The expression and solubility of each of the mutants is shown in Figure 7.4. Equal volumes (1μL of OD_{595} =100) of whole cell extract and cell-free lysate for each mutant were separated by 12% SDS PAGE (see section 2.2.6.1), transferred to nitrocellulose membrane, and detected (see section 2.2.6.5) with a mixture of purified mAbs 5A7, 6B5 and 27D7 (see section 2.2.9.4.2).

From a visual inspection of Figure 7.4 the AT:W452P mutant was ~50% soluble, and the AT:W456A and AT-N_{440}:N169G mutants were both fully soluble. The AT:W452P mutation introduced a turn into the hydrophobic side of the Q1 linker, which may have exposed hydrophobic regions of the protein normally hidden in wild type ATase, reducing solubility.

7.3.2 Comparative activity levels of ATase catalytic site and predicted reversal mutants

All the previously produced ATase catalytic site mutants and predicted activity reversal mutants (McLoughlin, 1999) were used in the initial rate adenylylation and deadenylylation assays (see section 7.2.2) to assess any changes in activity due to their mutations (Table 7.2).

Protein	Adenylylation		Deadenylylation	
	Rate (R^2 coeff)	proportion	Rate (R^2 coeff)	proportion
AT_{wt}	-2.7787 (0.9874)	1.00	1.4836 (0.9925)	1.00
pND707	na	0.00	na	0.00
Deadenylylation catalytic site mutants				
AT:D173A	-2.1607 (0.9536)	0.78	na	0.00
AT:D175A	-2.3996 (0.9868)	0.86	na	0.00
AT:D173AD175A	-1.7885 (0.9793)	0.64	na	0.00
Adenylylation catalytic site mutants				
AT:D701E	na	0.00	1.5228 (0.9913)	1.03
AT:D703E	na	0.00	0.9312 (0.9797)	0.63
AT:D701ED703E	na	0.00	0.5730 (0.9558)	0.39
AT:D701N	na	0.00	0.7279 (0.9792)	0.49
AT:D703N	na	0.00	1.2938 (0.9948)	0.87
AT:D701ND703N	na	0.00	5.3313 (0.9964)	3.59
Reversal mutants				
AT:N169G	-1.6765 (0.9248)	0.60	na	0.00
AT:W694G	-2.3544 (0.9755)	0.85	0.9898 (0.9658)	0.67
AT:G697N	-2.0177 (0.9788)	0.73	1.3263 (0.9858)	0.89

Table 7.2 ***Comparative adenylylation and deadenylylation rates for ATase and ATase mutants.*** The activity of the ATase proteins, was assessed by measuring the γ-glutamyl hydroxamate produced by GS/GS-AMP. Standard assay conditions (see section 7.2.2) were used except the ATase and ATase mutants were used at half normal concentration i.e 12.5nM. All assays were performed in duplicate and with AT_{wt} protein as a reference. The initial rate curves have been fitted with a linear regression using Microsoft Excel. The R^2 coefficient is shown in brackets. The initial rates for all the mutants have been expressed as a proportion of wild type activity. ATase mutants that had no activity are listed as na.

All the mutations that targeted the highly conserved putative metal binding sites within the β-polymerase motifs in ATase resulted in a complete loss of activity as shown by McLoughlin (1999). Hence, Asp173 and Asp175 in the N-terminal region or Asp701 and Asp703 in the C-terminal region became inactive in their respective

deadenylylation and adenylylation activities when these residues were mutated. In fact, mutating just one of each of the conserved Asp residues was enough to eliminate all activity for that particular site (Table 7.2). Subtle changes such as D701E or D701N resulted in the total loss of adenylylation activity.

The predicted adenylylation reversal mutants (AT:W694G and AT:G697N) had activity in both assays. The predicted deadenylylation reversal mutant (AT:N169G) had no activity in the deadenylylation assay. None of the predicted activity reversal mutants had activity higher than that of wild type ATase (Table 7.2). Therefore, none of the mutations appeared to have the effect of reversing the activity of the opposing domain.

The impact of mutations in one domain on the activity of the opposing domain was also examined. The single mutation of the Asp701 residue to Glu in the adenylylation active site of ATase had no impact on deadenylylation. Mutation of the Asp703 residue to Glu had some impact on the deadenylylation activity of ATase (activity dropped by ~30%), but the combination of the two mutations (D701ED703E) had a far more dramatic effect, reducing deadenylylation activity in the ATase protein by ~60% (Table 7.2).

The single mutation of residues Asp701 or Asp703 to Asn resulted in a reduction in deadenylylation activity, with the deadenylylation activity for D701N nearly half that of $ATase_{wt}$. Intriguingly however, when the two mutations were combined the resulting double mutant D701ND703N had deadenylylation activity more than 3 fold higher than $ATase_{wt}$ (Table 7.2).

As stated previously the potential activity reversal mutant AT:N169G did not have detectable activity in the initial rate assay (Table 7.2) and none of the reversal mutants showed increased activity in the opposing assay (Table 7.2). From the sequence alignment the residues Gly166 and Asn169 in the deadenylylation domain are swapped with Trp694 and Gly697 in the adenylylation domain (see Chapter 1). Addition of the opposing effector-protein to each assay (data not shown) i.e. PII to the deadenylylation assay and PII-UMP to the adenylylation assay (to ensure the lack of increase was not

due to the opposing mutated active site being exposed incorrectly) did not increase the opposing activity.

Mcloughlin (1999) suggested that the C-terminal region of the protein may have been inhibiting the action of the reversed deadenylylation active site of AT:N169G in some way. With this in mind this same mutation was introduced into the AT-N_{440} construct in this study. This protein was also tested for deadenylylation and adenylylation activity (data not shown), but it was inactive for both. This means there must be other residues besides Asn169, Trp694 and Gly697 contributing to the differences in the two active sites.

7.3.3 Glutamine binding

7.3.3.1 ATase C-terminal truncation constructs in adenylylation

Studies reported by Jaggi *et al.*, (1997) broadly established that gln binds in the C-terminal region of ATase (anywhere within Q1-R-Q2-C). Using all the C-terminal truncation constructs produced more recently in this laboratory, the gln dependence of ATase was assessed in the standard adenylylation assay (see section 7.2.2) (Table 7.3).

Condition	Protein				
	AT_{wt}	AT-C_{518}	AT-C_{396}	AT-C_{340}	AT:ΔR
PII, gln	1.00	1.00	1.00	1.00	1.00
PII, no gln	0.39	0.35	0.49	0.30	0.15

Table 7.3 ***Glutamine binding to entire ATase and the C-terminal truncation constructs in adenylylation.*** This table shows the gln dependence of the entire ATase protein and the C-terminal truncation constructs in adenylylation. The assay was run with standard conditions (see section 7.2.2) and standard conditions without gln. Activity was measured by the production of γ-glutamyl hydroxamate by GS. All assays were performed in duplicate and with AT_{wt} protein as a reference. The initial rate curves have been fitted with a linear regression using Microsoft Excel. The initial rates for all the constructs have been expressed as a proportion of their standard activity.

Each of the C-terminal truncation constructs and the construct missing the R domain showed a drop in adenylylation activity when gln was omitted from the assay (Table 7.3). The smallest C-terminal truncation construct used was AT-C_{340}. This construct

encompasses the second Q-linker (Q2) and C domain of ATase, therefore gln must be binding somewhere within this region of the ATase protein.

7.3.3.2 Glutamine independence of the predicted adenylylation reversal mutants

From previous studies McLoughlin demonstrated the AT:W694G mutant had no requirement for gln in adenylylation. All the predicted adenylylation reversal mutants were assessed for their ability to adenylylate GS in the absence of gln using the initial rate assay. Table 7.4 shows the relative activities of the predicted adenylylation reversal mutants with and without gln under standard conditions (see section 7.2.2) and also with 10μM α-kg added to the assay.

Assay effectors	Protein			
	AT_{wt}	AT:G697N	AT:W694G	AT:W694G G697N
PII, gln	1.00	1.00	1.00	1.00
PII, no gln	0.23	0.26	1.00	1.01
PII, gln, 10uM α-kg	1.40	1.38	1.39	1.45
PII, no gln, 10uM α-kg	0.36	0.39	1.36	1.46

Table 7.4 Glutamine dependence of the ATase adenylylation reversal mutants in adenylylation. The activity of the ATase proteins, was assessed by measuring the γ-glutamyl hydroxamate produced by GS. Standard assay conditions (see section 7.2.2) were used. All assays were performed in duplicate and with AT_{wt} protein as a reference. The initial rate curves were fitted with a linear regression using Microsoft Excel. The R^2 coefficients were generally >0.9. The initial rates for all the mutant ATase proteins have been expressed as a proportion of their standard activity.

All the ATase adenylylation reversal mutants had activity in the adenylylation assay and they all responded to addition of 10uM α-kg to a similar degree. Removal of gln from the assay had no impact on the two ATase adenylylation reversal mutants that contain the W694G mutation (Table 7.4).

7.3.3.3 Inhibition of adenylylation active site mutants in deadenylylation

Glutamine binds somewhere within the Q2-C region of ATase (Table 7.3) and the predicted active site reversal mutants AT:W694G and AT:W694GG697N are gln independent (Table 7.4). The possibility that gln might bind at or near the adenylylation active site within ATase was investigated further. In this series of deadenylylation assays a range of gln concentrations were examined for inhibitory effects on AT_{wt} and various adenylylation active site mutants. Some of these mutants have no adenylylation activity, hence inhibition of deadenylylation activity was assessed. The gln inhibition profiles for the AT_{wt} protein and adenylylation active site mutants are shown in Figure 7.5.

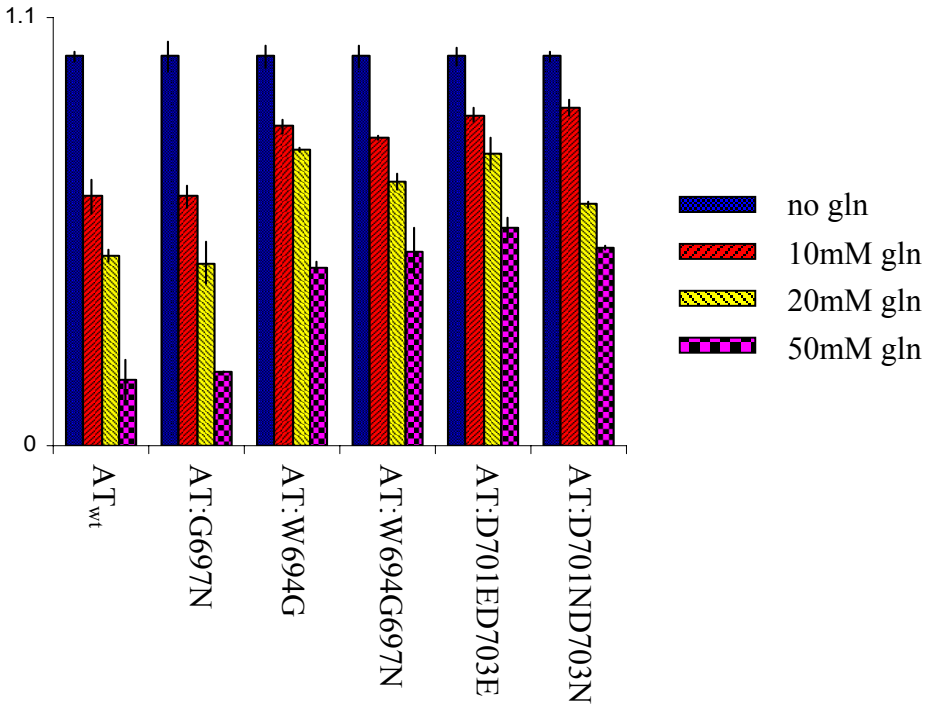

Figure 7.5 ***Glutamine effects in deadenylylation using ATase and various adenylylation active site mutants.*** This graph shows, the deadenylylation rate inhibition profiles for AT_{wt} and adenylylation active site mutants with various concentrations of gln added to the standard deadenylylation assay (see section 7.2.2). Activity was measured by the production of γ-glutamyl hydroxamate by GS-AMP. All assays were performed in duplicate and with AT_{wt} protein as a reference. The initial rate curves have been fitted with a linear regression using Microsoft Excel. The initial rates for all the proteins have been expressed as a proportion of their standard activity.

The AT:G697N mutant had the same profile as wild type ATase, responding to the different concentrations of gln to a similar degree (see discussion). The other

adenylylation catalytic site mutants AT:W694G, AT:W694GG697N, AT:D701ED703E and AT:D701ND703N all had similar gln inhibition profiles and appear to be less responsive to gln inhibition than $ATase_{wt}$ and AT:G696N (10-50mM gln) (Figure 7.5). It is possible these mutations partly impaired gln binding.

7.3.4 α-Ketoglutarate binding within the adenylylation catalytic complex

7.3.4.1 Direct binding of α-kg to PII and ATase

The PII and ATase proteins (10μM) were assessed for their ability to bind α-kg in the presence of ATP over a concentration range of 0-5μM α-kg ^{14}C (see section 7.2.3) the raw DPM have been converted to μM α-kg ^{14}C (see section 2.2.10.1.3) (Figure 7.6).

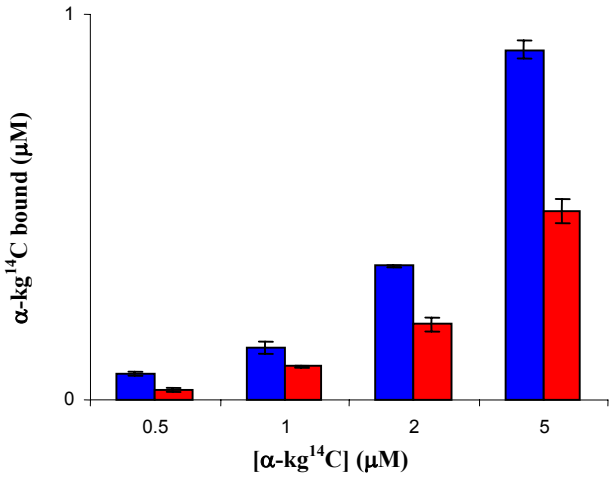

Figure 7.6 ***α-Ketoglutarate binding to PII and ATase.*** PII and ATase (10μM) were assessed for α-kg binding (see section 7.2.3) using radio-labelled ^{14}C α-kg in the presence of ATP (2mM). PII (blue) and ATase (red).

Both PII and ATase bound to α-kg, with PII binding more α-kg than ATase at these concentrations of α-kg (Figure 7.6).

7.3.4.2 ATase N-terminal truncation constructs in deadenylylation

The above results imply that ATase is capable of binding to α-kg. In this series of assays all the N-terminal truncation constructs were assessed for their independence of α-kg stimulation in the standard deadenylylation assay (see section 7.2.2) (Table 7.5).

Condition	Protein			
	AT_{wt}	AT-N_{440}	AT-N_{501}	AT-N_{548}
PII-UMP, α-kg	1.00	1.00	1.00	1.00
PII-UMP, no α-kg	0.04	0.97	1.03	1.04

Table 7.5 ***α-Ketoglutarate binding to ATase and the N-terminal truncation constructs in deadenylylation.*** This table shows the effect of α-kg on the activity of ATase and the N-terminal truncation constructs in deadenylylation. The assay was run with standard conditions (see section 7.2.2) and standard conditions without α-kg. Activity was measured by the production of γ-glutamyl hydroxamate by GS-AMP. All assays were performed in duplicate and with AT_{wt} protein as a reference. The initial rate curves have been fitted with a linear regression using Microsoft Excel. The R^2 coefficient is generally >0.9. The initial rates for all the proteins have been expressed as a proportion of their standard activity.

Wild type ATase showed a dramatic drop in deadenylylation activity when α-kg was omitted from the assay. The activity of each N-terminal truncation construct on the other hand was independent of α-kg. There was no drop in activity when α-kg was removed from the assay when the N-terminal truncation constructs were used (Table 7.4). This result suggests that if deadenylylation activity is due to α-kg binding to a low affinity site on ATase, then it must be binding outside the AT-N_{548} region of the protein.

The smallest C-terminal construct, which shows inhibition of adenylylation when 40mM α-kg is present in the assay is AT-C_{340} (Q2-C) (Table 7.6) and the largest N-terminal construct that is independent of α-kg for deadenylylation is AT-N_{548} (N-Q1-partR) (Table 7.5). These results are in accordance and suggest that α-kg may bind to ATase somewhere in the Q2-C region of the protein.

7.3.4.3 ATase C-terminal truncation constructs in adenylylation

α-Ketoglutarate has two effects on adenylylation activity. Addition of a small amount of α-kg (10μM) stimulates adenylylation activity and addition of a large amount of α-kg (>10mM) depresses adenylylation activity (Jiang *et al.*, 1998b). The high affinity α-kg binding site is situated on the PII protein (Kamberov *et al.*, 1995), and now that it has been shown in this work that ATase can probably also bind to α-kg (see section 7.3.4.1) the question arises as to the position of the second low affinity site within the adenylylation catalytic complex. Are there two α-kg binding sites on PII, one which has a high affinity for α-kg and stimulates adenylylation, and one which has a low affinity for α-kg that inhibits adenylylation? Or is the low affinity inhibitory α-kg binding site in the Q2-C region of ATase? In this series of adenylylation assays the interplay of α-kg binding between the PII and ATase proteins was investigated (Table 7.6).

Condition	Protein		
	AT_{wt}	$AT\text{-}C_{518}$	$AT\text{-}C_{341}$
PII, gln	1.00	1.00	1.00
PII, gln, α-kg (10μM)	1.16	1.02	0.96
no PII, no gln	0.06	0.64	0.71
no PII, no gln, α-kg (10μM)	0.05	0.65	0.70
no PII, no gln, α-kg (40mM)	0.04	0.32	0.17

Table 7.6 ***α-Ketoglutarate binding to ATase and several C-terminal truncation constructs in adenylylation.*** This table shows the effect of α-kg on the activity of ATase and several C-terminal truncation constructs in adenylylation. Standard assay conditions (see section 7.2.2) were used, except twice as much GS was used. Activity was measured by the production of γ-glutamyl hydroxamate by GS. All assays were performed in duplicate and with AT_{wt} protein as a reference. The initial rate curves were fitted with a linear regression using Microsoft Excel. The R^2 coefficient is generally >0.9. The initial rates for all the proteins have been expressed as a proportion of their standard activity.

Wild type ATase showed an increase in adenylylation activity when a small amount of α-kg (10μM) was added to the assay. Neither of the PII independent C-terminal truncation constructs showed any increase in activity with the addition of 10μM α-kg to the assay (Table 7.6). Therefore the high affinity site is probably on the PII protein, which is in accordance with the findings of Kamberov *et al.*, (1995).

Removal of the two effectors PII and gln renders ATase virtually inactive in adenylylation, whereas the two PII independent C-terminal truncation constructs retained nearly 65-70% of their activity when PII and gln, or gln alone were omitted from the assay (Table 7.6). Addition of α-kg (10μM) to the assay without PII or gln present did not change the adenylylation activity of ATase or the two truncated constructs. This result further supports the argument presented earlier that the high affinity stimulatory α-kg binding site must reside within PII, as per the findings of Kamberov *et al.*, (1995).

Interestingly, addition of α-kg to a concentration of 40mM (no PII or gln present) causes the adenylylation activities of the two C-terminal constructs AT-C_{518} and AT-C_{341} to drop by a further 32 and 54%, respectively (Table 7.5). Therefore the drop in adenylylation activity with the addition of 40mM α-kg is probably mediated by α-kg bound to ATase (PII is not present) and the low affinity site is probably situated on the ATase protein. To assure this effect was not due to a pH shift associated with addition of large amounts of α-kg, the stock solution was produced in 50mM HEPES pH 7.6 in keeping with the assay conditions.

The fact that α-kg still inhibited adenylylation activity of the C-terminal constructs when there was no gln present in the assay (Table 7.5), suggests the mechanism of inhibition is not via reduced gln binding.

7.3.4.4 PII and GlnK in adenylylation

The different effects of a range of α-kg concentrations on the adenylylation activity stimulated by both the effector-proteins, PII and GlnK was investigated in this section (Figure 7.7). This assay was designed to give a better estimate of the concentration of α-kg where stimulation of adenylylation stops and inhibition starts.

The adenylylation rate profiles for PII and GlnK with varying concentrations of α-kg were quite different (Figure 7.7). As shown previously (Chapter 5) the stimulatory effect of 10μM α-kg is only demonstrated when PII is the effector-protein. When either

effector-protein is present concentrations of α-kg greater than 50μM are inhibitory in the adenylylation assay (Figure 7.7).

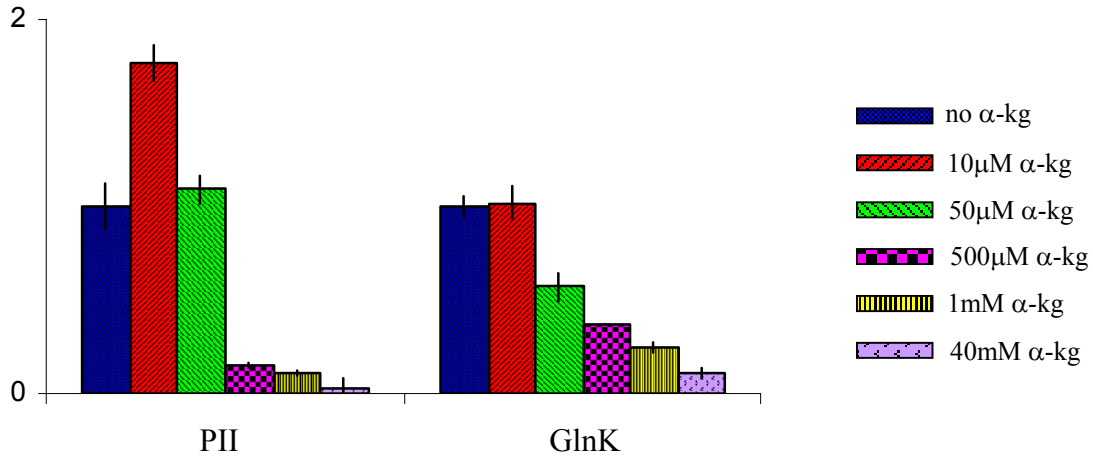

Figure 7.7 ***α-Ketoglutarate effects in adenylylation using PII and GlnK as the effector-protein.*** This curve shows, the adenylylation rate profiles for PII and GlnK with various concentrations of α-kg added to the standard adenylylation assay (see section 7.2.2). Activity was measured by production of γ-glutamyl hydroxamate by GS. All assays were performed in duplicate and with PII_{wt} protein as a reference. The initial rate curves have been fitted with a linear regression using Microsoft Excel. The R^2 coefficient is generally >0.9. The stimulated initial rates for all the effector-proteins have been expressed as a proportion of their standard stimulated activity.

The results of Jiang *et al.*, (1998b) suggested >10mM α-kg was inhibitory. The results from this assay in Figure 7.7 suggest a concentration of α-kg as low as 50μM may be inhibitory, which is just below the suggested physiological range in *E. coli* of 0.1-0.9mM (Senior, 1975). The majority of the inhibition effect of α-kg is demonstrated in the 50-500μM range, which is well within the physiological range.

7.3.5 Intramolecular signalling of small effector-molecule binding within ATase

The activity of ATase is moderated by the effector-protein, PII (in both its native and uridylylated form) and by the small effector-molecules, gln and α-kg. In the adenylylation assay PII and gln are required for ATase to efficiently adenylylate GS. In the deadenylylation assay PII-UMP and α-kg are required for ATase to deadenylylate GS-AMP. Previous studies by Stadtman and colleagues, (1979) showed that small effector-molecules that stimulate one activity have an inhibitory effect with respect to

the other activity eg. PII and gln are synergistic inhibitors of deadenylylation activity. Within the bacterial cell this would prevent futile cycling of the two mechanistically distinct, reversible functions. This series of assays examined the inhibitory effects of the two allosteric effectors on the opposing activity of the ATase Q1 linker mutants and a truncation construct with two Q1 linkers (Table 7.7).

The initial rates for all the proteins included in this study were expressed as a proportion of their respective activities, so that any inhibitory effect due to the small effector-molecule for the particular protein can be viewed separately from any global effect due to the introduced mutation or truncation.

Protein	Adenylylation		Deadenylylation	
	PII, gln	PII, gln, α-kg (40mM)	PII-UMP, α-kg	PII-UMP, α-kg, gln (20mM)
AT_{wt}	1.00	0.18	1.00	0.42
AT:$Q1^2$	1.00	0.06	1.00	0.00
AT:W452A	1.00	0.61	1.00	0.45
AT:W452P	1.00	0.41	1.00	0.39
AT:E454A	1.00	0.24	1.00	0.49
AT:W456A	1.00	0.28	1.00	0.21

Table 7.7 ***Inhibition of the activity of ATase, mutants and truncation constructs by small effector-molecules in the opposing assay.*** This table shows the effect of α-kg (40mM) and gln (20mM) on the opposing activity of ATase, Q1 linker mutants and a truncation construct with two Q1 linkers in adenylylation. The assays were run with standard conditions (see section 7.2.2) and standard conditions with the opposing small effector-molecule. Activity was measured by the production of γ-glutamyl hydroxamate by GS/GS-AMP. All assays were performed in duplicate and with AT_{wt} protein as a reference. The initial rate curves were fitted with a linear regression using Microsoft Excel. The initial rates for all the proteins have been expressed as a proportion of their standard activity.

Wild type ATase and all the mutants showed partial inhibition of adenylylation activity with the addition of 40mM α-kg to the standard assay and partial inhibition of deadenylylation when 20mM gln was added to the standard deadenylylation assay (Table 7.7). The fact that each mutant showed inhibition suggests the Q1 linker is not directly involved in signalling small effector-molecule binding within ATase, because an inhibitory signal is still being transmitted within all the mutants. However the degree of inhibition was not always equivalent to wild type ATase. The Q1 linker is probably involved in signalling effector-protein binding (Chapter 6). It is possible the differing

levels of response to the opposing effectors for the mutants derived from differences in the signalling of effector-protein binding. In the case of the construct with two Q1 linkers the inhibition by either small effector-molecule was virtually complete for both activities. This was probably due to the overall poorer activity (~20% of wild type) of this construct, which is in keeping with the Q1 linker signalling effector-protein binding.

7.4 DISCUSSION

In previous chapters the studies focussed on the protein elements of the adenylylation cascade. In this final results chapter the role of the small effector-molecules, gln and α-kg in the regulation of the two opposing activities of ATase is examined.

Firstly the ATase active site mutants (including various mutants that were predicted to be potentially critical for reversing activities of the two enzymatic domains) were examined more rigorously using initial rate reaction conditions. This method revealed certain features of ATase that will play a critical role in explaining its various mechanisms when 3D structures for the protein become available.

As in the case of human DNA polymerase-β (Davies *et al.*, 1994), mutation of the conserved Asp residues in the two polymerase motifs of ATase (Chapter 1, Figure 7.1) shows they are critical for the adenylylation and deadenylylation activities of ATase. The 3D structure for AT-N_{440} (Figure 7.1) shows that the polymerase motif fold is conserved (Chapter 1) in the deadenylylation domain of ATase, and is very similar to that of the eukaryotic DNA polymerases, even though this domain in ATase is not a polymerase, but a protein nucleotidyl removase (AMP group removed from GS-AMP by phosphorylysis of the phosphotyrosine link in deadenylylation). Replacement of the Asp residues at either position 173 or 175 with Ala completely eliminates deadenylylation activity. The fact that the ATase mutants bearing these changes were fully soluble and still able to carry out adenylylation activity indicates that the change to Ala can be tolerated, albeit with a reduction in initial rate activites ranging from 25-40% compared to wild type ATase.

The more subtle changes in the adenylylation motif, where Asp 701 or 703 were changed to Asn or Glu also resulted in the complete inhibition of mutant adenylylation activity, with varying effects on their deadenylylation activity. The change of Asp 701 to Glu had no affect at all on mutant deadenylylation activity, although it eliminated their adenylylation activity. The same single change at position 703 resulted in a mutant with no adenylylation activity, and impaired deadenylylation activity (~60% of wild type ATase activity). The double mutant where the Asp residues at both positions were changed to Glu resulted in a ~60% reduction in the deadenylylation initial rate. One possible explanation for this result may be that the negative charges on the side chain when extended by a methylene group destablise the deadenylylation site by affecting PII-UMP binding. This notion is supported by the almost 3-fold increase in the deadenylylation initial rate when the Asp residues at positions 701 and 703 are changed to Asn. It is difficult with the available results to suggest if the two active sites are physically close to each other in the entire ATase protein, but the present results further support the notion that there is continuous cross-talk between the two domains to minimise/prevent futile cycling, i.e. the domains are involved in intramolecular signal transduction.

The close sequence similarity between the polymerase motifs of the two domains (Chapter 1) suggested that perhaps their activities could be reversed by making key changes to several amino acid residues within the motif. Based on a simple alignment changes were made to achieve a reversal. The key residue Asn 169 thought to bind the inorganic phosphate substrate involved in the phosphorylysis reaction in deadenylylation was mutated to Gly. The entire protein carrying this mutation (AT:N169G) (Table 7.2), and the deadenylylation domain carrying this mutation (AT-N_{440}:N169G) did not demonstrate reversed adenylylation activity. In this context the mutation in the C-terminal domain W694G turned up an important phenotype, ie. a gln independent ATase protein in adenylylation (see below).

The binding of gln to ATase was investigated extensively using all the constructs that contained the C domain (AT-C_{518}, AT-C_{396}, AT-C_{340}, AT:ΔR) as well as various mutants. Firstly it was demonstrated that gln binds somewhere in the AT-C_{340} region of

ATase (Table 7.3). This is the domain that contains the Q2 linker and the C domain, which also includes the adenylylation active site. All of the C domain truncation constructs are PII independent (in terms of activity in the *in vitro* assay), but still gln dependent. Further investigation of several ATase mutants with mutations in the putative adenylylation catalytic site suggested that gln may be binding in this region of ATase (see later).

In wild type ATase if gln is removed from the adenylylation assay the activity drops dramatically, but with ATase containing the Trp694 to Gly mutation there is no drop in activity (Table 7.4). By changing the Trp to Gly the mutant behaves as if gln is permanently bound to ATase, i.e. ATase is in the gln activated form. The Trp at 694 may undergo a shift, which moves the side-chain away (effectively what happens when mutated to Gly) when gln is bound. Maybe when the side chain moves away it allows GS to dock in the adenylylation active site more efficiently.

The AT:W694G, AT:W694GG697N, AT:G697N (all reversal mutants swapping adenylylation residues to deadenylylation residues), AT:D701ED703E, AT:D701ND703N (conserved catalytic aspartates) ATase mutants and wild type ATase were run in a series of deadenylylation assays to investigate the inhibitory effect different concentrations of gln would have on their deadenylylation activity (Figure 7.5). In adenylylation and deadenylylation the mutant AT:G697N protein responded to small effector-molecules in the same manner as the AT_{wt} protein. Both proteins showed a drop in adenylylation activity if gln was removed (Table 7.4) and both had the same gln inhibition profile in deadenylylation (Figure 7.5). It's unlikely the Gly697 residue of ATase is involved in the interaction with gln.

The two ATase mutants that contained the W694G mutation had adenylylation activity independent of gln, these mutants showed no drop in activity when gln was removed from the assay (Table 7.4). Changing the Trp to Gly gave the protein a gln bound conformation in terms of adenylylation activity, but whether gln was binding to the protein or not, could not be determined from that assay. The two double Asp mutants had no activity in adenylylation (Table 7.2). These four mutants all had similar gln

inhibition profiles in deadenylylation (Figure 7.5), which were different from the AT_{wt} and AT:G697N proteins. These four mutants were not as responsive to gln. The deadenylylation activity of these mutants was still inhibited with increasing concentrations of gln, but not to the same degree. These results suggest the three residues Trp694, Asp701 and Asp703 in the adenylylation active site of ATase may potentially play a role in gln binding.

Evidence that gln was still binding to the AT:W694G mutant was demonstrated when it was shown that an increasing concentration of gln inhibited deadenylylation in a dose dependent manner. Having a gln bound conformation in terms of adenylylation did not reduce normal deadenylylation activity. Therefore, the inhibitory effect due to inclusion of gln in the deadenylylation assay is not due to having a gln bound conformation in the adenylylation active site. This is further support for the concept (from SPR data in Chapter 5) that gln binding to ATase may cause a reduction in deadenylylation activity by reducing the amount of PII-UMP binding to ATase.

The next area of investigation was the binding of α-kg to the adenylylation catalytic complex. An interesting phenomenon is observed in the adenylylation assay; if α-kg is added to the assay at 10μM there is an increase in activity (Jiang et al., 1998b). This effect is only observed when the effector-protein is PII (Chapter 5) (Atkinson and Ninfa, 1999), but if the α-kg concentration is increased, adenylylation activity is dramatically reduced with either PII or GlnK as the effector-protein. The inhibitory effect starts from 50μM α-kg onwards (Figure 7.7), which is just below the physiological range of 0.1-0.9mM for α-kg in *E. coli* (Senior, 1975). At a concentration of 1mM, α-kg reduced the adenylylation activity of ATase (PII as effector-protein) to ~10% of normal activity. Concentrations of α-kg above 1mM in the assay did not increase the inhibition much further. This means from this work that the main inhibitory concentration range for α-kg is 50μM to 1mM, which ties in nicely with the estimated physiological range of 0.1-0.9mM (Senior, 1975).

The results from the α-kg studies in this chapter suggest the high affinity binding site within the adenylylation catalytic complex is positioned on the PII protein, which is in

accordance with the results from previous studies (Kamberov *et al.*, 1995; Jiang *et al.*, 1998b). It was demonstrated with direct binding studies that ATase could also bind to α-kg. The PII protein bound more α-kg than ATase at these low concentrations (Figure 7.6); therefore when 10μM α-kg is added to the assay more α-kg should be bound to PII than ATase. The second piece of supporting evidence for this concept came from the activity of the two C-terminal truncation constructs AT-C_{518} and AT-C_{341} in adenylylation. Both the constructs have activity independent of PII and both the constructs did not have an increase in activity when 10μM α-kg was added to the assay.

Contrary to previous studies by Jiang *et al.*, (1998b) the results from ATase truncation constructs in this current study suggest that the low affinity inhibitory α-kg binding site is situated on the ATase protein rather than the PII protein. As mentioned previously, it was demonstrated that α-kg was capable of binding to ATase. Adenylylation inhibition studies using C-terminal truncation constructs demonstrated the smallest C-terminal truncation construct inhibited by α-kg was AT-C_{340} (Table 7.6), which includes the Q2-C domain. Further adenylylation assays with this construct demonstrated that the activity of this protein was still inhibited by α-kg even when there was no PII or gln present (Table 7.6). The concentration, used in this assay for α-kg (40mM) was way in excess of the physiological range, and was chosen for maximal effect.

A far better concentration to use would have been 1mM, which reduced activity by 90% as mentioned previously. Not withstanding this, the mechanism should still be the same at either concentration, and this would mean the mechanism of inhibition is not by reduced gln binding, but some other factor. These results support the concept that the low affinity binding site is situated on the ATase protein. Surface plasmon resonance data presented in Chapter 5 suggested α-kg had no impact on the binding of PII to ATase; therefore it is possible that α-kg binding to ATase at the higher concentration may disrupt the interaction between GS and ATase.

The high concentration of α-kg that leads to inhibition of adenylylation activity alternately stimulates deadenylylation activity in the ATase protein. The two ATase double Asp adenylylation catalytic site mutants, which had no activity in adenylylation,

behaved quite differently in the deadenylylation assay. The AT:D701ED703E mutant had significantly lower than wild type ATase activity, and the AT:D701ND703N mutant had significantly higher then wild type ATase activity (Table 7.2). Two different subtle changes in the adenylylation active site gave rise to two mutants with dramatically different behaviour in deadenylylation. How then does a minor change in the adenylylation domain contribute to the deadenylylation activity in the domain at the opposite end of the ATase protein?

The close association of the two domains provides a possible mechanism. In SPR the two domains bind to each other and entire ATase (data not shown). The conformational change in the C domain associated with α-kg binding may disrupt an interaction between the N and C domains, which normally keeps them together inhibiting the opposing activity.

The improvement in PII-UMP binding to the ATase protein with higher concentrations of α-kg is another possible mechanism. In SPR when the concentration of α-kg was increased from 2μM to 1mM (no gln present), the K_D went from 15.7μM to 220nM. Deadenylylation activity assays using ATase with and without the two allosteric effectors favour the second hypothesised mechanism, because α-kg on its own does not stimulate any deadenylylation activity, whereas PII-UMP does. This mechanism would also tie in nicely with the "open" and "closed" ATase conformation model with effector-protein binding proposed in Chapter 6.

The only region of the ATase protein that could not be assessed for an inhibitory α-kg effect in adenylylation was the adenylylation active site (mutants at this site have no adenylylation activity). If the two different activities demonstrated by the double Asp mutants arises from the second signalling mechanism proposed above, then the differences in the active site are probably affecting α-kg binding. If α-kg binding to ATase disrupts the interaction between ATase and GS, then the adenylylation active site would be the best place for that to occur. In evolutionary terms, if the bifunctional enzyme arose from the fusion of two monofunctional enzymes, and the ancestral form

had to sense both the key small effector-molecules, then they would both bind to the same domain.

The Q1 linker probably plays a significant role in signalling effector-protein binding within ATase (Chapter 6), so this region of the protein was also assessed for its potential role in signalling small effector-molecule binding. All the constructs and mutants tested had activity and demonstrated allosteric inhibition by the opposing small effector-molecule (Table 7.7). Even a truncation construct which had two Q1 linkers transmitted the various signals. These results suggest the Q1 linker does not play a major role in signalling small effector-molecule binding. The results from this study suggest that both the small effector-molecules are potentially binding in the adenylylation active site, affecting PII-UMP binding to ATase in the N-terminal region of the R domain (Chapter 6), and consequently affecting its enzymatic activity. These results suggest the Q2 linker between these two regions of ATase warrants closer attention.

In closing, the results from this chapter suggest that the stimulatory high affinity α-kg binding site in the adenylylation catalytic complex is found within the PII protein and the inhibitory low affinity α-kg binding site is probably found within the ATase protein. This same low affinity site stimulates the deadenylylation activity of ATase. It is possible that both of these small effector-molecules bind in or near the adenylylation active site of ATase and the binding event is not signalled through the first Q-linker.

CHAPTER 8 General Discussion

The N signal transduction pathway in *E. coli* bacteria has been studied extensively, but the details and subtleties at the molecular level have yet to be fully elucidated. The results described in this thesis are all related to the goal of understanding the adenylylation cascade that is used to regulate the activity of GS. This simple system has been studied using various approaches:

1. Using monoclonal antibodies generated against PII and ATase
2. Utilising point mutations in the T-loop and ATP-binding cleft of PII
3. Using an extensive series of ATase truncation constructs, and point mutations within the active site motifs and Q1 linker
4. Enzymatic assay for adenylylation and deadenylylation activity
5. Direct binding using SPR

The overall aim of this study was to investigate the molecular mechanisms of the adenylylation cascade by studying the behaviour of the proteins involved, in various binding and activity assays. Of particular interest were the subtleties of the interactions between the signalling effector-proteins PII and GlnK and the receptor-proteins UTase and ATase (in particular ATase), including the influences of small effector-molecules. In this final chapter all the results from this study have been assessed and a new model is proposed.

In this work the existence of a central regulatory domain within the ATase protein was confirmed (Chapter 6). The new topology of the protein is as follows: N (deadenylylation active site)-Q1-central (regulatory)-Q2-C (adenylylation active site). A panel of mAbs produced against ATase (Chapter 3) was used to determine the region of ATase where the four effector-proteins, PII, PII-UMP, GlnK and GlnK-UMP probably bind. The two R domain mAbs 39G11 (binding in the region of residues 466-501) and 5A7 (binding in the region of residues 502-548) completely blocked the binding of the four effector-proteins to ATase (Chapter 6). This means that all four effector-proteins could potentially bind at the same site within ATase. Competitive assays using two effector-proteins with widely differing K_Ds for ATase (SPR data) and different activity

levels in the assays suggested they do not all bind at the same site in ATase, but near each other in the N-terminal region of the R domain (Chapter 5).

The "open" effector-protein-complexed and "closed" uncomplexed conformation theory for ATase activity proposed by Jaggi (1998) was supported by this work. Three C-terminal truncations (AT-C_{518}, AT-C_{396}, AT-C_{340}) and a construct that had no R domain (AT:ΔR) had adenylylation activity that was independent of the PII effector-protein, and the N domain of ATase AT-N_{440} had deadenylylation activity that was independent of PII-UMP (Chapter 6).

The above results suggested that the central regulatory domain positioned the two terminal domains such that they were inhibiting the activity of the opposing domain in uncomplexed "closed" ATase. When either PII or PII-UMP binds to ATase in the N-terminal region of the R domain it causes a conformational change in ATase that positions the two active domains apart from each other in the active "open" conformation. The binding of PII-UMP probably also causes the deadenylylation active site to be presented in a conformation conducive to the binding of GS-AMP as well, because the AT-N_{440} construct is approximately 1000 times less active than the intact ATase protein (Chapter 6).

Various ATase truncation constructs that start in the N-terminal region of the R domain have problems with solubility (AT-C_{481} and AT-C_{439}), yet truncation constructs finishing in this same region have no solubility problems (AT-N_{501} and AT-N_{548}). A helical wheel secondary structure prediction for the Q1 linker (Schiffer and Edmundson, 1967) shows it to be amphipathic in nature (Chapter 1). These results suggest that the hydrophobic side of the amphipathic Q1 linker may lie along a hydrophobic patch in the N-terminal region of the R domain.

It is possible that the binding of the PII or PII-UMP effector-proteins in the N-terminal region of the R domain could disrupt the hydrophobic interaction between the two domains causing the N domain to move away from the R domain opening up the ATase protein, leaving both the active sites accessible to GS or GS-AMP. The lower

adenylylation and deadenylylation activities of an ATase truncation construct with two Q1 linkers (AT:$Q1^2$) (Chapter 7) is consistent with this hypothesis.

The opposing activities of ATase are also regulated by the small effector-molecules, gln and α-kg. In this work it was demonstrated that both these small effector-molecules may bind in the C domain (truncation construct stimulation and inhibition in assays) (Chapters 6 and 7) of ATase, possibly at or near the adenylylation active site. The residues Trp694, Asp701 and Asp703 within the adenylylation active site may play a role in gln binding and the two Asp residues are potentially involved in α-kg binding (Chapter 7).

Mutation of the Trp694 residue in the adenylylation active site to Gly had a profound effect on the behaviour of the ATase mutant. This protein was no longer dependent on gln for full adenylylation activity. It had adenylylation activity as though gln was present. Removing the bulky Trp side-chain from the active site by mutation to Gly signalled that gln was bound to ATase for adenylylation activity (whether it had or not) (Chapter 7).

The above result suggests that the binding of gln at or near the adenylylation active site causes the bulky Trp side chain to move away allowing the adenylylation reaction to proceed more efficiently. Surface plasmon resonance data (Chapter 5) suggested gln binding did not impact on the interaction between PII and ATase. The function of gln may be to serve as a molecular switch inducing a conformational change that permits the entry of the GS loop into the active site allowing GS to dock more efficiently and be adenylylated.

Having an adenylylation active site with a gln bound conformation did not impact on the capacity of AT:W694G mutant to deadenylylate GS-AMP, this mutant still needed to be bound to the gln molecule for the deadenylylation activity to be inhibited (Chapter 7). This supported SPR data which suggested that gln binding to ATase reduced the binding of PII-UMP (Chapter 5), which would in turn reduce the deadenylylation activity.

Adenylylation assays using the two PII independent C-terminal truncation constructs AT-C_{518} (Q1-R-Q2-C domains) and AT-C_{341} (Q2-C domain) demonstrated that the α-kg molecule could still inhibit adenylylation without PII or gln present (Chapter 7). This suggests that the inhibition mechanism may not be via a reduction in gln binding. The binding of PII to ATase was not affected by α-kg in SPR (Chapter 5), therefore it is possible the binding of the α-kg molecule at or near the adenylylation active site inhibits the interaction between ATase and GS. Analysis of the interactions between the ATase (ATase adenylylation catalytic site mutants and ATase C-terminal truncation constructs also) and GS proteins using SPR with various allosteric effector combinations would increase the understanding of the adenylylation inhibition mechanism.

Various mutations introduced into the Q1 linker of ATase designed to disrupt the hydrophobic region of the Q1 linker, and an ATase truncation construct with two Q1 linkers (AT:$Q1^2$), all showed deadenylylation activity that was inhibited by gln and adenylylation activity that was inhibited by α-kg (Chapter 7). It is unclear if this Q-linker is involved with intramolecular signalling of small effector-molecule binding. However, initial evidence suggests it is possibly only involved in signalling effector-protein binding. This result supports the previous data, where gln binding inhibits deadenylylation activity in the ATase protein by preventing PII–UMP from binding in the R domain, and α-kg inhibits adenylylation activity by inhibiting the binding of GS. All of these interactions are in the region of the ATase protein past the Q1 linker.

Although the Q1 linker is possibly not involved in intramolecular signalling of small effector-molecule binding, it is quite possible that the Q2 linker signals small effector-molecule binding within ATase. Both the small effector-molecules binding in the C domain are potentially affecting PII-UMP binding in the N-terminal region of the R domain. The Q2 linker needs to be investigated further. Crystallisation of an ATase truncation construct of Q1-R-Q2-C (R-Q2-C would potentially have solubility problems) could shed light on this issue. Activity studies using point mutations within the Q2 linker of ATase could also help provide more information regarding the role of the Q2 linker in intramolecular signalling of small effector-molecule binding.

How then does α-kg potentially binding in the C-terminal adenylylation active site contribute to the N-terminal deadenylylation activity at the other end of the ATase protein? A possible answer comes from the close association of the two activity domains. In SPR the two domains bind to each other and the entire ATase protein (data not shown). The conformational change in the C domain associated with α-kg binding could disrupt an interaction between the N and C domains, which normally keeps them together inhibiting the opposing activity.

Another possible mechanism is the improvement in PII-UMP binding to ATase with higher concentrations of α-kg (in SPR when the α-kg concentration was increased from 2μM to 1mM when no gln was present, the K_D went from 15.7μM to 220nM) (Chapter 5). Deadenylylation activity assays using entire ATase with and without the two allosteric-effectors favour the second hypothesised mechanism, because α-kg alone does not stimulate deadenylylation activity (Chapter 6).

Jaggi (1998) suggested that PII might also interact with GS in the adenylylation reaction. The results generated in Chapter 5 of this work are consistent with this hypothesis. Under adenylylation conditions PII binds less tightly to ATase than GlnK, yet PII is far more effective at stimulating the adenylylation activity of ATase. Increasing the concentration of GlnK in the adenylylation assay also improves the adenylylation activity of ATase. Addition of α-kg (10μM) to the adenylylation assay increases the adenylylation activity of ATase when PII is the effector-protein, but not when GlnK is the effector-protein (the adenylylation rate is unchanged). Under these conditions the binding of PII to ATase does not change and the binding of GlnK to ATase is weakened. The disparity between the impact of the two effector-proteins on ATase in adenylylation and their direct binding to ATase suggests another interaction is the key to the differences in the behaviour of PII and GlnK in adenylylation. The dissociation constants determined using SPR (Chapter 5) are a measure of direct binding between two proteins, and may not necessarily reflect the actions of those proteins when used in assays involving other proteins as well.

The above results strongly suggest there is an interaction between the effector-proteins and GS. Swapped T-loop PII mutants showed there is only one residue at position 54 in the T-loop that distinguishes the differences between PII and GlnK in their response to α-kg (10μM) in adenylylation (Chapter 5). This suggests the interaction with GS only involves the T-loop of the two effector-proteins. A similar SPR study to the one carried out in this work using the same effector-molecule conditions with the GS protein ligated to a chip would help determine the nature of these interactions. Inclusion of the uridylylated forms of the effector-proteins in this experiment would also establish if uridylylation of the T-loop inhibits the interaction with GS.

Under deadenylylation conditions PII-UMP binds to the ligated ATase protein 40 times more tightly than GlnK-UMP (Chapter 5). When both of these effector-proteins are used in the deadenylylation assay at 25nM only PII-UMP stimulates deadenylylation activity in ATase, but if the concentration of GlnK-UMP is increased 40-fold, ATase is capable of deadenylylation activity. In this instance binding of the uridylylated effector-protein to ATase appears to be the main determinant of the difference in the deadenylylation activity they stimulate. Deadenylylation assays using uridylylated forms of the swapped T-loop PII mutants demonstrated that the region of the effector-proteins, PII-UMP and GlnK-UMP that distinguishes them is not the T-loop, but some other part of the protein (Chapter 5).

The results generated in this work from uridylylation assays using PII mutants are in accordance with previous studies using PII mutants (Jiang *et al.*, 1997a). The binding of ATP and α-kg to PII, and the T-loop conformation are very important to the interaction of PII and UTase. The new contribution from this work is the determination of the two T-loop residues at positions 43 and 54, which are the major contributors to the difference between the PII and GlnK proteins as a substrate for the UTase enzyme (Chapter 5).

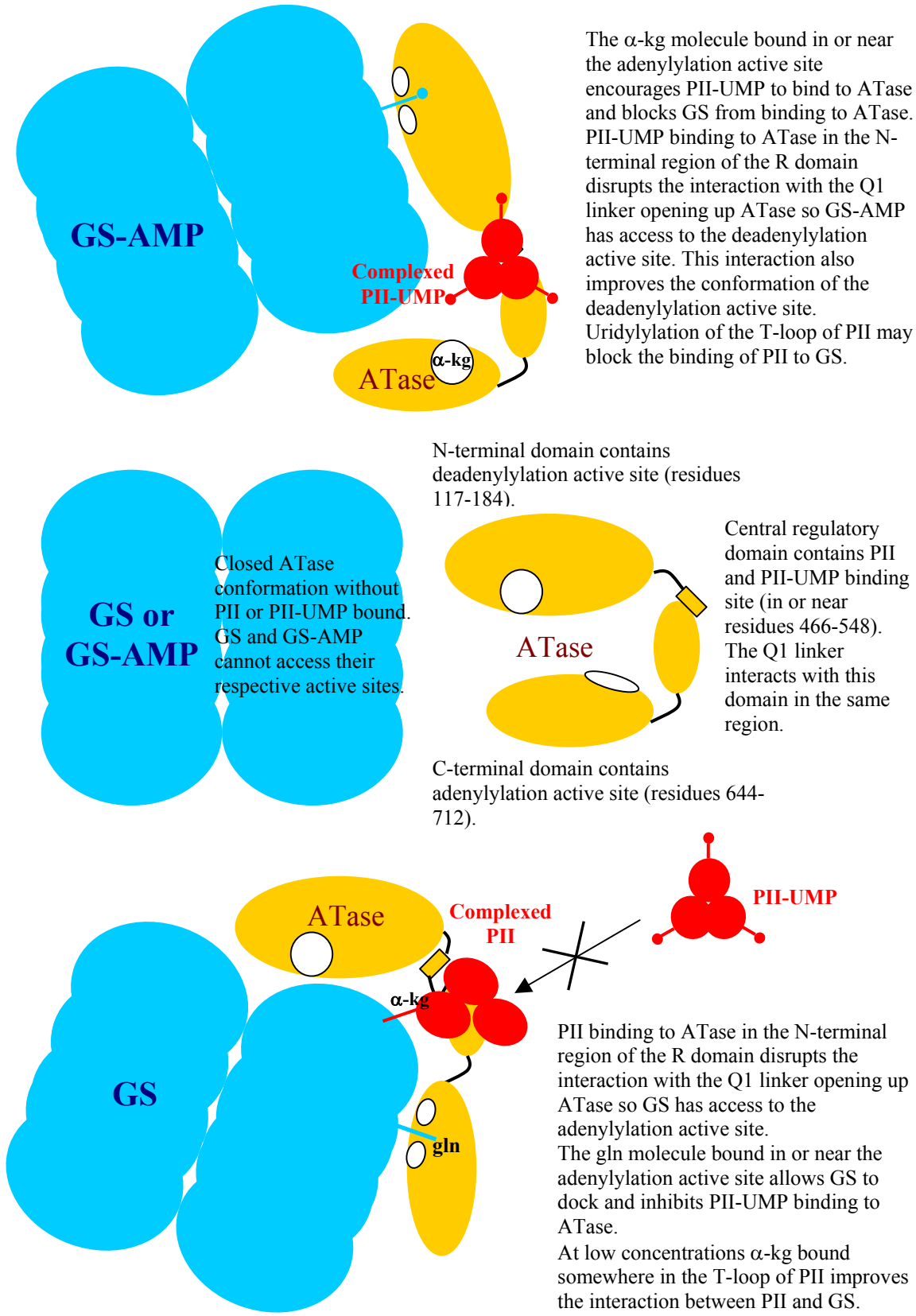

Figure 8.1 Diagrammatic representation of the proposed new adenylylation cascade model.

In summary this work has given rise to a greater understanding of the molecular mechanisms of the adenylylation cascade. The model that is postulated based on the results in this thesis is as follows (see Figure 8.1):

1. In uncomplexed ATase the two activity domains are held in place by the central regulatory domain. There is a close association between the two activity domains such that they sterically inhibit the activity of the opposing domain.

2. The two forms of the effector-protein, PII bind to ATase in the N-terminal region of the central regulatory domain (possibly at different sites, which are close to each other) causing a disruption of the Q1 linker interaction in the same region of the protein. The Q1 linker disruption caused by PII-UMP binding causes the deadenylylation active site to be exposed and held in a conformation that encourages GS-AMP binding to ATase. The disruption to the Q1 linker interaction caused by PII binding exposes the adenylylation active site.

3. Glutamine binding in the adenylylation active site enables GS to bind to ATase more effectively, encouraging adenylylation, and inhibits the binding of PII-UMP, inhibiting deadenylylation activity.

4. The binding of α-kg to ATase in or near the adenylylation active site encourages PII-UMP to bind to ATase, favouring deadenylylation, and inhibits the binding of GS, stopping adenylylation activity.

5. The PII protein binds to GS as well as ATase. A small amount of α-kg (<50μM) improves the interaction between the PII and GS proteins, further favouring adenylylation, and uridylylation of the T-loop of PII might block the interaction with the GS protein, further favouring deadenylylation.

REFERENCES

Adler, S. P., Purich, D., and Stadtman, E. R. (1975). Cascade control of *Escherichia coli* glutamine synthetase. Properties of the PII regulatory protein and the uridylyltransferase-uridylylremoving enzyme. *J. Biol. Chem.* **250**: 6264-6272.

Aravind, L., and Koonin, E. V. (1999). DNA polymerase β-like nucleotidyltransferase superfamily: identification of three new families, classification and evolutionary history. *Nucleic Acids Res.* **27**: 1609-1618.

Arcondeguy, T., Huez, I., Fourment, J., and Kahn, D. (1996). Symbiotic nitrogen fixation does not require adenylylation of glutamine synthetase I in *Rhizobium meliloti. FEMS Microbiol. Lett.* **145**: 33-40.

Arcondeguy, T., Lawson, D., and Merrick, M. (2000). Two residues in the T-loop of GlnK determine NifL-dependent nitrogen control in *nif* gene expression. *J. Biol. Chem.* **275**: 38452-38456.

Arcondeguy, T., Jack, R, and Merrick, M. (2001). P_{II} signal transduction proteins, pivotal players in microbial nitrogen control. *Microbiol. Mol. Biol. Rev.* **65**: 80-105.

Atkinson, M. R., and Ninfa, A. J. (1998). Role of the GlnK signal transduction protein in the regulation of nitrogen assimilation in *Escherichia coli*. *Mol. Microbiol.* **29**: 431-447.

Atkinson, M. R., and Ninfa, A. J. (1999). Characterisation of the GlnK protein of *Escherichia coli. Mol. Microbiol.* **32**: 301-313.

Austin, S., and Dixon, R. (1992). The prokaryotic enhancer binding protein NTRC has an ATPase activity which is phosphorylation and DNA dependent. *EMBO J.* **11**: 2219-2228.

Ausubel, F. M., Brent, R., Kingston, R. E., Moore, D. D., Seidman, J. G., Smith, J. A., and Struhl, K. (1994). In Current Protocols in Molecular Biology (New York: Greene Publishing and John Wiley & Sons).

Bard, J., Zhelkovsky, A. M., Helmling, S., Earnest, T. N., Moore, C. L., and Bohm, A. (2000). Structure of yeast poly(A) polymerase alone and in complex with 3'-dATP. *Science* **289**: 1346-1349.

Benelli, E. M., Buck, M., Polikarpov, I., de Souza, E. M., Cruz, L. M., and Pedrosa, F. O. (2002). *Herbaspirillum seropedicae* signal transduction protein PII is structurally similar to the enteric GlnK. *Eur. J. Biochem.* **269**: 3296-3303.

Blattner, F. R., Plunkett, G. III, Bloch, C. A., Perna, N. T., Burland, V., Riley, M., Collado-Vides, J., Glasner, J. D., Rode, C. K., Mayhew, G. F., Gregor, J., Davis, N. W., Kirkpatrick, H. A., Goeden, M. A., Rose, D. J., Mau, B. and Shao, Y. (1997). The complete genome sequence of *Escherichia coli* K-12. *Science* **277**: 1453-1474.

Blauwkamp, T. A., and Ninfa, A. J. (2003). Antagonism of PII signalling by the AmtB protein of *Escherichia coli. Mol. Microbiol.* **48**: 1017-1028.

Bradford, M. M. (1976). A rapid and sensitive method for the quantification of microgram quantities of protein utilising the principle of protein dye binding. *Anal. Biochem.* **72**: 248-254.

Bueno, R., Pahel, G., and Magasanik, B. (1985). Role of *glnB* and *glnD* products in regulation of the *glnALG* operon of *Escherichia coli. J. Bacteriol.* **164**: 816-822.

Canyon, S. J. (1998). Investigation of the stability of PII and GlnK by mutagenesis. (Townsville, Australia: Honours thesis, James Cook University).

Carr, P. D., Cheah, E., Suffolk, P. M., Vasudevan, S. G., Dixon, N. E., and Ollis, D. L. (1996). X-Ray structure of the signal transducing protein PII from *Escherichia coli* at 1.9 Å. *Acta Cryst.* **D52**: 93-104.

Cheah, E., Carr, P. D., Suffolk, P. M., Vasudevan, S. G., Dixon, N. F., and Ollis, D. L. (1994). Structure of the *Escherichia coli* signal transducing protein PII. *Structure* **2**: 981-990.

Chien, A., Edgar, D., and Trela, J. (1976). Deoxyribonucleic acid polymerase from the extreme thermophile *Thermus aquaticus*. *J. Bacteriol.* **127**: 1550.

Colonna-Romano, S., Riccio, A., Guida, M., Defez, R., Lamberti, A., Iaccarino, M., Arnold, W., Priefer, U., and Puehler, A. (1987). Tight linkage of *glnA* and a putative regulatory gene in *Rhizobium leguminosarum*. *Nucleic Acids Res.* **15**: 1951-1964.

Contreras, A., and Drummond, M. (1988). The effect on the function of the transcriptional activator NtrC from *Klebsiella pneumoniae* of mutations in the DNA recognition helix. *Nucleic Acids Res.* **16**: 4025-4039.

Davies, J., Almassy, R. J., Hostomska, Z., Ferre, R. A., and Hostomsky, Z. (1994). 2.3 Å crystal structure of the catalytic domain of DNA polymerase beta. *Cell* **76**: 1123-1133.

Coutts, G., Thomas, G., Blakey, D., and Merrick, M. (2002). Membrane sequestration of the signal transduction protein GlnK by the ammonium transporter AmtB. *The EMBO J.* **21**: 536-545.

de Sal, G., Mantioletti, G., and Schneider, C. (1988). One-tube plasmid mini preparation suitable for sequencing. *Nucleic Acids Res.* **16**: 9878.

de Zamarockzy, M., Delorme, F., and Elmerich, C. (1990). Characterisation of three different nitrogen-regulated promoter regions for the expression of *glnB* and *glnA* in *Azospirillum brasilense. Mol. Gen. Genet.* **224**: 421-430.

Edelman, G. M., and Poulik, M. D. (1961). Studies on structural units of the γ-globulins. *J. Exp. Med.* **113**: 861.

Eisenberg, D., Gill, H. S., Pfuegel, G. M. U., and Rotstein, S. H. (2000). Structure-function relationships of glutamine synthetases. *Biochim. Biophys. Acta* **1477**: 122-145.

Elvin, C. M., Dixon, N. E., and Rosenburg, H. (1986). Molecular cloning of the phosphate (inorganic) transport (*pit*$^+$) gene of *Escherichia coli* K12. Identification of the *pit*$^+$gene product and physical mapping of the *pit-gor* region of the chromosome. *Mol. Gen. Genet.* **204**: 477-484.

Elvin, C. M., Thompson, P. R., Argall, M. E., Hendry, P., Stamford, N. P. J., Lilley, P. E., and Dixon, N. E. (1990). Modified bacteriophage λ promoter vectors for over-production of proteins in *Escherichia coli*. *Gene* **87**: 123-126.

Engelman, D. M., Steitz, T. A., and Goldman, A. (1986). Identifying non-polar transbilayer helices in amino acid sequences of membrane proteins. *Annu. Rev. Biophys. Biophys. Chem.***15**: 321-353.

Engelman, E., and Francis, S. (1978). Cascade control of *E. coli* glutamine synthetase. II. Metabolite regulation of the enzymes in the cascade. *Arch. Biochem. Biophys.* **191**: 602-612.

Feng, J., Atkinson, M., McCleary, W., Stock, J., Wanner, B., and Ninfa, A. (1992). Role of phosphorylated metabolic intermediates in the regulation of glutamine synthetase synthesis in *Escherichia coli. J. Bacteriol.* **174**: 6061-6070.

Fiedler, U., and Wiess V. (1995). A common switch in activation response regulators NtrC and PhoB: phosphorylation induces dimerisation of the receiver module. *EMBO J.* **14**: 3696-3705.

Fleischmann, R. D. (1995). Whole-genome random sequencing and assembly of *Haemophilus influenzae* RD. *Science* **269**: 496-512.

Forchhammer, K., Hedler, A., Strobel, H., and Weiss, V. (1999). Heterotrimerisation of P_{II}-like signalling proteins: implications for P_{II}-mediated signal transduction systems. *Mol. Microbiol.* **33**: 338-349.

Forchhammer, K. (2003). PII signal transduction in Cyanobacteria. *Symbiosis* **35**: 101-115.

Galfre, C., Howe, S. C., Milstein, C., Butcher, and Howard, V. C. (1977). Antibodies to major histocompatability antigens produced by hybrid cell lines. *Nature* **266**: 550-552.

Garcia, E., and Rhee, S. G. (1983). Cascade control of *Escherichia coli* glutamine synthetase. Purification and properties of PII uridylyltransferase and uridylylremoving enzyme. *J. Biol. Chem.* **258**: 2246-2253.

Gibson, T. J. (1984). Studies of the Epstein-Barr virus genome. (Cambridge, UK: PhD thesis, Cambridge University).

Gill, H. S., Pfuegel, G. M. U., and Eisenberg, D. (2002). Multicopy crystallographic refinement of a relaxed glutamine synthetase from *Mycobacterium tuberculosis* highlights flexible loops in the enzymatic mechanism and its regulation. *Biochemistry* **41**: 9863-9872.

Goding, J. W. (1983). Monoclonal Antibodies: Principles and Practice. Academic Press, London.

Grisshammer, R., and Nagai, K. (1995). Purification of over-produced proteins from *E. coli* cells. In DNA cloning 2, D. M. Glover and B. D. Hames, eds. (Oxford: Oxford University Press).

Harlow, E., and Lane, D. (1988). Antibodies, a Laboratory Manual. Cold Spring Harbor Press, New York.

Harth, G., Clemens, D. L., and Horwitz, M. A. (1994). Glutamine synthetase of *Mycobacterium tuberculosis*: extracellular release and characterization of its enzymatic activity. *Proc. Nat. Acad. Sci. U.S.A.* **91**: 9342-9346.

Hastings, C. A., Lee, S-Y., Cho, H. S., Yan, D., Kustu, S., and Wemmer, D. E. (2003). High-resolution solution structure of the beryllofluoride-activated NtrC receiver domain. *Biochemistry* **42**: 9081-9090.

He, L., Soupene, E., and Kustu, S. (1997). NtrC is required for control of *Klebsiella pneumoniae* NifL activity. *J. Bacteriol.* **179**: 7446-7455.

He, L., Soupene, E., Ninfa, A., and Kustu, S. (1998). Physiological role for the GlnK protein of enteric bacteria: relief of NifL inhibition under nitrogen-limiting conditions. *J. Bacteriol.* **180**: 6661-6667.

Holm, L., and Sander, C. (1995). DNA polymerase β belongs to an ancient nucleotidyl transferase superfamily. *Trends Biochem. Sci.* **20**: 345-347.

Holtel, A., and Merrick, M. (1988). Identification of the *Klebsiella pneumoniae glnB* gene: nucleotide sequence of wild type and mutant alleles. *Mol. Gen. Genet.* **215**: 134-138.

Hulme, E. C. (1990). Receptor Biochemistry, A Practical Approach. Oxford University Press, Oxford.

Hunt, J. B., and Ginsburg, A. (1972). Some kinetics of the interaction of divalent cations with glutamine synthetase from *Escherichia coli*. Metal ion induced conformational changes. *Biochemistry* **26**: 3723-3735.

Ikeda, T. P., Shauger, A. E., and Kustu, S. (1996). *Salmonella typhimurium* apparently perceives external nitrogen limitation as internal glutamine limitation. *J. Mol. Biol.* **259**: 589-607.

Jaggi, R., Ybarlucea, W., Cheah, E., Carr, P. D., Edwards, K. J., Ollis, D. L., and Vasudevan, S. G. (1996). The role of the T-loop of the signal transducing protein PII from *Escherichia coli*. *FEBS Lett.* **391**: 223-228.

Jaggi, R., van Heeswijk, W. C., Westerhoff, H. V., Ollis, D. L., and Vasudevan, S. G. (1997). The two opposing activities of adenylyltransferase reside in distinct homologous domains, with intramolecular signal transduction. *EMBO J.* **16**: 5562-5571.

Jaggi, R. (1998). Structure, function and molecular recognition of proteins in the signalling cascade that controls nitrogen assimilation in *Escherichia coli.* (Townsville, Australia: PhD thesis, James Cook University).

James, C. L., and Viola, R. E. (2002). Production and characterisation of bifunctional enzymes. Domain swapping to produce new bifunctional enzymes in the aspartate pathway. *Biochemistry* **41**: 3720-3725.

Jiang, P., Zucker, P., Atkinson, M. R., Kamberov, E. S., Tirasophon, W., Chandran, P., Schefke, B. R., and Ninfa, A. J. (1997a). Structure/function of PII signal transduction protein of *Escherichia coli:* genetic separation of interactions with protein receptors. *J. Bacteriol.* **179**: 4342-4353.

Jiang, P., Zucker, P., and Ninfa, A. J. (1997b). Probing interactions of the homotrimeric PII signal transduction protein with its receptors by use of PII heterotrimers formed *in vitro* from wild type and mutant subunits. *J. Bacteriol.* **179**: 4354-4360.

Jiang, P., Peliska, J. A., and Ninfa, A. J. (1998a). Enzymological characterisation of the signal-transducing uridylyltransferase/uridylyl-removing enzyme (EC 2.7.7.59) of *Escherichia coli* and its interaction with the PII protein. *Biochemistry* **37**: 12782-12794.

Jiang, P., Peliska, J. A., and Ninfa, A. J. (1998b). The regulation of *Escherichia coli* glutamine synthetase revisited: role of 2-ketoglutarate in the regulation of glutamine synthetase adenylylation state. *Biochemistry* **37**: 12802-12810.

Jiang, P., Atkinson, M. R., Srisawat, C., Sun, Q., and Ninfa, A. (2000). Functional dissection of the dimerisation and enzymatic activities of *Escherichia coli* nitrogen regulator II and their regulation by the PII protein. *Biochemistry* **39**: 13433-13449.

Jin, Q., Yuan, Z. H., Xu, J. G., Wang, Y., Shen, Y., Lu, W. C., Wang, J. H., Liu, H., Yang, J., Yang, F., Qu, D., Zhang, X. B., Zhang, J. Y., Yang, G. W., Wu, H. T., Dong, J., Sun, L. L., Xue, Y., Zhao, A. L., Gao, Y. S., Zhu, J. P., Kan, B., Chen, S. X., Yao, Z. J., He, B. K., Chen, R. S., Ma, D. L., Qiang, B. Q., Wen, Y. M., Hou, Y. D. and Yu, J. (2002). Genome sequence of *Shigella flexneri* 2a: insights into pathogenicity through comparison with genomes of *Escherichia coli* K12 and O157. *Nucleic Acids Res.* **30**: 4432-4441.

Johansson, M., and Nordlund, S. (1996). Transcription of the *glnB* and *glnA* genes in the photosynthetic bacterium *Rhodospirillum rubrum. Microbiol.* **142**: 1265-1272.

Kabat, E.A., Wu, T.T. and Bilofsky, H. (1977). Unusual distribution of amino acids in complementarity determining (hypervariable) segments of heavy and light chains of immunoglobulins and their possible roles in specificity of antibody combining sites. *J. Biol. Chem.* **252**: 6609.

Kamberov, E. S., Atkinson, M. R., Chandarn, P., and Ninfa, A. J. (1994a). Effect of mutations in *Escherichia coli gln* (*ntrB*), encoding nitrogen regulator II (NRII or NtrB),

on the phosphatase activity involved in bacterial nitrogen regulation. *J. Biol. Chem.* **269**: 28294-28299.

Kamberov, E. S., Atkinson, M. R., Feng, J., Chandran, P., and Ninfa, A. J. (1994b). Sensory components controlling bacterial nitrogen assimilation. *Cell. Mol. Biol. Res.* **40**: 175-191.

Kamberov, E. S., Atkinson, M. R., and Ninfa, A.J. (1995). The *Escherichia coli* PII signal transduction protein is activated upon binding 2-ketoglutarate and ATP. *J. Biol. Chem.* **270**: 17797-17807.

Kantrowitz, E. R., and Lipscomb, W. N. (1988). Escherichia coli aspartate transcarbamylase: the relation between structure and function. *Science* **241**: 669-674.

Keener, J., and Kustu, S. (1988). Protein kinase and phosphoprotein phosphatase activities of nitrogen regulatory proteins NTRB and NTRC of enteric bacteria: roles of the conserved amino-terminal domain of NTRC. *Proc. Natl. Acad. Sci. USA* **85**: 4976-4980.

Kessler, P. S., Blank, C., and Leigh, J. A. (1998). The *nif* gene operon of the methanogenic archaeon *Methanococcus maripaludis*. *J. Bacteriol.* **180**: 1505-1511.

Kohler, G., and Milstein, C. (1975). Continuous cultures of fused cells secreting antibody of predefined specificity. *Nature* **256**: 495-497.

Kranz, R. G., Pace, V. M., and Caldicot, I. M. (1990). Inactivation, sequence and *lacZ* fusion analysis of a regulatory locus required for repression of nitrogen fixation genes in *Rhodobacter capsulatus*. *J. Bacteriol.* **172**: 53-62.

Kustu, S., Santern, E., Keener, J., Popham, D., and Weiss, D. (1989). Expression of σ^{54} (*ntrA*) -dependent genes is probably united by a common mechanism. *Microbiol. Rev.* **53**: 367-376.

Laemmli, U. K. (1970). Cleavage of structural proteins during the assembly of the head of the bacteriophage T4. *Nature* **227**: 680-685.

Lee, S. J., Gray, M. C., Guo, L., Sebo, P., and Hewlett, E. L. (1999). Epitope Mapping of Monoclonal Antibodies against *Bordetella pertussis* Adenylylate Cyclase Toxin. *Infect. Immun.* **67**: 2090-2095.

Li, H., and Walker, D. H. (1998). rOmpA is a critical protein for the adhesion of *Rickettsia rickettsii* to host cells. *Microb. Pathog.* **24**: 289-298.

Liaw, S.H., Kuo, I. and Eisenberg, D. (1995). Discovery of the ammonium substrate site on glutamine synthetase, a third cation binding site. *Protein Sci.***4**: 2358-2365.

Liu, J., and Magasanik, B. (1995). Activation of the dephosphorylation of nitrogen regulator I-phosphate of *Escherichia coli*. *J. Bacteriol.* **177**: 926-931.

Lilley, P. E., Stamford, N. P. J., Vasudevan, S. G., and Dixon, N. E. (1993). The 92-min region of the *E. coli* chromosome: location and cloning of *ubiA* and *alr* genes. *Gene* **129**: 9-16.

Love, C. A., Lilley, P. E., and Dixon, N. E. (1996). Stable high-copy-number-bacteriophage lambda promoter vectors for overproduction of proteins in *Escherichia coli. Gene* **176**: 49-53.

Magasanik, B. (1993). The regulation of nitrogen utilisation in enteric bacteria. *J. Cell. Biochem.* **51**: 34-40.

Martin, G. B., Thomashow, M. F., and Chelm, B. K. (1989). *Bradyrhizobium japonicum glnB*, a putative nitrogen-regulatory gene, is regulated by NtrC at tandem promoters. *J. Bacteriol.* **139**: 2667-2675.

Martin, G., Keller, W., and Doublie, S. (2000). Crystal structure of mammalian poly(A) polymerase in complex with an analog of ATP. *EMBO J.* **19**: 4193-4203.

McLoughlin, S. (1999). Identification of the residues responsible for the opposing catalytic activities of adenylyl transferase (ATase) in *Escherichia coli.* (Townsville, Australia: Honours thesis, James Cook University).

Merrick, M. J., and Edwards, R. A. (1995). Nitrogen control in bacteria. *Microbiol. Rev.* **59**: 604-622.

Miller, R. E., and Stadtman, E. R. (1972). Glutamate synthase from *Escherichia coli. J. Biol. Chem.* **247**: 7407-7419.

Moore, J., Shiau, S. P. and Reitzer, L. (1993). Alterations of highly conserved residues in the regulatory domain of nitrogen regulator I (NtrC) of *Escherichia coli*. *J. Bacteriol.* **175**: 2692-2701.

Neylon, C., Brown, S. E., Kralicek, A. V., Miles, C. S., Love, C. A., and Dixon, N. E. (2000). Interaction of the *Escherichia coli* replication terminator protein (Tus) with

DNA: a model derived from DNA binding studies of mutant protein by surface plasmon resonance. *Biochemistry* **39**: 11989-11999.

Ninfa, A. J., Ueno-Nishio, S., Hunt, T. P., Robustell B. and Magasanik, B. (1986). Purification of nitrogen regulator II, the product of the *glnL* (*ntrB*) gene of *Escherichia coli. J. Bacteriol.* **168**: 1002-1004.

Ninfa, A. J., and Bennet, R. L. (1991). Identification of the site of the autophosphorylation of the bacterial protein kinase/phosphatase NRII. *J. Biol. Chem.* **266**: 6888-6893.

Ninfa, A. J., Atkinson, M. R., Kamberov, E. S., Feng, J. and Ninfa, E. G. (1995). Control of nitrogen assimilation by the NRI-NRII two component system of enteric bacteria. In: Two Component Signal Transduction (Hoch, J.A. and Silhavy, T.J. eds.). ASM Press, Washington, DC.

Ninfa, A. J., and Atkinson, M. R. (2000). PII signal transduction proteins. *Trends Microbiol.* **8**: 172-179.

Ninfa, E. G., Atkinson, M., Kamberov, E., and Ninfa, A. J. (1993). Mechanism of autophosphorylation of *E. coli* nitrogen regulator II (NRII or NtrB): *trans*-phosphorylation between subunits. *J. Bacteriol.* **175**: 7024-7032.

O'Donnell, R. (2000). The role of Q-linkers in the intramolecular signalling mechanisms of adenylyl transferase (ATase). (Townsville, Australia: Honours thesis, James Cook University).

Pancholi, V., and Fischetti, V. A. (1998). α-Enolase, a novel strong plasmin(ogen) binding protein on the surface of pathogenic streptococci. *J. Biol. Chem.* **273**: 14503-14515.

Parish, T., and Stoker, N., G. (2000). *glnE* is an essential gene in *Mycobacterium tuberculosis. J. Bacteriol.* **182**: 5715-5720.

Pedersen, L. C., Benning, M. M., and Holden, H. M. (1995). Structural investigation of the antibiotic and ATP-binding sites in kanamycin nucleotidyltransferase. *Biochem.* **34**: 13305-13311.

Pelletier, H., Sawaya, M. R., Kumar, A., Wilson, S. H., and Kraut, J. (1994). Structures of ternary complexes of rat DNA polymerase β, a DNA template primer, and ddCTP. *Science* **264**: 1891-1903.

Pelton, J. G., Kustu, S., and Wemmer, D. E. (1999). Solution structure of the DNA-binding domain of NtrC with three alanine substitutions. *J. Mol. Biol.* **292**: 1095-1110.

Porter, R. R. (1959). The hydrolysis of rabbit γ-globulin and antibodies with crystalline papain. *Biochem. J.* **73**: 119-126.

Raleigh, E. A., Lech, K., and Brent, R. (1989). In Current Protocols in Molecular Biology, F. M. Ausubel, R. Brent, R. E. Kingston, D. D. Moore, J. G. Seidman, J. A. Smith and K. Struhl, eds. (New York: Publishing Associates and Wiley Interscience), pp. 1.4.8-1.4.9.

Reith, M., and Munholland, J. (1993). A high-resolution gene map of the chloroplast genome of the red algae *Porphyra purpurea. Plant Cell* **5**: 465-475.

Rhee, S. G., Chock, P. G., and Stadtman, E. R. (1989). Regulation of *Escherichia coli* Glutamine Synthetase. *Adv. Enzymol. Relat. Areas Mol. Biol.* **62**: 37-92.

Roitt, I. (1988). In Essential Immunology. (Oxford: Blackwell Scientific Publications).

Rost, B., and Sander, C. (1993). Prediction of protein secondary structure at better than 70% accuracy. *J. Mol. Biol.* **232**: 584-599.

Sambrook, J., Fritsch, E. F., and Maniatis, T. (1989). In Molecular Cloning: A Laboratory Manual. (Cold Spring Harbor, NY: Cold Spring Harbor Laboratory Press).

Sanger, F., Niklen, S., and Coulson, A. R. (1977). DNA sequencing with chain-terminating inhibitors. *Proc. Nat. Acad. Sci. U.S.A.* **74**: 5463-5467.

Sawaya, M. R., Pelletier, H., Kumar, A., Wilson, S. H., and Kraut, J. (1994). Crystal structure of rat DNA polymerase beta: evidence for a common polymerase mechanism. *Science* **264:** 1930-1935.

Sawaya, M. R., Prasad, R., Wilson, S. H., Kraut, J., and Pelletier, H. (1997). Crystal structures of human DNA polymerase beta complexed with gapped and nicked DNA: evidence for an induced fit mechanism. *Biochemistry* **36**: 11205-11215.

Sayers, J. R., Krekel, C., and Eckstein, F. (1992). Rapid high-efficiency site directed mutagenesis by the phosphorothioate approach. *Biotechniques* **13**: 592-596.

Severinova, E., Severinova, K., Fenyo, D., Marr, M., Brody, E. N., Roberts, J. W., Chait, B. T., and Darst, S. A. (1996). Domain organisation of the *Escherichia coli* RNA polymerase sigma 70 subunit. *J. Mol. Biol.* **263**: 637-647.

Schiffer, M., and Edmundson, A. B. (1967). Use of helical wheels to represent the structures of proteins and to identify segments with helical potential. *Biophys. J.* **7**: 121-135.

Schulman, M., Wilde, C. D., and Kohler, G. (1978). A better cell line for making and secreting specific antibodies. *Nature* **276**: 269-270.

Senior, P. J. (1975). Regulation of nitrogen metabolism in *Escherichia coli* and *Klebsiella aerogenes*: Studies with the continuous-culture technique. *J. Bacteriol.* **123**: 407-418.

Shapiro, B. M., and Stadtman, E. R. (1970). Glutamine synthetase (*Escherichia coli*). *Methods Enzymol.* **17A**: 910-922.

Smith, C. S., Aalim, M. W. and Moorhead, G. B. G. (2003). Molecular properties of the putative nitrogen sensor PII from *Arabidopsis thaliana. Plant J.* **33**: 353-360.

Son, H. S., and Rhee, S. G. (1987). Cascade control of *Escherichia coli* glutamine synthetase. Purification and properties of PII protein and nucleotide sequence of its structural gene. *J. Biol. Chem.* **262**: 8690-8695.

Stadtman, E. R., Smyrniotis, P. Z., Davis, J. N., and Wittenberger, M. E. (1979). Enzymatic procedures for determining the average state of adenylylation of *Escherichia coli* glutamine synthetase. *Anal. Biochem.* **95**: 275-285.

Stock, J. B., Ninfa, A. J., and Stock, A. M. (1989). Protein phosphorylation and regulation of adaptive responses in bacteria. *Microbiol. Rev.* **53**: 450-490.

Studier, F. W., Rosenberg, A. H., Dunn, J. J., and Dubendorff, J. W. (1990). Use of T7 RNA polymerase to direct expression of cloned genes. *Methods Enzymol.* **185**: 60-89.

Su, W., Porter, S., Kustu, S. and Echols, H. (1990). DNA-looping and enhancer activity: association between DNA-bound NtrC activator and RNA polymerase at the bacterial *glnA* promoter. *Proc. Nat. Acad. Sci. U.S.A.* **87**: 5504-5508.

Sun, R., Anderson, T. J., Erickson, A. K., Nelson, E. A., and Francis, D. H. (2000). Inhibition of adhesion of *Escherichia coli* K88ac fimbria to its receptor, intestinal mucin-type glycoproteins, by a monoclonal antibody directed against a variable domain of the fimbria. *Infect. Immun.* **68**: 3509-3515.

Tainer, J., and Russell, P. (1994). Enzyme structure. Cracking tyrosine phosphatases. *Nature* **370**: 506-507.

Taylor, J. W., Ott, J., and Eckstein, F. (1985). The rapid generation of oligonucleotide-directed mutations at high frequency using phosphorothioate-modified DNA. *Nucleic Acids Res.* **13**: 8765-8785.

Tikasingh, E. S., Spence, L., and Downs, W. G. (1965). The use of adjuvant and sarcoma 180 cells in the production of mouse hyperimmune ascitic fluids to arboviruses. *Amer. J. Trop. Med. Hyg.* **15**: 219-226.

Towbin, H., Stehelin, T., and Gordon, N. (1979). Electrophoretic transfer of proteins from polyacrylamide gels to nitrocellulose sheets, procedure and some applications. *Proc. Nat. Acad. Sci. U.S.A.* **76**: 4350-4354.

Tsinoremas, N. F., Castets, A. M., Harrison, M. A., J. F., A., and Tandeau de Marsac, N. (1991). Photosynthetic electron transport controls nitrogen assimilation in cyanobacteria by means of post-translational modification of the *glnB* gene product. *Proc. Natl. Acad. Sci. USA* **88**: 4565-4569.

van Heeswijk, W. C., Rabenberg, M., Westerhoff, H. V., and Kahn, D. (1993).The genes of the glutamine synthetase adenylylation cascade are not regulated by nitrogen in *Escherichia coli. Mol. Microbiol.* **9**: 443-457.

van Heeswijk, W. C., Stegeman, B., Hoving, S., Molenaar, D., Kahn, D., and Westerhoff, H. V. (1995). An additional PII in *Escherichia coli*: a new regulatory protein in the glutamine synthetase cascade. *FEMS Microbiol. Lett.* **132**: 153-157.

van Heeswijk, W. C., Hoving, S., Molenaar, D., Stegeman, B., Kahn, D., and Westerhoff, H. V. (1996). An alternative PII protein in the regulation of glutamine synthetase in *Escherichia coli. Mol. Microbiol.* **21**: 133-146.

van Heeswijk, W.C. (1998). The glutamine synthetase adenylylation cascade: A search for its control and regulation. (Amsterdam, Netherlands: PhD thesis, Free University).

van Heeswijk, W. C., Wen, D., Clancy, P., Jaggi, R., Ollis, D. L., Westerhoff, H. V. and Vasudevan, S. G. (2000). The *Escherichia coli* signal transducers PII (GlnB) and GlnK form heterotrimers *in vivo*: fine tuning the nitrogen signal cascade. *Proc. Nat. Acad. Sci. U.S.A.* **97**: 3942-3947.

Vasudevan, S. G., Armarego, W. L., Shaw, D. C., Lilley, P. E., Dixon, N. E., and Poole, R. K. (1991). Isolation and nucleotide sequence of the *hmp* gene that encodes a haemoglobin-like protein in *Escherichia coli* K-12. *Mol. Gen. Genet.* **226**: 49-58.

Vasudevan, S. G., Gedye, C., Dixon, N., Cheah, E., Carr, P., Suffolk, P., Jeffrey, P., and Ollis, D. (1994). *E. coli* PII protein: purification, crystallisation and oligomeric structure. *FEBS Lett.* **337**: 255-258.

Vieira, J., and Messing, J. (1987). Production of single-stranded plasmid DNA. *Methods Enzymol.* **153**: 3-11.

Volkman, B. F., Nohaile, M. J., Amy, N. K., Kustu, S., and Wemmer, D. E. (1995). Three dimensional solution structure of the N-terminal receiver domain of NTRC. *Biochemistry* **34**: 1413-1424.

Walter, M. R., Windsor, W. T., Nagabushan, T. L., Lundell, D. J., Lunn, C. A., Zauodny, P. J., and Narula, S. K. (1995). Crystal structure of complex between interferon and its soluble high-affinity receptor. *Nature* **376**: 230-235.

Wei, J., Goldberg, M. B., Burland, V., Venkatesan, M. M., Deng, W., Fournier, G., Mayhew, G. F., Plunkett, G. III, Rose, D. J., Darling, A., Mau, B., Perna, N. T., Payne, S. M., Runyen-Janecky, L. J., Zhou, S., Schwartz, D. C. and Blattner, F. R. (2003). Complete Genome Sequence and Comparative Genomics of *Shigella flexneri* Serotype 2a Strain 2457T. *Infect. Immun.* **71**: 2775-2786.

Welch, R. A., Burland, V., Plunkett, G. D. III, Redford, P., Roesch, P., Rasko, D. A., Buckles, E. L., Liou, S. -R., Boutin, A., Hackett, J., Stroud, D., Mayhew, G. F., Rose, D. J., Zhou, S., Schwartz, D. C., Perna, N. T., Mobley, H. L. T., Donnenberg, M. S. and Blattner, F. R. (2002). Extensive mosaic structure revealed by the complete genome sequence of uropathogenic *Escherichia coli*. *Proc. Natl. Acad. Sci. U.S.A.* **99**: 17020-17024.

Wen, D. (2000). Studies on PII/GlnK heterotrimer formation and truncated domains of adenylyl transferase (ATase) in the adenylylation cascade of glutamine synthetase in *Escherichia coli*. (Townsville, Australia: Masters thesis, James Cook University).

Wiess, V., Batut, J., Klose, K., Keener, J. and Kustu, S. (1991). The phosphorylated form of the enhancer binding protein NtrC has ATPase activity that is essential for activation of transcription. *Cell* **67**:155-167.

Wooton, J. C., and Drummond, M. H. (1989). The Q-linker: a class of interdomain sequences found in bacterial multidomain regulatory proteins. *Prot. Eng.* **2**: 535-543.

Wray, L. V., Atkinson, M. R., and Fisher, S. H. (1994). The nitrogen-regulated *Bacillus subtilis nrg AB* operon encodes a membrane protein and protein highly similar to the *Escherichia coli glnB*-encoded PII protein. *J. Bacteriol.* **176**: 108-114.

Xu, Y., Carr, P. D., van Heeswijk, W. C., Westerhoff, H. V., Vasudevan, S. G., and Ollis, D. L. (1998). GlnK, a PII-homologue, structure reveals ATP binding site and indicates how the T-loops may be involved in molecular recognition. *J. Mol. Biol.* **282**: 149-165.

Xu, Y., Carr, P. D., Huber, T., Vasudevan, S. G. and Ollis, D. L. (2001). The structure of the PII-ATP complex. *Eur. J. Biochem.* **268**: 2028-2037.

Xu, Y., Carr, P. D., Clancy, P., Garcia-Dominguez, M., Forchhammer, K., Florencio, F., Tandeau de Marsac, N., Vasudevan, S., and Ollis, D. (2003). The structures of the PII proteins from the cyanobacteria *Synechococcus* sp. PCC 7942 and *Synechocystis* sp. PCC 6803. *Acta Cryst D.* **59**: 2183-2190.

Xu, Y., Wen, D., Clancy, P., Carr, P. D., Ollis, D. L., and Vasudevan, S. G. (2004). Expression, purification, crystallization and preliminary X-ray analysis of the N-terminal domain of *Escherichia coli* ATase. *Protein Express. Purif.* **34**: 142-146.
Yamashita, M. M., Almassy, R. J., Janson, C. A., Cascio, D., and Eisenberg, D. (1989). Refined atomic model of glutamine synthetase at 3.5.A resolution. *J. Biol. Chem.* **264**: 17681-17690.

Yanisch-Perron, C., Vieira, J., and Messing, J. (1985). Improved M13 phage cloning vectors and host strains: nucleotide sequences of the M13mp18 and pUC19 vectors. *Gene.* **33**: 103-119.

Yi, J., Cheng, H., Andrake, M. D., Dunbrack, R. L., Roder, H., and Skalka, A. M. (2002). Mapping the epitope of an inhibitory monoclonal antibody to the C-terminal DNA-binding domain of HIV-1 integrase. *J. Biol. Chem.* **277**: 12164-12174.